



Fate and transport of lignin in the soil-water continuum

Jonathan Simon Williams

Thesis submitted for the degree of Doctor of Philosophy

School of Civil Engineering and Geosciences, Faculty of Science Agriculture and
Engineering, Newcastle University,

and

Rothamsted Research

February 2014



Abstract

Vascular plants comprise 20-30% lignin, constituting a considerable organic input to soils. Lignin is not necessarily preserved in soils, but the fate of its decomposition products in the wider environment is not well understood. Therefore, the overarching hypothesis tested herein was that a significant proportion of lignin is solubilised and lost from soils by transport in water.

Solid phase extraction was used to extract lignin phenols from dissolved organic matter (DOM) from water outlets adjacent to major land use types (grazed grassland, deciduous woodland, and moorland) and compared to the lignin phenols from representative vegetation types, animal dungs and soils from each land use type. The phenols were identified and quantified using thermally assisted hydrolysis and methylation using tetramethylammonium hydroxide.

Leachates from lysimeters treated with four vegetation types (grass, buttercup, ash, and oak) were sampled in a 22 month chronosequence, showing that some of the dominant phenols detected in the vegetation were also dominant in the respective DOM. A proportional relationship between increasing temperature and loss of representative lignin phenols in DOM was observed. Comparison of the dominant phenols in vegetation, soil and water sampled from field sites suggested specific lignin phenols could be used as biomarkers for different land uses. The concentrations of organic carbon-normalised total lignin phenols in the soils were similar to those in water, indicating that a considerable proportion of lignin in soils is lost *via* leaching. There was no significant difference in losses of lignin phenols between each land use type. Application of different rates of dissolved lignin to lysimeters indicated that the amount of water added was a dominant driver of transport through soil over 16 days, and that molecular structure also influenced transport rates of individual phenols. The impact of this research is that climate change (increased precipitation and warming) may significantly affect the loss of lignin by increased solubilisation and leaching from soils.

Acknowledgements

I would like to thank my supervisory team: Drs. Geoffrey Abbott, Jennifer Dungait, and Roland Bol for encouraging me to take up this challenge, and their inspiration. Each of them contributed valuable expertise, and without their mentorship, I could not have completed it. “When you are a Bear of Very Little Brain, and you Think of Things, you find sometimes that a Thing which seemed very Thingish inside you is quite different when it gets out into the open and has other people looking at it.” (A.A. Milne, *Winnie-the-Pooh*).

I thank Dan Dhanoa for his advice and help with experimental design and statistical analysis.

The laboratory support staff at Newcastle University have been fantastic. I thank Berni Bowler for his endless wisdom, the opportunity to talk ideas through, and his boundless knowledge of how to find things and get things to work. I thank Ian Harrison and Paul Donohoe for their gas chromatograph expertise and Phil Green, David Race for their patience when I needed to analyse samples at short notice.

I thank the laboratory analysts Andrew Bristow, Liz Dixon, Trish Butler, and Denise Headon at Rothamsted Research North Wyke for their support and who analysed total carbon samples for me.

I thank Farm Managers Paul Redmore at Bicton College, Devon, and David Watson at Cockle Park Farm, and for supplying topsoil for my lysimeter experiments.

I acknowledge NERC and BBSRC for funding this project and providing my stipend. I also thank Newcastle University for the fantastic broad array of workshops to develop hard and soft skills.

I thank Ini Edem, Farouk Saeed, and Siraj, and the whole company of Newcastle’s West End Operatic Society who helped me enjoy my free time.

Finally, I thank my family for being there. I love you. Thank you for all your support and encouragement.

Table of Contents

Abstract	i
Acknowledgements.....	ii
List of tables.....	viii
List of figures.....	xi
Chapter 1: Introduction.....	1
1.1 The carbon cycle and climate change.....	1
1.2 Land use, management practices and soil carbon stocks.....	2
1.3 The importance of lignin in the carbon cycle.....	3
1.4 Lignin chemistry and biosynthesis.....	4
1.5 Lignin degradation.....	8
1.5.1 Lignin degrading microorganisms and enzymes.....	9
1.6 Chemistry of lignin degradation.....	10
1.7 Chemical analysis of lignin.....	13
1.8 The formation and structure of soils.....	18
1.9 Dissolved organic matter.....	19
1.10 Dissolved lignin.....	20
1.11 Lignin transport.....	21
1.12 Fate of lignin in aquatic systems.....	24
1.13 Overarching thesis aims.....	24
Chapter 2: General methods.....	25
2.1 Sample sites.....	25
2.2 Vegetation sampling.....	27
2.3 Soil and livestock dung sampling.....	28

2.4 Water sampling.....	28
2.5 Lysimeter experiments.....	29
2.5.1 <i>Bucket lysimeters (6.4 L) (Chapter 4)</i>	29
2.5.2 <i>Soil cores (0.645 L) (Chapter 6)</i>	31
2.6 Bulk analysis.....	32
2.6.1 <i>Vegetation, soil and dung</i>	32
2.6.2 <i>Water and leachates</i>	32
2.6.3 <i>Extraction of organic carbon from water</i>	33
2.6.4 <i>Bulk total carbon, total nitrogen, bulk stable $^{13}\text{C}/^{15}\text{N}$ isotope analysis of solid samples</i>	35
2.7 Sample derivatisation.....	35
2.7.1 <i>Sample derivatisation with N,O-bis(trimethylsilyl) trifluoroacetamide (BSTFA)</i>	35
2.7.2 <i>Thermally assisted hydrolysis and methylation using tetramethylammonium hydroxide and on-line py-GC-MS</i>	36
2.8 Gas chromatographic analysis.....	38
2.9 Statistical analysis.....	39
Chapter 3. Methodology comparison study: solid phase extraction vs. freeze-drying, and on-line TMAH thermochemolysis vs. GC-MS of trimethylsilyl derivatives for extraction and analysis of water-transportable lignin phenols.....	40
3.1. Introduction.....	40
3.1.1 <i>Extraction of dissolved lignin</i>	40
3.1.2 <i>Lignin analysis techniques</i>	43
3.1.3 <i>Experiment aims and hypotheses</i>	50
3.2. Methodology.....	50
3.2.1 <i>Experimental Design</i>	50
3.2.2 <i>Sampling Sites and collection</i>	51

3.2.3 <i>Sample extraction, derivatisation and analysis</i>	51
3.3. Results.....	52
3.3.1 <i>Sample TOC, pH and WBM yields</i>	52
3.3.2 <i>Total lignin phenol concentrations</i>	54
3.3.3 <i>Water borne lignin phenols</i>	55
3.4 Discussion.....	58
3.4.1 <i>Extracted WBM yields</i>	59
3.4.2 <i>Extraction of lignin phenols from water</i>	59
3.4.3. <i>Detection of lignin phenols extracted from water samples</i>	60
3.5 Conclusions.....	63
Chapter 4. Investigation of leaf litter lignin decomposition and subsequent loss as dissolved organic matter over time in a model system.....	64
4.1 Introduction.....	64
4.1.1 <i>Experiment aims and hypothesis</i>	67
4.2 Methodology.....	67
4.2.1 <i>Experimental Design</i>	67
4.2.2 <i>Field sampling</i>	68
4.2.3 <i>Lysimeter preparation, sampling and analysis</i>	69
4.2.4 <i>Statistical analysis</i>	69
4.3 Results.....	69
4.3.1 <i>Bulk fresh and degraded litter</i>	70
4.3.2 <i>Lignin phenols in fresh and degraded litter</i>	71
4.3.3 <i>Acid/aldehyde ratios in litter</i>	77
4.3.4 <i>Lignin phenols in leachates</i>	77

4.4 Discussion.....	89
4.4.1 <i>Mass loss of litter, total C, total N, and total lignin phenols</i>	89
4.4.2 <i>Lignin phenol composition of litters and leachate</i>	90
4.4.3 <i>Leached lignin phenol concentrations with respect to temperature</i>	92
4.5 Conclusions.....	93
Chapter 5: Lignin phenols in soils and natural waters as indicators of land use type....	95
5.1 Introduction.....	95
5.1.1 <i>Aims and hypotheses</i>	96
5.2 Methodology.....	96
5.2.1 <i>Experimental design</i>	96
5.2.2 <i>Approach</i>	96
5.3 Results and discussion.....	97
5.3.1 <i>Total lignin phenols</i>	97
5.3.2 <i>Lignin phenols in soils and DOM from different land use type</i>	100
5.3.3 <i>Dung</i>	107
5.3.4 <i>Lignin phenols as indicators of land use type</i>	108
5.4 Conclusions.....	109
Chapter 6. Transport of phenols through soil.....	110
6.1 Introduction.....	110
6.1.1 <i>Aims and hypotheses</i>	113
6.2 Methodology.....	113
6.2.1 <i>Experimental design</i>	113
6.2.2 <i>Preparation of soil cores, dung DOC, irrigation, and sampling</i>	114
6.2.3 <i>Data handling, sample derivatisation and analysis</i>	115

6.2.4 <i>Predictions of mass of DOC and total lignin phenols leached</i>	116
6.3 Results.....	116
6.3.1 <i>Soluble dung C characterisation</i>	116
6.3.2 <i>Leachate DOC</i>	119
6.3.3 <i>Leached total lignin phenols</i>	120
6.3.4 <i>Leached lignin phenols</i>	122
6.4 Discussion.....	125
6.4.1 <i>Relative leaching rates of lignin phenols</i>	125
6.4.2 <i>Effect of application rate of soluble fraction of dung on the mass of lignin phenols leached</i>	127
6.4.3 <i>Mechanisms of SOC contribution to leachates</i>	129
6.5 Conclusions.....	131
Chapter 7. Synthesis and future research.....	132
7.1 Overall thesis aims and objectives.....	132
7.2 Thesis hypotheses and conclusions.....	133
7.3 Synthesis of outcomes.....	136
7.4. Future research.....	138
References.....	143

List of tables

Table 1.1. Lignin proxies associated with analysis of lignin using thermally assisted hydrolysis and methylation using TMAH, assembled from Nierop and Filley (2007)...	17
Table 1.2. mean dissolved lignin vanillyl (V) and cinnamyl (C) phenol concentrations and vanillyl acid/aldehyde ratios (ac/al) _v in compartments at Wülfersreuth and Oberwarmensteinach forest sites (Guggenberger and Zech, 1994).....	21
Table 2.1. Sample site descriptions where vegetation, soil, dung, and water samples were collected. Grid References (G.R.) are located in figure 2.1. The chapter number refers to the experimental chapter in which the sample was used. Water sample Moorland* represents a mixed land use sample since the river source was on Dartmoor but flows through agricultural grassland.....	26
Table 3.1. Structure and retention properties of polar to highly polar pre-packed polymer and silica-based solid phase sorbents (Dittmar et al., 2008).....	41
Table 3.2. Mean (n = 3) water sample pH, TOC, and recovered water-borne matter yields extracted using freeze drying (FD) and solid phase extraction (SPE) from water samples collected from six sites. s.e. = standard error of the mean.....	52
Table 3.3. Mean (± standard error of the mean (s.e.), n = 3) total organic carbon (TOC) percentages in solid phase extracted (SPE) and freeze dried (FD) extracted water-borne matter for six water samples.....	54
Table 3.4. Mean (± standard error of the mean, n = 3) water borne lignin phenols concentrations from six sites (TBF, St, TRT, JC, RT, and ODC) extracted using freeze drying and detected using TMAH/GC-MS. Site name abbreviations are described in table 3.2. Phenol abbreviations (Abb.) with * contain an unmethylated hydroxyl group.....	56
Table 3.5. Mean (± standard error of the mean, n = 3) water borne lignin phenol concentrations (mg (100 mg OC) ⁻¹) from six sites (TBF, St, TRT, JC, RT, and ODC), extracted using SPE and detected using GC-FID. G6 ^{me} refers to a G6 compound with a demethylated 3-methoxy group. Site name abbreviations are described in table 3.2....	56
Table 3.6. Mean (± standard error of the mean, n = 3) water borne lignin phenol concentrations from six sites (TBF, St, TRT, JC, RT, and ODC) extracted using solid phase extraction and detected using TMAH/GC-MS. Site name abbreviations are	

described in table 3.2. Each * in the phenol abbreviation (Abb) column denotes an unmethylated hydroxyl group.....	57
Table 4.1. Randomised block experimental design showing the allocation of treatments to packed soil cores.....	68
Table 4.2. Characterisation of freeze-dried undegraded litters applied to lysimeters, comprising leaf and shoots showing mean and standard error of the mean (s.e., n = 4).	69
Table 4.3. Mean (\pm standard error of the mean (s.e.), n = 4) normalised lignin phenol concentrations and aromatic carboxylic acids (/100 mg OC) from TMAH/GC-MS analysis of fresh mixed grass, <i>Ranunculus repens</i> , <i>Fraxinus excelsior</i> , and <i>Quercus robur</i> . Total lignin (sum of compounds: 1,2,4,5,6,8,9,11-29) and acid/aldehyde ratios for compounds 21/18 (G6/G4 ratio) and compounds 27/22 (S6/S4 ratio) are also reported.....	72
Table 4.4. Mean (\pm standard error of the mean (s.e.), n = 4) TMAH/GC-MS product concentrations from analysis of degraded mixed grass, <i>Ranunculus repens</i> , <i>Fraxinus excelsior</i> , and <i>Quercus robur</i> . Total lignin (sum of compounds: 1,2,4,5,6,8,9,11-29) and acid/aldehyde ratios for compounds 21/18 (G6/G4 ratio) and compounds 27/22 (S6/S4 ratio) are also reported.....	76
Table 4.5. Litter types and lignin phenols where hypothesis 3 could be accepted, labelled ✓	94
Table 5.1. Mean (\pm standard error of the mean (s.e.), n = 3) dissolved lignin phenol concentrations from the six water samples. TBF = Taw Barton Farm drain, S = Sticklepath drain, TRT = Tributary of River Taw, JC = Josephs Carr pond, RT = River Taw, ODC = Orchard Dean Copse stream. The last six compound names with abbreviations (Abb.) in the table identify lignin degradation products detected in soils but not in water samples.....	106
Table 6.1. Experimental design for the allocation of slurry treatments to packed soil cores and the re-randomisation of cores after each sampling event.....	113
Table 6.2. Mean (\pm standard deviation; n = 3) concentrations ($\mu\text{g L}^{-1}$) of major lignin phenols extracted from the soluble fraction of cattle dung. Compound labels instead of the full compound name are used in the text.....	117

Table 6.3. Mean ($n = 5$) recovery ($\text{Mass}/\text{Mass}_0$) ratios of individual lignin monomers, total lignin phenols, and dissolved organic carbon (DOC) recovered in leachates after passage of 13.5 pore volumes. Differences in masses recovered at 65 and 163 $\text{m}^3 \text{ha}^{-1}$ application rates are expressed as a Multiplication factor. Compound labels are defined in table 6.2.....124

List of figures

Figure 1.1. The natural carbon (C) cycle displaying storages (Pg C) and fluxes (Pg C year ⁻¹) for its main components. Thick arrows highlight important fluxes. Dashed lines represent fluxes of C as CaCO ₃ which operate over long time-scales (IPCC, 2001). Values for pools with superscripts ^b and ^a were sourced elsewhere (Denman et al., 1996, US-DOE, 2008), respectively.....	1
Figure 1.2. The secondary cell wall in plant cells (www.ccruc.uga.edu/~mao/intro/outline.htm).....	4
Figure 1.3. Molecular structures of the monolignol precursor phenylalanine, and three monolignols: <i>p</i> -coumaryl alcohol, coniferyl alcohol, and sinapyl alcohol.....	5
Figure 1.4. The β -O-4 linkage between lignin monomer units, highlighted in red. R = the continuation of the lignin biopolymer.....	6
Figure 1.5. The two lignin configurations found in the secondary cell wall of spruce wood. Lignin bound principally to xylan has a linear configuration (A). Lignin principally bonded to glucomannans form a more branched configuration (B) (Chen and Sarkanen, 2010, Gellerstedt, 2007).....	7
Figure 1.6. Molecular structures of incompletely biosynthesized monolignols.....	8
Figure 1.7. Principal lignin degradation reactions by white-rot (side chain oxidation, and aromatic ring cleavage) and brown-rot fungi (ring hydroxylation, and ring demethylation). Figure is modified from Filley, et al. (2000) and Geib, S. et al. (2008).....	11
Figure 1.8. Incorporation rates of S (plot A), V (plot B), and C (plot C) maize-derived lignin phenols into soil through time (Bahri et al., 2006).....	12
Figure 1.9. Proportion of dung-derived lignin moieties incorporated in the 0-1cm soil horizon beneath C ₄ dung pats, 56 and 372 days after dung deposition. 1 = 4-vinylphenol, 3 = syringol, 7 = 4-vinylguaiacol, 9 = 4-vinylsyringol, 12 = 4-(2- <i>Z</i> -propenyl)syringol, 13 = 4-(2- <i>E</i> -propenyl)syringol, 14 = 4-acetylsyringol, 15 = 4-(2-propanone)syringol (Dungait et al., 2008).....	13

Figure 1.10. Names, abbreviation symbol, and molecular structure of the lignin phenols detected in samples analysed in this thesis.....	15
Figure 1.11. Development of soil horizons as materials are added to the upper part of the profile and other materials translocated to deeper zones (Brady and Weil, 2008)...	18
Figure 1.12. The lignin cycle, as a component of the carbon cycle. Lignin pools and concentrations are in solid boxes, fluxes in dashed-line boxes.....	22
Figure 2.1. Ordnance Survey map showing the approximate location of sampling sites in the vicinity of the Rothamsted Research North Wyke institute, Devon.....	27
Figure 2.2. Solid phase extraction (SPE) setup used for the extraction of dissolved lignin phenols from natural waters using C ₁₈ -SPE cartridges.....	34
Figure 2.3. Molecular structure of <i>N,O</i> -bis(trimethylsilyl) trifluoroacetamide (BSTFA) derivatising agent.....	35
Figure 2.4. Tetrahedral geometry of the tetramethylammonium hydroxide salt.....	36
Figure 2.5. Pyroprobe temperature calibration. Mean (\pm standard error of the mean, n = 3) observed temperatures of five inorganic salts of known melting points.....	37
Figure 3.1. Six-centre concerted retro-ene pyrolysis reaction mechanism for breaking the β -O-4 bond in the lignin macromolecule (Klein and Virk, 1983, van der Hage et al., 1993).....	44
Figure 3.2. Reaction of <i>N,O</i> -bis(trimethylsilyl) trifluoroacetamide (BSTFA) with an active hydrogen atom on a sample compound via a SN ₂ -type mechanism.....	44
Figure 3.3. Proposed general mechanism for the cleavage of the lignin β -O-4 bond using tetramethylammonium hydroxide ((CH ₃) ₄ N ⁺ OH ⁻), modified from Filley et al., (1999) for the reaction of (CH ₃) ₄ N ⁺ OH ⁻ in aqueous solution, rather than in methanol.....	46
Figure 3.4. Proposed mechanism for the degradation of lignin by DFRC (Holtman et al., 2003, Ralph and Grabber, 1996).....	48
Figure 3.5. Proposed mechanism for thioacidolysis of lignin (Holtman et al., 2003, Rolando et al., 1992).....	49
Figure 3.6. Schematic describing the split-split plot experimental design comparing extraction and analysis techniques.....	51

Figure 3.7. Mean (\pm standard error of the mean (s.e.), $n = 3$) total organic carbon (TOC, plot A), solid phase extracted (SPE) water-borne matter (WBM, plot B), freeze dried (FD) extracted WBM (plot C), and TOC of the solid freeze-dried WBM extract (plot D) in six water samples. Site name abbreviations are described in table 3.2.....	53
Figure 3.8. Mean (\pm standard error of the mean, $n = 3$) total lignin phenol concentrations after freeze-drying (FD, plot A) and solid phase extraction (SPE, plot B), detected using cold on column GC-FID and TMAH/GC-MS.....	54
Figure 4.1. Experiment setup showing lysimeters with decomposing plant litter on packed soil cores with an overhead irrigation system, and provision for leachate collection below the trolleys.....	68
Figure 4.2. Percentage (%) mass loss (\pm standard error of the mean; $n = 4$) for parameters: total organic carbon, total nitrogen, total lignin, and litter biomass from initial undegraded vegetation after 671 days of decomposition for mixed grass, <i>Ranunculus repens</i> , <i>Fraxinus excelsior</i> , and <i>Quercus robur</i> . Litter types are grouped (a, b, or c) to show significant differences (FPLSD test) for the same parameter. P values highlight significant differences (two-sample t-test) between parameters for the same litter type.....	70
Figure 4.3. Mean (\pm standard error of the mean, $n = 4$) total lignin phenol concentrations normalised to TOC for fresh and decomposed (after 671 days) leaf litter.....	73
Figure 4.4. A principal component biplot of first and second components of individuals (individual lignin phenol concentrations, shown in red, defined in table 4.3), and variates (mixed grass, <i>Ranunculus repens</i> , <i>Fraxinus excelsior</i> , and <i>Quercus robur</i> litter samples, shown in blue), for fresh and degraded litter.....	74
Figure 4.5. Mean (\pm standard error of the mean, $n = 4$) carbon normalised phenol concentrations in fresh and degraded mixed grass, <i>Ranunculus repens</i> , <i>Fraxinus excelsior</i> , and <i>Quercus robur</i> species. Phenol abbreviations are defined in figure 1.10.....	75
Figure 4.6. Mean (\pm standard error of the mean, $n = 3$) normalised total lignin concentrations in topsoil leachates from decomposing litter (mixed grass, <i>Ranunculus repens</i> , <i>Fraxinus excelsior</i> , and <i>Quercus robur</i>) through time. Mean ($n = 3$) topsoil temperature is shown in red.....	78

Figure 4.7. Mean (\pm standard error of the mean, n = 3) concentrations of selected lignin phenols detected in topsoil leachates from decomposing litter (mixed grass, <i>Ranunculus repens</i> , <i>Fraxinus excelsior</i> , and <i>Quercus robur</i>) through time. Phenol abbreviations are defined in figure 1.10.....	80
Figure 4.8. Mean lignin phenols and aromatic acids (n = 3) detected in soil leachates with different vegetation treatments applied using TMAH/GC-MS at time 1. Phenol abbreviations are defined in figure 1.10.....	81
Figure 4.9. Mean lignin phenols and aromatic acids (n = 3) detected in soil leachates with different vegetation treatments applied using TMAH/GC-MS at time 2. Phenol abbreviations are defined in figure 1.10.....	82
Figure 4.10. Mean lignin phenols and aromatic acids (n = 3) detected in soil leachates with different vegetation treatments applied using TMAH/GC-MS at time 3. Phenol abbreviations are defined in figure 1.10.....	83
Figure 4.11. Mean lignin phenols and aromatic acids (n = 3) detected in soil leachates with different vegetation treatments applied using TMAH/GC-MS at time 4. Phenol abbreviations are defined in figure 1.10.....	84
Figure 4.12. Mean lignin phenols and aromatic acids (n = 3) detected in soil leachates with different vegetation treatments applied using TMAH/GC-MS at time 5. Phenol abbreviations are defined in figure 1.10.....	85
Figure 4.13. Mean lignin phenols and aromatic acids (n = 3) detected in soil leachates with different vegetation treatments applied using TMAH/GC-MS at time 6. Phenol abbreviations are defined in figure 1.10.....	86
Figure 4.14. Mean lignin phenols and aromatic acids (n = 3) detected in soil leachates with different vegetation treatments applied using TMAH/GC-MS at time 7. Phenol abbreviations are defined in figure 1.10.....	87
Figure 5.1. Mean (\pm standard error of the mean, n = 3) total lignin phenol concentrations of soils, dung, and dissolved organic matter (DOM) extracts, defined as the sum of lignin phenols in table 5.1. G = grassland, F = woodland, M = moorland. Subscripts o and a denote the soil organic and A horizons respectively. SD = sheep dung, and CD = cattle dung. Letters above each column group label the statistical difference grouping according to the Fisher's protected least significant difference test.....	98

Figure 5.2. Mean (\pm standard error of the mean, n = 3) grazed grassland lignin phenol concentrations in soil organic- (O), A-horizon (A), and DOM (Taw Barton Farm). Lignin phenol abbreviations are defined in figure 1.10.....	100
Figure 5.3. Lignin phenol correlations between grassland soil organic (Go) and A horizons (Ga, plot A) and between the A horizon and DOM (Taw Barton Farm, plot B).....	101
Figure 5.4. Mean (\pm standard error of the mean, n = 3) woodland lignin phenol concentrations in soil organic- (O), A-horizon (A), and DOM from Oak woodland (Orchard Dean Copse stream). Lignin phenol abbreviations are defined in figure 1.10.....	102
Figure 5.5. Lignin phenol correlations between woodland soil organic (Fo) and A horizons (Fa, plot A) and between the organic horizon and DOM (Orchard Dean Copse stream, plot B).....	103
Figure 5.6. Mean (\pm standard error of the mean, n = 3) moorland lignin phenol concentrations in soil organic- (O), A-horizon (A), and River Taw DOM (DOM). Lignin phenol abbreviations are defined in figure 1.10.....	104
Figure 5.7. Lignin phenol correlations between moorland soil organic (Mo) and A horizons (Ma, plot A) and between the A horizon and DOM (River Taw, plot B).....	105
Figure 5.8. Mean (\pm standard error of the mean, n = 3) lignin phenol concentrations in sheep and cattle dung. Lignin phenol abbreviations are defined in figure 1.10.....	107
Figure 5.9. A principal component biplot of first and second components of individuals (individual lignin phenol concentrations, shown in red, table 5.1), and variates (different soil and dissolved organic matter samples, shown in blue). Site A_DOM, Site B_DOM, Site C_DOM, Site D_DOM, Site E_DOM, Site F_DOM, represent dissolved lignin samples from Taw Barton Farm, Sticklepath drain, Tributary of River Taw, Josephs Carr pond, River Taw, and Orchard Dean Copse stream, respectively. Go_mean, G_mean, Fo_mean, F_mean, Mo_mean, and M_mean represent soil organic and A horizon samples for grassland, woodland, and moorland land uses, respectively. Tree, and grass/short vegetation ecosystems, and dung-association regions are labelled.....	108

Figure 6.1. Processes resulting in protection of root carbon in soils (Rasse et al., 2005).....	111
Figure 6.2. Experimental setup showing how irrigation water was pumped to each lysimeter, and subsequent leachate collection. The Insert shows the top of a lysimeter, utilising an inverted cone of filter paper to distribute irrigation water evenly.....	114
Figure 6.3. Molecular structure of phenols identified in soluble dung DOC and leachates reported in table 6.2.....	118
Figure 6.4. Mean values (and cumulative σ) for cumulative release of dung DOC in leachate from soil cores at 65 and 163 m ³ ha ⁻¹ application rates, where the control treatment (blue) received no dung DOC. The predicted amount of DOC leached following 163 m ³ /ha slurry application is shown (brown circles and dotted line) calculated using equation 6.1.....	119
Figure 6.5. Release curves for mean ($\pm \sigma$) recovery of total lignin phenols applied to soil cores at 0 (n = 3), 65 (n = 5), and 163 m ³ ha ⁻¹ (n = 5) application rates. Total lignin defined as the sum of the compound concentrations listed in table 6.2. Predicted mass of total lignin phenols recovered in leachate at 163 m ³ ha ⁻¹ slurry application rate is also shown (brown circles and dashed line), calculated using equation 6.2. The insert is an expanded view of 0 – 10 μ g mass recovered.....	121
Figure 6.6. Release curves for mean masses (and standard deviation, n = 5) of P6, G6, G12, P18, G12*, P12, G18, and S6 lignin phenols determined in leachates from soil cores after application of dung DOC at 0, 65, and 163 m ³ ha ⁻¹ . Compound labels are defined in table 6.2.....	122
Figure 7.1. The lignin cycle, identifying future research lignin flux determination requirements highlighted in red.....	140

Chapter 1. Introduction

1.1 The carbon cycle and climate change

Pre-industrial global atmospheric carbon dioxide (CO₂) concentrations have been estimated as 280 ± 10 ppm (Solomon et al., 2007), and industrialisation has since increased this to 394.3 ppm, currently increasing at 2.4 ppm year⁻¹ (Tans and Keeling, 2013). The rate of warming averaged over the last 50 years is 0.13 ± 0.03 °C/decade (Solomon et al., 2007), which is greater than the critical rate of 0.1 °C/decade above which ecosystems cannot adapt (Lal, 2004). Furthermore, a warming of 2-7 °C of the mean global air temperature is expected by 2100 (Allison et al., 2009), therefore there is increased importance on reducing atmospheric CO₂ concentrations.

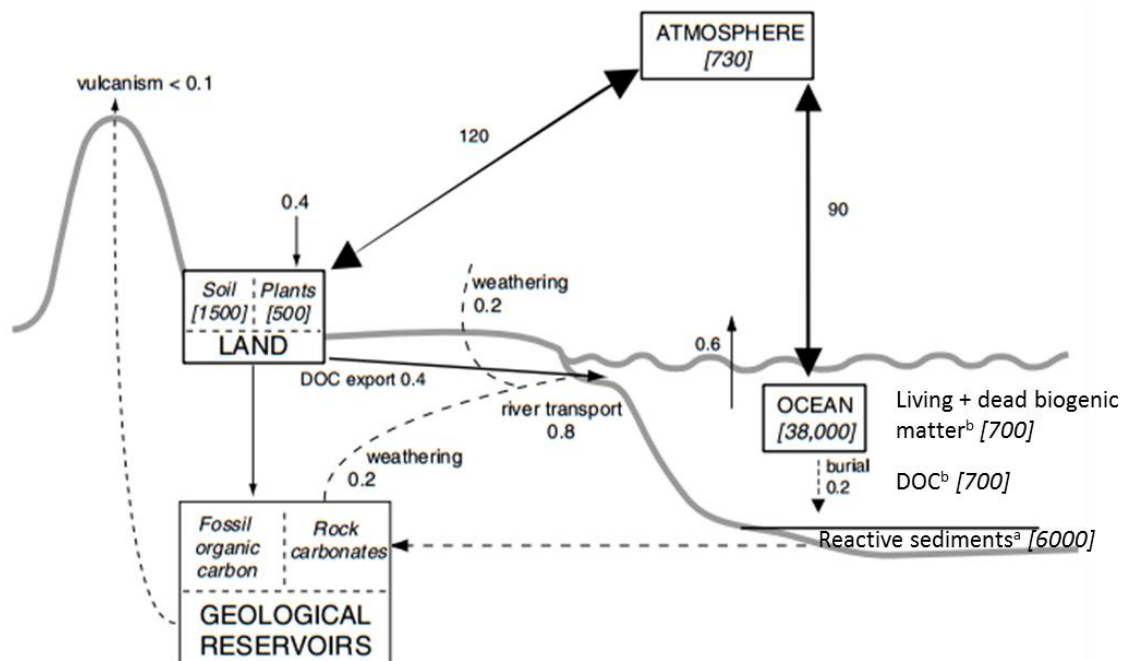


Figure 1.1. The natural carbon (C) cycle displaying storages (Pg C) and fluxes (Pg C year⁻¹) for its main components. Thick arrows highlight important fluxes. Dashed lines represent fluxes of C as CaCO₃ which operate over long time-scales (IPCC, 2001). Values for pools with superscripts ^b and ^a were sourced elsewhere (Denman et al., 1996, US-DOE, 2008), respectively.

Figure 1.1 shows the storages and fluxes for the atmospheric, ocean, land, and geological carbon (C) reservoirs for the natural carbon cycle. The ocean is the largest active pool at 38,000 PgC and land plants the smallest at 500 PgC. A considerable proportion of C is exchanged between the atmosphere and ocean, and between the atmosphere and land pools, with fluxes of 90 PgC year⁻¹ and 120 PgC year⁻¹, respectively (IPCC, 2001). The size of the terrestrial carbon sink at any point in time depends on (i) the magnitude of Net Primary Productivity (NPP), defined as the amount

of organic carbon remaining from the total amount of organic carbon produced by photosynthesis, minus autotrophically respired carbon (IPCC, 2001), (ii) the rate at which NPP is increasing, and (iii) the turnover time of carbon in the system (Kicklighter et al., 1999, White et al., 2000).

1.2 Land use, management practices and soil carbon stocks

Changes in land use and management practices have been highlighted as mechanisms that can reduce the amount of C stored in soils and plant biomass through oxidation of soil organic carbon (SOC) and vegetation decomposition (Wang et al., 2013b, Lal, 2004). Some cultivated soils, for example, have cumulatively lost 30-40 Mg C ha⁻¹, constituting one half to two-thirds of the original SOC (Lal, 2004). Conversion of land use types and adoption of recommended management practices can also result in net C sequestration, as well as providing ecosystem services such as supporting food security, water quality, and agro-industries (Guo and Gifford, 2002, Murty et al., 2002, Lal, 2004, Yan et al., 2012, Lal, 2013), and reduce emissions of the greenhouse gas methane (Shrestha et al., 2013).

Grassland and woodland land uses are a central theme in this thesis since they represent important land uses in the UK. Temperate grassland soils have been estimated to contain 33100 g OM m⁻², or 12% of the Earth's SOM (Schlesinger, 1977) and with improved management, such as earthworm introduction, conversion from cultivation to pasture, introduction of legumes, and improved grass species, can be a significant carbon sink (Conant et al., 2001). Species of deep rooted grasses such as *Andropogon gayanus* and *Brachiaria humidicola* can increase carbon sequestered deep in the soil due to high root production and store most of their C in soils where turnover is relatively slow (Fisher et al., 1994). However, tropical pastures subjected to seasonal drought and overgrazing have been demonstrated to be a strong carbon source (261 g C m⁻²), whereas tropical afforestation was a strong sink, sequestering 442 g C m⁻² (Wolf et al., 2011). Soils under coniferous plantations have also been shown to sequester 10⁵ g C m⁻² year⁻¹ down to a depth of one metre (Chapman et al., 2013).

In enhancing soil C sequestration, the aim is to: increase SOC density in the soil, improve SOC depth distribution, and stabilize SOC in a recalcitrant form with a long turnover time or encapsulate it within micro-aggregates to protect it physically from microbial activity (Lal, 2004). Association of SOC with minerals has been identified as

the most important factor in its stabilisation, irrespective of land use, vegetation, and soil type (Schrumpf et al., 2013). Carbon sequestration in soils to mitigate anthropogenic CO₂ emissions is finite in magnitude and duration and is therefore a short term strategy to combat global warming (Lal, 2004).

1.3 The importance of lignin in the carbon cycle

After cellulose, lignin is the second most abundant biopolymer in the biosphere (Boerjan et al., 2003) and the most abundant renewable natural aromatic material on Earth (Kirk and Farrell, 1987), with an estimated global pool size of 3×10^{14} kg (Whittaker and Likens, 1975). Its roles within plants is integral to plant cell wall structure (figure 1.2) (Chabannes et al., 2001), plant stem strength (Jones et al., 2001), restricts microorganism attack on plant polysaccharides and plant disease resistance (Crawford, 1981). It comprises 18-35% of the dry weight of vascular plants such as angiosperms, gymnosperms, and monocotyledons (Pometto III and Crawford, 1986), where it is estimated to constitute a pool of 1.75×10^{14} kg (Hedges et al., 1997), thus forming a considerable organic input into soils.

Traditionally, lignin was perceived to be a recalcitrant component of soil organic matter (SOM), where its decomposition was regarded as the rate limiting step in the biospheric carbon-oxygen cycle (Crawford, 1981). Some research suggests accumulation and stabilisation of a part of lignins in soils (Rasse et al., 2006, Thevenot et al., 2010). Other studies indicate that lignin degradation may be more rapid in mineral soils than degradation of bulk SOC, alkanolic acids, *n*-alkanes, Gram-positive phospholipid fatty acids, proteins, and total saccharides (Gleixner et al., 2002, Dungait et al., 2008, Schmidt et al., 2011). In arable soils, lignin did not accumulate within the refractory C pool compared to more labile SOC fractions, whereas polysaccharides of microbial origin were stabilised long term (Kiem and Kogel-Knabner, 2003). Alkyl structures were selectively preserved over phenols in dystric cambisol B horizons (Rumpel et al., 2002). This body of conflicting evidence brings into question the potential of soil to capture and store C in the form of lignin or lignin-derived compounds.

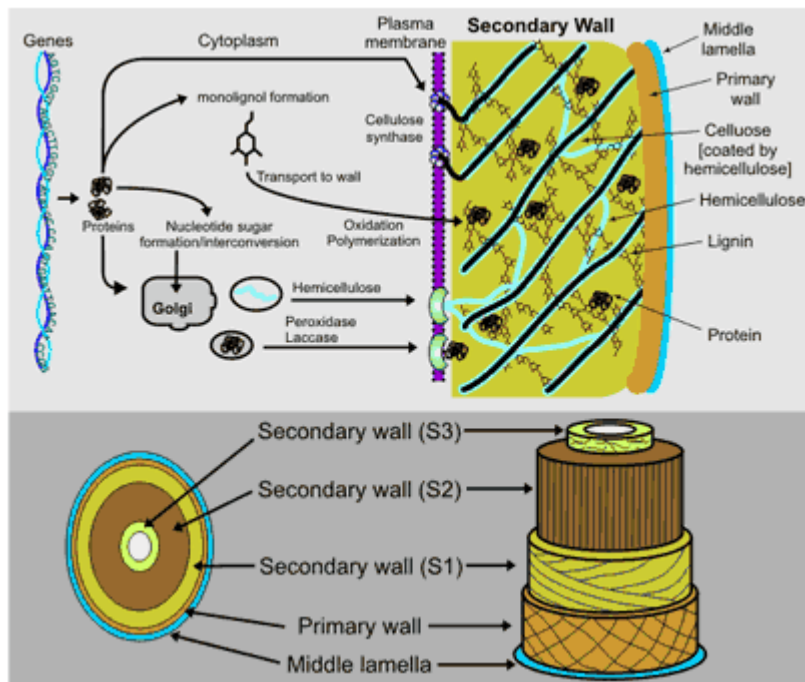


Figure 1.2. The secondary cell wall in plant cells (www.ccrcc.uga.edu/~mao/intro/outline.htm).

1.4 Lignin chemistry and biosynthesis

Lignin is a polymer consisting of 4-hydroxyphenylpropanoid units (Ralph et al., 2004), forms an essential component of higher vascular plants (Leo and Barghoorn, 1970, Faix et al., 1987) and is virtually absent in all other organisms. Vascular plants almost exclusively grow on land, allowing lignin-derived compounds to be used as geochemical biomarkers of terrestrial plant input (Ertel et al., 1986).

The lignin macromolecule is principally made up of three monolignols: *p*-coumaryl alcohol, coniferyl alcohol, and sinapyl alcohol (Freudentberg, 1965) that are biosynthesized from phenylalanine (Boerjan et al., 2003) (figure 1.3).

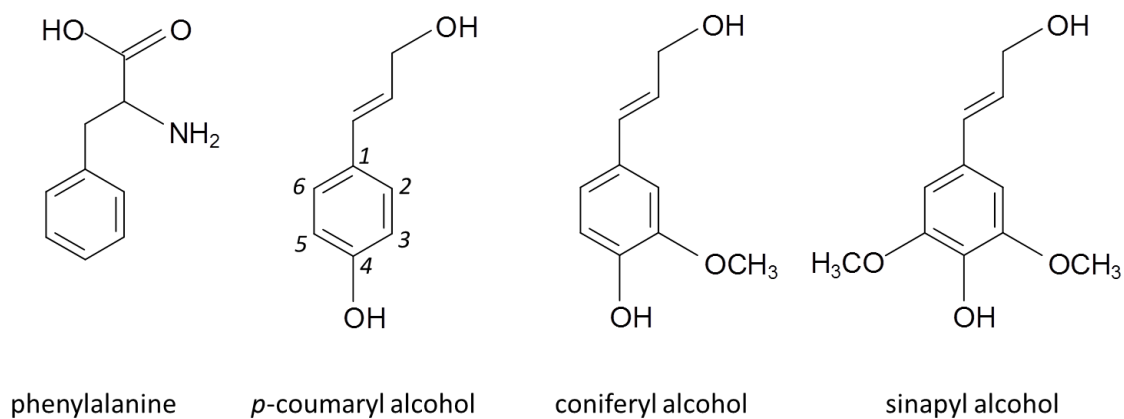


Figure 1.3. Molecular structures of the monolignol precursor phenylalanine, and three monolignols: *p*-coumaryl alcohol, coniferyl alcohol, and sinapyl alcohol.

They are transported to the cell secondary wall (figure 1.2) before being oxidised to phenoxy radicals by abstraction of a hydrogen atom, and polymerised (Christensen et al., 2000) to produce *p*-hydroxyphenyl (P), guaiacyl (G), and syringyl (S) units when incorporated into the macromolecule (Boerjan et al., 2003). P phenols have a hydroxyl group at position 4 of the phenyl ring, e.g. *p*-coumaryl alcohol (figure 1.3), G phenols have a methoxy group at position 3 of the phenyl ring in addition to a hydroxyl group at position 4, e.g. coniferyl alcohol (figure 1.3), and S phenols have a methoxy group at positions 3 and 5 of the phenyl ring together with a hydroxyl group at position 4, e.g. sinapyl alcohol (figure 1.3). P, G, and S phenols within the lignin macromolecule also have a three carbon side chain, attached at position 1 of the phenyl ring. The main lignification reactions are radical coupling reactions where monomer units are added on to the end of the existing chain, to generate a 600-1000 kDa macromolecule (Kirk and Farrell, 1987). The most common linkage between monomer units is the β -O-4 linkage (Boerjan et al., 2003)(figure 1.4). Coupling reactions between lignin oligomers results in 5-5 and 5-O-4 as well as β -5, β - β , and β -1 linkages. The relative contribution of specific monomers during the polymerization process affect the relative abundance of the different inter-unit linkages (Boerjan et al., 2003).

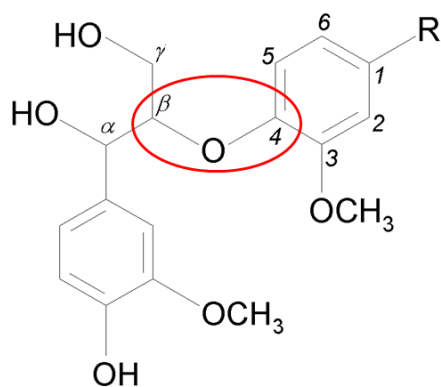


Figure 1.4. The β -O-4 linkage between lignin monomer units, highlighted in red. R = the continuation of the lignin biopolymer.

The sequence of individual lignin monomer units was considered random, described as fortuitous in spruce lignin (Freudenberg, 1965). Later research revealed that plant cells carefully control the supply of monolignols, the conditions in the wall for polymerization, and monolignol radical-generating ability. This indicated a combinatorial rather than random mechanism that is highly evolved, allowing plants to adapt when subjected to various environmental stresses (Ralph et al., 2004). The amount and composition of lignins can differ within taxa, cell types, and individual cell wall layers, and can be modified by developmental and environmental cues (Campbell and Sederoff, 1996).

Recent research has identified two lignin configurations in the secondary cell wall of spruce wood according to the proportion of xylan and glucomannan carbohydrates they are bonded to: lignin bound principally to xylan has a linear configuration of monomer units, almost exclusively connected via β -O-4 alkyl-aryl ether links (figure 1.5A). Lignin principally bonded to glucomannans forms a more branched configuration (figure 1.5B) containing all of the substructures found in softwood lignin (Lawoko et al., 2005, Gellerstedt, 2007, Chen and Sarkanen, 2010). The remaining lignin has been identified as galactoglucomannan-lignin (8%), and glucan-lignin (4%) (Gellerstedt, 2007). This indicates a controlled mechanism, such as a template polymerisation mechanism where lignin primary structure is replicated by noncovalent interactions controlling lignol radical placement before coupling (Chen and Sarkanen, 2010).

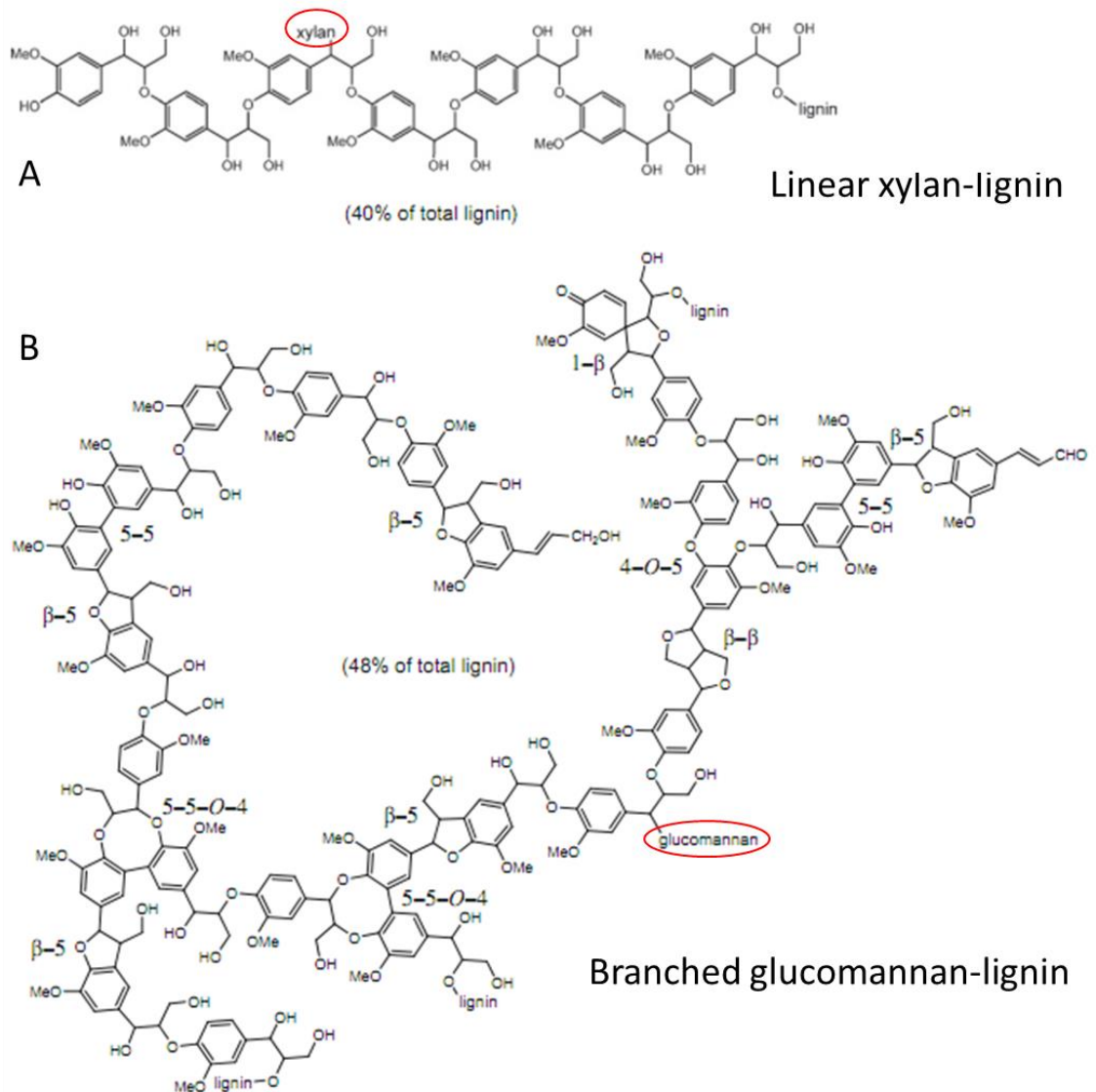


Figure 1.5. The two lignin configurations found in the secondary cell wall of spruce wood. Lignin bound principally to xylan has a linear configuration (A). Lignin principally bonded to glucomannans form a more branched configuration (B) (Chen and Sarkanen, 2010, Gellerstedt, 2007).

All lignins contain traces of incompletely biosynthesized monolignols or other units derived from side reactions that occur during biosynthesis (Ralph et al., 2001). Boerjan et al (2003) suggest that all of the acylated lignins: (*p*-hydroxybenzoates in poplars, palms, and willows; *p*-coumarates in all grasses; and acetates in palms and kenaf, as well as small amounts in several hardwoods) derive from acylated monolignols (See figure 1.6 for structures). Also, cinnamyl, benzyl aldehyde groups are always detected in lignins, although it is not clear whether these derive from aldehydic monomers being incorporated into the lignin polymer or post-lignification oxidation (Boerjan et al., 2003).

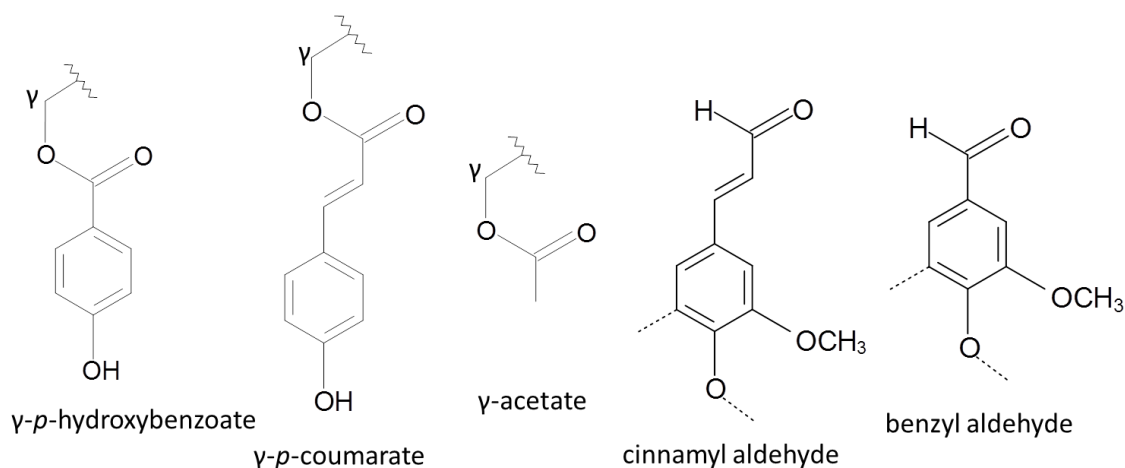


Figure 1.6. Molecular structures of incompletely biosynthesized monolignols.

1.5 Lignin degradation

Lignin enters the soil from aboveground litter such as shoots and leaves, or belowground litter from the root system (Abiven et al., 2005, Feng and Simpson, 2007). Roots are more lignified than the aerial parts of the same plant (Fernandez et al., 2003, Rasse et al., 2005). Research has shown that the mean residence time of root derived C is 2.4 times that of shoot derived C (Rasse et al., 2005).

Lignin degradation is related to: the nature of the vegetation and land use; climate, including mean annual temperature; and soil acidity, which could affect fungal activity (Thevenot et al., 2010). Optimal degradation is reported between pH 4 to 4.5 (Kirk et al., 1978), and pH 6.5 for the mineralization of lignin by *Streptomyces*, and pH 8.5 for optimum lignin solubilisation (Pometto III and Crawford, 1986). Lignin concentration in soils, as a proportion of SOC, generally decreases from the litter to the A horizon and with increasing depth in the subsoil (Guggenberger and Zech, 1994). However, in Sitka spruce soils increasing concentrations with depth, and passing through a maximum, are attributable to land preparation practices (Mason et al., 2009). Lignin degradation results in a decrease in total lignin through mineralization, structural transformations into non-lignin products, and incorporation into SOM (Thevenot et al., 2010). Thevenot, et al (2010) suggest that a part of lignins accumulate and become stabilized in soils, particularly the clay fraction, due to lignin-clay binding (Grunewald et al., 2006).

It has been proposed that antioxidants such as phenols present in soils protecting SOM from oxidation by scavenging the reactive free radicals and terminating the oxidative

chain reaction (Rimmer, 2006). There is evidence that lignin phenols are important contributors to the antioxidant capacity (AOC) of soils (Rimmer and Abbott, 2011). This was supported by other work that quantified the electron donating capacities of natural organic matter by a mediated electrochemical oxidation (Aeschbacher et al., 2012). These lignin phenols were more recently identified using pyrolysis-field ionisation mass spectrometry (Py-FIMS) as one of a number of classes of molecules that contribute to the AOCs of a range of UK soils (Schlichting et al., 2013). Antioxidant molecules will terminate the free radical chain reactions and thereby inhibit oxidation processes.

Lignin is susceptible to transport in water, in which case, degradation increases progressively along the following sequence: plant material, coarse suspended sediment, fine suspended sediment, and into the dissolved phase (Ertel et al., 1986).

As well as biotic lignin degradation, discussed more in section 1.6, lignin also degrades abiotically, e.g. photochemically, where greater photodegradation rates in litter has been observed at higher lignin concentrations (Austin and Ballare, 2010). Photochemical lignin degradation also occurs in dissolved organic matter (DOM), where for example, in the Mississippi River water, 75% of the total dissolved lignin was lost in a 28 day incubation study in sunlight. At the start of the same study, 90% of the dissolved lignin was high molecular weight (>1000 Dalton (Da)), and at the end of the incubation 80% of the remaining lignin was low molecular weight (<1000 Da). However, dissolved lignin >1000 Da from the equatorial Pacific Ocean was resistant to photooxidation. The authors concluded that under photodegradative conditions, abiotic degradation can be the dominant driver, where lignin is selectively degraded as it absorbs UV and visible light over a wide range of wavelengths (Opsahl and Benner, 1998). Another study investigating Mississippi River plume water revealed that at water salinities <25 psu, dissolved lignin concentrations were mostly affected by flocculation and microbial degradation. Photooxidation was a dominant driver controlling lignin concentrations and compositions at salinities >25 psu, where microbial degradation rate of dissolved lignin was approximately 30% that of photooxidation rates in surface waters in a 10 day incubation experiment (Hernes and Benner, 2003).

1.5.1 Lignin degrading microorganisms and enzymes

Lignin degradation is mainly biotic, aerobic, and cometabolic. Its initial biodegradation is oxidative, nonspecific, and extracellular due to its large molecular size,

nonhydrolyzability, and molecular complexity (Kirk and Farrell, 1987). The few organisms able to degrade lignin include: (i) some bacteria belonging to the genera *Pseudomonas* and *Flavobacterium* (Sorensen, 1962); (ii) actinomycetes such as *Streptomyces* spp.; and (iii) fungi, particularly basidiomycetes brown-rot and white-rot fungi, with the white-rot variety able to degrade the macromolecule more rapidly and extensively than any other microorganism (Kirk and Farrell, 1987), and able to fully oxidise it to CO₂ and H₂O (Crawford, 1981). *Pleurotus ostreatus*, a white-rot fungus, has been shown to degrade lignin within 7 to 63 days (Vane et al., 2001b, Robertson et al., 2008b). In addition, species of ascomycetes and Fungi Imperfecti lead to soft-rot wood decay, although polysaccharides are selectively degraded over lignin (Kirk and Cowling, 1984).

Lignin biodegradation is carried out by extracellular enzymes such as lignin peroxidase (ligninase), manganese peroxidase, and laccase released by the aforementioned microorganisms (Glenn et al., 1983, Tien and Kirk, 1983, Higuchi, 2004). Lignin peroxidase oxidises susceptible aromatic substrates by one electron, producing an unstable cation radical, which subsequently undergoes various nonenzymatic reactions. The manganese peroxidase enzyme oxidises Mn(II) to Mn(III) which then oxidises the organic substrate. Laccases catalyze the one-electron oxidation of phenols generating phenoxy radicals, and later transferring four electrons to O₂ (Kirk and Farrell, 1987). Lignin is also degraded in the guts of wood-feeding insects such as the Asian longhorned beetle (*Anoplophora glabripennis*) and Pacific dampwood termite (*Zootermopsis angusticollis*) where oxidation of propyl side chain, and demethylation of ring methoxyl groups was detected (Geib et al., 2008).

1.6 Chemistry of lignin degradation

White-rot fungi simultaneously degrade lignin, cellulose, and hemicellulose in the plant cell wall (Geib et al., 2008). Analysis of lignin in wood degraded by white-rot fungi (*Phanerochaete chrysoaporium*) revealed that the reactions involve aromatic ring cleavage, oxidation of α and γ hydroxyl groups, oxidative cleavage of C α -C β and C β -C γ bonds and demethylation (Chen et al., 1983). Brown-rot fungi degrade the cellulose and hemicellulose with minor alteration to lignin (Green and Highley, 1997), with an increase in aromatic hydroxyl groups through a net demethylation (Kirk and Adler,

1969, Kirk et al., 1970). This results from demethoxylation or methoxyl demethylation (Filley et al., 2000) (figure 1.7).

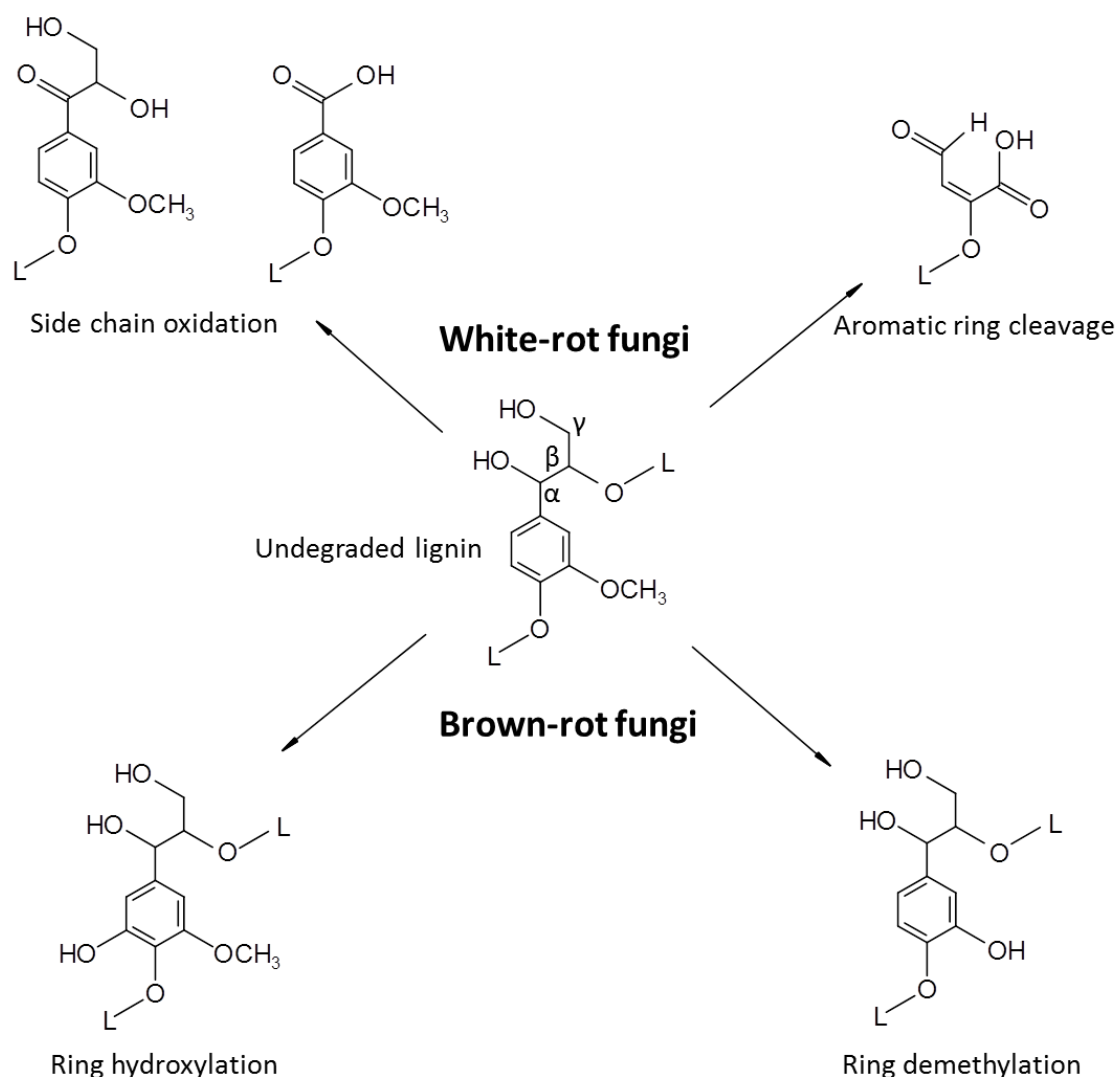


Figure 1.7. Principal lignin degradation reactions by white-rot (side chain oxidation and aromatic ring cleavage) and brown-rot fungi (ring hydroxylation and ring demethylation). Figure is modified from Filley, et al. (2000) and Geib, S. et al. (2008).

Natural lignin ($\delta^{13}\text{C}$ -12‰) incorporation into native lignin phenols in agricultural soils ($\delta^{13}\text{C}$ -30.2 to -36.3‰) has been studied at the compound specific level under C3-C4 crop succession (Dignac et al., 2005, Bahri et al., 2006), and in dung-lignin ($\delta^{13}\text{C}$ -12.6‰) incorporation into soil ($\delta^{13}\text{C}$ -30.3‰) (Dungait et al., 2008). Bahri et al (2006) observed that the rate of maize-derived lignin phenol (C4) incorporation into C3 soil varied between different lignin phenols, i.e. that lignin turnover in soils is monomer specific (figure 1.8).

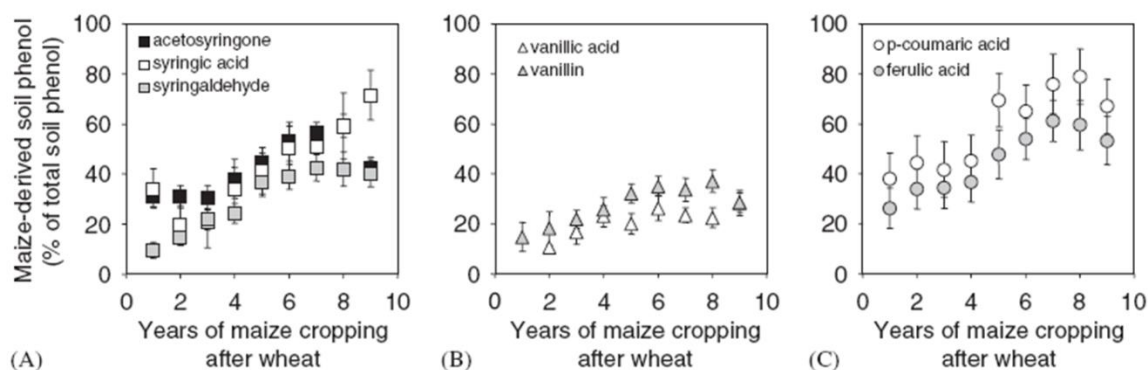


Figure 1.8. Incorporation rates of S (plot A), V (plot B), and C (plot C) maize-derived lignin phenols into soil through time (Bahri et al., 2006).

Figure 1.8 shows how Bahri et al (2006) determined that maize-derived vanillic acid (G6, see figure 1.10 for structures), vanillin (G4), *p*-coumaric acid (P18), ferulic acid (G18), acetosyringone (S5), and syringaldehyde (S4) phenols were incorporated into soil lignin OC fastest during the first six years before reaching a plateau, whereas syringic acid increased to year 9. Cinnamyl (C) phenols, defined as *p*-coumaric (P18) and ferulic acids (G18), derived from maize always constituted the highest proportion of monomer units, and vanillyl (V) the lowest. Variation in monomer turnover rate was attributed to: the localisation of specific lignin monomer types in plant tissues; and the greater resistance of V over syringyl (S)-types due to more cross-linked coupling between V phenols at the aromatic C5 position. Bahri et al (2006) also determined that within C, V, and S phenols, the side chain structure also influenced turnover kinetics: aldehyde groups on V phenols turned over faster than the corresponding carboxylic acid, whereas for S phenols the opposite was observed. Accumulation of phenols from most to least rapid was: *p*-coumaric acid = syringic acid > acetosyringone > ferulic acid > syringaldehyde > vanillin > vanillic acid (Bahri et al., 2006).

Dungait et al. (2008) observed that after 372 days, the proportions of dung-derived 4-vinylphenol (1), syringol (3), 4-vinylguaiacol (7), and the *E* isomer of 4-(2-propenyl)syringol (13) in the 0-1 cm soil horizon had reduced considerably compared with 56 days (figure 1.9), indicating that these phenols degraded relatively rapidly in soils. However, the proportion of dung-derived 4-vinylsyringol (9), and the *E* isomer of 4-(2-propenyl)syringol (12) in soil did not change. The *Z* isomer of 4-(2-propenyl)syringol (12) was much more resistant to degradation than the *E* isomer (13) between days 56 and 372, indicating specific conformations of propenyl side chains is

important for lignin phenol stability in soil (Dungait et al., 2008). Bahri et al. (2006) found that *p*-coumaric acid, which also has an unsaturated C₃ side chain, accumulated most rapidly in soil until year 6.

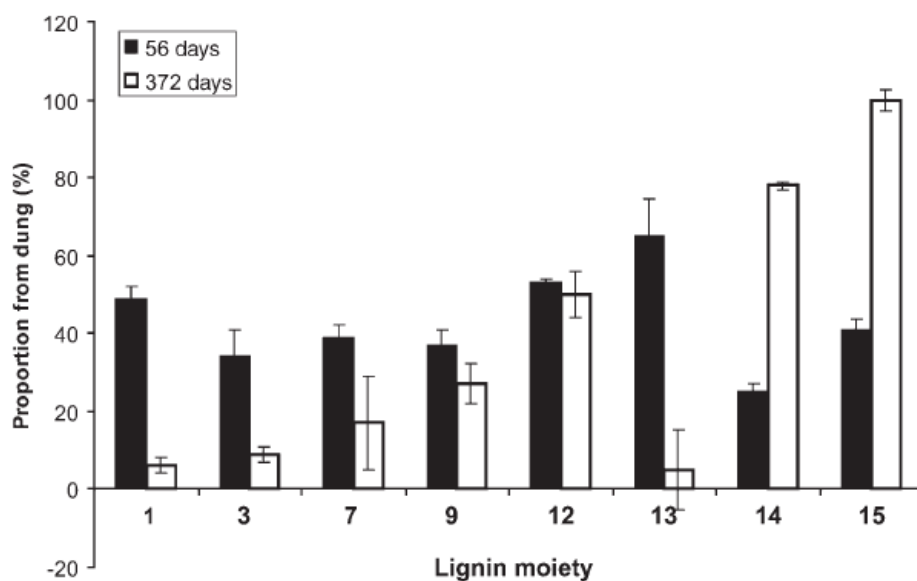


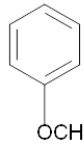
Figure 1.9. Proportion of dung-derived lignin moieties incorporated in the 0-1cm soil horizon beneath C₄ dung pats, 56 and 372 days after dung deposition. 1 = 4-vinylphenol (P3), 3 = syringol, 7 = 4-vinylguaiacol (G3), 9 = 4-vinylsyringol, 12 = 4-(2-*Z*-propenyl)syringol, 13 = 4-(2-*E*-propenyl)syringol, 14 = 4-acetylsyringol (S5), 15 = 4-(2-propanone)syringol (Dungait et al., 2008). The structures of the compound abbreviations in brackets are shown in figure 1.10.

The abundance of 4-acetylsyringol (14) and 4-(2-propanone)syringol (15) in figure 1.9, having oxidised side chains, both increased considerably up to 372 days suggesting that they derive from a resistant source of lignin in the dung (Dungait et al., 2008). Dungait et al. (2008) concluded that individual lignin moieties either: (i) move into soil, (ii) are degraded, or (iii) are diagenetically transformed at different rates.

1.7 Chemical analysis of lignin

In addition to natural degradation, the lignin macromolecule can be broken up using degradative analysis techniques that release lignin phenols by cleaving the β-O-4 bonds (figure 1.4), such as on- or off-line pyrolysis techniques (Faix et al., 1987, Dungait et al., 2008) as well as pyrolysis in the presence of derivatising agents such as tetramethylammonium hydroxide (TMAH) e.g. (Clifford et al., 1995, Filley et al., 1999,

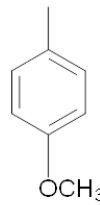
Mason et al., 2009, Mason et al., 2012). CuO oxidation is another commonly used technique to analyse lignin phenols e.g. (Hedges and Ertel, 1982, Wysocki et al., 2008). Lignin phenols released by CuO oxidation include a suite of vanillyl, syringyl, and cinnamyl monomer units, enabling gymnosperm woods, nonwoody gymnosperm tissues, angiosperm woods, and nonwoody angiosperm tissues to be distinguished (Hedges and Mann, 1979a). These lignin source differences were also detected in marine sediments (Hedges and Mann, 1979b). Whilst vanillyl and syringyl units are exclusively derived from lignin, *p*-hydroxyl phenols are also produced from other sources (Benner et al., 1990). Cinnamyl phenols also released are typically bound to lignin via ester linkages (Higuchi et al., 1967). An analogous suite of lignin phenols is released using pyrolysis in the presence of TMAH which are also indicative of vegetation source: gymnosperm tissue generated principally methylated guaiacyl derivatives and methylated carboxyl groups; angiosperm tissue generated methylated guaiacyl and syringyl derivatives; nonwoody angiosperm generated methylated cinnamyl derivatives as well as methylated guaiacyl and syringyl derivatives (Clifford et al., 1995). The names, abbreviation symbol, and molecular structure of the lignin phenols detected in samples analysed in this thesis are reported in figure 1.10.



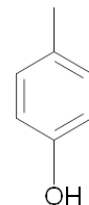
P1
Methoxybenzene



P1*
Phenol



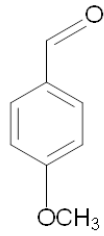
P2
4-methoxytoluene



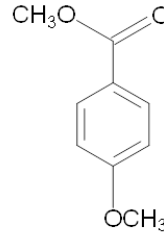
P2*
4-hydroxytoluene



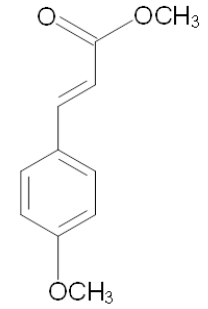
P3
4-methoxybenzeneethylene



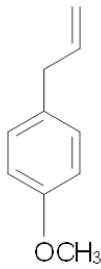
P4
4-methoxybenzaldehyde



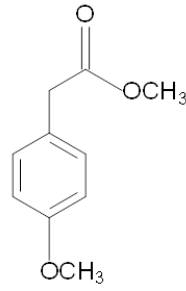
P6
4-methoxybenzoic acid
methyl ester



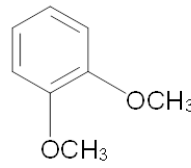
P18
2-propenoic acid, 3-(4-
methoxyphenyl) methyl ester



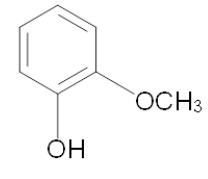
P21
1-(4-methoxyphenyl)-3-
propene



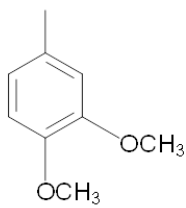
P24
4-methoxybenzeneacetic
acid methyl ester



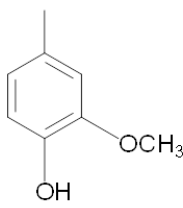
G1
1,2-dimethoxybenzene



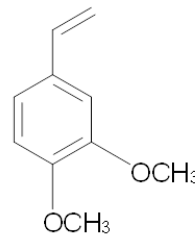
G1*
2-methoxyphenol



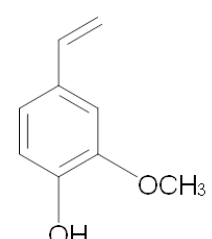
G2
3,4-dimethoxytoluene



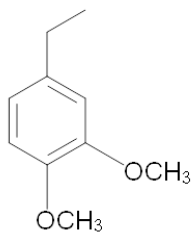
G2*
3-methoxy- 4-hydroxytoluene



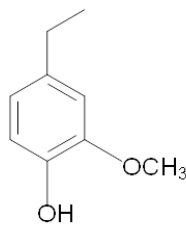
G3
3,4-dimethoxybenzeneethylene



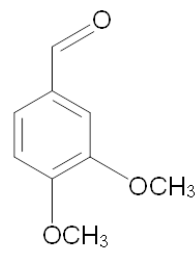
G3*
3-methoxy- 4-hydroxybenzeneethylene



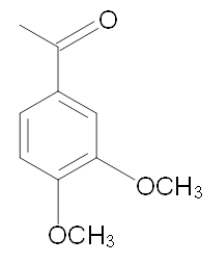
Gx
3,4-dimethoxyethylbenzene



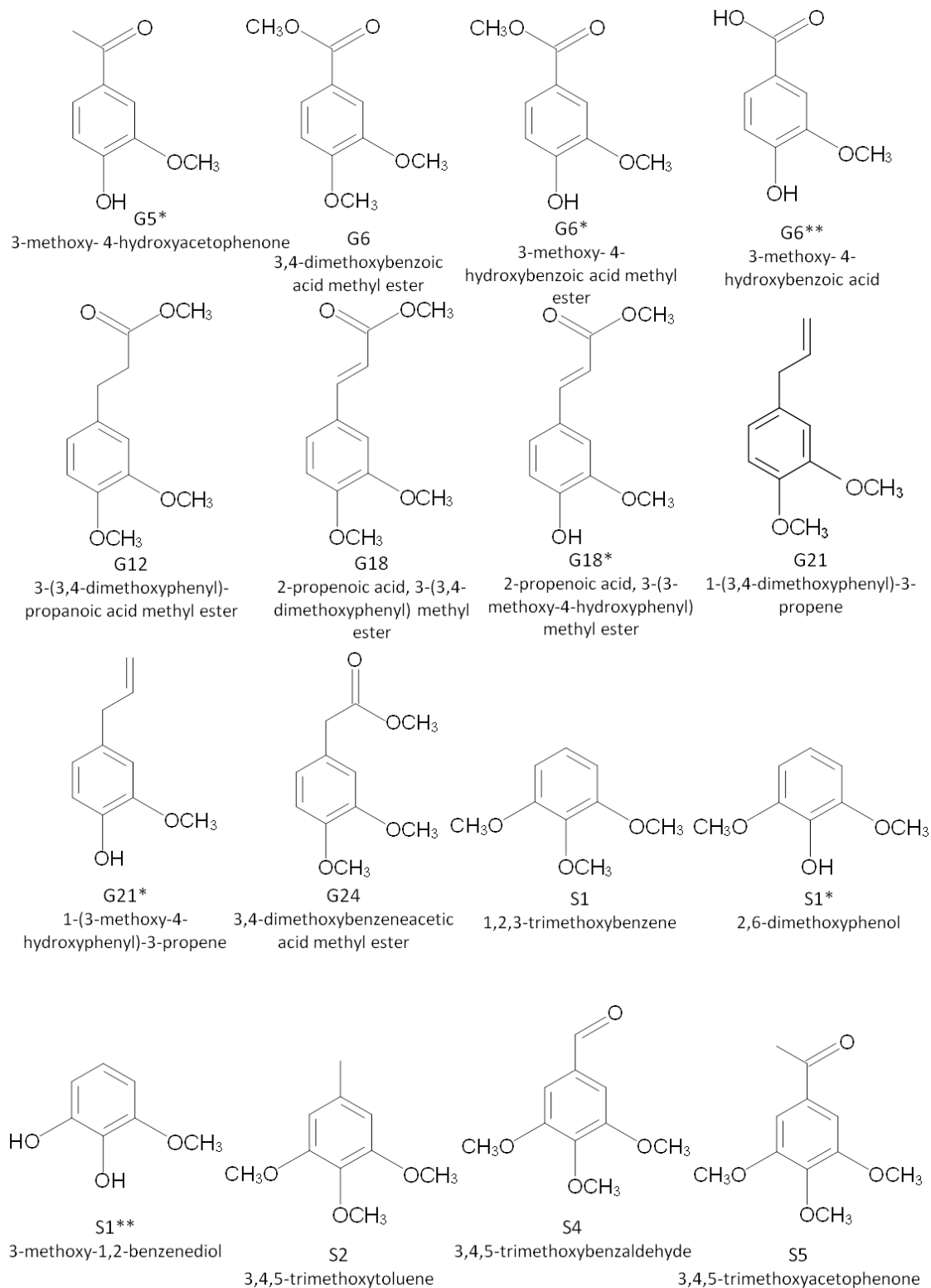
Gx*
3-methoxy- 4-hydroxyethylbenzene



G4
3,4-dimethoxybenzaldehyde



G5
3,4-dimethoxyacetophenone



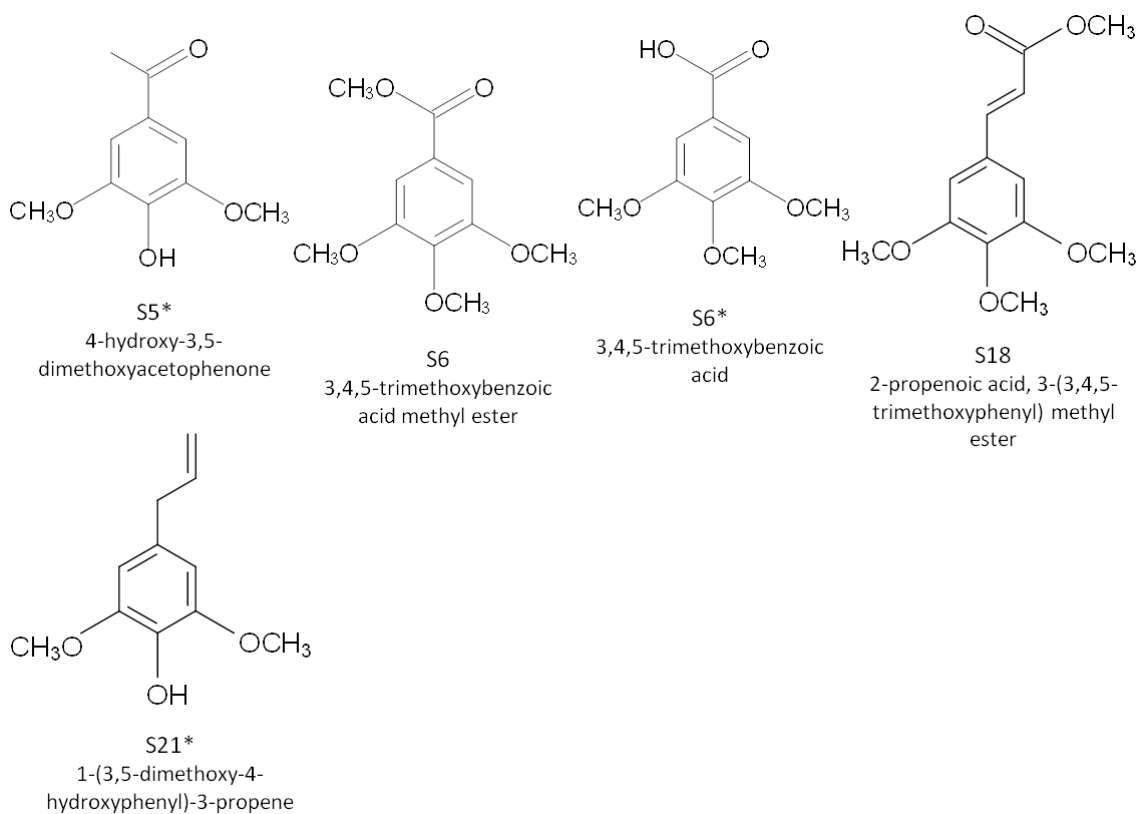


Figure 1.10. Names, abbreviation symbol, and molecular structure of the lignin phenols detected in samples analysed in this thesis.

The release and oxidation of lignin phenols upon degradation in natural environments has therefore led to the development of proxies as a means to determine the lignin source and extent of oxidation (table 1.1).

Table 1.1. Lignin proxies associated with analysis of lignin using thermally assisted hydrolysis and methylation using TMAH, assembled from Nierop and Filley (2007).

Proxy	Description	Use
$\Lambda_{SG}, \Lambda_{SGC}$	The sum of methylated syringyl + guaiacyl (+ cinnamyl) compounds (mg/100 mg OC)	Total lignin concentration
S/G	Ratio of syringyl to guaiacyl lignin phenols, where $S = (S4 + S5 + S6)$, $G = (G4 + G5 + G6)$.	Assess relative angiosperm & gymnosperm input. Indicator of selective S or G degradation (Van der Heijden and Boon, 1994).
C/G	Ratio of cinnamyl to guaiacyl lignin phenol concentrations.	Determine relative input of non-woody lignin
F/P	Ratio of ferulic acid to <i>p</i> -coumaric acid concentrations.	Non-woody angiosperm/non-woody gymnosperm ratio (Hedges & Mann, 1979), marker for root and bark input (Filley et al. 2006)
$Ac/Al_{G(S)}$	Acid-to-aldehyde ratio for guaiacyl and syringyl units. $G6/G4$ or $S6/S4$, respectively	Relative decomposition state proxy
$\Gamma_{G(S)}$	Concentration of G(S)6 divided by the sum of G(S)14 and G(S)15.	Indicator of lignin side chain shortening

Proxies such as Ac/Al and I , which can be used to monitor fungal degradation of lignin (Robertson et al., 2008a), and F/P ratios (table 1.1) can be distorted by non-lignin sources such as gallic acid from tannins, protocatechuic acid, and caffeic acid which are more water soluble and therefore more transportable than lignin polymers. Such distortions have been observed in soil lower C horizons, although they can be corrected for using ^{13}C -labelled TMAH (Nierop and Filley, 2007).

1.8 The formation and structure of soils

Soil is a material composed of minerals, gases, water, organic substances, and animals such as macrofauna (>2 mm), mesofauna (0.1-2 mm), and microfauna (<0.1 mm). Soil formation is governed by: parent materials, climate, biota, topography, and time. A soil is the product of destructive and creative processes that lead to the development of soil layers or horizons, generally aligned parallel to the land surface. The horizons form as a result of influences such as plant material, air, water, and solar radiation at the soil-atmosphere interface (figure 1.11) (Brady and Weil, 2008).

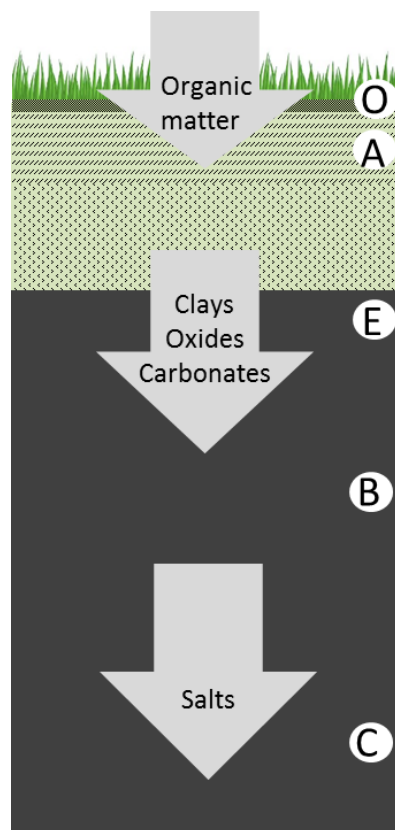


Figure 1.11. Development of soil horizons as materials are added to the upper part of the profile and other materials translocated to deeper zones (Brady and Weil, 2008).

O horizons constitute organic materials formed from fallen leaves and other plant and animal remains that accumulate on the soil surface, that undergo physical and biochemical degradation. Soil fauna and percolating water moves some of these organic materials downward to mix with underlying mineral grains. A horizons are dominated by mineral particles although darkened by the accumulation of organic matter. An E horizon may be present in some soils underlying the A horizon, which is an intensely weathered and leached layer that has not accumulated organic matter. B horizons contain relatively less organic matter than the overlying E, A, and O horizons, containing silicate clays, aluminium and iron oxides, gypsum, or calcium carbonate. These minerals may have been transported down the soil profile or formed in situ. C horizons may form below B horizons where plant roots and microorganisms may change the water chemistry and biochemically alter the soil (figure 1.11) (Brady and Weil, 2008).

1.9 Dissolved organic matter

Dissolved organic matter (DOM) is defined as consisting of organic molecules of varying sizes up to 0.45 μm (Michalzik and Matzner, 1999, Kalbitz et al., 2000), originating from decomposed plant litter, SOM, microbial biomass, and root exudates (Kalbitz et al., 2000). Research suggests that it constitutes the most bioavailable carbon source as soil microorganisms are aquatic and microbial assimilation mechanisms require an aqueous environment (Marschner and Kalbitz, 2003). Later research suggests that plant-derived carbohydrates were easily degradable and aromatic compounds, such as those from lignin, form the most stable components of DOM (Kalbitz and Kaiser, 2008). Observed soil DOM concentrations or flux is the net result of processes that release DOM (e.g. leaching from litter, desorption from solids) and those that remove DOM (e.g. adsorption, decomposition). These processes are influenced by factors such as: amount of litter, land use, microbial activity and community composition, Fe- and Al-oxides/hydroxides, clay, solution pH, ionic strength, phosphate, polyvalent cations, temperature, precipitation, and land management practices, e.g. clear felling, liming, and organic fertilization (Kalbitz et al., 2000).

Previous research indicates that sorption of labile DOM, comprising carbohydrates and low molecular weight fatty acids, to soil mineral horizons doubles the portion of stable C, and that sorption of recalcitrant DOM, high in aromatics, increased its stability by

20%. Furthermore, stable DOM sorbed much more readily than labile DOM, suggesting that selective sorption of stable compounds to the mineral soil with strong chemical bonds and/or physical inaccessibility of OM to microorganisms are key DOM stabilisation mechanisms (Kalbitz et al., 2005). Later research discovered that between 20 – 55 Mg C ha⁻¹ was DOM-derived in the mineral soil of a haplic podzol, representing 19 – 50% of the total soil C. The mean residence time of DOM from the Oa horizon increased from < 30 years to > 90 years after sorption, indicating that DOM contributes to storage of stable C in soil (Kalbitz and Kaiser, 2008).

DOM has been categorised into mobile- and immobile organic matter (OM) depending on the soil pore volume size it occupies. Mobile OM is chiefly present in pore sizes > 0.2 µm and transportable convectively by seepage. Immobile OM occupies smaller pores (< 0.2 µm), is only transportable by diffusion, and is inaccessible to bacteria or plant roots (Zsolnay, 1996).

Whilst biotic factors and environmental conditions largely control DOC concentrations, hydrological conditions are more important in terms of DOC fluxes, particularly at increasing time scales (Kalbitz et al., 2000). Riverine DOC has a weighted worldwide concentration of 5.75 mg C litre⁻¹ and exports around 6 (± 4) × 10¹⁴ g C yr⁻¹ to the oceans (Meybeck, 1982).

1.10 Dissolved lignin

DOC comprises lignin phenols, carbohydrate-derived compounds, protein-derived compounds, fatty acids and *n*-alkanes (Christman and Ghassemi, 1966, Lytle and Perdue, 1981, Guggenberger and Zech, 1994, Frazier et al., 2003), with lignin constituting between 4.6 – 15% of products of DOC analysed using TMAH thermochemolysis (Frazier et al., 2003).

Dissolved lignin phenol concentrations and fluxes have been investigated in coniferous forest ecosystems from bulk and forest canopy precipitation as lignin input into the forest floor (table 1.2), equating to a flux of 12.8 and 15.0 kg ha⁻¹ year⁻¹ at Wülfersreuth and Oberwarmensteinach forests, respectively. Decreasing dissolved lignin phenol concentrations were observed with increasing soil depth between the mineral soil input and output, attributed to sorption to the soil matrix rather than biodegradation since the acid/aldehyde ratios did not alter with depth (table 1.2). This represents mineral soil input fluxes of 28.6 and 32.0 kg ha⁻¹ year⁻¹, decreasing with depth to mineral soil output fluxes of 0.18 and 0.31 kg ha⁻¹ year⁻¹ at Wülfersreuth and Oberwarmensteinach forests,

respectively (Guggenberger and Zech, 1994). They also observed that highly carboxylated lignin-derived substances selectively entered the soil solution, and concluded that the extent of lignin oxidation controls its solubilization (Guggenberger and Zech, 1994).

Table 1.2. mean dissolved lignin vanillyl (V) and cinnamyl (C) phenol concentrations and vanillyl acid/aldehyde ratios $(ac/al)_v$ in compartments at Wülfersreuth and Oberwarmensteinach forest sites (Guggenberger and Zech, 1994).

Compartment	Wülfersreuth		Oberwarmensteinach	
	V + C (mg C g ⁻¹ DOC)	$(ac/al)_v$	V + C (mg C g ⁻¹ DOC)	$(ac/al)_v$
Bulk precipitation	3.3	0.7	3.5	0.9
Canopy precipitation	8.6	0.8	7.6	0.7
Mineral soil input	9.2	1.2	8.9	1.1
B horizon solution (30 cm)	2.1	1.1	1.5	1.1
Mineral soil output (90 cm)	1.6	1.1	1.3	1

Lignin phenols have been detected in fresh, estuarine and marine waters (Louchouart et al., 2000, Frazier et al., 2003), in deep ocean DOM (Opsahl and Benner, 1997, Opsahl et al., 1999), and in stalagmites (Blyth and Watson, 2009), allowing them to be used as molecular tracers of terrestrial OM input, and to determine the fate of riverine DOC in estuaries and oceans (Ertel et al., 1986). Approximately 1% of DOM in seawater is terrigenous-derived as estimated using carbon-normalised lignin phenol yields and $\delta^{13}C$ measurements (Hernes and Benner, 2002). Increasing total lignin phenol concentrations with increasing depth were observed in the North Pacific ocean, ranging between 1.3 – 5.6 $\mu\text{g (100 mg OC)}^{-1}$ for the LMW (< 1 nm) fraction, and 5.7 – 35 $\mu\text{g (100 mg OC)}^{-1}$ for the HMW (1-100 nm) fraction from surface to intermediate water (approx. 750 m depth). This increase with depth was attributed to riverine input. Particulate organic carbon (POC, 0.1-60 μm) concentrations ranged from 58 – 469 $\mu\text{g (100 mg OC)}^{-1}$ to a depth of 2500 m (Hernes and Benner, 2002).

1.11 Lignin transport

Figure 1.12 presents the ‘lignin cycle’ as a component of the carbon cycle, summarizing the extent of our current knowledge of the size of global lignin pool, lignin phenol concentrations within compartments, and fluxes.

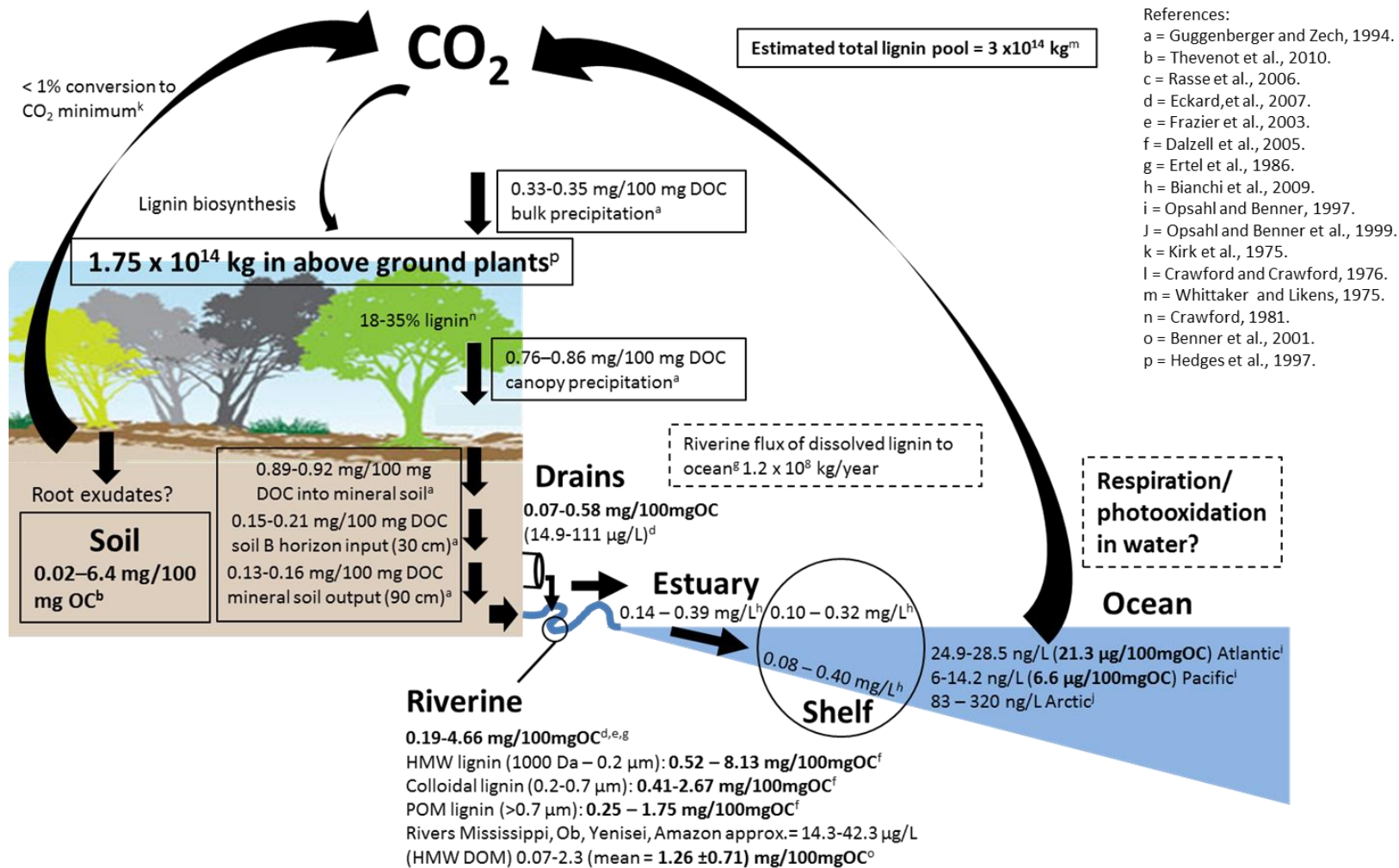


Figure 1.12. The lignin cycle, as a component of the carbon cycle. Lignin pools and concentrations are in solid boxes, fluxes in dashed-line boxes.

Of the total global lignin pool, estimated at 3×10^{14} kg (Crawford, 1981), the largest single lignin pool, constituting an estimated 1.75×10^{14} kg, is in above-ground plants (Hedges and Oades, 1997). Once lignin enters the soil and is exposed to the processes of decomposition, solubilisation, and transport, it is present in concentrations ranging between $0.02 - 6.4$ mg $(100 \text{ mg OC})^{-1}$ (Thevenot et al., 2010). Previous research indicates that as a minimum, less than 1% of lignin in some forest soils can be oxidized to CO_2 (Kirk et al., 1975).

Lignin fluxes of 2.6 and $3.1 \text{ kg ha}^{-1} \text{ year}^{-1}$ were observed into the forest ecosystem from bulk precipitation at Wülfersreuth and Oberwarmensteinach coniferous forests, respectively, which entered the forest floor as canopy precipitation with fluxes of 12.8 and $15.0 \text{ kg ha}^{-1} \text{ year}^{-1}$, respectively (Guggenberger and Zech, 1994). In a mixed broadleaved woodland, comparable bulk precipitation fluxes of $2.69 \text{ kg ha}^{-1} \text{ year}^{-1}$ were estimated (McDowell and Likens, 1988). Guggenberger and Zech (1994) measured lignin fluxes of 28.6 and $32.0 \text{ kg ha}^{-1} \text{ year}^{-1}$ into the mineral soil at Wülfersreuth and Oberwarmensteinach forests respectively, translating into fluxes of 0.43 and $0.89 \text{ kg ha}^{-1} \text{ year}^{-1}$ as soil B horizon input. In the mixed broadleaved woodland, estimated fluxes of total hydroxylated aromatics (lignin and tannin) were $35.4 \text{ kg ha}^{-1} \text{ year}^{-1}$ into the mineral soil, $5.12 \text{ kg ha}^{-1} \text{ year}^{-1}$ in the upper B horizon, reducing to $1.41 \text{ kg ha}^{-1} \text{ year}^{-1}$ at 30 cm depth in the B horizon, and $1.67 \text{ kg ha}^{-1} \text{ year}^{-1}$ in stream water within the catchment (McDowell and Likens, 1988).

Riverine lignin concentrations for $< 0.2 \mu\text{m}$ range from $0.19 - 8.13 \text{ mg (100 mg OC)}^{-1}$ (Ertel et al., 1986, Frazier et al., 2003, Dalzell et al., 2005, Eckard et al., 2007), colloidal ($0.2 - 0.7 \mu\text{m}$) concentrations range between $0.41 - 2.67 \text{ mg (100 mg OC)}^{-1}$, and particulate lignin ($> 0.7 \mu\text{m}$) between $0.25 - 1.75 \text{ mg (100 mg OC)}^{-1}$ (Dalzell et al., 2005) (figure 1.9). Estuarine and shelf dissolved lignin concentrations have been detected as $0.14 - 0.39 \mu\text{g L}^{-1}$, and surface and bottom dissolved lignin concentrations ranged between $0.10 - 0.32 \text{ mg L}^{-1}$ and $0.08 - 0.4 \text{ mg L}^{-1}$ (Bianchi et al., 2009). Dissolved lignin concentrations in the ocean varied widely between oceans: $24.9 - 28.5 \text{ ng L}^{-1}$ in the Atlantic Ocean, $6 - 14.2 \text{ ng L}^{-1}$ in the Pacific Ocean (Opsahl and Benner, 1997), and $83 - 320 \text{ ng L}^{-1}$ in the Arctic Ocean (Opsahl et al., 1999).

1.12 Fate of lignin in aquatic systems

Dissolved lignin can be reduced from higher (> 1000 Da) to lower (< 1000 Da) molecular weight due to photooxidation, which has been observed in river waters, although high molecular weight lignin in Pacific Ocean waters was highly resistant to photooxidation (Opsahl and Benner, 1998). Research indicates that the CO_2 emitted from riverine and shelf waters to the atmosphere from bacterial degradation of riverine floodwater DOC was of terrestrial origin. The authors concluded that flooding leads to rapid transfer of soil carbon to the atmosphere via aquatic pathways (Bianchi et al., 2013). When compared with the atmosphere, streams and rivers in the US are supersaturated with CO_2 , and global temperate rivers (between 25 and 50 degrees N) are estimated to emit $0.5 \text{ Pg C year}^{-1}$ to the atmosphere. In addition, CO_2 emissions have been shown to be positively correlated with annual precipitation (Butman and Raymond, 2011).

1.13 Overarching thesis aims

(H_0) The central hypothesis being tested by this thesis was that a significant proportion of lignin in soils is solubilised and lost from the soil by transport in water.

The overarching aim of this project was to understand the contribution of lignin to the soluble fraction of SOC and its delivery to associated watercourses in a range of terrestrial ecosystems by addressing four major questions:

- (1) What is the dominant form of lignin moving through soils and into water courses?
- (2) Does the form of lignin differ between soil, different vegetation and land use types?
- (3) Do lignin decomposition products and concentrations vary seasonally?
- (4) What are the relative rates of lignin phenol transport through the soil?

Chapter 2. General methods

Four experiments are reported in this thesis in separate chapters:

Chapter 3: Methodology comparison study to compare solid phase extraction or freeze drying to extract water borne lignin phenols, and cold on-column GC-FID or TMAH/GC-MS to detect water-borne lignin phenols.

Chapter 4: Leaf litter degradation study which explored the lignin in leachates from different vegetation types and the relationship with temperature.

Chapter 5: Land use study that characterised the lignin phenols in soil organic, A horizons, and associated dissolved phases from grassland, woodland, and moorland ecosystems.

Chapter 6: Lignin transport experiment that used the dissolved fraction of C4 dung to compare relative transport rates of different lignin phenols through soil.

The following chapter describes the methodology used in each of these chapters.

2.1. Sample sites

Coordinates for each sample collection site were determined using a Trimble Geo XT global positioning system (GPS), which is accurate to 1 m². At each site, a mean of 11 fixes was used to define the exact position. Samples were collected within a 30 metre radius of the GPS point. All samples were stored at 4°C immediately after sampling.

Table 2.1 describes the sites where vegetation, soil, dung, and water samples were collected, including the immediate land use and dominant vegetation species, grid reference (G.R.), date sampled, and the chapter in which analysis of these samples is reported. The G.R.s reported in table 2.1 are located on figure 2.1.

Table 2.1. Sample site descriptions where vegetation, soil, dung, and water samples were collected. Grid References (G.R.) are located in figure 2.1. The chapter number refers to the experimental chapter in which the sample was used. Water sample Moorland* represents a mixed land use sample since the river source was on Dartmoor but flows through agricultural grassland.

Sample	Land use	Replicate	Site location & information	G.R.	Date sampled	Chapter
Mixed grass sward	Mixed grass sward	all 4	Little Burrows. <i>Lolium perenne</i> and <i>Holcus lanatus</i> dominant	SX659982	10/12/2009	4
<i>Ranunculus repens</i>	Mixed grass sward	all 4	Little Burrows <i>L. perenne</i> and <i>H. lanatus</i> dominant	SX659982	12/12/2009	4
<i>Fraxinus excelsior</i>	Agroforestry	all 4	Agroforestry West. <i>F. excelsior</i> plantation in grazed grassland	SX637990	11/12/2009	4
<i>Quercus robur</i>	Woodland	all 4	Woodland south of Agroforestry West	SX637989	11/12/2009	4
Gleysol	Grazed grassland	1	Taw Barton Farm. Blithe soil series. <i>L. perenne</i> dominated	SX654971	01/11/2011	5
Gleyi-eutric fluvisol	Grassland	2	Josephs Carr. Fladbury soil series. <i>Juncus acutiflorus</i> & <i>Deschamsia cespitosa</i> dominated	SX654988	01/11/2011	5
Eutric regosol	Grazed grassland	3	Caters Field. Teign soil series. <i>Holcus lanatus</i> & <i>L. perenne</i> dominated	SX653984	01/11/2011	5
Stagni-vertic cambisol	Woodland	1	Orchard Dean Copse. Hallsworth soil series. <i>Quercus robur</i> dominated	SX653982	01/11/2011	5
Stagni-vertic cambisol	Woodland	2	Yonder Wyke Moor Copse. Hallsworth soil series. <i>Q. robur</i> dominated	SX665979	01/11/2011	5
Stagni-vertic cambisol	Woodland	3	Woodland south of Joseph's Carr. Hallsworth soil series. <i>Q. robur</i> dominated	SX654987	01/11/2011	5
Histosol	Moorland	1	Cosdon Hill, Dartmoor. <i>Festuca ovina</i> & <i>Calluna vulgaris</i> dominated	SX637917	02/11/2011	5
Histosol	Moorland	2	Cosdon Hill, Dartmoor. <i>Festuca ovina</i> & <i>Calluna vulgaris</i> dominated	SX636915	02/11/2011	5
Histosol	Moorland	3	Cosdon Hill, Dartmoor. <i>Festuca ovina</i> & <i>Calluna vulgaris</i> dominated	SX637916	02/11/2011	5
Well drained brown earth	Grassland	n/a	Bicton College. Topsoil (< 230 mm depth) Bromsgrove soil series. Coarse sandy loam	SY071865	05/02/2010	4
Rivington soil	Grazed grassland	n/a	Cockle Park Farm, Ulgham, Northumberland. Well drained sandy loam	NZ204914	01/12/2011	6
Sheep dung	Grazed grassland	1	Taw Barton Farm	SX654971	01/11/2011	5
Sheep dung	Grazed grassland	2	Poor Field, North Wyke	SX655985	01/11/2011	5
Sheep dung	Grazed grassland	3	Poor Field, North Wyke	SX655985	01/11/2011	5
Cattle dung	Grazed grassland	1	Josephs Moor, North Wyke	SX654988	01/11/2011	5
Cattle dung	Grazed grassland	2	North end of Caters Field, N. Wyke	SX653984	01/11/2011	5
Cattle dung	Grazed grassland	3	South end of Northern field of Caters Field, N. Wyke	SX653984	01/11/2011	5
Water	Grazed grassland	1, 2 & 3	Taw Barton Farm. Water from artificial drain	SX654971	11/05/2010 & 20/07/2010	3, 5
Water	Grazed grassland	1, 2 & 3	Sticklepath. Grassland drainage & underground spring water	SX641939	11/05/2010 & 21/07/2010	3, 5
Water	woodland	1, 2 & 3	Tributary of River Taw. <i>Quercus robur</i> dominated woodland	SX665979	11/05/2010 & 21/07/2010	3, 5
Water	Grassland	1, 2 & 3	Josephs Carr. Pond in a wet mire	SX654988	11/05/2010 & 21/07/2010	3, 5
Water	Moorland*	1, 2 & 3	River Taw, originating on Dartmoor, flowing through grassland, lined with trees	SX653984	11/05/2010 & 21/07/2010	3, 5
Water	Woodland	1, 2 & 3	Orchard Dean Copse. Seasonally flowing ditch	SX653982	11/05/2010 & 24/01/2011	3, 5

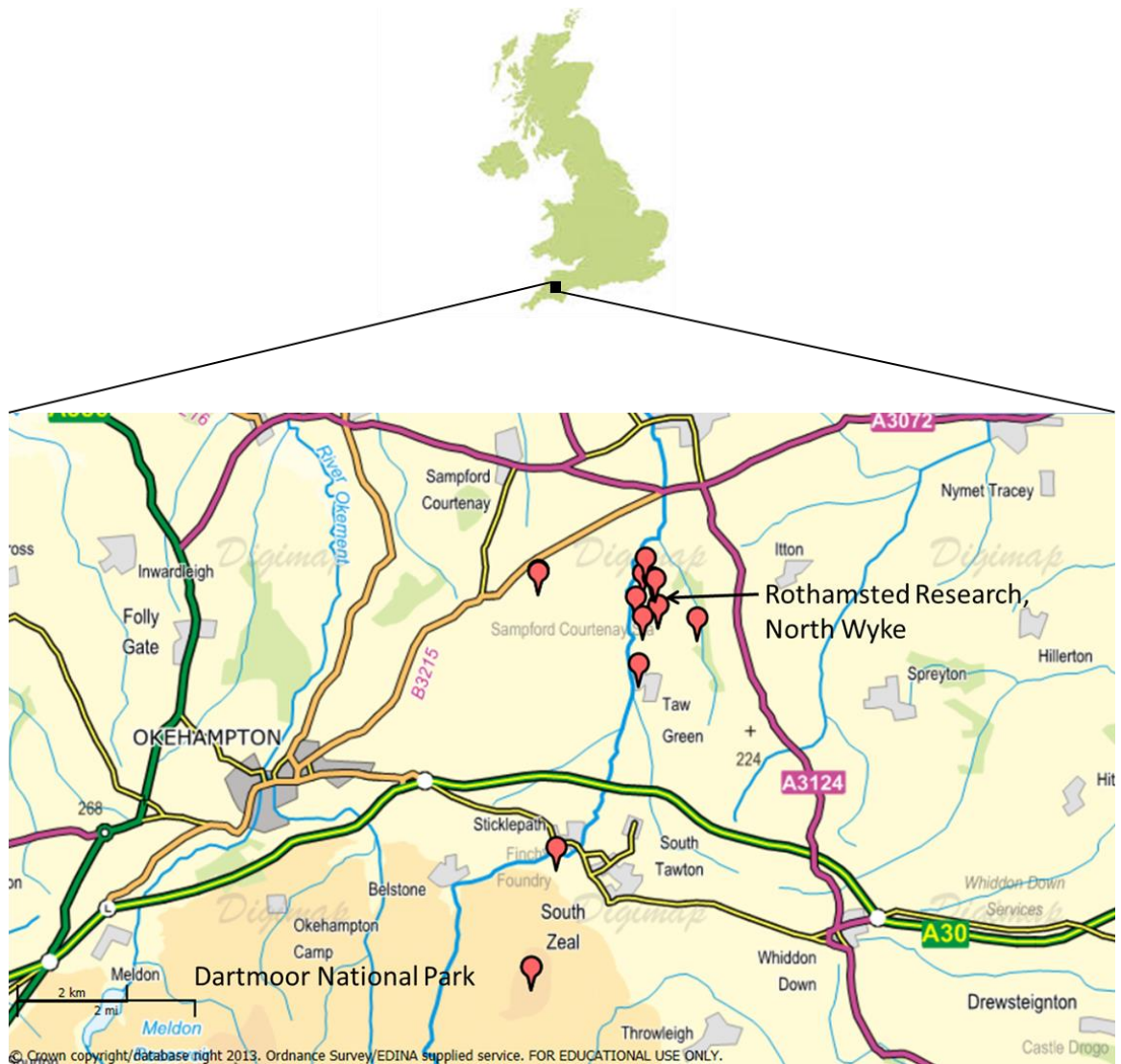


Figure 2.1. Ordnance Survey map showing the approximate location of sampling sites in the vicinity of the Rothamsted Research North Wyke institute, Devon.

2.2. Vegetation sampling

All vegetation samples were leaves and shoots that were taken in replicates of 5 in a ‘W’ shaped spatial sampling pattern, with the G.R. in table 2.1 being the middle point. Four different vegetation types were collected to represent local land uses that were examined in the litter degradation experiment (Chapter 4). All samples were collected from the field and immediately stored at 4 °C until required.

2.2.1 Grassland

a. Monocot (grass) leaves from a recently cut mixed grass sward dominated by *Lolium perenne* (ryegrass) and *Holcus lanatus* (Yorkshire fog) (>30%) with *Phleum pratense* common Timothy), *Agrostis stolonifera* (creeping bentgrass), *Cynosurus cristatus* (crested dogtail grass), *Elytrigia repens* (couch grass), and *Arrhenatherum* species.

b. Dicot (forb) leaves from *Ranunculus repens* (creeping buttercup).

2.2.2 Woodland

c. Pinnate tree leaves from *Fraxinus excelsior* (ash) that fall green.

d. Simple leaves from *Quercus robur* (common oak) that fall brown.

2.3 Soil and livestock dung sampling

Different soils were used for each of the experiments depending on the requirements to test the hypotheses (given at the end of the Introduction to each chapter). The soil characteristics are given in table 2.1.

Half a ton of free-draining top soil used for the litter degradation experiment (Chapter 4) was supplied by Bicton College, East Budleigh, Budleigh Salterton, EX9 7BY. UK.

The soils used for the land use study (Chapter 5) were sampled from 3 grassland, woodland, and moorland areas which had adjacent water outlets for sampling within 100 m (see section 2.4), apart from the moorland soils. Fifteen soil cores (25 mm Ø, < 30 cm depth) were taken in 3 replicates of 5 in a 'W' spatial sampling pattern using a soil auger for each land use. The O and A horizons were separated for analysis, and the impermeable clay B horizon was discarded. The five samples constituting each of the 3 replicates were homogenised.

Representative samples of fresh cattle and sheep dung solids (n = 3) were collected from each of the grassland plots (table 2.1).

Rivington soil used for the phenol transport study (Chapter 6) was supplied by Cockle Park Farm, Morpeth, Northumberland. NE61 3EA. It has a pH 6.2, TOC = 0.62 ± 0.14%, TN = 0.24%, annual mean temperature 8.3 °C, with an annual rainfall of 1314 mm in 2011, and is managed for grazing. It has never been used to grow a C4 crop and has a characteristic C3 soil $\delta^{13}\text{C}$ value of -27.9‰ (Boutton and Yamasaki, 1996). Soil cores were prepared as described in section 2.5.2.

2.4 Water sampling

Sites for water sample collection (table 2.1) were chosen to represent an assumed range of freshwater DOM concentrations including river water, drainage water, and pond water. Seasonal variation was captured in the data since the first replicate for each site was collected on 11/05/2010, and replicates 2 and 3 for sites: Taw Barton Farm,

Sticklepath, Tributary of River Taw, Josephs Carr pond, and River Taw were collected on 21/07/2010. For Orchard Dean Copse stream, replicates 2 and 3 were collected on 24/01/2011 since this site was dry until this time.

Water samples were collected in a bucket (15 litres) to approximately half-full. Subsamples (5 L) were measured into amber glass bottles on-site. Sample pH was measured and then all samples were adjusted to pH 2 with concentrated HCl (Trace analysis grade, 37%, Fisher Scientific) before being stored in a fridge overnight to prevent microbial activity during storage.

2.5 Lysimeter experiments

Packed soil cores were used for Chapter 4 (leaf litter degradation) and Chapter 6 (lignin transport). Soils were sieved (6.35 mm) to remove stones, grass, roots, and soil macrofauna such as beetles, earthworms, and millipedes. The soil was then homogenised to the same water content (detailed below) by mixing before being stored in plastic bags until required. The experimental design is given in each chapter, and the set up is described here.

2.5.1 Bucket lysimeters (6.4 L) (Chapter 4)

Twenty bucket lysimeters were set up using soil of the Bromsgrove series from Bicton College (table 2.1) in plastic buckets (15 L) lined with aluminium foil to prevent contamination, with a drain hole (15 mm) in the centre of the bottom. Four vegetation types plus no vegetation (control) were used (n = 4).

A trial experiment was carried out to determine the optimum soil-water content and bulk density (ρ_d). The soil was packed at 7.2 (field conditions), 8.3, 12.2, 17.2 and 20.5% soil water contents. The soil ρ_d was determined at each soil water content using a corer (i.d. = 5.046 cm, height = 3.780 cm, volume = 75.59 cm³), before drying the soil at 105 °C to constant weight. At 20.5% water content the soil had little mechanical strength and behaved increasingly like a liquid. A leaching test using two litres of distilled water over a set time period showed that 93% of applied water was recovered from the 17.2% soil water, whereas considerably less from 8.3 and 12.2% soil water content soil cores, and the 7.2% soil water content core collapsed. Therefore 17.2% soil water content was selected as most appropriate and was used to set up 20 bucket lysimeters at $\rho_b = 1.73 \text{ g cm}^{-3}$. Soil cores were packed in three equally thick layers. Each soil layer was compressed with a circular press-plate (235 mm diameter) and 18 kg

weight (415.7 kg m⁻² pressure) prior to adding the subsequent soil layer. The bucket lysimeters were placed in a polytunnel on trolleys for the duration of the experiment, suspended 300 mm above the ground to allow leachate collection vessels to be placed underneath. Aluminium rings (255 mm diameter, 127 mm height) were pressed into the lysimeter soil surface to a depth of approximately 10 mm to prevent boundary flow between the soil core and inner lysimeter wall.

Application of leaf litter to lysimeters

The weight of fresh vegetation applied to each lysimeter was determined based on the total carbon (TC) contents of each vegetation type (Chapter 4, table 4.2). The weights applied to each replicate (n = 4) were 1182 g (mixed grass, 43.8% carbon (C) of dry matter (DM) content), 163 g (*R. repens*, 40.6% C of DM), 640 g (*F. excelsior*, 47.1% C of DM) and 662 g (*Q. robur*, 49.1% C of DM). Due to difficulties collecting *R. repens* litter from the field, less was applied to lysimeters than other litter types. The treatments (vegetation types) were applied at random to each lysimeter by using a random number generator. Three temperature data loggers (Tinytag) connected to sensors (PB-5002-IM5 10K NTC, www.tinytag.info) were inserted into the soil of three different lysimeters at 30 mm (depth), and were programmed to record soil temperature every 30 min for 20 months.

Irrigation system set up

An irrigation system consisting of a water pressure reducer (Gardena Micro Drip Master Unit 2000 01354-20) applied water to each lysimeter via an adjustable valve (Gardena, part no. 1374-20) connected to a micro mist nozzle (Gardena, part no. 1371-20) mounted approximately 10 cm above the vegetation surface. Nozzle mean flow rate for each lysimeter was 275 ± 36 mL min⁻¹, which was the flow rate which provided an even coverage of water to the vegetation litter surface. Each lysimeter was irrigated for 15 sec with tap water (mean volume = 66 mL) once per week.

Leachate sampling

Leachate samples were collected at seven time periods (after 82, 143, 200, 263, 381, 459, and 671 days, on 10/08/2010, 11/10/2010, 06/12/2010, 08/02/2011, 06/06/2011, 22/08/2011, and 21/03/13 respectively) by applying 2300 mL tap water to the top of each lysimeter via a watering-can with a rose head. This volume was chosen based on the calculated lysimeter soil pore volume (2246 cm³), to encourage piston-flow to flush

out water transportable lignin-derived material. The leachate was collected in amber glass bottles (Fisher Scientific, part no. FB73180) over a period of approximately 2 hours before being weighed to determine leachate volume.

2.5.2 Soil cores (0.645 L) (Chapter 6)

Rivington top soil (0 - 17 cm depth) sampled with a spade on 01/12/2013 was sieved (6.35 mm) before readjustment to field water content (22%) at the time of collection, determined via weight loss of oven dried soil (30 °C). Soil cores of known volume (10.3 cm Ø x 12.6 cm depth) were used to calculate a soil ρ_b of 1.92 g cm⁻³ which suggest the soil was compacted by management (Brady and Weil, 2002). Thirteen lysimeters (7.4 cm diameter x 17 cm depth) were lined with Al foil to prevent sample contamination. Soil was packed into the lysimeters to a depth of 15 cm (similar to soil cores used in Chapter 4) at field soil ρ_b . An Al foil ring was inserted into the top of the soil to ensure subsequent applied slurry and simulated rainfall irrigation water was not lost as boundary flow between the soil core and inner lysimeter wall.

Preparation and application of dung DOC

The soluble fraction of cattle dung (dung DOC) was prepared using natural abundance ¹³C-labelled dung ($\delta^{13}\text{C} = -12.6\text{‰}$, 21.1% dry matter (DM)) derived from maize (C4) applied at a recommended slurry application rate (28 mL, equivalent to 65 m³ ha⁻¹; (Chambers et al., 2001)). Dung (403 g) was mixed with MilliQ water (1020 mL) to form a slurry (6% DM). The slurry was homogenised using an orbital shaker (Medline Scientific SK-71) at 150 rpm for 2 h, and then centrifuged (Sorvil) at 10,000 rpm for 20 min to extract the dissolved fraction by leaving the dung particulates as a solid pellet in the bottom of the centrifuge tube. The supernatant (735 mL) was decanted and re-centrifuged under the same conditions to ensure particulates were removed. The supernatant from this, the dung DOC, (approx. 700 mL) was decanted into a dark glass bottle to limit microbial activity and stored in a fridge (4°C) until required. Dung DOC was applied to soil cores at three rates: (i) control (28 mL MilliQ water, n=3), (ii) standard application rate (65 m³ ha⁻¹, 28 mL, n=5), (iii) 2.5 x the standard application rate (163 m³ ha⁻¹, 70 mL, n=5), corresponding to the addition of 0, 41, and 103 mg DOC to individual soil cores, respectively.

Rainfall simulation.

To simulate rainfall, starting on Day 2, MilliQ water was applied daily using peristaltic pumps (Watson Marlow 520S) at 24 mL h^{-1} for 3 h 56 min day^{-1} for 60 d. This rate was equivalent to the annual rainfall (1314 mm for Cockle Park farm in 2011) and generated sufficient leachate volume for analysis. An inverted cone of glass fibre filter paper (GF/A Whatman) was placed on the soil surface under the irrigation pipe to distribute the water over the whole soil surface and prevent water droplets eroding a depression in the soil surface.

Leachate sampling.

The first leachate sample was collected after slurry application (Day 1) before irrigation started. Leachate samples were also collected on Day 2, 4, 8, and 16 and were weighed to determine their volume. The leachate (typically $94\text{-}162 \text{ mL day}^{-1}$) was adjusted to pH 2 by addition of a few drops of conc. HCl acid before a 7 mL sample was taken for DOC analysis as described in section 2.6.2. The remainder of the leachate was processed by SPE as described in section 2.6.3 to characterise the lignin phenols present.

2.6 Bulk analysis

2.6.1 Vegetation, soil and dung

Vegetation, soil and dung samples were oven dried at 40°C to constant weight before grinding to a fine powder with a ball mill (SPEX Industries, inc. Metuchen, N.J. 08840, U.S.A.) for 15 min. The soils were stored in the dark at room temperature until analysis.

Soil pH was determined by shaking 5 mL dried soil with 25 mL water ($15 \text{ M}\Omega\cdot\text{cm}$) for 15 min. The soil-water suspension was left to equilibrate for 24 hours before measuring the pH (BSI, 1995). Where pH of soils was >6.7 inorganic carbon was removed using hot acidification ($60 - 70^\circ\text{C}$; 4M HCl) prior to total carbon determination (see section 2.6.4).

2.6.2 Water and leachates

Acidified sub-samples of water samples from the land use experiment (Chapter 5) and the leachates (pH 2; 10 mL) from the leaf litter degradation experiment (Chapter 4) were analysed directly for total organic carbon (TOC) concentration (mg L^{-1}) using a

TOC analyser (CA14 Formacs, Skalar (UK) Ltd). The carrier gas was purified air, supplied by a TOC gas generator (scrubbed of CO₂ and moisture), and the inorganic catalyst solution was 2% orthophosphoric acid.

Acidified sub-samples (7 mL) of leachates from the lignin phenol transport study (Chapter 6) were filtered through 0.2 µm filters to remove particulate organic matter before analysis for TOC concentration (mg L⁻¹) using a TOC analyser (Shimadzu 5050A, with an ASI-5000A auto sampler). The carrier gas was zero grade air, and the inorganic catalyst solution was 25% phosphoric acid.

2.6.3 Extraction of organic carbon from water

Solid organic residues from water were prepared for analysis by freeze-drying (Chapter 3) or solid phase extraction (SPE; Chapters 3, 4, 5, and 6).

Freeze-drying water samples

Freeze-drying removes water by sublimation (Bruttini et al., 1991). Water samples for freeze drying were transferred from the amber glass bottles to pre-cleaned (Decon solution, rinsed three times with deionised water, MilliQ water, then furnace at 500 °C for four hours) Al foil trays (220 mm x 220 mm x 50 mm). Half of each water sample was poured into one pre-weighed Al tray, the other half into another pre-weighed tray. The samples were frozen then freeze-dried (Edwards Super Modulyo) at -50 °C and 10⁻¹ mbar pressure until the water-borne material (WBM) residue remained. The trays containing the residue were weighed again to determine the mass of WBM residue. As much of the residue as possible was transferred to a glass vial using a spatula, before being stored in a freezer under N₂ until analysis.

Solid phase extraction of water samples and leachates

Solid phase extraction (SPE) of water samples was carried out using a modified version of the method described previously (Louchouart et al., 2000) in that the samples were not initially filtered (0.2 µm). Reverse phase C₁₈ end capped solid phase extraction (SPE) cartridges (60 mL, 10 g, Mega-Bond Elut, Agilent Technologies) were mounted on a vacuum manifold (VAC ELUT-20, 13 x 75 mm, Varian) connected to a vacuum pump (Gast Diaphragm pump, model: DOA-P504-BN. Gast Manufacturing, Inc. U.S.A.) via a liquid trap (Carboy Bottle 20 L, part 2226-0050 with filling venting closure, part 2161-0830, Varian Ltd.), enabling up to 10 SPE cartridges to be used simultaneously (figure 2.2). Each cartridge was preconditioned with 100 mL methanol (HPLC grade, Fisher

Scientific) followed by 50 mL pure water (MilliQ Gradient A10) acidified to pH 2 (Trace analysis grade HCl acid, 37%, Fisher Scientific). Water samples (2.5 L) were drawn through the SPE cartridges at an average flow rate of approximately 20 mL min⁻¹ via a Teflon transfer pipe (1/8 in. x 0.1 in. Part AL20096, Varian Ltd.) and adapters (part 12131004, Varian Ltd.) to seal the SPE cartridge. After samples were extracted, cartridges were rinsed with 50 mL pure water (pH 2) to remove any residual salts. Louchouart et al. (2000) rinsed with one litre of acidified water as they analysed saline in addition to freshwater. Then, collection bottles (60 mL, Part BTF-543-030X, Fisher Scientific) were placed inside the vacuum manifold under each SPE cartridge prior to eluting the retained WBM in one fraction with 50 mL methanol. The methanol was evaporated from the collection bottles at 40 °C under a stream of N₂. When 1-2 mL of the methanol-DOC solution remained, this was transferred quantitatively to a 5 mL glass vial by rinsing the 60 mL collection bottle twice with 1.5 mL methanol. The methanol solution was evaporated to dryness under the same conditions before being capped and stored under N₂ in a freezer until analysis.

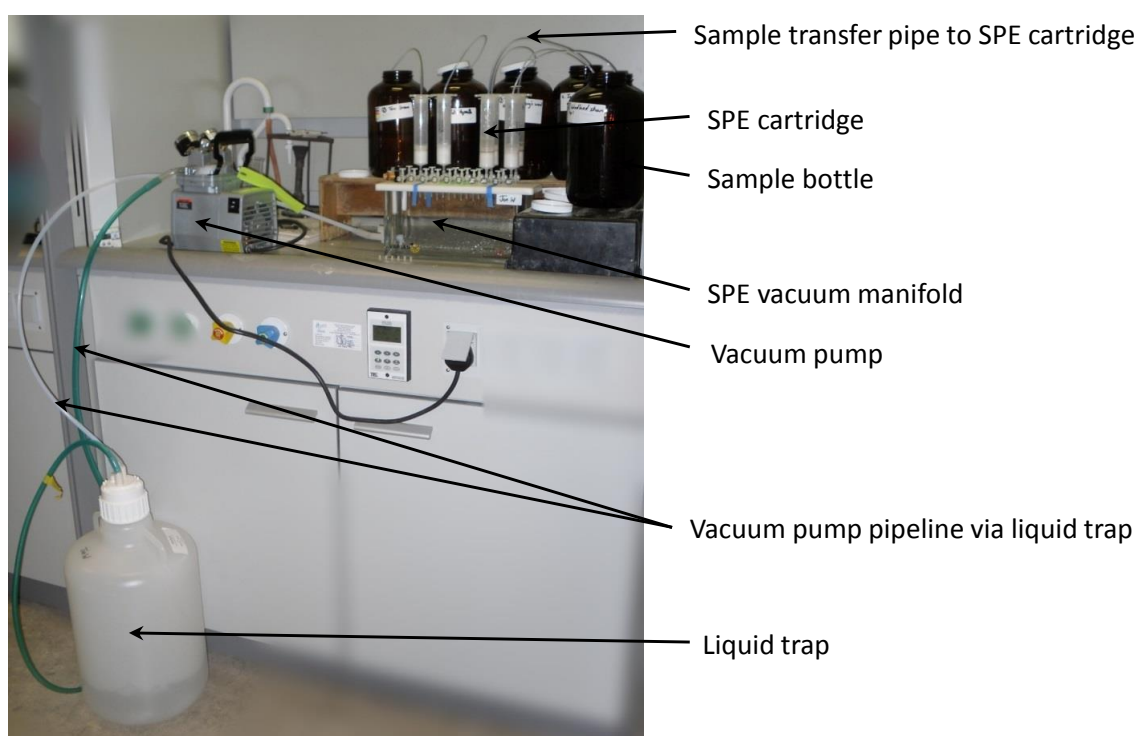


Figure 2.2. Solid phase extraction (SPE) setup used for the extraction of dissolved lignin phenols from natural waters using C₁₈-SPE cartridges.

2.6.4 Bulk total carbon, total nitrogen, and bulk stable $^{13}\text{C}/^{15}\text{N}$ isotope analysis of solid samples

Sub-samples of dry, ground vegetation (3.0–4.0 mg), soil (4.0–60 mg), dung (2.5–2.9 mg) and water residue (2–4 mg) were analysed for total carbon and total nitrogen using a Carlo Erba NA2000 analyser (CE Instruments, Wigan, UK) and a SerCon 20-22 isotope ratio mass spectrometer (SerCon Ltd, Crewe, UK) at Rothamsted Research North Wyke. Wheat flour (1.91 %N, 41.81 %C, 4.80 $\delta^{15}\text{N}$ and -26.41 $\delta^{13}\text{C}$) calibrated against IAEA-N-1 by Iso-Analytical, Crewe, UK was used as a reference standard.

2.7 Sample derivatisation

The phenols extracted from the samples using freeze-drying or SPE were analysed using GC-FID, GC-MS and thermally assisted hydrolysis and methylation using tetramethylammonium hydroxide. To volatilise the phenols for GC analysis, two derivatisation methods (trimethylsilylation and methylation) were used:

2.7.1 Sample derivatisation with *N,O*-bis(Trimethylsilyl) trifluoroacetamide (BSTFA).

The molecular structure of BSTFA is shown in figure 2.3 and the derivatisation reaction mechanism in Chapter 3, figure 3.2.

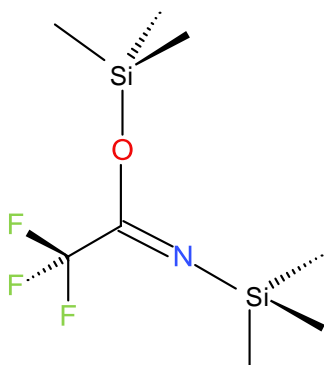


Figure 2.3. Molecular structure of *N,O*-bis(Trimethylsilyl) trifluoroacetamide (BSTFA) derivatising agent.

An aliquot (approx. 1–2 mg for SPE, 10 mg for FD samples) of the extracted samples was accurately weighed into a GC vial (part: STV12-02L, Kinesis) with limited volume insert (part: INWC-01, Kinesis), before being dissolved in 50 μL pyridine, and whirlimixed for 15 sec. *N,O*-bis(trimethylsilyl) trifluoroacetamide (5 drops, BSTFA)

with 1% trimethylchlorosilane (TMCS) were added before capping the vials and heating the samples at 60 °C for 1 hr. The samples were blown down to dryness under N₂ before being re-dissolved in 3 drops of DCM and blown down again to dryness under N₂. Once samples appeared dry, they were given an additional hour to dry to ensure all pyridine had evaporated. 5 α -Androstane (3 μ L; 0.1 mg/mL) was added to each sample as an internal standard. Samples were re-dissolved in DCM and whirlmixed prior to analysis.

2.7.2 *Thermally assisted hydrolysis and methylation using tetramethylammonium hydroxide and on-line py-GC-MS*

Figure 2.4 shows the molecular structure of tetramethylammonium hydroxide (TMAH) derivatising agent used in thermally assisted hydrolysis and methylation that cleaves the β -O-4 bond (figure 1.4) linkage between lignin phenols via the reaction mechanism described in Chapter 3 in figure 3.3.

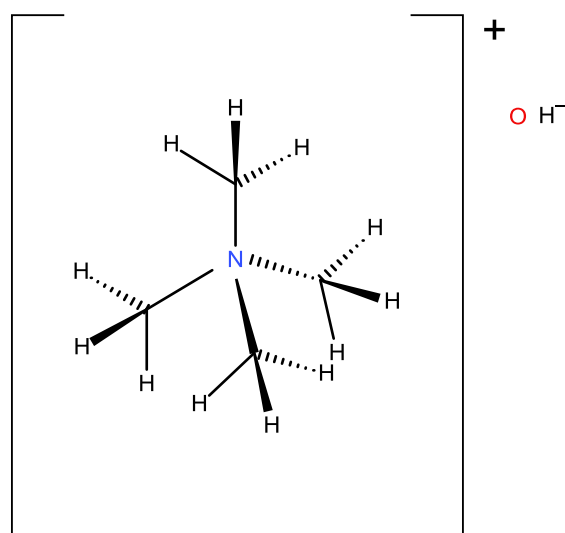


Figure 2.4. Tetrahedral geometry of the tetramethylammonium hydroxide salt.

Temperature calibration of the pyroprobe in preparation for thermally assisted hydrolysis and methylation using tetramethylammonium hydroxide

In order to determine the real temperature that samples were exposed to during flash pyrolysis, the pyroprobe was calibrated using five inorganic salts: PbCl₂, LiCl, CsCl, KI, and KCl, with known melting points: 501, 605, 646, 681, and 770 °C, respectively (Haynes, 2010). Approximately 2 mg of inorganic salt was introduced into a quartz pyrolysis tube before being placed into the pyroprobe heating coil and mounted inside a

heated brass GC inlet block maintained at 360 °C. A viewing window built into the heated block was mounted below a microscope allowing salt melting to be observed. He gas flowed through the heated block at approximately 1 mL min⁻¹ to represent the carrier gas in normal pyrolysis operational conditions. The inorganic salts were repeatedly pyrolysed for 15 sec at incrementing temperatures. The pyroprobe temperature set point at which the salt began to melt was noted together with the temperature at which the salt had completely melted. The mid-point of this temperature range, averaged over three replicates of each salt, was used to determine the pyroprobe temperature calibration curve (figure 2.5).

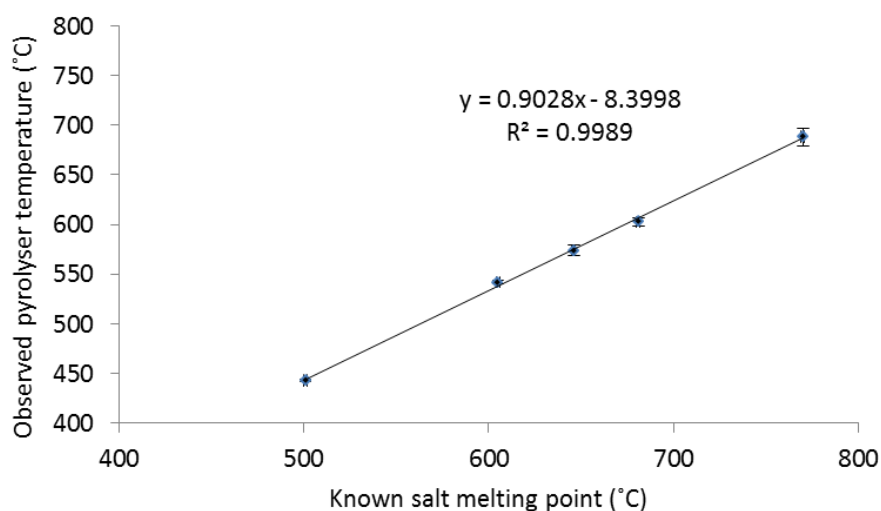


Figure 2.5. Pyroprobe temperature calibration. Mean (\pm standard error of the mean, n = 3) observed temperatures of five inorganic salts of known melting points.

Previous work carried out at Newcastle and elsewhere has shown that a pyrolysis temperature of 610 °C is effective for the analysis of lignin phenols (Clifford et al., 1995, Huang et al., 1998, Mason et al., 2009, Mason et al., 2012). Therefore, according to the equation of the line in figure 2.5, an actual temperature of 610 °C corresponded to a pyroprobe temperature set point of 542 °C, therefore this set point was used for all thermally assisted hydrolysis and methylation using tetramethylammonium hydroxide (TMAH/GC-MS).

Analysis of vegetation, soil, and solid water extracts by thermally assisted hydrolysis and methylation using tetramethylammonium hydroxide

Extracted sample (0.5 to 1.5 mg for extracted DOC, 1.0 to 2.0 mg for vegetation, see section 5.2.2 for soil weights) was weighed into quartz pyrolysis tubes plugged with

glass wool. The glass wool had been pre-extracted with dichloromethane:methanol (93:7; v:v) in a Soxhlet apparatus for 24 h prior to use. 5 α -androstane in dichloromethane (3 μ L; 0.1 mg/mL) was added as an internal standard to each pyrolysis tube. Immediately prior to analysis, 5 μ L of an aqueous solution of tetramethylammonium hydroxide (TMAH) (25%; w/w) was added to the sample (10 μ L for samples > 12 mg). The tube was inserted into the platinum pyrolysis coil and flash pyrolysed at 610 °C for 10 sec (20 °C/ms temperature ramp). This temperature and ramp rate was chosen as it was successful in previous studies investigating lignin phenols (Clifford et al., 1995, Huang et al., 1998, Mason et al., 2009, Mason et al., 2012) and sphagnum phenols (Abbott et al., 2013). The pyroprobe interface was maintained at 340 °C with the products passing into an HP6890 gas chromatograph (GC) with an open split (30 mL/min) and a 60 m HP5-MS column (0.25 mm internal diameter, 0.25 μ m film thickness, J&W Scientific, USA). Helium was used as the carrier gas at a flow rate of 1 mL/min. The GC oven was programmed from 50 °C to 220 °C at a rate of 1.5 °C/min, where it was held isothermally for 1 min and then raised to a final temperature of 320 °C at a rate of 15 °C/min where it was held for 16 min. Product detection was carried out using an HP5973 series mass selective detector in full scan mode (m/z 50 to 700). Compound identification was based on the NIST98 mass spectral library, literature (Vane et al., 2001a, Vane, 2003), and spectra from synthetic lignin standards (Geoff Abbott, personal communication).

2.8 Gas chromatographic analysis

2.8.1 Cold on-column GC-FID

Cold on-column GC-FID (Carlo Erba Strumentazione HRGC 5160 Mega Series) was used for compound quantification. The GC column was a HP-5 ((5% Phenyl)-methylpolysiloxane), 60 m, 0.25 mm dia., 0.25 μ m film thickness (Agilent J & W). The GC oven temperature programme was 40 °C held isothermally for 2 min, then ramped at 2 °C min⁻¹ to 300 °C where it was held isothermally for 1 min, then ramped at 20 °C min⁻¹ to a final temperature of 320 °C held for 40 min (run time = 174 min). Carrier gas was H₂ at 2 mL min⁻¹. Injection volume was 1 μ L.

2.8.2 GC-MS

GC-MS analysis of the derivatised total solvent extract was performed on a Agilent 7890A GC split/splitless injector (280 °C) linked to an Agilent 5975C mass selective detector (electron voltage 70eV, source temperature 230 °C, quad temperature 150 °C multiplier voltage 1800V, interface temperature 310 °C). Samples were manually injected (1 µL) into the GC in splitless mode for 1 min before switching to an open split (30 mL min⁻¹), and a 60 m HP5 ((5% phenyl)-methylpolysiloxane) column (0.25 mm internal diameter, 0.25 µm film thickness, Agilent J&W Scientific, USA). Hydrogen was used as the carrier gas at a flow rate of 1 mL min⁻¹. The GC oven was programmed from 40 °C held isothermally for 2 min, then ramped at 2 °C min⁻¹ to 300 °C where it was held isothermally for 1 min, then ramped at 20 °C min⁻¹ to a final temperature of 320 °C held for 40 min (run time = 174 min). Product detection was carried out in full scan mode (m/z 50 to 700), EM Voltage was 2176. The acquisition was controlled by a HP Compaq computer using Chemstation software. Compound identification was based on the NIST98 mass spectral library, the literature (Vane, 2003), and spectra from synthetic lignin standards (Geoffrey Abbott, personal communication).

2.9 Statistical analysis

Data was analysed by analysis of variance (ANOVA) and PCA using GenStat 64-bit Release 14.1 and specific differences were determined using the Fisher's protected least significant difference (FPLSD) test. Statistical significance was tested at the 95% level. ANOVA is used when there are more than two mean values to compare, for normally distributed data. The test compares the variance within sample groups to that between sample groups, generating an F value, which is used to calculate an F pr. value, which if <0.05 means that there is a significant difference at the 95% confidence limit. A further test, such as the FPLSD test for example, is required to determine which means are significantly different from each other.

Chapter 3. Methodology comparison study: solid phase extraction vs. freeze-drying, and on-line TMAH thermochemolysis vs. GC-MS of trimethylsilyl derivatives for extraction and analysis of water-transportable lignin phenols

3.1. Introduction

Decomposed plant litter, soil organic matter, root exudates, and microbial biomass are thought to be the most important sources of dissolved organic matter (DOM) in soils (Kalbitz et al., 2000), comprising carbohydrate-derived compounds, lignin-derived phenols, fatty acids, alkanes, and smaller amounts of N-containing compounds such as amino acids (Frazier et al., 2003, Frazier et al., 2005, Bowen et al., 2009) which are thought to have a rapid turnover time (Herbert and Bertsch, 1995). Riverine dissolved organic carbon (DOC) concentrations vary from approximately 1 mg L⁻¹ in alpine environments to 25 mg L⁻¹ for rivers draining swamps or in poorly drained soils. The worldwide average of 5.75 mg L⁻¹ (Meybeck, 1982), equates to a flux of 0.25 x 10¹⁵ g riverine DOC year⁻¹ transported to the ocean (Hedges et al., 1997). With total dissolved lignin concentrations ranging, for example, from 0.07 mg/100 mg OC from Island drains in the Sacramento-San Joaquin River Delta (Eckard et al., 2007) to 8.13 mg/100 mg OC (for the 1000 Da - 0.2 μm DOC fraction) for the Big Pine Creek watershed (Dalzell et al., 2005), this represents a substantial loss of carbon (C) in the form of lignin lost from soil C stocks. Due to the molecular structure of lignin monomers, unique to vascular plants (Hedges and Mann, 1979a), lignin monomers are used as terrestrial biomarkers (Gardner and Menzel, 1974, Goni et al., 1997) which can be used as indicators of losses of terrestrial C as inputs into the aquatic C reservoir.

3.1.1 *Extraction of dissolved lignin*

Various techniques have been used to extract DOM from aqueous samples prior to chemical analysis:

(i) Solid phase extraction (SPE)

Various SPE techniques have been used to extract DOM from aqueous solutions. SPE is used to clean up or purify an analyte, concentrate up an analyte, or to solvent switch. It works by providing a solid surface that the analyte of interest can interact with by adsorption to the surface or penetrating an outer layer of molecules on that surface. An

equilibrium is established between analyte adsorbed to the solid phase and that remaining in the liquid phase. The analyte is subsequently eluted using a solvent, whereby the solvent provides a more desirable environment for the analyte than the solid phase does. An advantage of SPE versus liquid-liquid extraction is the ability to elute the analyte with a solvent that is miscible with the original sample matrix solvent since in SPE the elution solvent does not come into direct contact with the sample matrix solvent. Therefore a polar solvent can be used to elute an analyte originally in aqueous solution (Simpson, 2000). Hydrophobic macroreticular resins (XAD) have been used to extract fulvic acid from aqueous solutions (Aiken et al., 1979), to distinguish radiolabelled ‘new’ from ‘old’ DOC in seawater (Lara and Thomas, 1994) and lignin phenols from ocean water (Meyersschulte and Hedges, 1986, Moran et al., 1991). A study comparing different solid phase sorbents (C₁₈, C₁₈EWP, C₁₈OH, C₈, PPL, and ENV) in SPE cartridges (table 3.1) found that whilst the PPL sorbent achieved the highest extraction efficiency of DOC, C₁₈ was more selective for terrigenous compounds, and was the most efficient silica-based sorbent (Dittmar et al., 2008). Due to the non-specificity of the C₁₈ sorbent, as a cartridge or a disc, molecules with a hydrophobic nature will sorb to it (Liska, 2000). C₁₈ SPE in disc form was used to extract riverine DOM and NMR analysis indicated that the C₁₈ extract and original DOM had a similar distribution of functional groups (Kim et al., 2003). Another extraction study compared hydrophobic SPE (C₂, C₈, C₁₈, cyclohexyl, or phenyl sorbents), XAD-2, and ultrafiltration to extract marine humic substances. C₁₈ achieved the greatest extraction efficiency (Amador et al., 1990).

Table 3.1. Structure and retention properties of polar to highly polar pre-packed polymer and silica-based solid phase sorbents (Dittmar et al., 2008).

Sorbent	Structure	Pore size (Å)	Retention properties
C ₁₈	Octadecyl bonded phase, silica-based	60	Retention of nonpolar compounds
C ₁₈ EWP	Octadecyl bonded phase, silica-based	500	More efficient retention of large molecules, compared with C ₁₈
C ₁₈ OH	Non-encapped octadecyl bonded phase, silica-based, with active silanol groups	150	Enhanced retention of basic compounds, compared with C ₁₈
C ₈	Octa bonded phase, silica-based	60	Not as retentive for nonpolar compounds as C ₁₈
PPL	Styrene divinyl benzene polymer	150	Retention of highly polar to nonpolar substances from large volumes of water
ENV	Styrene divinyl benzene polymer	450	Similar to PPL, larger pore size

Although the PPL sorbent has been used to extract lignin from oilfield product water DOM (Wang et al., 2012c), many studies investigating dissolved lignin degradation products have favoured C₁₈ SPE. These include extracts from freshwaters (Louchouart et al., 2000) estuarine waters (Dittmar et al., 2007, Bianchi et al., 2009), oceans (Hernes and Benner, 2006), and from stalagmites (Blyth and Watson, 2009). Using C₁₈ SPE, Louchouart *et al* (2000) achieved 101 ± 4% recoveries of lignin-derived phenols from riverwaters compared with a direct dry down approach using rotary evaporation followed by drying under vacuum in a Savant SpeedVac concentrator. There has even been experimentation with solvents for the C₁₈ extraction protocol where CH₃OH or CH₃CN was used to activate and subsequently elute sorbed fresh, estuarine, and marine DOM from SPE cartridges (Spencer et al., 2010). For freshwater samples they achieved 76.2 – 91.1% recovery (mean = 86.0%) for Σ₈ lignin phenols using CH₃OH versus 48.3 to 77.4% recovery (mean = 67.4%) with CH₃CN, compared to the rotary evaporated sample, and found little fractionation of C:V, S:V, and acid : aldehyde ratios between techniques.

(ii) Freeze-drying (FD), or lyophilisation, is the process whereby a solvent, usually water, is removed from a frozen sample by sublimation (Bruttini et al., 1991). Its main use is preservation of moisture-laden materials, particularly labile biological materials, by preventing microorganism growth and any damaging chemical reactions during sample distribution and storage. Freeze-drying requires the following steps: (i) Sample preparation, whereby samples should have large surfaces and thin uniform cross-sections, or small spherical shapes; (ii) prefreezing the sample in a freezer; (iii) primary drying which allows the frozen free and weakly bound H₂O to sublime slowly under partial vacuum which is subsequently trapped in a refrigerated condenser; (iii) secondary drying which removes moisture that was trapped under the ice crystal; (iv) Rehydration, if the dried sample has to be restored to its original hydrated condition. (Mellor, 1978). For the purposes of this thesis, sample rehydration was not required.

FD has been used to extract dissolved organic material exuded from freshwater microalgae cultures (Lombardi et al., 2005). However FD in combination with other techniques has successfully been used to extract water borne lignin in other studies e.g. using reverse osmosis followed by FD for lake water (O'Driscoll et al., 2006), or cation exchange column followed by FD (Huang et al., 1998), although FD alone has not been used to extract lignin from aqueous samples to the best of our knowledge.

(iii) Ultrafiltration has been used to isolate different molecular size fractions of DOM in fresh and marine waters (Amon and Benner, 1996, Opsahl and Benner, 1998), and ocean water at various depths (McCarthy et al., 1996, Benner et al., 1997, Opsahl and Benner, 1997, Opsahl et al., 1999).

(iv) Combined electro dialysis and reverse osmosis has been used to remove inorganic ions and concentrate DOM from freshwater, wastewater (Drewes et al., 2002) and seawater (Vetter et al., 2007).

3.1.2 Lignin analysis techniques

DOC of freshwater and seawater has been determined by various high temperature combustion instrumental analysers (Sharp et al., 1995), and spectrophotometric methods, such as at 250 nm (Bolan et al., 1996), or specific UV absorbance (SUVA) at 254 nm to estimate the dissolved aromatic C content of water samples (Weishaar et al., 2003).

Characterising the precise macromolecular structure of lignin is inherently difficult due to its large size, estimated as 600-1000 kDa (Kirk and Farrell, 1987), and containing a variety of inter-monomer linkages (Boerjan et al., 2003). Its two principal proposed structures are shown in Chapter 1, figure 1.5 (Chen and Sarkanen, 2010). This means that it is first necessary to break the macromolecule down into its constituent monomeric units and then characterise these. Analysis techniques that give molecular structural and proxy information include:

(i) On-line pyrolysis-GC-MS. Pyrolysis has been defined in different ways: the thermal degradation of a compound brought about by the application of heat, in the absence or presence of air (van der Hage, 1995), commonly carried out between 500 – 800 °C (Moldoveanu, 1998). Upon pyrolysis, polymers and macromolecules decompose generating smaller volatile and semivolatile molecules which can be analysed using GC-MS (Moldoveanu, 2001), and may either be carried out on-line (Faix et al., 1987, Kuroda and Nakagawa-izumi, 2006), or off-line (see below). The pyrolysis mechanism for cleaving the β -O-4 bond in the lignin macromolecule (figure 3.1) has been described as a first-order six-centre concerted retro-ene mechanism (Klein and Virk, 1983, van der Hage et al., 1993).

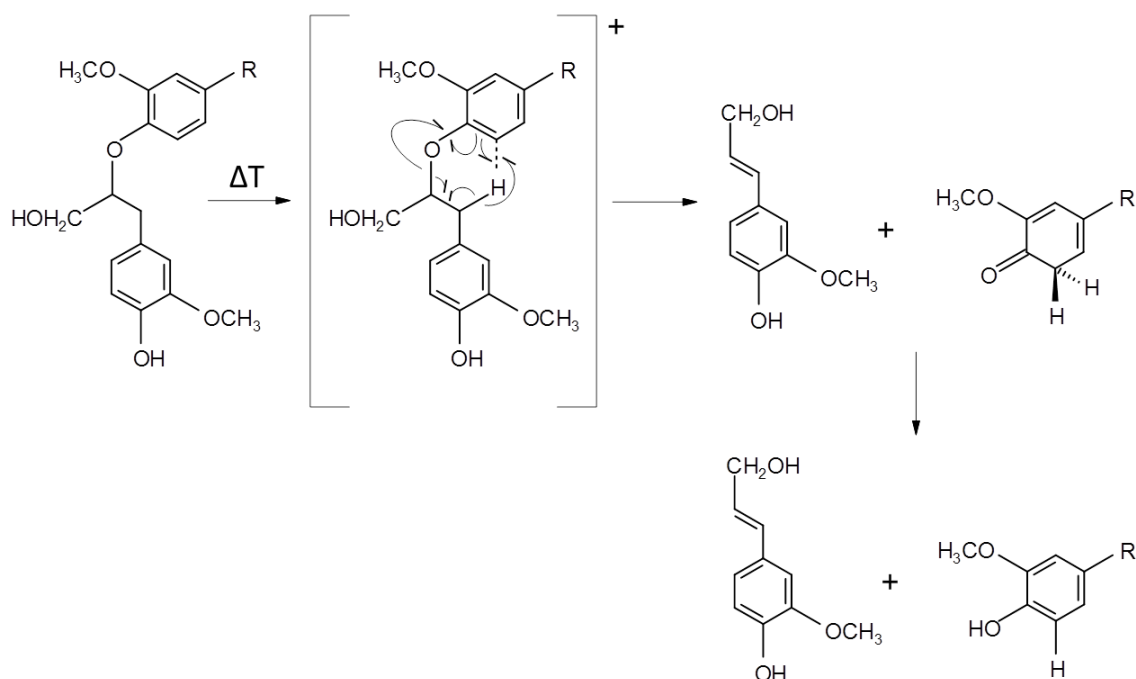


Figure 3.1. Six-centre concerted retro-ene pyrolysis reaction mechanism for breaking the β -O-4 bond in the lignin macromolecule (Klein and Virk, 1983, van der Hage et al., 1993).

(ii) Off-line pyrolysis followed by derivatisation of the pyrolysate with BSTFA (Vane and Abbott, 1999, Dungait et al., 2008). The pyrolysis mechanism for cleavage of the β -O-4 bond is the same as described in (i) above (figure 3.1). *N,O*-bis(trimethylsilyl) trifluoroacetamide (BSTFA) with 1% trimethylchlorosilane (TMCS) is a widely used derivatisation agent and functions by donating a trimethylsilyl (TMS) group to replace active hydrogen atoms on polar molecules via the mechanism in figure 3.2, making them more amenable GC analysis techniques.

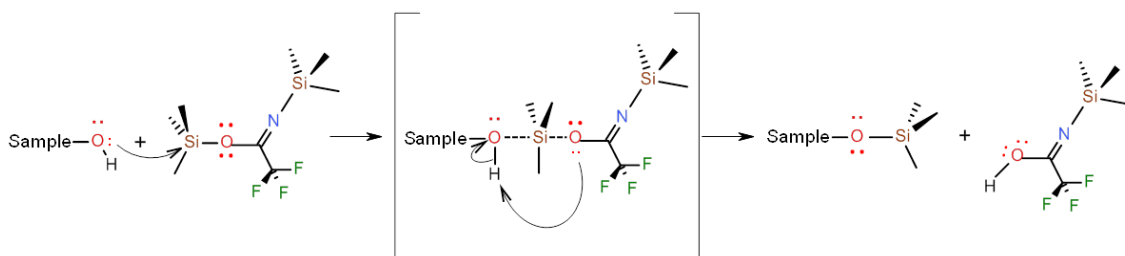


Figure 3.2. Reaction of *N,O*-bis(trimethylsilyl) trifluoroacetamide (BSTFA) with an active hydrogen atom on a sample compound via a SN2-type mechanism.

(iii) Thermally assisted hydrolysis and methylation using tetramethylammonium hydroxide (TMAH/GC-MS) has been used both off-line for the analysis of DOM, soils, and vegetation (Martin et al., 1995, del Rio et al., 1998, Huang et al., 1998, Frazier et al., 2003) and on-line in the analysis of vegetation, soils, aquatic humic substances (Saizjimenez et al., 1993, Challinor, 1995, Clifford et al., 1995, Mason et al., 2009, Mason et al., 2012), and terrestrial organic matter preserved in stalagmites (Blyth and Watson, 2009). TMAH/GC-MS principally cleaves lignin β -O-4 bonds (Hatcher et al., 1995) (Chapter 1, figure 1.4) via the mechanism reported in figure 3.3, which is modified from Filley et al., 1999 for the reaction of tetramethylammonium hydroxide (TMAH) in aqueous solution, rather than in methanol. The base OH^- from TMAH deprotonates the hydroxyl group on either the α or γ side chain carbon. Subsequent intramolecular nucleophilic attack on the β carbon results in the formation of the $\beta\gamma$ -epoxide or $\alpha\beta$ -epoxide, which cleaves the β -O-4 bond. Subsequent nucleophilic attack by OH^- (rather than CH_3O^- as reported in Filley et al. 1999), could proceed at the β or γ side chain carbon on the $\beta\gamma$ -epoxide, or at the α or β carbon on the $\alpha\beta$ -epoxide to open the epoxide ring. Further reaction with TMAH methylates all unprotected OH groups to yield the fully methylated product.

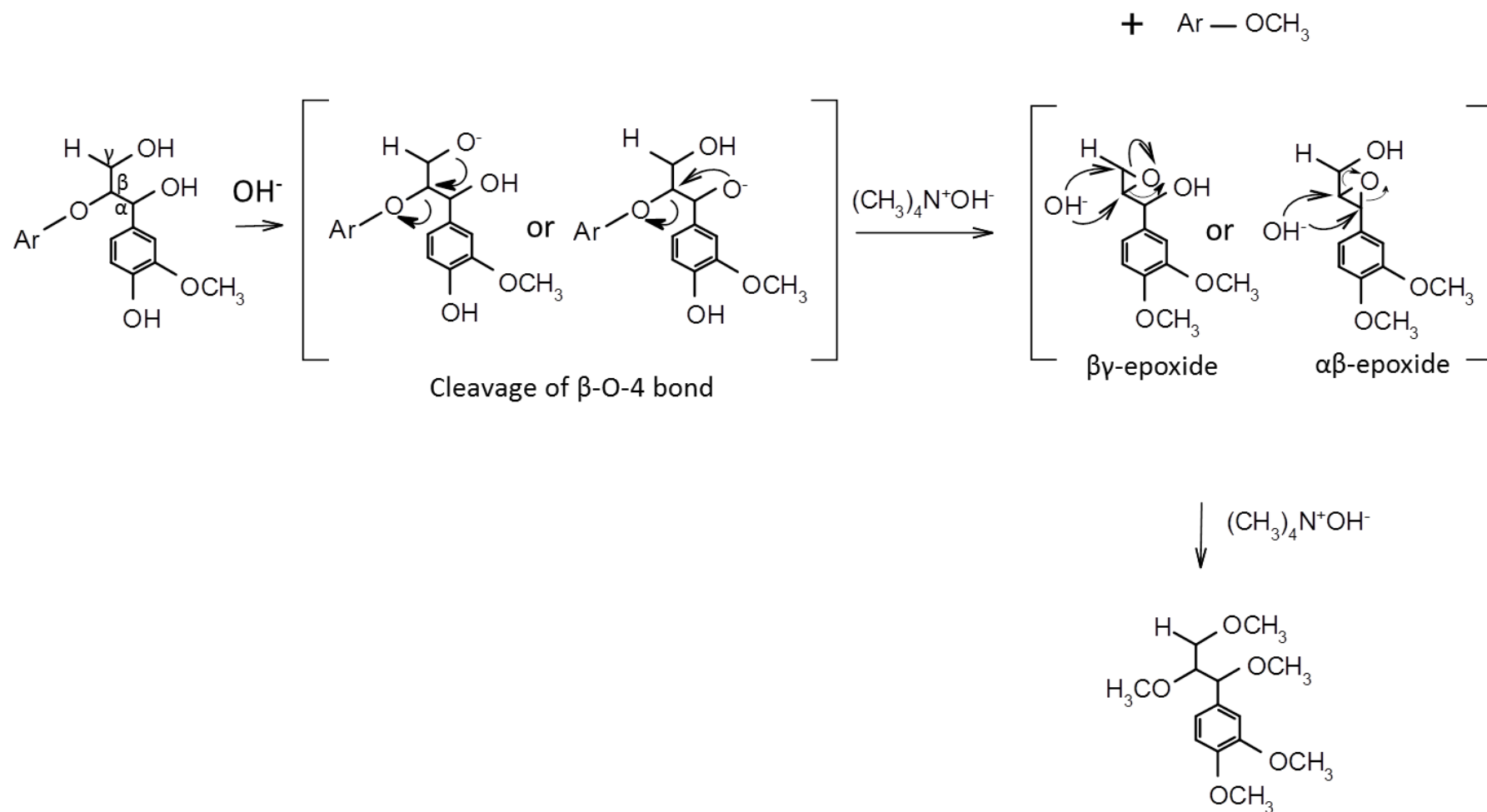


Figure 3.3. Proposed general mechanism for the cleavage of the lignin β -O-4 bond using tetramethylammonium hydroxide ($(\text{CH}_3)_4\text{N}^+\text{OH}^-$), modified from Filley et al., (1999) for the reaction of $(\text{CH}_3)_4\text{N}^+\text{OH}^-$ in aqueous solution, rather than in methanol.

(iv) CuO oxidation has been used to characterise lignin in plant tissue, soil, and sediments (Hedges and Mann, 1979a, Hedges and Ertel, 1982), and DOM (Kaiser et al., 2004). CuO oxidation has been compared with TMAH thermochemolysis to characterise lignin (Hatcher et al., 1995, Wysocki et al., 2008). Wysocki et al (2008) found that the CuO approach yielded greater amounts of total lignin from a given sample, although a wider range of lignin breakdown products, including a greater abundance of cinnamyl-based products were achieved by TMAH thermochemolysis. The CuO oxidation mechanism for the release of polar phenols involves the one electron oxidation of polymer linkages in dilute alkaline solution. Most of the ether bonds in the lignin polymer are hydrolysed at the ring side chain. The phenols are then derivatised prior to gas chromatography analysis (Opsahl and Benner, 1995, Wysocki et al., 2008).

(v) liquid chromatography-MS has been used to trace terrigenous DOM and its photochemical decay along a transect from the Brazilian mangrove-fringed coast to the ocean (Dittmar et al., 2007).

(vi) Derivatization followed by reductive cleavage (DFRC) has been used to investigate lignin in vegetation (Lu and Ralph, 1997), lignin dimers (Peng et al., 1998), pinewood (Ikeda et al., 2002), on model lignin compounds (Holtman et al., 2003), and lignin monomers in low rank coal humic acids (Grasset et al., 2010).

The DFRC approach breaks down the lignin macromolecular structure according to the mechanism shown in figure 3.4, consisting of the following steps (Lu and Ralph, 1997):

- (a) Acetyl bromide (CH_3COBr) reacts with the lignin macromolecule to cleave α -ether bonds resulting in β -bromo ethers. Free phenyl hydroxyl groups and γ -hydroxyl groups may also be acylated. This derivatisation step is accompanied by solubilisation of the cell-wall as a result of the bromination and acetylation (Lu and Ralph, 1998).
- (b) Reductive cleavage of the β -bromo ethers with zinc powder in an acidic medium cleaves the β -O-4 bonds, via zinc metal coordination, resulting in the formation of a carbon-carbon double bond between the side chain α and β carbons (Holtman et al., 2003).

- (c) Acylation with acetic anhydride ($\text{CH}_3\text{COOCOCH}_3$) and pyridine which acylates remaining free phenyl hydroxyl groups resulting in the formation of 4-acylcinnamyl acetate (4-acetoxycinnamyl acetate) monomers.

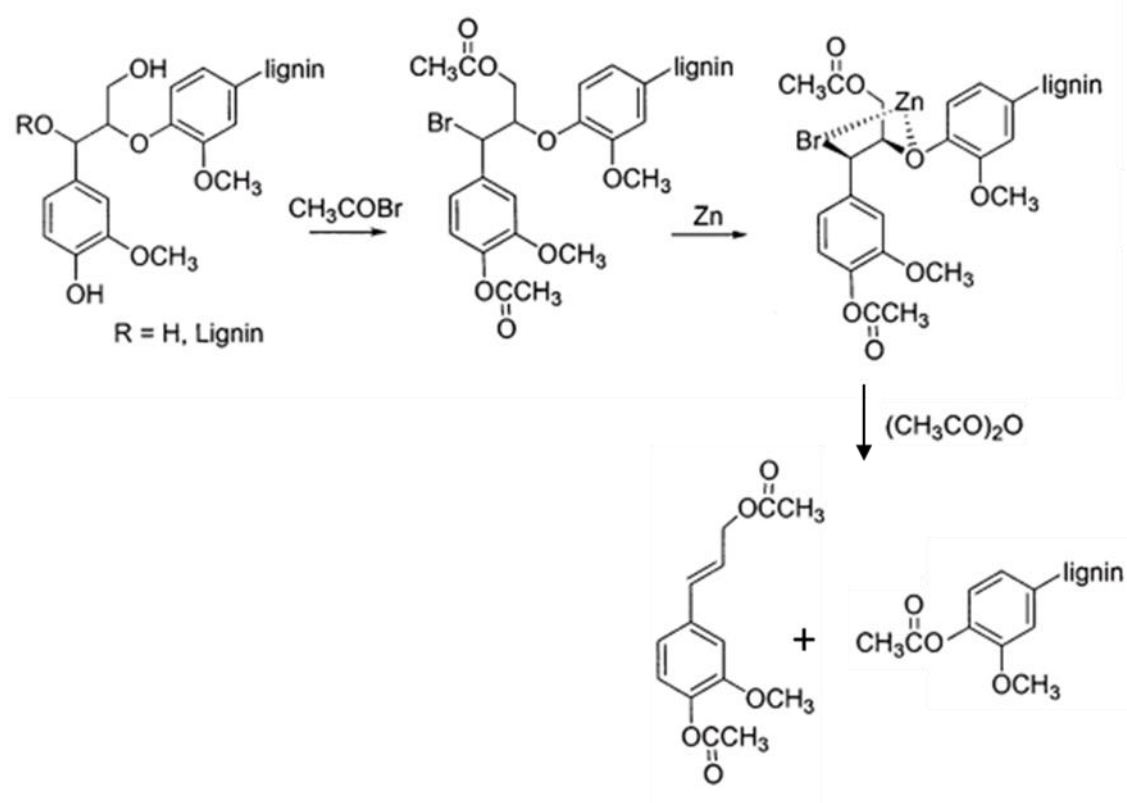


Figure 3.4. Proposed mechanism for the degradation of lignin by DFRC (Ralph and Grabber, 1996, Holtman et al., 2003).

(vii) Thioacidolysis is a type of acid-catalysed solvolysis reaction in dioxane-ethanethiol with boron trifluoride etherate ($\text{Et}_2\text{O}^+\text{-BF}_3$) depolymerising lignin mainly by cleavage of arylglycerol- β -aryl ether linkages (Rolando et al., 1992), and has been used for example for the analysis of pinewood and wheat straw lignin (Lapierre et al., 1988).

In thioacidolysis (figure 3.5), ethanethiol (EtSH) behaves as a soft nucleophile and boron trifluoride a hard Lewis acid (Fuji et al., 1979). BF_3 reacts at the O bonded to the α carbon through electron acceptance before ethanethiol attacks the α carbon leading to the thioether (A). Further reaction with more boron trifluoride, followed by ethanethiol generates the thioether at C_β (B). Reaction with yet more BF_3 then ethanethiol yields the tri-substituted thioether (C) (Rolando et al., 1992).

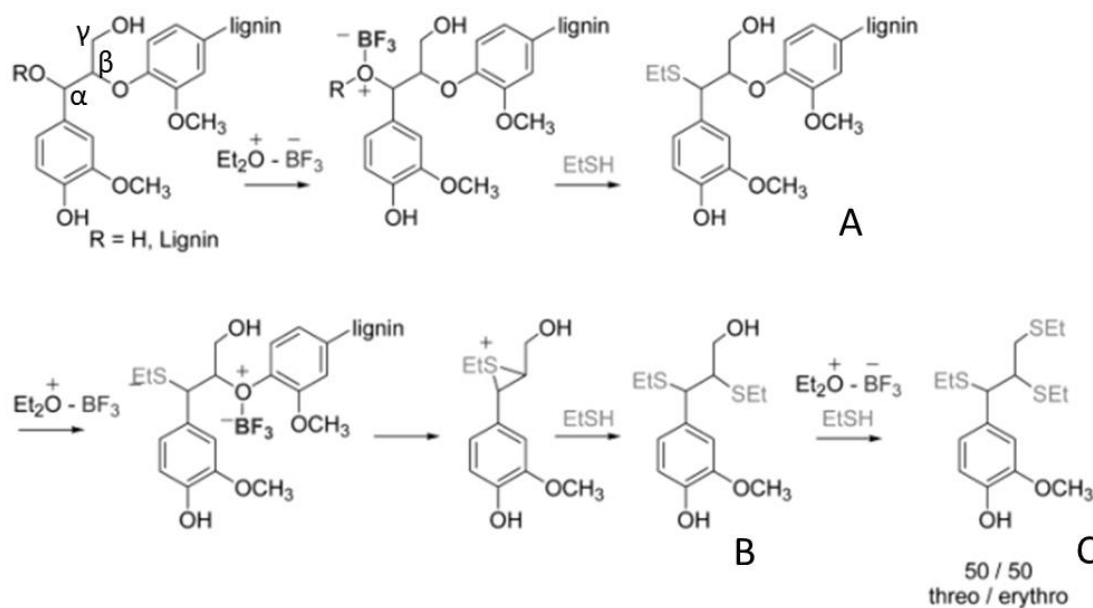


Figure 3.5. Proposed mechanism for thioacidolysis of lignin (Rolando et al., 1992, Holtman et al., 2003).

Cation exchange has been used prior to FD extraction and derivatisation with BSTFA to investigate DOM prior to GC-FID and GC-MS analysis of the resulting trimethylsilyl (TMS) derivatives (Huang et al., 1998) and they had virtually no detector response in their chromatographic traces, hypothesizing that DOM constituents are polymeric or oligomeric. However, detection of lignin phenols using cold on-column GC-FID has not been tried to the best of our knowledge, and has the potential benefit of characterising the water-borne lignin in its original molecular structure for those monomers/oligomers amenable to GC analysis.

In order to understand and characterise the water-borne lignin component, it was necessary to determine the best extraction and detection technique combination. FD in isolation has not been used to extract lignin degradation products from water-borne material (WBM) to the best of our knowledge. Hence, C_{18} SPE or FD was used to extract water-borne lignin from a range of natural freshwaters. Secondly, two different analysis techniques: cold on-column GC-FID and thermally assisted hydrolysis with methylation using TMAH were compared to detect extracted water-borne lignin phenols. The best combination of extraction and detection techniques would be used in later experiments in this thesis.

3.1.3 *Experiment aims and hypotheses*

The aims of this experiment were (i) to compare SPE or FD to extract water-transportable lignin-derived compounds from freshwater samples, in terms of total yield recovered and representation of the full range of lignin phenol molecular structures, and (ii) to compare derivatisation with BSTFA followed by cold on-column GC-FID or thermally assisted hydrolysis and methylation using TMAH (TMAH/GC-MS) to derivatise and detect extracted water-borne lignin phenols.

Hypotheses

H1. Freeze-drying extracts a greater concentration of water-transportable lignin-derived compounds from natural fresh water samples than SPE because everything should be recovered.

H2. TMAH/GC-MS analysis detects greater concentration, albeit less original macromolecular structure, of water-borne lignin than GC-FID of TMS derivatives.

3.2. Methodology

3.2.1 *Experimental Design*

Three replicate water samples were collected at six sites using a split-split-plot experimental design (figure 3.6) to compare water-borne lignin extraction and detection techniques. Mass of matter and phenols recovered from blanks (MilliQ water) were subtracted from the respective values recovered from samples.

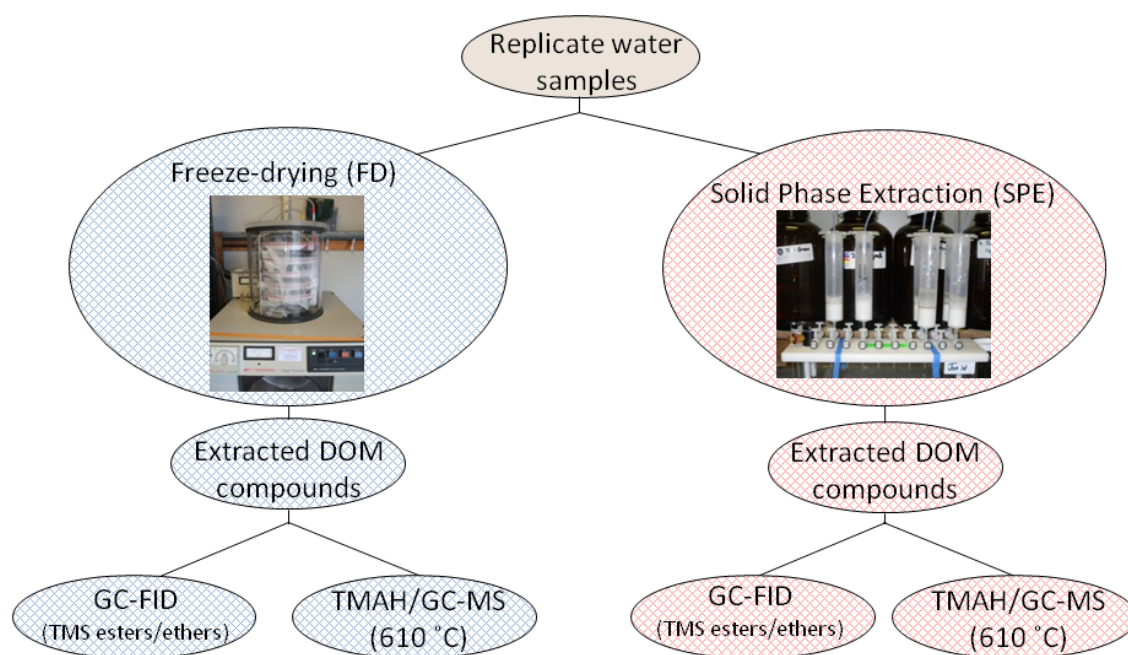


Figure 3.6. Schematic describing the split-split plot experimental design comparing extraction and analysis techniques.

3.2.2 Sampling Sites and collection

Water samples were collected from six locations in the vicinity of Rothamsted Research North Wyke, Devon, UK (G.R. SX660984, 50°45'N and 4°53'W) as described in Chapter 2, section 2.4, table 2.1, and analysed for total organic carbon as described in Chapter 2, section 2.6.2.

3.2.3 Sample extraction, derivatisation and analysis

Samples were extracted by freeze drying and SPE using the methods described in Chapter 2, section 2.6.3. All water-borne matter (WBM) extracted by SPE and FD were analysed for total carbon as described in Chapter 2, section 2.6.4.

An aliquot of FD and SPE extract was derivatised with BSTFA (Chapter 2, section 2.7.1) and analysed using cold on-column GC-FID (Chapter 2, section 2.8.1) for quantification, and GC-MS for identification (Chapter 2, section 2.8.2). Another aliquot of FD and SPE extract was derivatised with TMAH and analysed using on-line py-GC-MS (Chapter 2, section 2.7.2). Statistical analysis of the results was carried out as described in Chapter 2, section 2.9.

3.3. Results

3.3.1 Sample TOC, pH and WBM yields

Expressed as a concentration, FD recovered 159 and 90 mg L⁻¹ and SPE extracted 12 and 0.3 mg L⁻¹ water-borne matter from sites TBF and St, respectively, after background subtraction (table 3.2). At TRT, JC, and ODC sites SPE extracted 9, 21, and 3.2 mg L⁻¹ whereas FD extracted 0 mg L⁻¹ WBM from the same sites due to large amounts of WBM recovered from the blank (MilliQ water). The standard errors were consistently larger for FD than SPE. The most acidic water pH was at site St (pH 6.4) and the most basic was site RT (pH 7.35).

Table 3.2. Mean (n = 3) water sample pH, TOC, and recovered water-borne matter yields extracted using freeze drying (FD) and solid phase extraction (SPE) from water samples collected from six sites. s.e. = standard error of the mean.

Site	Location	pH	Water borne matter yield (mg L ⁻¹)			
			SPE	s.e.	FD	s.e.
TBF	Taw Barton Farm	7.33	11.92	2.69	159.13	63.98
St	Sticklepath field drain	6.39	0.30	0.30	90.45	90.45
TRT	TRT, Yonder Wyke Moor Copse	7.14	8.97	3.17	0.00	0.00
JC	Joseph's Carr	6.5	20.97	6.67	0.00	0.00
RT	River Taw, Caters Field	7.35	3.24	0.95	2.51	2.51
ODC	Orchard Dean Copse stream	6.54	6.93	0.97	0.00	0.00

Figure 3.7A & B show that the greatest SPE extracted WBM, recovered from the JC sites (21 mg L⁻¹), correlated with the greatest TOC concentration (13.9 mg L⁻¹) in the same original aqueous sample. The lowest SPE extracted WBM concentration, at site St (0.3 mg L⁻¹), and correlated with the lowest TOC concentration (1.5 mg L⁻¹).

Comparing figures 3.7A, B, and C, the concentrations of SPE extracted WBM are more consistent with TOC concentrations than FD extracted WBM, suggesting that TOC as a function of water-borne matter is better represented by SPE than FD extraction. The TOC percentage of FD extracted WBM (figure 3.7D) shows that the highest and lowest organic carbon contents were at the JC and St sites (4.7 and 0.2%, respectively), indicating that the proportion of organic carbon in the FD extract, rather than the extract yield, correlated with the aqueous TOC concentration (figure 3.7A) and with the WBM yield recovered using SPE (figure 3.7B). WBM was recovered from sites TRT and JC using FD extraction despite the zero values for these sites in figure 3.7C. The zero values arise by subtraction of the high mass of WBM recovered from the FD blank,

whereas the TOC analysis of the FD extract figure 3.7D) was carried out on the actual recovered material.

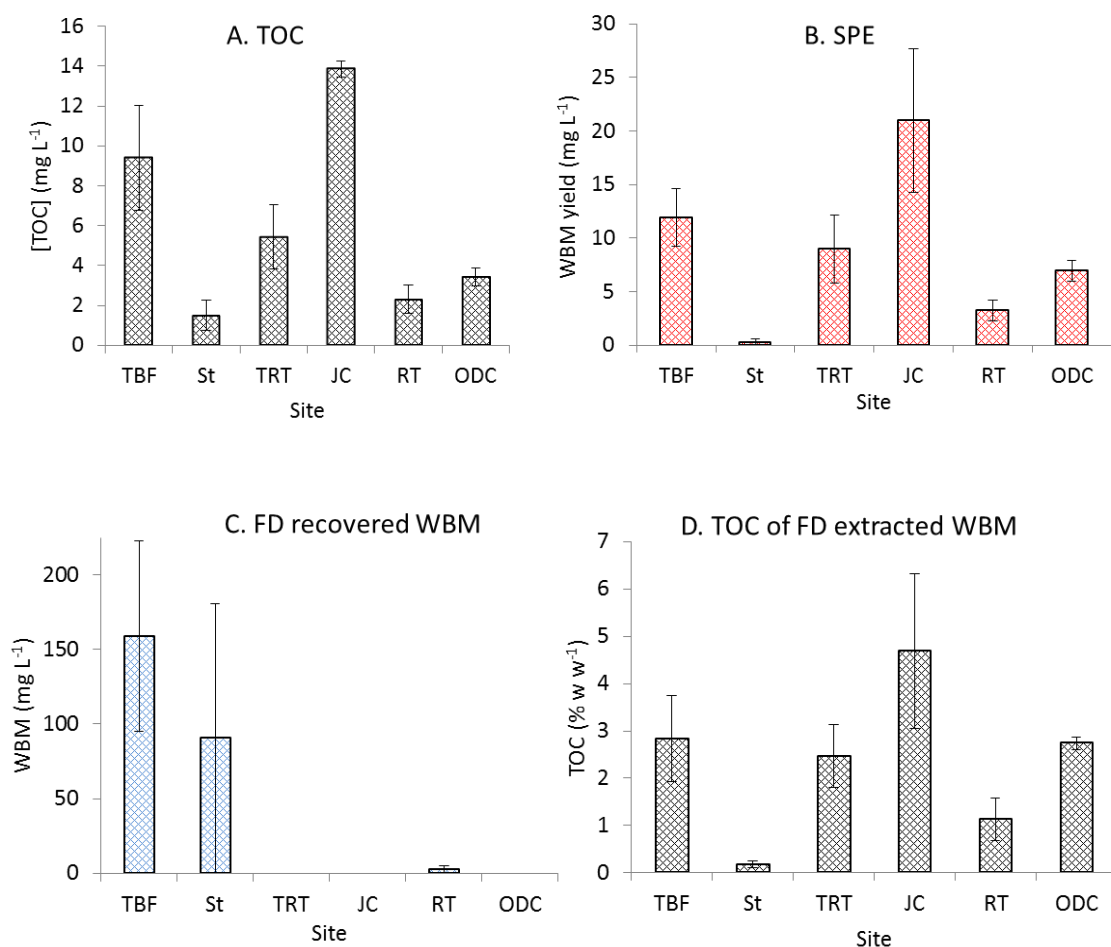


Figure 3.7. Mean (\pm standard error of the mean (s.e.), $n = 3$) total organic carbon (TOC, plot A), solid phase extracted (SPE) water-borne matter (WBM, plot B), freeze dried (FD) extracted WBM (plot C), and TOC of the solid freeze-dried WBM extract (plot D) in six water samples. Site name abbreviations are described in table 3.2.

As a proportion of the WBM extracted using SPE or FD, SPE recovered considerably more organic carbon than FD (table 3.3) for all six sites, with TOC values ranging between 41.9 – 59.1% for SPE and 0.2 – 4.7% for FD. Therefore the majority of WBM extracted by FD must have been inorganic.

Table 3.3. Mean (\pm standard error of the mean (s.e.), $n = 3$) total organic carbon (TOC) percentages in solid phase extracted (SPE) and freeze dried (FD) extracted water-borne matter for six water samples.

Site	TOC (%)			
	SPE	s.e.	FD	s.e.
TBF	47.2	2.2	2.8	0.9
St	59.1	4.8	0.2	0.1
TRT	44.2	3.7	2.5	0.7
JC	46.5	3.4	4.7	1.6
RT	50.6	2.0	1.1	0.5
ODC	41.9	2.9	2.7	0.1

3.3.2 Total lignin phenol concentrations

Total lignin concentration for each site in this study was defined as the sum of the individual compound concentrations reported in table 3.6, normalised to 100 mg OC. Following FD extraction of WBM (figure 3.8A), TMAH/GC-MS detected the highest total lignin phenol concentrations at site ODC ($3.1 \text{ mg (100 mg OC)}^{-1}$) and $0 \text{ mg (100 mg OC)}^{-1}$ at the St site. No lignin phenols were detected using on-column GC-FID at any of the sites.

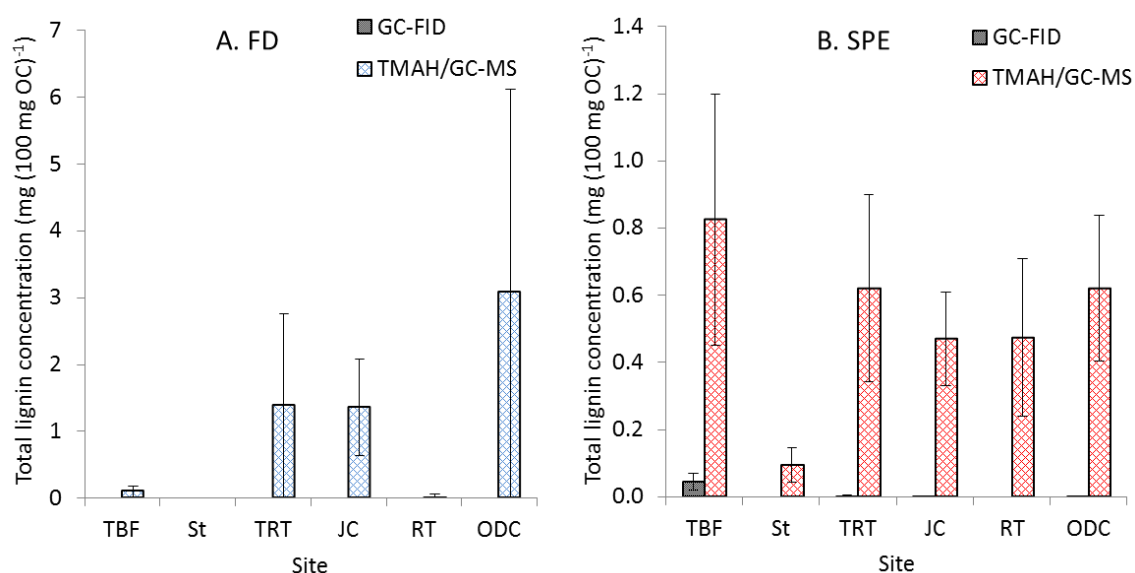


Figure 3.8. Mean (\pm standard error of the mean, $n = 3$) total lignin phenol concentrations after freeze-drying (FD, plot A) and solid phase extraction (SPE, plot B), detected using cold on column GC-FID and TMAH/GC-MS.

After SPE of WBM (figure 3.8B), lignin phenols were detected at all six sites by TMAH/GC-MS with concentrations ranging between 0.09 and 0.82 mg (100 mg OC)⁻¹ at sites St and TBF, respectively. On-column GC-FID detected lower concentrations of lignin phenols than TMAH/GC-MS, and only detected phenols at four of the six sites with concentrations ranging between 0 mg (100 mg OC)⁻¹ at sites St and RT to 0.05 mg (100 mg OC)⁻¹ at site TBF.

Comparison of figure 3.8A and B shows that TMAH/GC-MS detects more than an order of magnitude more total lignin phenols than on-column GC-FID. However, there were no significant differences between sites ($F_{pr} = 0.392$) or extraction techniques ($F_{pr} = 0.235$) due to the large number of zero concentration values for the FD extraction technique and large associated standard errors.

3.3.3 Water borne lignin phenols

Total lignin concentrations extracted by FD or SPE and detected by GC-FID or TMAH/GC-MS shown in figure 3.8 comprise of individual phenols, reported in tables 3.4, 3.5, and 3.6.

Table 3.4. Mean (\pm standard error of the mean, $n = 3$) water borne lignin phenols concentrations from six sites (TBF, St, TRT, JC, RT, and ODC) extracted using freeze drying and detected using TMAH/GC-MS. Site name abbreviations are described in table 3.2. Phenol abbreviations (Abb.) with * contain an unmethylated hydroxyl group.

Phenol	Abb.	mean conc. ($\mu\text{g (100 mg OC)}^{-1}$)											
		TBF	s.e.	St	s.e.	TRT	s.e.	JC	s.e.	RT	s.e.	ODC	s.e.
phenol	P1*	0	0	0	0	1270.7	1270.7	839.8	453.6	0	0	3220.9	1.9
4-methoxytoluene	P2	100.2	76.797	0	0	3.3	3.3	0	0	0	0	0	0
4-hydroxytoluene	P2*	0	0	0	0	0	0	429.1	222.0	21.4	21.4	3068.9	3045.9
1,2-dimethoxybenzene	G1	0	0	0	0	104.0	104.0	0	0	0	0	0	0
3-methoxy, 4-hydroxyethylbenzene	Gx*	0	0	0	0	0	0	0	0	0	0	1.9	1.9
3,4,5-trimethoxybenzoic acid	S6*	0	0	0	0	0	0	0	0	9.3	9.3	0	0

Table 3.5. Mean (\pm standard error of the mean, $n = 3$) water borne lignin phenol concentrations ($\text{mg (100 mg OC)}^{-1}$) from six sites (TBF, St, TRT, JC, RT, and ODC), extracted using SPE and detected using GC-FID. G6^{me} refers to a G6 compound with a demethylated 3-methoxy group. Site name abbreviations are described in table 3.2.

Phenol	Abb.	TBF	s.e.	St	s.e.	TRT	s.e.	JC	s.e.	RT	s.e.	ODC	s.e.
4-[(TMS)oxy]-benzoic acid TMS ester	P6	38.75	21.51	0	0	0	0	0.28	0.28	0	0	0.08	0.08
3-methoxy-4-[(TMS)oxy]-benzoic acid TMS ester	G6	3.40	2.82	0	0	0.3	0.3	0.57	0.57	0	0	0	0
3,4-bis[(TMS)oxy]-benzoic acid TMS ester	G6 ^{me}	3.61	0.70	0	0	0.27	0.27	0.36	0.36	0	0	0.73	0.73
3,4,5-tris(TMSoxy)-benzoic acid TMS ester	S6	0	0	0	0	1.63	1.63	0	0	0	0	0	0

Table 3.6. Mean (\pm standard error of the mean, $n = 3$) water borne lignin phenol concentrations from six sites (TBF, St, TRT, JC, RT, and ODC) extracted using solid phase extraction and detected using TMAH/GC-MS. Site name abbreviations are described in table 3.2. Each * in the phenol abbreviation (Abb) column denotes an unmethylated hydroxyl group.

Phenol	Abb.	mean concentration ($\mu\text{g (100 mg OC)}^{-1}$)											
		TBF	s.e.	St	s.e.	TRT	s.e.	JC	s.e.	RT	s.e.	ODC	s.e.
methoxybenzene	P1	8.3	6.6	7.4	4.4	21.5	11.8	17.0	3.1	23.8	9.1	15.9	2.9
phenol	P1*	152.9	12.3	4.0	4.0	113.0	24.9	68.7	14.5	140.1	50.9	102.6	17.4
4-methoxytoluene	P2	80.6	49.0	7.5	3.1	17.7	3.4	14.8	3.4	15.9	5.5	20.5	4.8
4-hydroxytoluene	P2*	68.0	17.9	0	0	80.1	30.0	84.0	10.1	87.3	33.1	60.4	5.2
2-methoxyphenol	G1*	126.4	39.6	0	0	52.7	26.5	38.7	21.2	25.0	25.0	73.1	31.2
1,2-dimethoxybenzene	G1	16.8	16.8	10.9	6.4	51.5	28.4	32.8	2.5	7.2	7.2	23.9	12.0
4-methoxybenzeneethylene	P3	0	0	7.3	4.3	0	0	0	0	0	0	0	0
3,4-dimethoxytoluene	G2	0	0	0.8	0.8	0	0	0	0	0	0	0	0
4-methoxybenzaldehyde	P4	0	0	1.6	1.6	0	0	0	0	0	0	0	0
3-methoxy-4-hydroxytoluene	G2*	20.7	20.7	0	0	11.9	11.9	3.4	1.9	8.0	8.0	11.1	5.6
3-methoxy-1,2-Benzenediol	S1**	0	0	0	0	8.4	8.4	0	0	0	0	0	0
3-methoxy-4-hydroxyethylbenzene	Gx*	20.7	10.8	0	0	18.2	9.2	0	0	3.2	3.2	0	0
1,2,3-trimethoxybenzene	S1	1.3	1.3	1.0	1.0	34.4	17.8	15.3	2.9	9.7	7.9	20.5	5.2
3-methoxy-4-hydroxybenzeneethylene	G3*	47.4	26.1	0	0	0	0	0	0	6.6	6.6	0	0
3,4-dimethoxybenzeneethylene	G3	15.9	8.8	19.0	7.1	0	0	4.8	4.8	9.0	5.2	0	0
2,6-dimethoxyphenol	S1*	67.6	34.8	0	0	33.8	15.2	15.1	4.4	16.1	8.4	29.1	6.1
4-methoxybenzoic acid methyl ester	P6	22.4	6.9	6.0	6.0	20.2	4.5	29.1	8.5	22.0	12.8	32.1	16.6
3,4,5-trimethoxytoluene	S2	0	0	0	0	4.7	4.7	0	0	0	0	0	0
1-(3-methoxy-4-hydroxyphenyl)-3-propene	G21*	0	0	0	0	2.7	2.7	0	0	0	0	0	0
3-methoxy-4-hydroxyacetophenone	G5*	10.9	10.9	0	0	13.6	6.9	0	0	0	0	9.9	5.1
3-methoxy-4-hydroxybenzoic acid methyl ester	G6*	6.3	6.3	0	0	7.2	7.2	16.1	5.5	0	0	4.8	4.8
3-methoxy-4-hydroxybenzoic acid	G6**	6.3	6.3	0	0	0	0	0	0	0	0	0	0
3,4-dimethoxyacetophenone	G5	7.8	7.8	0.9	0.9	11.0	4.1	7.4	3.7	5.8	5.8	16.8	5.1
3,4-dimethoxybenzoic acid methyl ester	G6	42.7	13.8	15.9	8.0	41.6	14.7	59.2	16.0	55.4	17.4	94.0	40.7
3,4-dimethoxybenzeneacetic acid methyl ester	G24	0	0	0	0	0	0	3.9	3.9	0	0	12.4	6.2
2-Propenoic acid, 3-(4-methoxyphenyl) methyl ester (E)-	P18	5.0	3.0	1.5	1.5	6.7	2.7	8.8	2.4	8.3	2.6	10.3	5.3
1-(3,5-dimethoxy-4hydroxyphenyl)-3-propene	S21*	4.4	4.4	0	0	3.1	3.1	0	0	0	0	0	0
3,4,5-trimethoxyacetophenone	S5	0	0	0	0	0	0	16.4	12.7	0	0	10.1	5.1
3,4,5-trimethoxybenzoic acid methyl ester	S6	0	0	0	0	0	0	20.0	11.0	6.7	6.7	43.8	22.0
3,4,5-trimethoxybenzoic acid	S6*	0	0	0	0	24.9	14.9	0	0	0	0	0	0
4-hydroxy-3,5-dimethoxyacetophenone	S5*	6.3	4.6	0	0	11.6	6.2	0	0	0	0	2.3	2.3
4-hydroxy-3,5-dimethoxybenzoic acid hydrazide		17.1	10.9	0	0	13.0	7.3	0	0	4.4	4.4	14.5	7.3
2-propenoic acid, 3-(3-methoxy-4-hydroxyphenyl) methyl ester	G18*	16.8	10.5	0	0	6.7	3.4	0	0	3.1	3.1	0	0
2-propenoic acid, 3-(3,4-dimethoxyphenyl) methyl ester	G18	10.9	5.9	10.4	2.2	5.8	3.7	9.1	2.9	8.4	3.6	12.1	6.1
2-propenoic acid, 3-(3,4,5-trimethoxyphenyl) methyl ester	S18	0	0	0	0	0.9	0.9	0	0	0	0	0	0

In this study, not all lignin phenols detected using TMAH/GC-MS were completely methylated to the methyl ether or ester. These compounds are denoted with * after the abbreviated product name in results tables 3.4, 3.5, and 3.6, indicating that they contain unmethylated hydroxyl groups. ** refers to compounds containing two unmethylated hydroxyl groups. Six phenols were identified in the six water samples by FD extraction and detection with TMAH/GC-MS (table 3.4). P1* was detected at TRT, JC, and ODC sites and was the most abundant phenol at concentrations of 1271, 840, and 3221 μg (100 mg OC)⁻¹, respectively. The phenol detected at lowest concentration was Gx at 1.9 μg (100 mg OC)⁻¹ at site ODC. No single phenol was detected at all six sites using FD extraction and TMAH/GC-MS analysis, and no lignin phenols were detected at site St. There were representatives of P, G, and S type lignin phenols, and side chain lengths ranged from zero to two carbons, with hydroxyl, alkyl, and carboxyl functional groups.

Four phenols were identified in the six water samples following SPE and detection with on-column GC-FID (table 3.5), and they were all benzoic acids (P6, G6, G6^{me}, and S6) with different degrees of substitution on the phenyl ring. The highest concentrations were detected at site TBF with P6 greatest, followed by G6^{me} and G6 phenols at 38.8, 3.4, and 3.6 μg (100 mg OC)⁻¹, respectively. No lignin phenols were detected at sites St or RT.

Considerably more phenol compounds were identified at all six sites after SPE extraction and TMAH/GC-MS detection (table 3.6) than any other combination of extraction and analysis technique, with P, G, and S monomer types present. Carbon side chains ranged from zero to three carbons in length, with functional groups including alkyl, alkenyl, ketone, aldehyde, and carboxyl groups. P1* was detected at highest concentration at site TBF (153 μg (100 mg OC)⁻¹), and was the most abundant phenol at all sites except St.

3.4 Discussion

The hypothesis tested in this experiment were that FD extracts a greater concentration water-transportable lignin-derived compounds from natural fresh water samples than SPE (H1), and that TMAH/GC-MS analysis detects greater concentration, albeit less original macromolecular structure, of water-borne lignin than GC-FID of TMS derivatives (H2). The following discussion leads to the rejection of H1 because of the inconsistency of FD, and acceptance of H2 because greater total lignin phenol

concentrations with a greater range of side chain structure were detected using TMAH/GC-MS, concluding that SPE followed by TMAH/GC-MS is the best extraction and detection technique combination from the approaches tested.

3.4.1 *Extracted WBM yields*

Greater concentration of WBM was expected for FD than SPE since FD should not selectively extract any compounds, i.e. all water-borne material (dissolved and particulate organic and inorganic matter) should be recovered. However, greater recovery with FD was only achieved at sites TBF and St (table 3.2), and the extract recovered from all sites contained a large proportion of inorganics (table 3.3). Previous research using low-temperature, low pressure evaporation and freeze-drying to extract natural waters also discovered comparable low percentage TOC values by weight in the extract, and was attributed to substantial contribution of salts to the weight of total dissolved solids (Frazier et al., 2003). Comparison of figures 3.7A, B and C indicates that water TOC concentration, as a function of WBM, is more closely represented by SPE extraction than FD extraction. C₁₈ SPE selectively extracted compounds such as lignin degradation products, carbohydrate derived material, and FAMES. The mean pore diameter of the solid phase (73 Å; 0.0073 µm) only extracts dissolved compounds, defined as molecules < 0.45 µm (Michalzik and Matzner, 1999, Kalbitz et al., 2000). Thus, material not recovered comprised either compound classes that do not sorb to the C₁₈ solid phase, or was in the form of colloids or particulates > 0.0073 µm in diameter, and therefore would not have been able to pass through the SPE cartridge and remained as a layer on the upper surface of the sorbent bed.

3.4.2 *Extraction of lignin phenols from water*

Greater normalised total lignin phenol concentrations were extracted by FD than SPE at sites TRT, JC, and ODC following detection with TMAH/GC-MS (figure 3.8), although greater concentrations were extracted by SPE at sites TBF, St, and RT. The large standard error bars associated with FD suggest that SPE is more reproducible and lignin phenols were detected at all six sites, therefore H1 was rejected. Previous research has shown that C₁₈ recovered 101 ± 4% of lignin derived phenols compared with direct dry-down of freshwater samples (Louchouart et al., 2000), indicating that it achieves good recovery of lignin phenols and is repeatable.

Total lignin phenol concentrations extracted using low-temperature, low-pressure evaporation and freeze-drying and detected using TMAH/GC-MS ranged from 0.15 to

0.49 mg (100 mg OC)⁻¹ for river waters from differing climates and land uses (Frazier et al., 2003), which are comparable to the TBF site (0.10 ± 0.08 mg (100 mg OC)⁻¹) in this study, although Frazier *et al.* (2003) detected considerably more lignin phenols from all of their sites.

Carbon normalised total lignin concentrations extracted with SPE and detected using TMAH/GC-MS for sites St, TRT, JC, RT, and ODC were comparable to total lignin phenol (*A*₈) concentrations in another study. Between 0.16 – 0.42 mg (100 mg OC)⁻¹ was extracted using C₁₈ SPE and analysed by CuO oxidation for water samples collected from organic rich blackwater in the Florida Everglades and the organic rich Penobscot River, Maine, New England (Spencer et al., 2010).

Total lignin concentrations extracted with SPE and detected using GC-FID were 3.05 ± 1.53, 0, 0.06 ± 0.06, 0.11 ± 0.11, 0, and 0.04 ± 0.04 µg L⁻¹ for sites TBF, St, TRT, JC, RT, and ODC respectively, all of which are considerably lower than total lignin concentration of 10.6 ± 0.7 µg L⁻¹ in river water (Nueces River, Texas) of another study, also extracted using C₁₈ SPE followed by CuO oxidation (Louchouart et al., 2000). However, our samples analysed using TMAH/GC-MS yielded total lignin concentrations of 61.2 ± 33.4, 0.42 ± 0.20, 30.97 ± 17.23, 41.81 ± 8.91, 11.10 ± 6.19, 19.68 ± 6.64 µg L⁻¹ for sites TBF, St, TRT, JC, RT, and ODC respectively.

Comparison of FD and SPE extracted individual lignin phenols detected using TMAH/GC-MS (tables 3.4 and 3.6, respectively) shows that SPE extracted considerably more lignin phenol compounds than FD. Also, phenols extracted by FD were generally detected at higher concentration than the same phenol compound extracted by SPE from the same water sample using the same detection technique. For example, P1* extracted by FD was detected at 3221 µg (100 mg OC)⁻¹ in the ODC sample (table 3.4), whereas for the same sample SPE extracted (table 3.6) it was detected at 103 µg (100 mg OC)⁻¹. P2 was detected at similar concentrations: 100 ± 77 µg (100 mg OC)⁻¹ FD extracted, and 81 ± 49 µg (100 mg OC)⁻¹ after SPE extraction. Furthermore, no more than three phenols were detected by TMAH/GC-MS from any single site using FD extraction and there was less consistency between FD water samples than SPE in terms of phenols present. Therefore, SPE was relatively better than FD at extracting water-borne phenols.

3.4.3. Detection of lignin phenols extracted from water samples

More lignin phenols were detected using TMAH/GC-MS than GC-FID, whether FD or SPE extracted, in terms of summed total lignin phenol concentration (figure 3.8), and

number of phenol compounds detected (tables 3.4, 3.5, and 3.6). A greater range of phenol side chain structure was detected by TMAH/GC-MS than GC-FID, therefore H2 was accepted.

No lignin phenols were detected in FD extracted WBM via GC-FID analysis (figure 3.8A). This may be due to the low total carbon content, thus low lignin content of FD extracted WBM. The WBM residue from FD was barely soluble in pyridine prior to derivatisation with BSTFA, which may have led to incomplete derivatisation of the phenols. Organic matter may have been physically protected by encapsulation within the residue or crystal lattice structure of salts, due to the high proportion of inorganics. Even after reaction with BSTFA the residue remained, therefore the proportion of successfully derivatised lignin products could not be known. It is possible that trace levels of phenols below detection limits for on-column GC-FID analysis were successfully derivatised into TMS esters and ethers. Alternatively, the lignin phenols in the water samples were in a dimer, trimer, or oligomeric form. These may have been undetected using GC-FID or unrecognisable using normal GC-MS due to a lack of authentic lignin phenol oligomer standards or having too high a molecular weight beyond the maximum m/z limit of the MS detector ($> m/z$ 700) to get an accurate mass spectrum. In another study, virtually no GC or GC-MS chromatographic responses were also observed in DOM samples extracted by cation exchange followed by FD and derivatised with BSTFA, leading to the suggestion that DOM constituents were in polymeric or oligomeric forms (Huang et al., 1998). TMAH/GC-MS analysis successfully detected FD extracted lignin phenols (table 3.4) which could be due to the higher temperatures (610 °C) involved in this technique that may have been able to volatilise the FD residue releasing the lignin phenols. Any oligomers would be depolymerised by cleavage of β -O-4 linkages into their constituent phenols upon reaction with TMAH (see figure 3.3) facilitating their identification.

In this study, lignin phenols detected using TMAH/GC-MS were not always completely methylated to the methyl ether or ester, which has also been observed in another study (Klingberg et al., 2005). Methylated and unmethylated analogues of P1, G1, and S6 extracted with FD and detected with TMAH/GC-MS in this study (table 3.4) were only detected as the fully methylated derivatives in another study (Huang et al., 1998). In addition they detected P6, G6, G12, and G18 from an upland grassland site sampled in spring, and furthermore G4, but no P18 from the same site sampled in autumn. Frazier et al. (2003) using a combination of low-temperature, low pressure evaporation and

freeze-drying extraction followed by TMAH/GC-MS analysis detected P3, G1, P4, S1, P5, G3, P6, S2, G4, G5, G6, S5, and S6 from river waters of differing land uses and climates. Concentrations from a temperate stream at White Clay Creek, PA encompassing all these products ranged from 2.51 – 23.4 µg/100 mg OC.

SPE extracted lignin phenol hydroxyl groups were derivatised to completion with BSTFA to their respective trimethylsilyl ethers and esters prior to GC-FID analysis, although only four compounds were detected using this combination of extraction and analysis techniques (table 3.5). G6^{me} could either be a lignin phenol partially degraded by microbes such as brown-rot fungi (Kirk and Adler, 1969, Kirk et al., 1970) or tannin derived (Jin et al., 1990, Filley et al., 2000, Kogel-Knabner, 2002, Filley et al., 2006, Nierop and Filley, 2008). TMAH/GC-MS would not have detected this compound unless ¹³C-labelled TMAH was used, since with unlabelled TMAH it would be detected as G6 (3,4-dimethoxybenzoic acid, methyl ester) (Filley et al., 2006), assuming that TMAH derivatisation went to completion. SPE extracted G6 (3,4-dimethoxybenzoic acid, methyl ester) was detected by TMAH/GC-MS at all six sites (table 3.6), although derivatisation with BSTFA revealed that at sites TBF, TRT, JC, and ODC a proportion of the compound detected as 3,4-dimethoxybenzoic acid, methyl ester by TMAH/GC-MS was in fact present as 3,4-dihydroxybenzoic acid in the original water sample. This highlights an advantage of derivatisation with BSTFA being able to detect original molecular structure of water-borne phenols compared to TMAH.

The standard errors of the mean reported in this study are larger than the errors reported in other studies that have either used SPE extraction (Louchouart et al., 2000), and detection of lignin phenols using TMAH/GC-MS from water samples (Frazier et al., 2003) and in soil samples (Mason et al., 2009, Mason et al., 2012). Perhaps the combination of SPE and on-line TMAH/GC-MS may lead to large errors, although a lack of literature using the extraction and detection techniques in this study prevents error comparison. Furthermore, water sample collection in this study occurred in May, July, and January in order to incorporate a wide range of dissolved lignin concentrations, therefore the effect of seasonality was incorporated into the DOM samples. This would increase the variance in the data without necessarily being due to error during sample processing or analysis.

3.5 Conclusions

Whilst FD extraction recovered a greater concentration of lignin phenols than SPE from half of the water samples, SPE was more consistent at extracting phenols and more selective at extracting organic compounds from all of the water samples. Additionally, more phenol compounds were detected following SPE than FD for a given analysis technique, therefore H1 was rejected, and SPE was selected as the best extraction technique.

Analysis of extracted phenols using TMAH/GC-MS led to greater concentration of summed lignin phenols detected for both extraction techniques, therefore H2 was accepted. SPE combined with TMAH/GC-MS enabled detection of a wide array of P, G, and S type lignin phenols exhibiting a variety of side chain structures from zero to three carbons in length with alkyl, alkenyl, ketone, aldehyde, and carboxyl functional groups, therefore this was selected as the best approach to extract water-borne phenols in the experiments described in Chapters 4, 5, and 6.

Chapter 4. Investigation of leaf litter lignin decomposition and subsequent loss as dissolved organic matter over time in a model system

4.1 Introduction

In the development of traditional models describing soil organic carbon (SOC) dynamics in order to better understand the relationship between soil carbon processes and climate change or crop production and to make predictions, components of SOC have been allocated into different compartments, or pools. This allocation has been based on their turnover time in pools such as: decomposable plant material, resistant plant material, soil biomass, physically stabilised organic matter, and chemically stabilized organic matter; young and old carbon (C); structural C, metabolic C, active soil C, slow soil C, or passive soil C; or variations thereof (Jenkinson and Rayner, 1977, Parton et al., 1988, Andren and Katterer, 1997, Coleman et al., 1997, Bruun et al., 2003). This approach of allotting biological inputs or classes of molecules to a particular pool of SOC, or defining the resistance of SOC to decomposition based solely on its chemical structure, has recently been disputed in favour of factors pertaining to its accessibility to decomposer organisms and/or their enzymes, and environmental conditions such as soil moisture and temperature (Gleixner et al., 2002, Dungait et al., 2012b). Where substrates including plant litter and soil C *are* accessible to decomposition enzymes, rates of decomposition increase exponentially with increasing temperature, at least between 20 – 35 °C, in agreement with classical reaction kinetics (Davidson and Janssens, 2006, Wallenstein et al., 2012, Wang et al., 2012a). However, there is evidence to suggest that initial increases in soil microbial respiration rates at elevated temperature may not persist long-term due to reduced observed mass-specific respiration rates when seasonal temperatures were higher, possibly due to acclimation of the metabolism of soil microbes (Bradford et al., 2008). Furthermore, it has been hypothesized that the composition of the microbial community changes with increasing temperature, enabling dominant populations to metabolize substrates not utilized by the microbial community at lower temperatures (Zogg et al., 1997). Other research observed remarkably constant organic carbon decomposition rates in forest soils on five continents with varying mean annual temperature (Giardina and Ryan, 2000). Lack of a general consensus of the temperature dependence of organic matter decomposition may be due to confounding factors such as different experimental conditions such as

substrate availability, management history, soil water limitations, and root respiration (Kirschbaum, 2006).

The magnitude of the increasing rate of decomposition with temperature is described by the Q_{10} parameter, which is defined as the factor by which the rate increases with an increase in temperature of 10 Kelvin (K) (Davidson and Janssens, 2006), however, there is evidence to suggest Q_{10} parameters in nature decrease with increasing temperatures (Tjoelker et al., 2001). Understanding the temperature dependence of the rate of SOC reactions and processes is important in order to determine the effect of global warming on soil C storage (Bol et al., 2003). The relative sensitivity to temperature of microbial assimilation rate (u) of a substrate can be shown as:

$$\frac{\partial \ln u}{\partial T} = \frac{-|\Delta G^0|}{RT^2q} \quad \text{Equation 4.1}$$

Where ΔG^0 is the Gibbs free energy at standard temperature and pressure, R is the universal gas constant, T (K) is absolute temperature, and q is the substrate quality, which has been defined as the number of enzymatic steps required to convert a C atom from an organic compound to CO_2 , with 1 being the maximum possible quality (Bosatta and Agren, 1999). A consequence of equation 4.1 is that: (i) temperature sensitivity of the rate of decomposition of a substrate increases as the substrate quality decreases (Bosatta and Agren, 1999), i.e. that low quality substrates should decompose more rapidly upon warming than high quality substrates, which has been observed in forest soils (Bol et al., 2003), grassland soils (Conant et al., 2008), and cultivated soils (Hartley and Ineson, 2008). Microbial respiration of old soil carbon (> 14 years) was greater at higher temperatures (20 and 35 °C) compared to lower (5 °C) temperature (Waldrop and Firestone, 2004), although there is evidence to suggest decomposition of old SOC in boreal forest soils is resistant to temperature changes (Liski et al., 1999); and (ii) the rate of degradation of a substrate is more temperature sensitive at lower temperatures, particularly for low quality substrates (Bosatta and Agren, 1999). Furthermore, it has been hypothesized that variation in temperature sensitivity also plays a strong role in adsorption and desorption of SOC (Conant et al., 2011).

Research has shown that lignin is not necessarily preserved in soils, for example intact lignin has been detected at lower abundance than amino acids in the mineral layer of grassland soils of low pH (van Bergen et al., 1998) as well as forming part of the resistant portion of SOC (Martin et al., 1980). Conflicting evidence of the relative

stability of lignin has led to the development of a two-reservoir model describing its behaviour in soil (Rasse et al., 2006). A field microcosm experiment showed warming increased the relative abundance of the lignin-degrading enzymes polyphenol oxidase and peroxidase and suggested that there would be enhanced depletion of recalcitrant C pools (including lignin) over labile C pools with warming, in agreement with equation 4.1; however, lignin concentrations were not measured directly in this study (Wang et al., 2012b). Decreasing lignin phenol acid/aldehyde ratios associated with clay particles were observed with increasing mean annual temperature, indicating decreased degree of lignin decomposition with increasing temperature (Amelung et al., 1999). Another study using artificial soils and model compounds found that the rate of lignin degradation was not temperature sensitive (Zhang et al., 2011), whereas slightly increased, but not significant, lignin turnover rates have been observed with increasing temperatures in grassland soils (Feng and Simpson, 2008). Moreover, increasing temperature has been shown to exponentially increase the rate of dissolved organic carbon (DOC) production ($Q_{10} = 1.7$) in forest soils, at least between the temperature range: 3 – 28 °C (Christ and David, 1996, Kalbitz et al., 2004), but also to have no effect on DOC production in other forest soils (Froberg et al., 2013). Increased riverine DOC concentration has been observed over a period of 29 years with increasing temperatures (Worrall et al., 2003). Therefore, uncertainty remains regarding the susceptibility of lignin to decomposition in soils, and the influence of temperature on its rate of loss from soil by leaching as a component of DOC. Furthermore, lignin degradation is also monomer specific (Bahri et al., 2006, Dungait et al., 2008), and passage of lignin through soil in the dissolved phase can fractionate lignin degradation products through the processes of adsorption and desorption (Hernes et al., 2007).

In summary, although there is evidence to support increased rate of SOC decomposition with increasing temperature, the evidence is less clear or absent with regard to the effect of temperature on lignin decomposition, dissolved lignin production, and subsequent leaching. Therefore the overarching hypothesis tested in this experiment was that total lignin phenol concentrations determined in leachate increase with increasing topsoil temperature. The experiment aims to investigate the effect of seasonal temperature on the combined processes of lignin degradation and subsequent transport at the compound specific level in order to determine losses of lignin from the soil C sink in leachate.

A range of angiosperm species were chosen for this study (described in Chapter 2, section 2.2): a mixed grass sward, *Ranunculus repens* (Creeping Buttercup), *Fraxinus*

excelsior (Ash), and *Quercus robur* (Common Oak), because of their potential as indicator species of different land-uses in the UK, particularly with respect to soil carbon sequestration and food security.

Thermally assisted hydrolysis and methylation using tetramethylammonium hydroxide (TMAH/GC-MS) has been used widely for the detection and characterisation of lignin in plants (Clifford et al., 1995, Robertson et al., 2008a, Klotzbucher et al., 2011a), soils (Mason et al., 2009, Mason et al., 2012) and waters (Huang et al., 1998, Frazier et al., 2003), and it is described in Chapter 2 section 2.7.2. In plant tissues, it can be used to distinguish three types of material: angiosperm wood, gymnosperm wood, and non-woody angiosperm according to the proportions of monomethoxyphenyl, dimethoxyphenyl, trimethoxyphenyl, and analogs of cinnamyl monomer units (Clifford et al., 1995).

4.1.1 Experiment aims and hypothesis

The aims of this experiment were: (i) to characterise the lignin phenols in fresh and degraded litter (mixed grass sward, *R. repens*, *F. excelsior*, and *Q. robur*) and their leachates representing different land use types and to determine the dominant form of lignin moving through soils and into water courses for each, and (ii) to determine the effect of seasonal temperature on lignin phenols leached from topsoil below each vegetation through time.

Hypotheses

H3. Dominant lignin phenols found in topsoil leachate DOM are the same as those in the source litter type.

H4. Total lignin concentrations determined in leachate increase with increasing topsoil temperature.

4.2 Methodology

4.2.1 Experimental Design

Collected leaf litter samples were applied to lysimeters using a randomised block design (4 treatments + Control (soil only) x 4 reps = 20 lysimeters total) as shown in table 4.1 and figure 4.1.

Table 4.1. Randomised block experimental design showing the allocation of treatments to packed soil cores.

Block 1	Mixed grass	<i>R. repens</i>	<i>F. excelsior</i>	Control	<i>Q. robur</i>
Block 2	<i>F. excelsior</i>	Mixed grass	<i>Q. robur</i>	<i>R. repens</i>	Control
Block 3	<i>R. repens</i>	Control	<i>F. excelsior</i>	Mixed grass	<i>Q. robur</i>
Block 4	<i>F. excelsior</i>	Control	Mixed grass	<i>Q. robur</i>	<i>R. repens</i>



Figure 4.1. Experiment setup showing lysimeters with decomposing plant litter on packed soil cores with an overhead irrigation system, and provision for leachate collection below the trolleys.

4.2.2 Field sampling

Leaf litter vegetation samples were collected from the sites described in Chapter 2, table 2.1, using the approach described in Chapter 2, section 2.2 and four of the five replicates collected were used in a randomised block design (table 4.1). Subsamples of the four leaf litter types were freeze-dried (Edwards Super Modulyo), to determine the dry matter content, then ball milled as described in Chapter 2 section 2.6.1. Dried and ground litter samples were then characterised for total C, total N (table 4.2), ^{13}C and ^{15}N contents, and lignin using TMAH/GC-MS, as described in Chapter 2, sections 2.6.4 and 2.7.2, respectively.

Approximately half a ton of well drained brown earth topsoil that was previously permanent pasture (Chapter 2, table 2.1) was collected from Bicton College (Bicton Farm Manager, *personal communication*).

4.2.3 Lysimeter preparation, sampling and analysis

Soil preparation, lysimeter and soil core preparation, application of leaf litter to lysimeters, irrigation to maintain background levels of moisture to support microbial activity, and leachate sampling is described in Chapter 2, section 2.5 and 2.5.1.

Leachates were acidified to pH 2 to measure TOC as described in Chapter 2, section 2.6.2, prior to SPE as described in section 2.6.3. Dried extracted DOM was analysed by TMAH/GC-MS to characterise the lignin as described in Chapter 2, section 2.7.2. At the end of the experiment the vegetation was characterised again for total C, total N, ^{13}C , and lignin by TMAH/GC-MS.

4.2.4 Statistical analysis

The data was analysed for statistical differences as described in Chapter 2, section 2.9. Additionally, a two-sample t-test was used to compare differences between the following parameters in litter vegetation: litter % mass loss, % carbon mass loss, % nitrogen mass loss, and % lignin mass loss, within the same leaf litter type. Replication was 4 for vegetation analysis and 3 for leachate analysis due to the greater number of leachate samples collected.

4.3 Results

Undegraded *Q. robur* had the highest DM and total C (25.5 and 49%, respectively, table 4.2) and *R. repens* had the lowest DM, total C, and highest total N (12.6%, 40.5%, and 4.13%, respectively). The total C values (table 4.2) were used to determine the mass of each litter type to apply to lysimeters (Chapter 2, section 2.5).

Table 4.2. Characterisation of freeze-dried undegraded litters applied to lysimeters, comprising leaf and shoots showing mean and standard error of the mean (s.e., n = 4).

Litter type	Dry Matter (%)	s.e.	Total C (% of DM)	s.e.	Total N (% of DM)	s.e.
Mixed grass	16.3	1.1	43.75	0.46	1.94	0.10
<i>R. repens</i>	12.6	0.5	40.50	0.53	4.13	0.22
<i>F. excelsior</i>	22.1	1.3	47.08	0.18	1.43	0.04
<i>Q. robur</i>	25.5	1.0	49.09	0.28	1.56	0.05

4.3.1 Bulk fresh and degraded litter

R. repens showed the greatest mass loss for TOC, TN, total lignin, and litter biomass (figure 4.2). There were significant differences between litter types for litter % mass loss, % carbon mass loss, and % nitrogen mass loss (F pr. = < 0.001 for all three): where mixed grass was similar to *F. excelsior*, which were different from *R. repens*, which was different from *Q. robur* (see figure 4.2 for statistical groupings labelled as lower case letters above columns). There was no significant difference in % lignin mass loss between litter types (F pr. = 0.096). The two-sample t-test revealed significant differences, also shown in figure 4.2, within mixed grass between % carbon mass loss and litter % mass loss ($P = < 0.001$) and between % carbon mass loss and % nitrogen mass loss ($P = 0.016$). For *R. repens* there were no significant differences. For *F. excelsior* there were significant differences between % carbon mass loss and % nitrogen mass loss ($P = 0.006$) and litter % mass loss and % nitrogen mass loss ($P = 0.047$). For *Q. robur* there were significant differences between % carbon mass loss and litter % mass loss ($P = 0.002$), % carbon mass loss and % nitrogen mass loss ($P = 0.005$), and litter % mass loss and % nitrogen mass loss ($P = 0.019$).

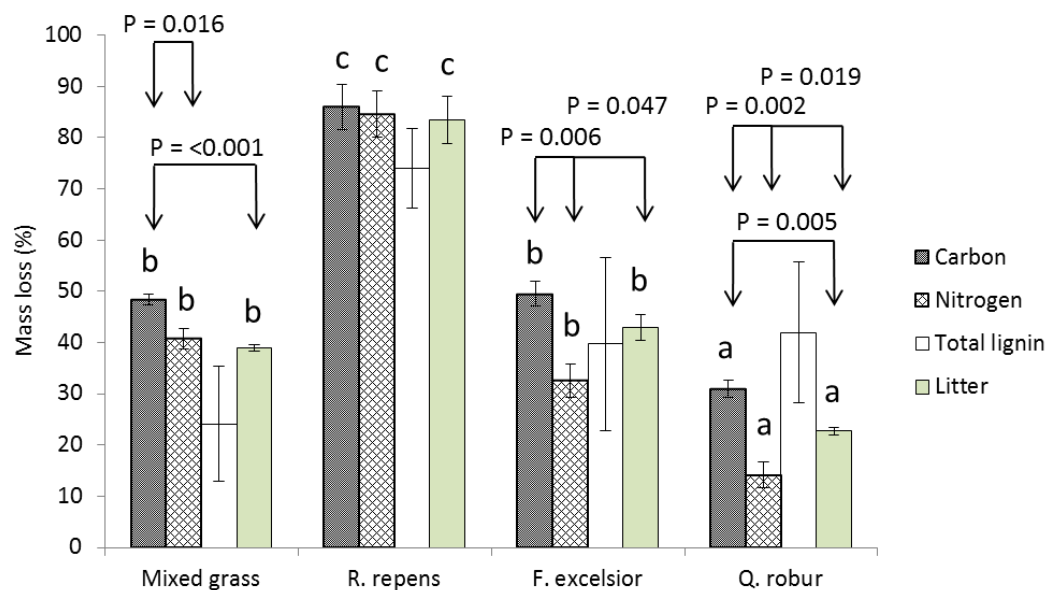


Figure 4.2. Percentage (%) mass loss (\pm standard error of the mean; $n = 4$) for parameters: total organic carbon, total nitrogen, total lignin, and litter biomass from initial undegraded vegetation after 671 days of decomposition for mixed grass, *Ranunculus repens*, *Fraxinus excelsior*, and *Quercus robur*. Litter types are grouped (a, b, or c) to show significant differences (FPLSD test) for the same parameter. P values highlight significant differences (two-sample t-test) between parameters for the same litter type.

4.3.2 Lignin phenols in fresh and degraded litter

Table 4.3 reports the lignin phenols and aromatic carboxylic acids detected in fresh mixed grass, *R. repens*, *F. excelsior* and *Q. robur* litter, and their molecular structures are shown in figure 1.10. Relatively dominant lignin phenols compared to other litter types, with significant differences (F pr. values), for mixed grass were: P6 (F pr. = 0.003), P18, and G18. In *R. repens*, there were no relatively dominant lignin phenols compared to other litter types although it was statistically different from mixed grass in G18 (F pr. = 0.042). In *F. excelsior*, relatively dominant lignin phenols were: P24* and G18. In *Q. robur*, relatively dominant lignin phenols were: P2, G2, S1, S2, G4, and S6 (F pr. = 0.004). G18 was a dominant lignin phenol in mixed grass and *F. excelsior* litters (figure 4.5 below and table 4.3) and there were multiple significant differences between litter types (F pr. = 0.042): The FPLSD test revealed that: mixed grass was significantly different from *R. repens* and *Q. robur*, and *F. excelsior* was significantly different from *Q. robur*.

Table 4.3. Mean (\pm standard error of the mean (s.e.), $n = 4$) normalised lignin phenol concentrations and aromatic carboxylic acids (/100 mg OC) from TMAH/GC-MS analysis of fresh mixed grass, *Ranunculus repens*, *Fraxinus excelsior*, and *Quercus robur*. Total lignin (sum of compounds: 1,2,4,5,6,8,9,11-29) and acid/aldehyde ratios for compounds 21/18 (G6/G4 ratio) and compounds 27/22 (S6/S4 ratio) are also reported.

compound no.	Compound	$\mu\text{g (100 mg OC)}^{-1}$							
		Mixed grass	s.e.	<i>R. repens</i>	s.e.	<i>F. excelsior</i>	s.e.	<i>Q. robur</i>	s.e.
1	methoxybenzene (P1)	75.5	14.8	80.8	19.7	81.8	8.0	133.9	76.5
2	4-methoxytoluene (P2)	72.1	9.3	93.8	26.8	67.8	11.0	310.0	205.7
3	benzoic acid, methyl ester	0	0	0	0	39.8	15.4	0	0
4	4-methoxyethylbenzene	11.7	1.7	19.8	4.4	19.9	10.3	14.1	4.9
5	1,2-dimethoxybenzene (G1)	27.8	4.3	59.9	18.7	58.3	11.3	69.0	47.6
6	4-methoxybenzeneethylene (P3)	69.2	6.7	18.4	3.7	44.8	16.0	93.2	53.4
7	benzeneacetic acid methyl ester	18.2	4.9	0	0	0	0	0	0
8	3,4-dimethoxytoluene (G2)	20.7	4.9	11.3	11.3	33.8	8.1	416.2	253.7
9	4-methoxybenzaldehyde (P4)	0	0	0	0	0	0	0	0
10	benzenepropanoic acid methyl ester	6.3	3.7	0	0	0	0	0	0
11	1-(4-methoxyphenyl)-3-propene (P21)	5.9	1.2	0	0	0	0	0	0
12	1,2,3-trimethoxybenzene (S1)	35.8	6.1	48.2	14.5	50.2	15.1	131.5	67.0
13	3,4-dimethoxyethylbenzene (Gx)	4.7	4.7	9.7	1.9	6.0	3.1	59.0	26.3
14	4-methoxybenzeneacetic acid (P24)	0	0	0	0	63.5	38.3	0	0
15	3,4-dimethoxybenzeneethylene (G3)	280.5	54.0	122.3	40.6	215.7	60.4	331.5	165.9
16	4-methoxybenzoic acid methyl ester (P6)	98.4	23.8	24.4	6.6	26.9	10.5	0	0
17	3,4,5-trimethoxytoluene (S2)	11.7	4.7	17.1	5.6	10.7	4.4	87.5	54.8
18	3,4-dimethoxybenzaldehyde (G4)	31.0	3.1	6.1	3.6	33.8	11.6	87.0	48.2
19	1-(3,4-dimethoxyphenyl)-3-propene (G21)	8.9	3.6	0	0	18.5	3.8	71.2	41.9
20	3,4-dimethoxyacetophenone (G5)	37.7	11.2	0	0	63.4	18.3	55.8	32.4
21	3,4-dimethoxybenzoic acid methyl ester (G6)	30.7	5.8	44.7	14.1	62.2	24.3	107.3	51.9
22	3,4,5-trimethoxybenzaldehyde (S4)	13.8	1.9	0	0	28.1	14.6	38.4	20.2
23	3,4-dimethoxybenzeneacetic acid methyl ester (G24)	0	0	0	0	15.2	8.3	0	0
24	1-(3,4,5-trimethoxyphenyl)-3-propene	2.2	0.8	0	0	51.4	21.6	105.2	56.3
25	2-Propenoic acid, 3-(4-methoxyphenyl) methyl ester (E)- (P18)	176.0	16.1	8.4	3.4	43.7	16.0	219.2	120.8
26	3,4,5-trimethoxyacetophenone (S5)	24.3	2.7	10.0	2.3	13.4	7.0	41.8	14.4
27	3,4,5-trimethoxybenzoic acid methyl ester (S6)	36.4	7.7	9.8	2.7	20.2	12.3	250.1	78.8
28	2-propenoic acid, 3-(3,4,5-trimethoxyphenyl)- (E)- (S18)	0	0	0	0	0	0	0	0
29	2-propenoic acid, 3-(3,4-dimethoxyphenyl) methyl ester (G18)	290.6	43.7	66.2	12.4	273.6	127.8	30.6	16.3
	Total lignin	1366.0	188.7	651.0	171.0	1302.7	378.8	2652.4	1362.9
	G6/G4 ratio	1.0	0.01	7.3	0.02	1.8	0.04	1.2	0.1
	S6/S4 ratio	2.6	0.01	0	0	0.7	0.03	6.5	0.1

Total lignin concentrations (figure 4.3) were determined as the sum of compounds 1, 2, 4, 5, 6, 8, 9, 11-29 defined in table 4.3 that are lignin phenols detected in fresh and degraded litter after 671 days.

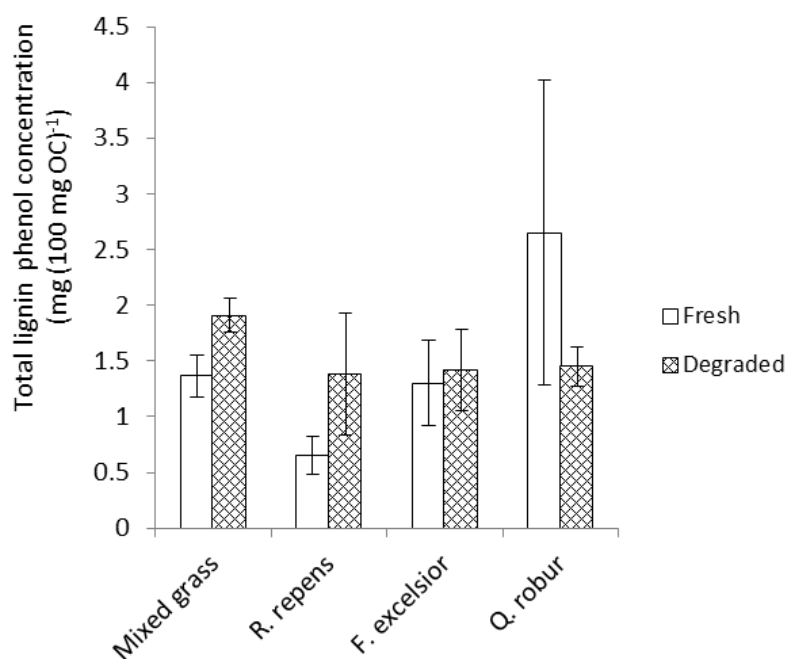


Figure 4.3. Mean (\pm standard error of the mean, $n = 4$) total lignin phenol concentrations normalised to TOC for fresh and decomposed (after 671 days) leaf litter.

There were no significant differences in total lignin concentrations between litter types in fresh or degraded litter ($F_{pr.} = 0.278$ and 0.701 , respectively), nor between undegraded and degraded litter of the same type. This suggests that lignin was not preferentially degraded nor preserved with respect to litter bulk organic carbon.

Concentrations of individual lignin phenol data (individuals, table 4.3) and litter type (variates) are displayed in a principal component biplot with first and second components on the x and y axis, respectively, for fresh and degraded litter (figure 4.4). Phenols positioned in the same line as a litter type have a strong association with that sample.

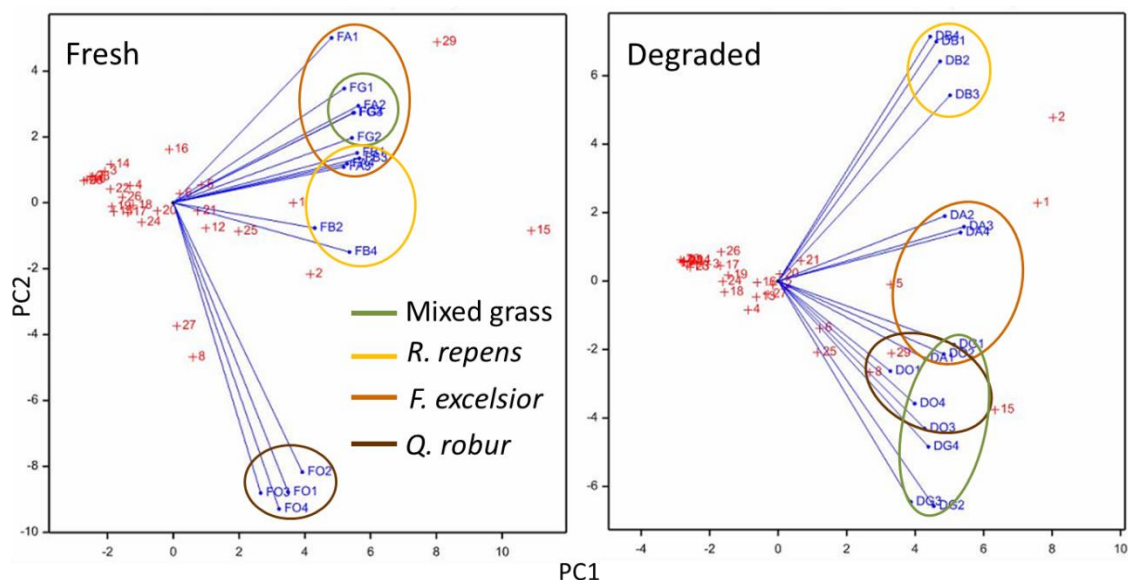


Figure 4.4. A principal component biplot of first and second components of individuals (individual lignin phenol concentrations, shown in red, defined in table 4.3), and variates (mixed grass, *Ranunculus repens*, *Fraxinus excelsior*, and *Quercus robur* litter samples, shown in blue), for fresh and degraded litter.

The fresh litter biplot clearly shows *Q. robur* is spatially distinct from the other litter types. The mixed grass region plotted within the *F. excelsior* region, whereas the *R. repens* region is almost separated from *F. excelsior*. Associated with fresh *Q. robur* were: S6 and G2. The concentration of S6 in fresh *Q. robur* was significantly different from other fresh vegetation types (F pr. = 0.004). For the mixed grass and *F. excelsior* regions, G18 was strongly associated. Lignin phenols associated with the *R. repens* region appeared to be: P1, P2, and G6. However none were more abundant in fresh *R. repens* than other vegetation types (table 4.3). P18 and G3 that also appeared in the *R. repens* region were less abundant in fresh *R. repens* than other fresh vegetation types, so may be associated with *R. repens* by negative association, or because these two compounds were more abundant in mixed grass and *Q. robur* and were therefore placed between the mixed grass and *Q. robur* regions rather than by association with *R. repens*.

Figure 4.5 shows the difference in concentration between fresh and decomposed litter for mixed grass, *R. repens*, *F. excelsior*, and *Q. robur* for those lignin phenols that are significantly different between litter types. Significant differences are reported in the text below. Table 4.4 reports the lignin phenols and aromatic carboxylic acids detected in degraded mixed grass, *R. repens*, *F. excelsior* and *Q. robur* litter.

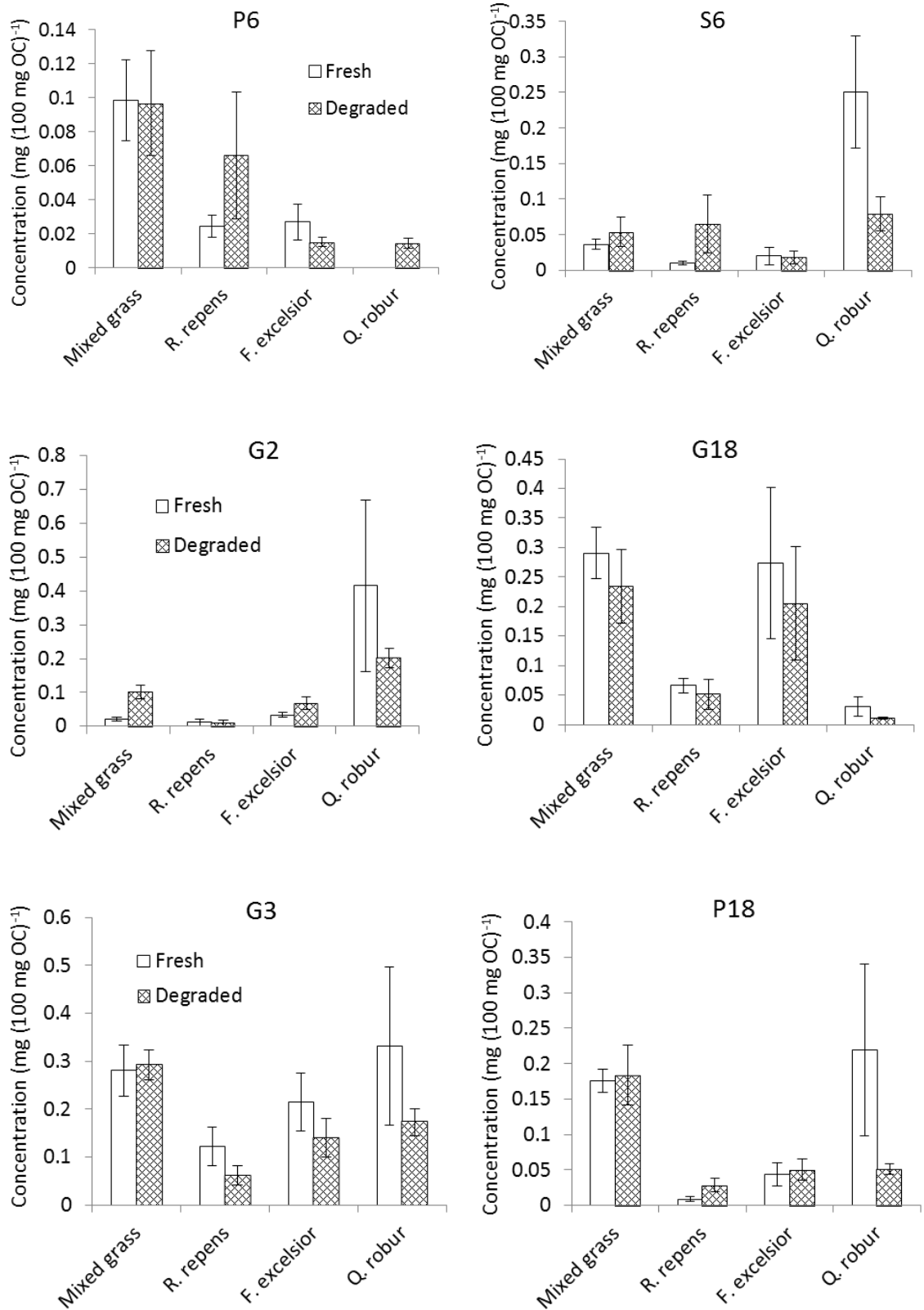


Figure 4.5. Mean (\pm standard error of the mean, $n = 4$) carbon normalised phenol concentrations in fresh and degraded mixed grass, *Ranunculus repens*, *Fraxinus excelsior*, and *Quercus robur* species. Phenol abbreviations are defined in figure 1.10.

Table 4.4. Mean (\pm standard error of the mean (s.e.), n = 4) TMAH/GC-MS product concentrations from analysis of degraded mixed grass, *Ranunculus repens*, *Fraxinus excelsior*, and *Quercus robur*. Total lignin (sum of compounds: 1,2,4,5,6,8,9,11-29) and acid/aldehyde ratios for compounds 21/18 (G6/G4 ratio) and compounds 27/22 (S6/S4 ratio) are also reported.

compound no.	Compound	$\mu\text{g (100 mg OC)}^{-1}$							
		Mixed grass	s.e.	<i>R. repens</i>	s.e.	<i>F. excelsior</i>	s.e.	<i>Q. robur</i>	s.e.
1	methoxybenzene (P1)	158.2	29.5	298.5	134.5	168.1	32.0	141.1	21.2
2	4-methoxytoluene (P2)	134.2	20.8	411.1	184.6	196.2	43.7	97.6	11.6
3	benzoic acid, methyl ester	0	0	0	0	16.9	11.2	24.2	6.7
4	4-methoxyethylbenzene	76.8	12.5	0	0	19.2	19.2	47.7	19.0
5	1,2-dimethoxybenzene (G1)	120.7	24.1	79.1	19.1	129.0	49.1	102.2	44.1
6	4-methoxybenzeneethylene (P3)	127.9	31.6	28.6	8.2	66.3	10.7	76.3	26.2
7	benzeneacetic acid methyl ester	0	0	0	0	0	0	0	0
8	3,4-dimethoxytoluene (G2)	102.3	19.7	9.5	9.5	69.2	18.8	202.2	29.0
9	4-methoxybenzaldehyde (P4)	5.1	3.0	0	0	0	0	0	0
10	benzenepropanoic acid methyl ester	0	0	0	0	0	0	0	0
11	1-(4-methoxyphenyl)-3-propene (P21)	9.0	2.1	0	0	1.7	1.7	4.7	2.0
12	1,2,3-trimethoxybenzene (S1)	41.7	20.3	21.1	10.4	45.8	16.8	82.0	38.1
13	3,4-dimethoxyethylbenzene (Gx)	49.4	13.5	7.6	5.7	32.3	15.5	61.2	10.0
14	4-methoxybenzeneacetic acid (P24)	0	0	0	0	25.2	12.7	0	0
15	3,4-dimethoxybenzeneethylene (G3)	293.3	31.1	62.0	20.7	139.9	40.4	173.4	28.3
16	4-methoxybenzoic acid methyl ester (P6)	96.7	30.6	66.1	37.2	15.0	2.7	14.4	3.0
17	3,4,5-trimethoxytoluene (S2)	15.9	6.3	12.9	5.4	24.9	9.5	25.7	9.4
18	3,4-dimethoxybenzaldehyde (G4)	42.7	13.4	5.9	3.4	38.1	20.5	28.1	11.4
19	1-(3,4-dimethoxyphenyl)-3-propene (G21)	20.5	3.5	7.2	5.3	33.0	10.9	37.7	18.1
20	3,4-dimethoxyacetophenone (G5)	39.1	1.1	73.5	37.8	31.7	11.5	82.6	6.8
21	3,4-dimethoxybenzoic acid methyl ester (G6)	62.3	8.5	101.8	51.3	59.0	18.8	58.5	16.4
22	3,4,5-trimethoxybenzaldehyde (S4)	0	0	0	0	1.9	1.9	5.1	3.0
23	3,4-dimethoxybenzeneacetic acid methyl ester (G24)	4.5	4.5	0	0	2.0	1.3	12.6	2.9
24	1-(3,4,5-trimethoxyphenyl)-3-propene	9.9	5.7	0	0	25.8	8.9	46.7	12.6
25	2-Propenoic acid, 3-(4-methoxyphenyl) methyl ester (E)- (P18)	183.7	42.6	28.4	9.6	50.4	14.5	51.5	7.3
26	3,4,5-trimethoxyacetophenone (S5)	27.9	10.4	54.7	33.1	14.6	3.3	8.2	2.0
27	3,4,5-trimethoxybenzoic acid methyl ester (S6)	53.4	20.6	65.1	40.8	17.9	8.6	79.2	23.8
28	2-propenoic acid, 3-(3,4,5-trimethoxyphenyl)- (E)- (S18)	0	0	0	0	8.3	6.5	0	0
29	2-propenoic acid, 3-(3,4-dimethoxyphenyl) methyl ester (G18)	233.7	62.1	51.2	26.1	205.0	96.3	11.1	2.0
	Total lignin	1908.8	151.4	1384.4	550.0	1420.6	368.2	1449.7	172.1
	G6/G4 ratio	1.5	0.02	17.3	0.1	1.5	0.04	2.1	0.0
	S6/S4 ratio	0	0	0	0	9.39	0.011	15.51	0.03

In the degraded litter biplot (figure 4.4), the mixed grass and *F. excelsior* regions moved down to overlap with the *Q. robur* region, leaving the *R. repens* region clearly isolated. Associated with *R. repens* were P2 and G6 (figure 4.4), where they were more abundant than in other degraded litter types (table 4.4), although not with statistical significance. G18 was located at the boundary between *F. excelsior* and mixed grass in figure 4.4 as it was abundant in both these degraded litter types (figure 4.5 & table 4.4), but not significantly different from other litter types (F pr. = 0.097). Associated with degraded mixed grass were: P3, G3, and P18 (F pr. = 0.005, figure 4.5) which were present in greater abundance than in other degraded vegetation. There were multiple significant differences with G3 between degraded litters (F pr. = 0.006, figure 4.5): mixed grass was different from *R. repens*, *F. excelsior*, and *Q. robur*; and *R. repens* was different from *Q. robur*.

Associated with *Q. robur* was G2 which was present in greater abundance than in other degraded litter types (figure 4.5 & table 4.4). There were multiple significant differences for G2 between litter types (F pr. = <0.001): *Q. robur* was different from mixed grass, *F. excelsior*, and *R. repens*; and mixed grass was different from *R. repens*.

4.3.3 Acid/aldehyde ratios in litter

Acid/aldehyde ratios for guaiacyl (3,4-dimethoxybenzoic acid, methyl ester/3,4-dimethoxybenzaldehyde (G6/G4)) and syringyl (3,4,5-trimethoxybenzoic acid, methyl ester/3,4,5-trimethoxybenzaldehyde (S6/S4)) lignin phenols for fresh and degraded litter are reported in tables 4.3 and 4.4, respectively. G6/G4 ratios increased from fresh to degraded litter for all litter types except *F. excelsior* which slightly reduced from 1.84 to 1.55. Fresh and degraded G6/G4 ratios were considerably greater for *R. repens* compared with other vegetation types. S6/S4 ratios increased substantially from fresh to degraded vegetation with the exception of *R. repens* as no S4 was detected. Increased acid: aldehyde ratios from fresh to degraded vegetation is in agreement with other studies and indicates increased state of lignin oxidation (Vane et al., 2001a).

4.3.4 Lignin phenols in leachates

Observed topsoil temperatures ranged from -7.16 to 33.61 °C (figure 4.6), with a mean temperature for the duration of the experiment of 11.33 °C. There was an associative relationship between TOC normalised total lignin concentrations detected in topsoil

leachates from mixed grass, *R. repens*, and *F. excelsior* through time with the topsoil seasonal temperature (figure 4.6).

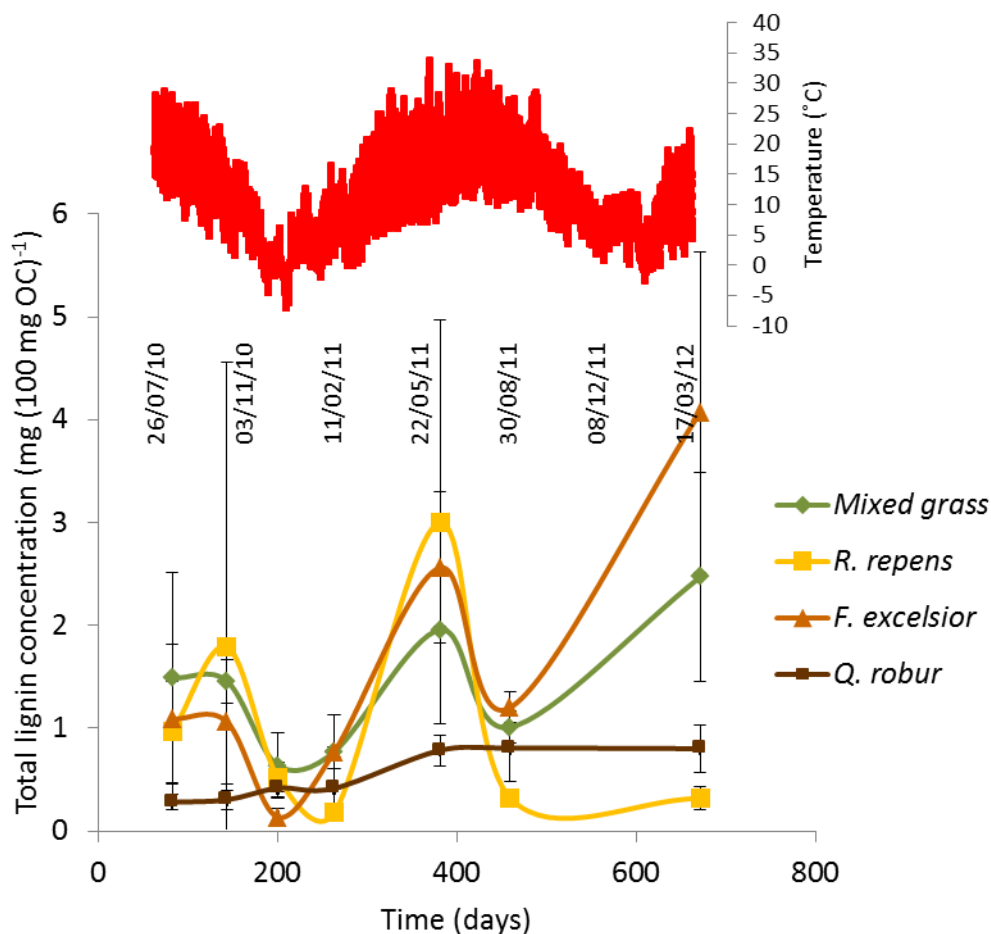


Figure 4.6. Mean (\pm standard error of the mean, $n = 3$) normalised total lignin concentrations in topsoil leachates from decomposing litter (mixed grass, *Ranunculus repens*, *Fraxinus excelsior*, and *Quercus robur*) through time. Mean ($n = 3$) topsoil temperature is shown in red.

Greatest total lignin concentrations with respect to bulk TOC were detected in late spring/early summer. This seasonal pattern was displayed most strongly in *R. repens*. *Q. robur* showed a gradual increase in total lignin concentration detected in leachate through time which appeared to be independent of temperature.

At the compound specific level, some phenols followed a similar seasonal trend through time (figure 4.7) to total lignin concentration (figure 4.6): P1 for all vegetation types; P2 for mixed grass, *R. repens*, and *Q. robur*; G1 for *R. repens*, *F. excelsior*, and *Q. robur*; G2, S1, and G3 for *F. excelsior*; P6, G6, P18, and S6 for mixed grass, *R. repens*, and *F. excelsior*; and finally G18 for *R. repens*.

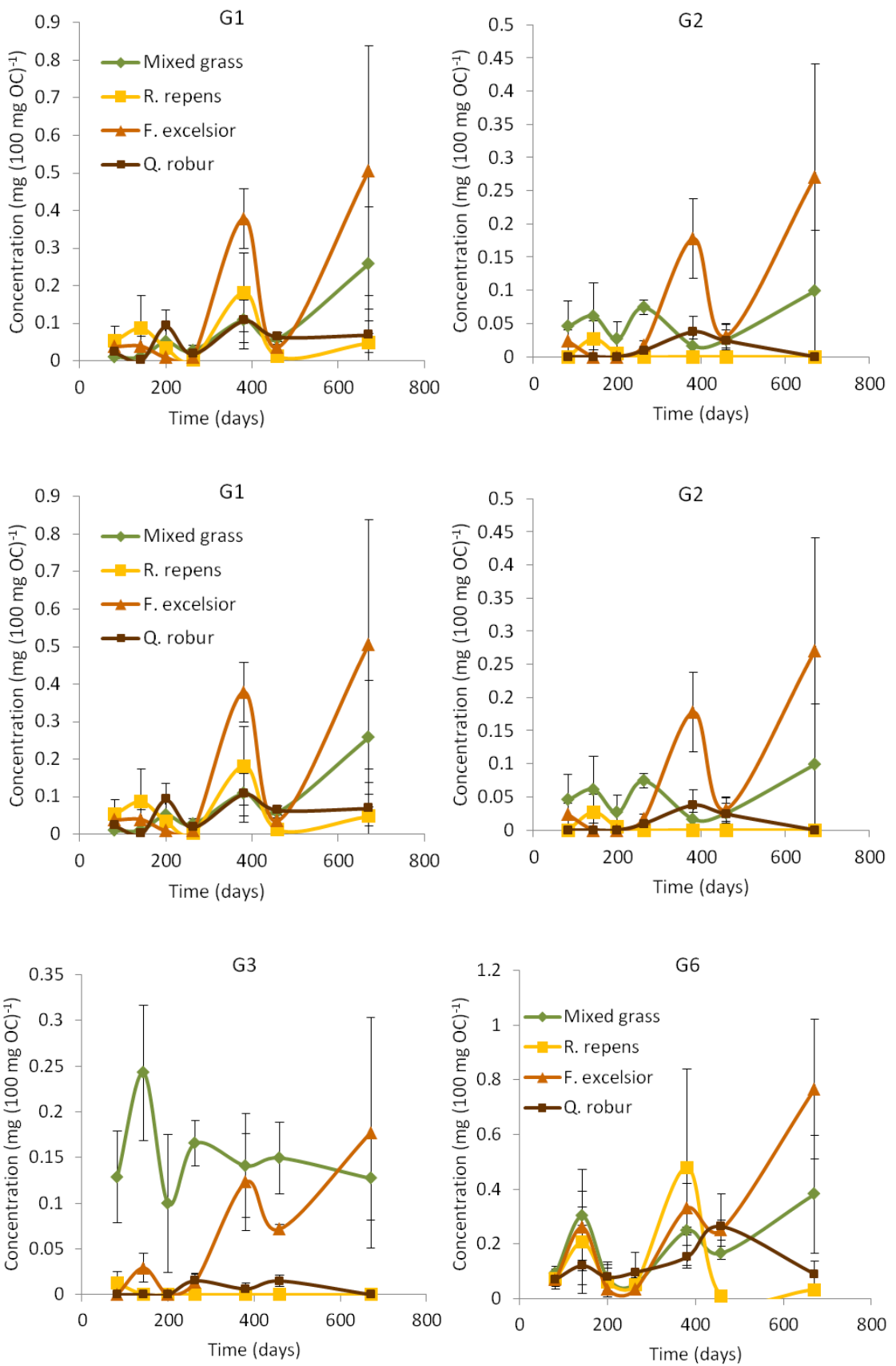


Figure continued on the next page.

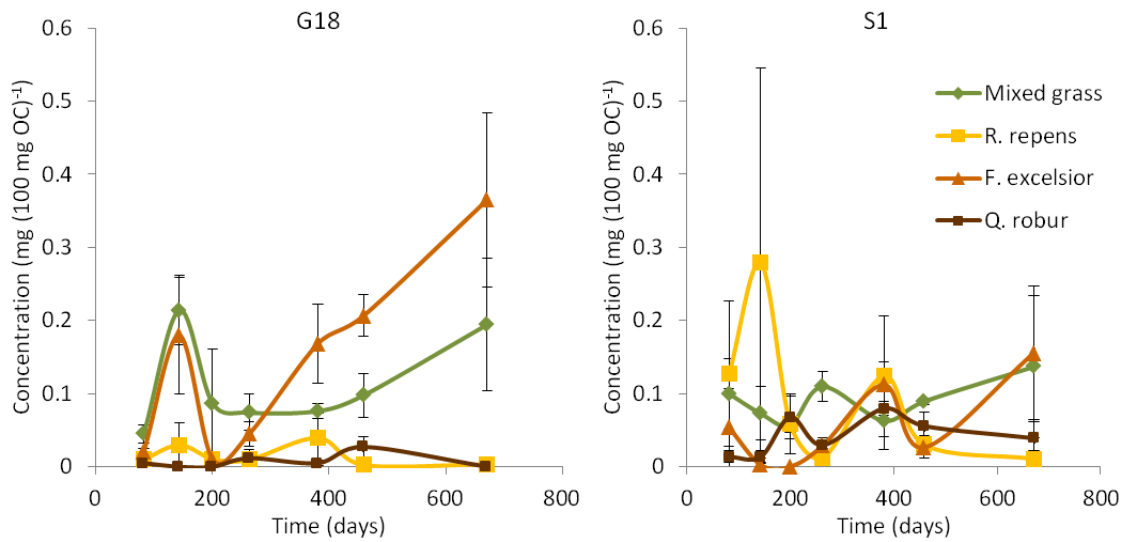


Figure 4.7. Mean (\pm standard error of the mean, $n = 3$) concentrations of selected lignin phenols detected in topsoil leachates from decomposing litter (mixed grass, *Ranunculus repens*, *Fraxinus excelsior*, and *Quercus robur*) through time. Phenol abbreviations are defined in figure 1.10.

Some phenols deviated from the seasonal trend: P2 for *F. excelsior*; G2, S1, and G3 for mixed grass and *R. repens*; G5, G24, and G18 for mixed grass; and finally, S5 for mixed grass, *R. repens*, and *Q. robur*.

Figures 4.8 to 4.14 below show the distributions of lignin phenols that constitute the total lignin concentration in leachates (figure 4.6) for each litter type at each sampling time, respectively.

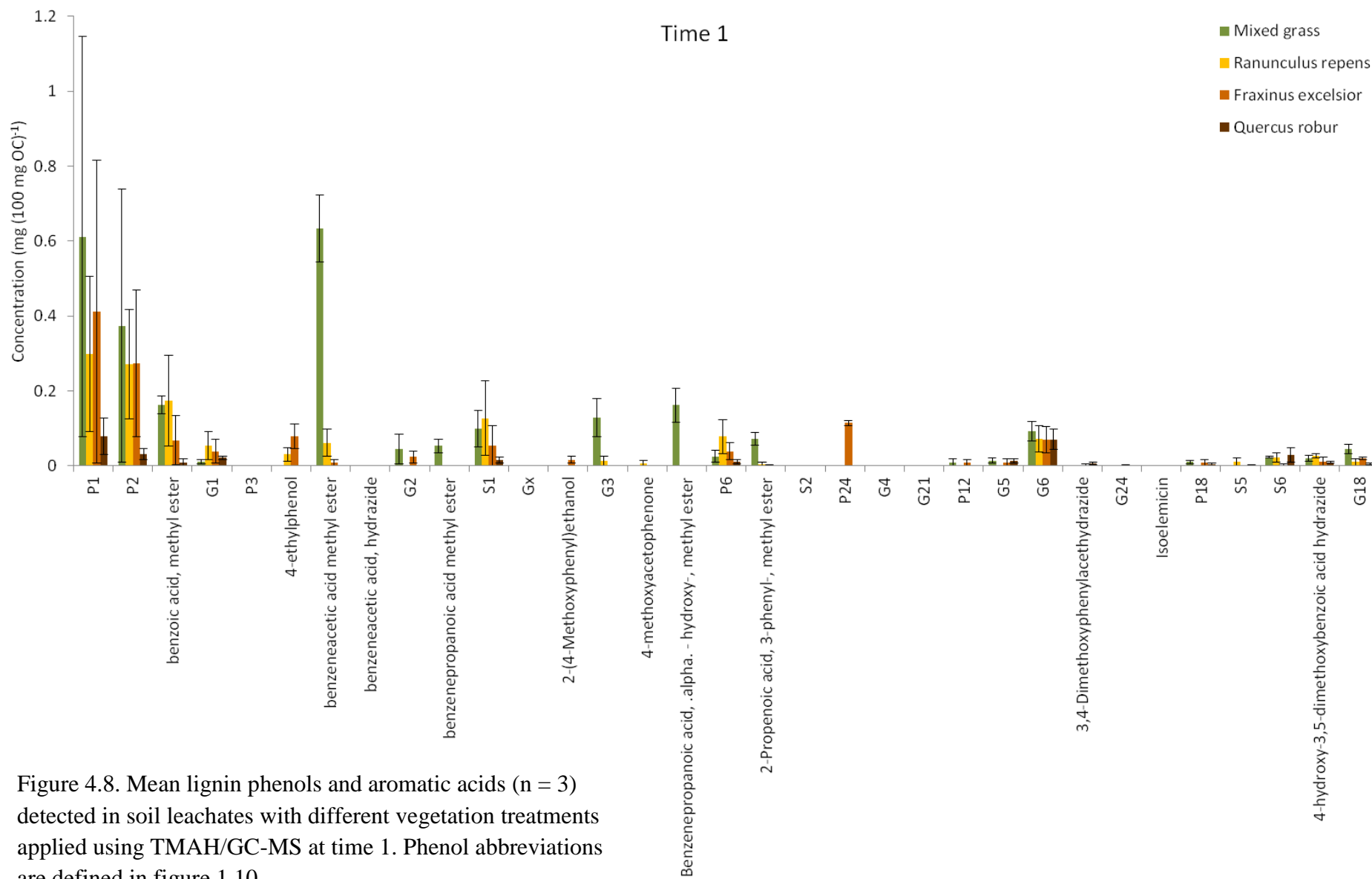


Figure 4.8. Mean lignin phenols and aromatic acids (n = 3) detected in soil leachates with different vegetation treatments applied using TMAH/GC-MS at time 1. Phenol abbreviations are defined in figure 1.10.

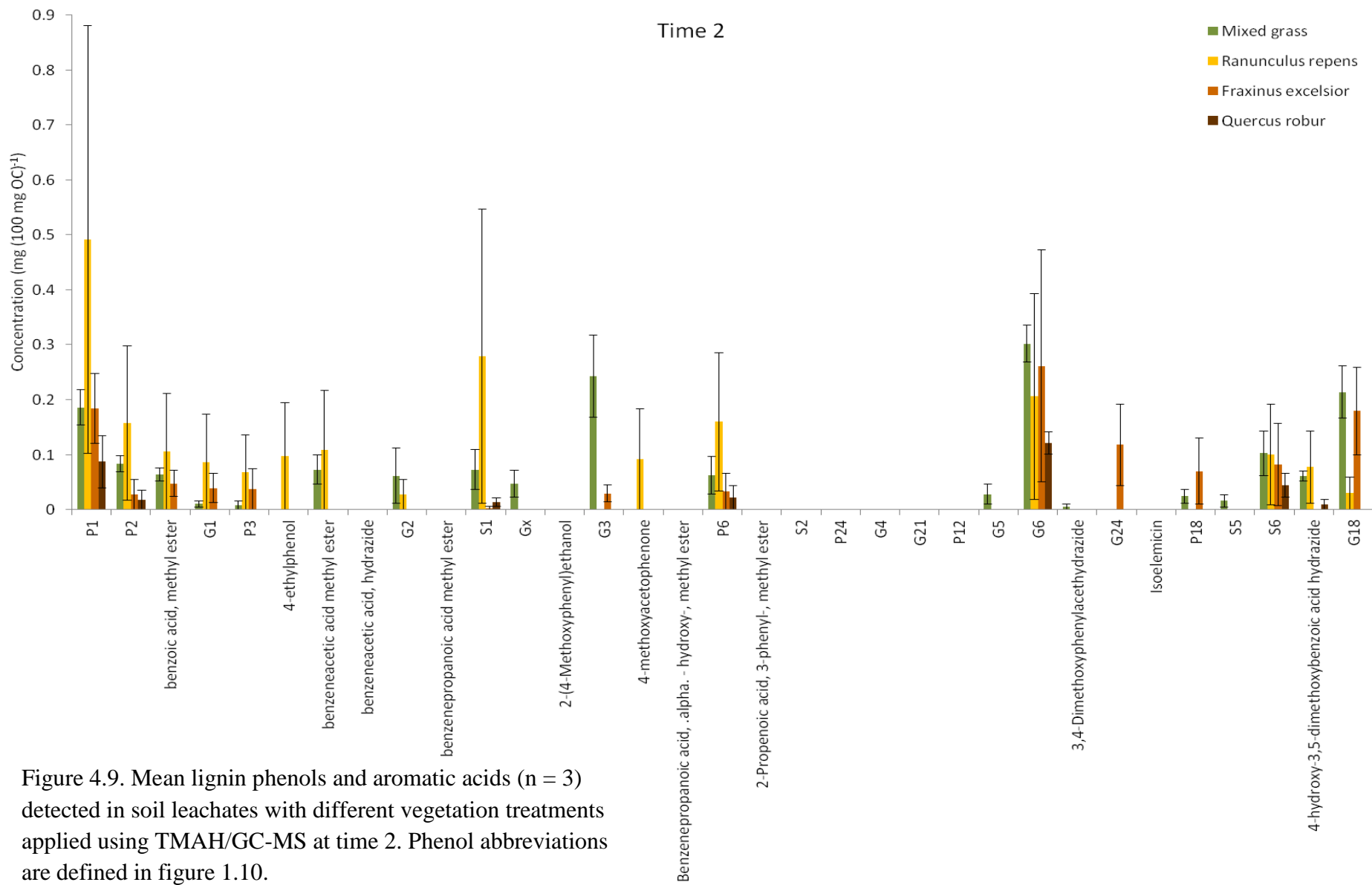


Figure 4.9. Mean lignin phenols and aromatic acids (n = 3) detected in soil leachates with different vegetation treatments applied using TMAH/GC-MS at time 2. Phenol abbreviations are defined in figure 1.10.

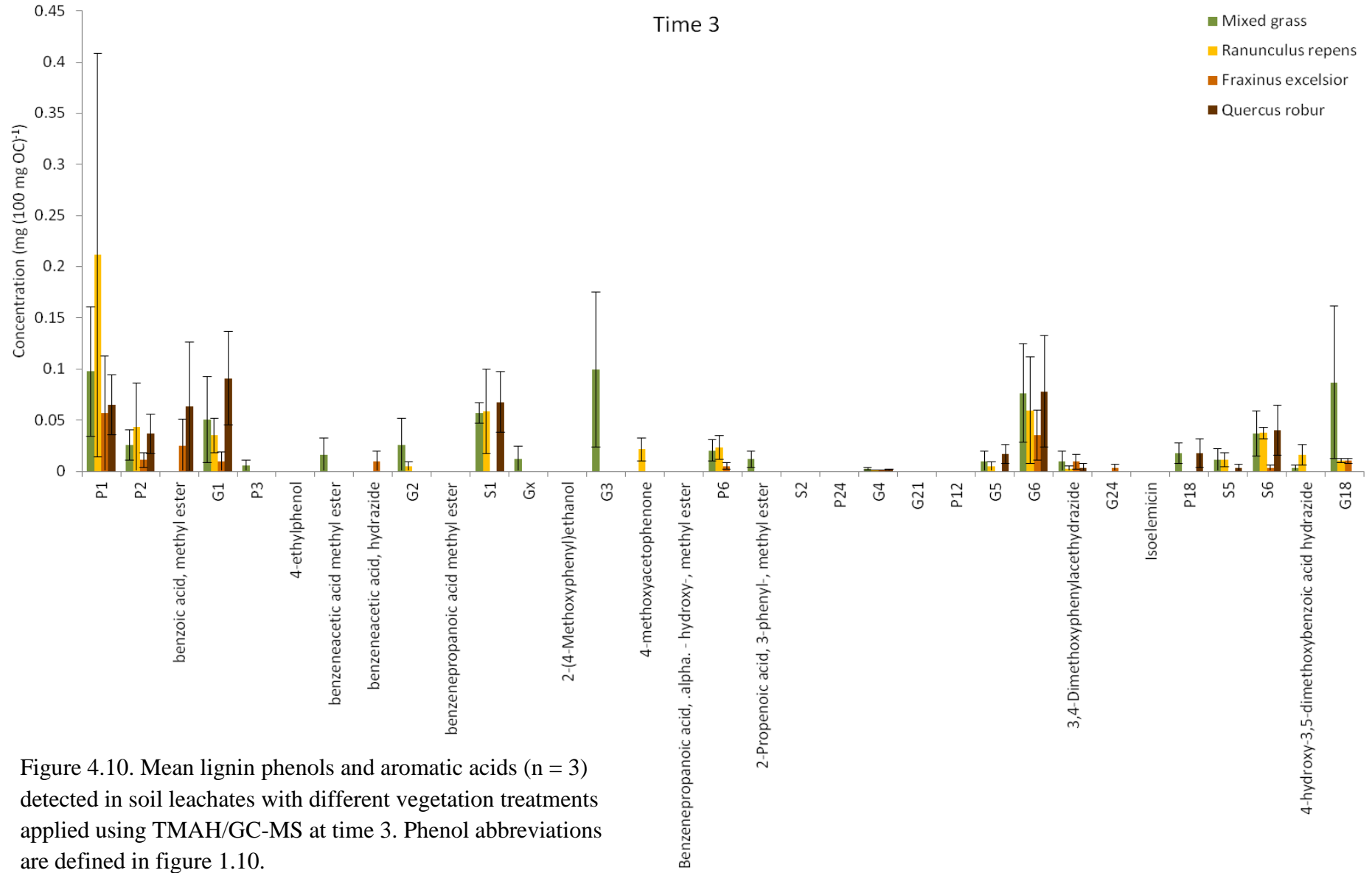


Figure 4.10. Mean lignin phenols and aromatic acids (n = 3) detected in soil leachates with different vegetation treatments applied using TMAH/GC-MS at time 3. Phenol abbreviations are defined in figure 1.10.

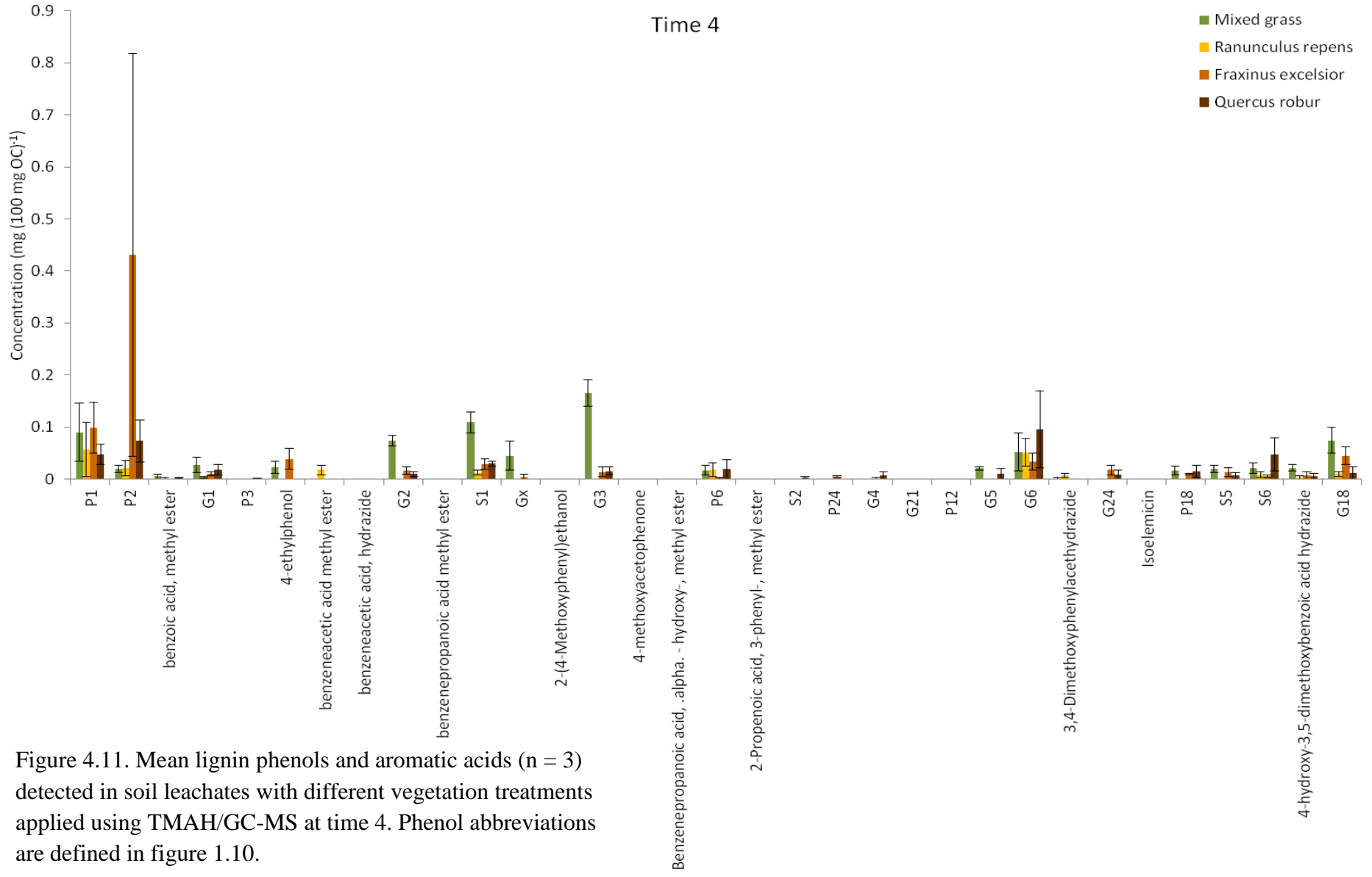


Figure 4.11. Mean lignin phenols and aromatic acids (n = 3) detected in soil leachates with different vegetation treatments applied using TMAH/GC-MS at time 4. Phenol abbreviations are defined in figure 1.10.

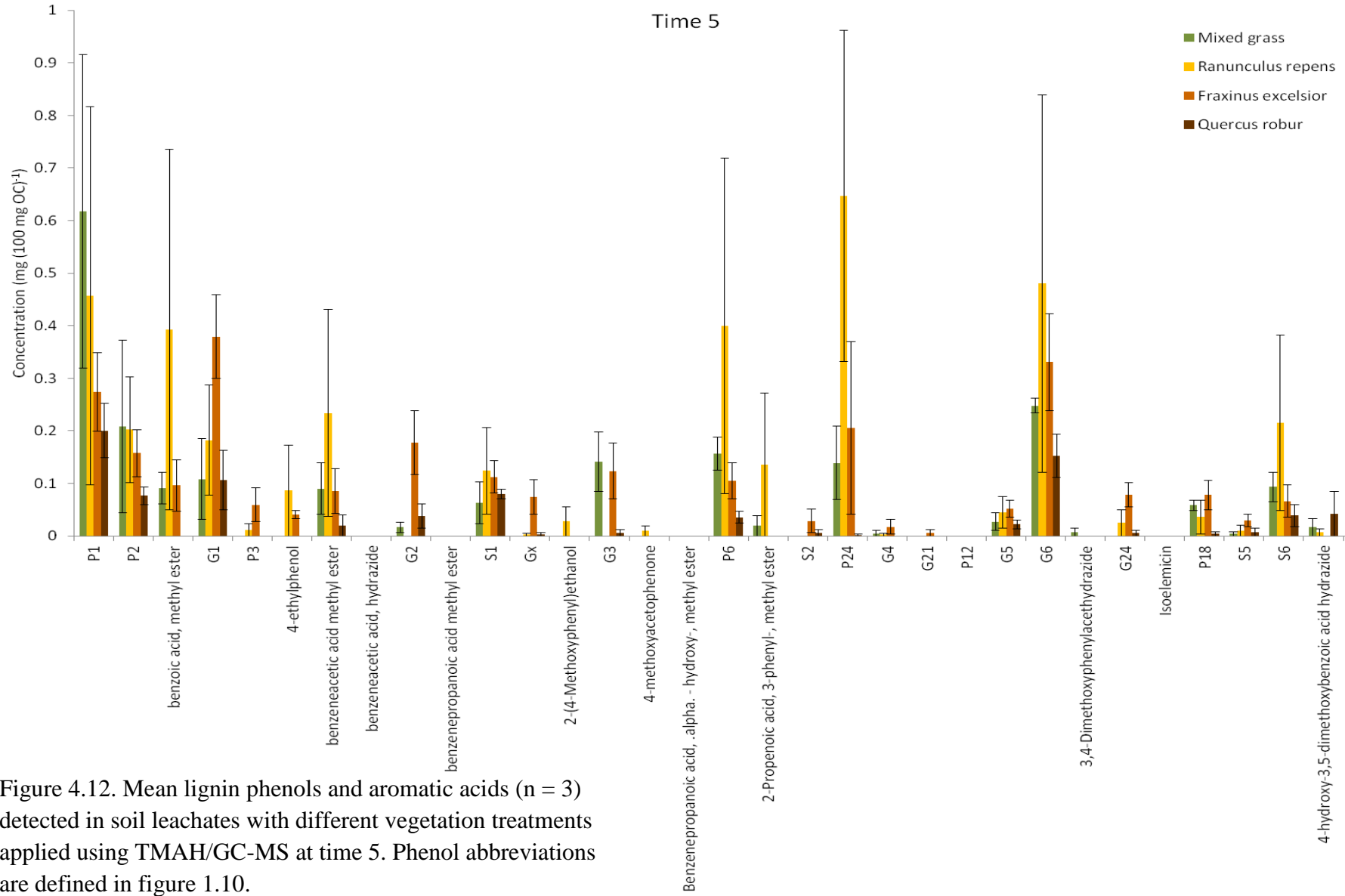


Figure 4.12. Mean lignin phenols and aromatic acids (n = 3) detected in soil leachates with different vegetation treatments applied using TMAH/GC-MS at time 5. Phenol abbreviations are defined in figure 1.10.

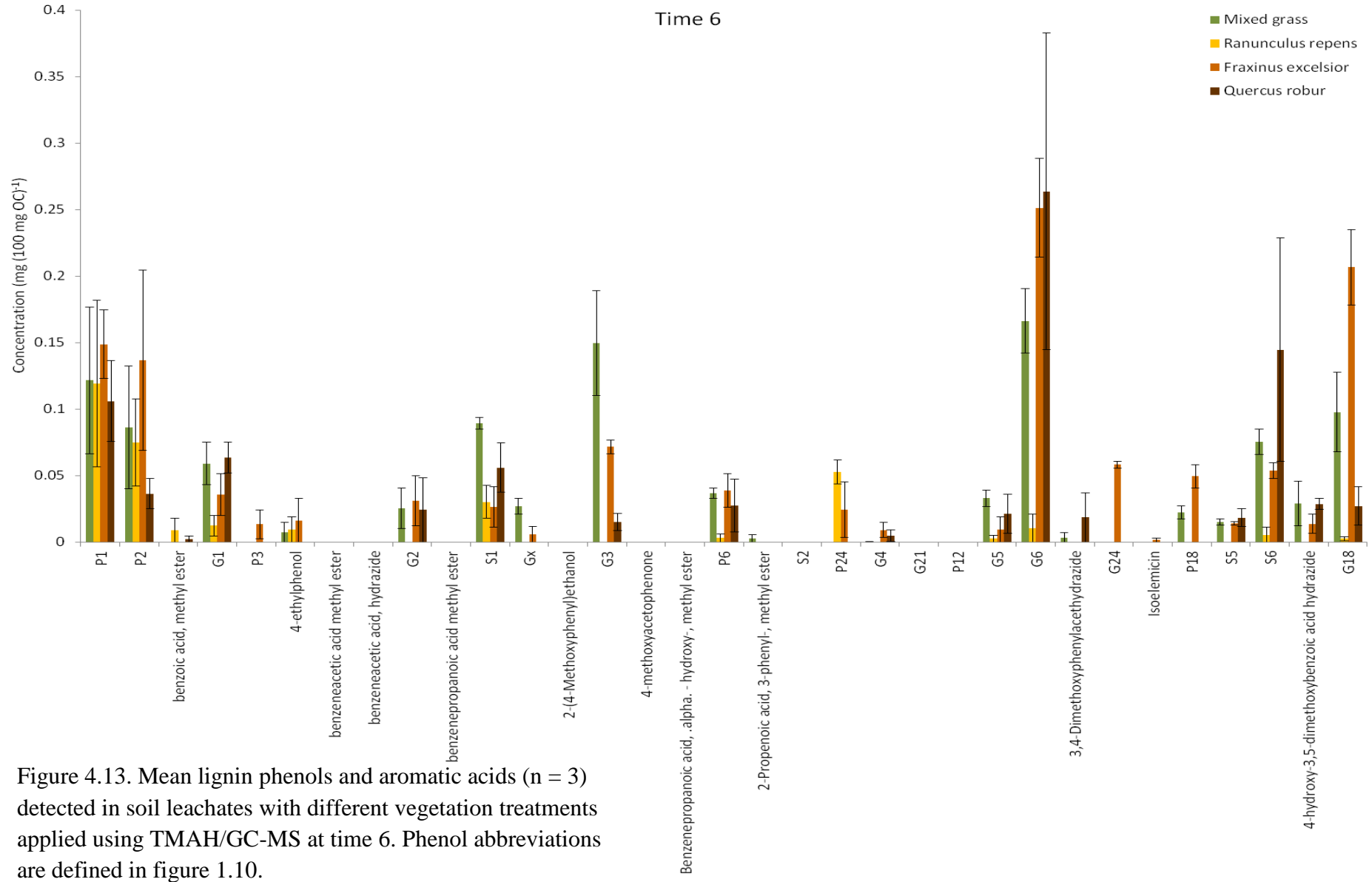


Figure 4.13. Mean lignin phenols and aromatic acids (n = 3) detected in soil leachates with different vegetation treatments applied using TMAH/GC-MS at time 6. Phenol abbreviations are defined in figure 1.10.

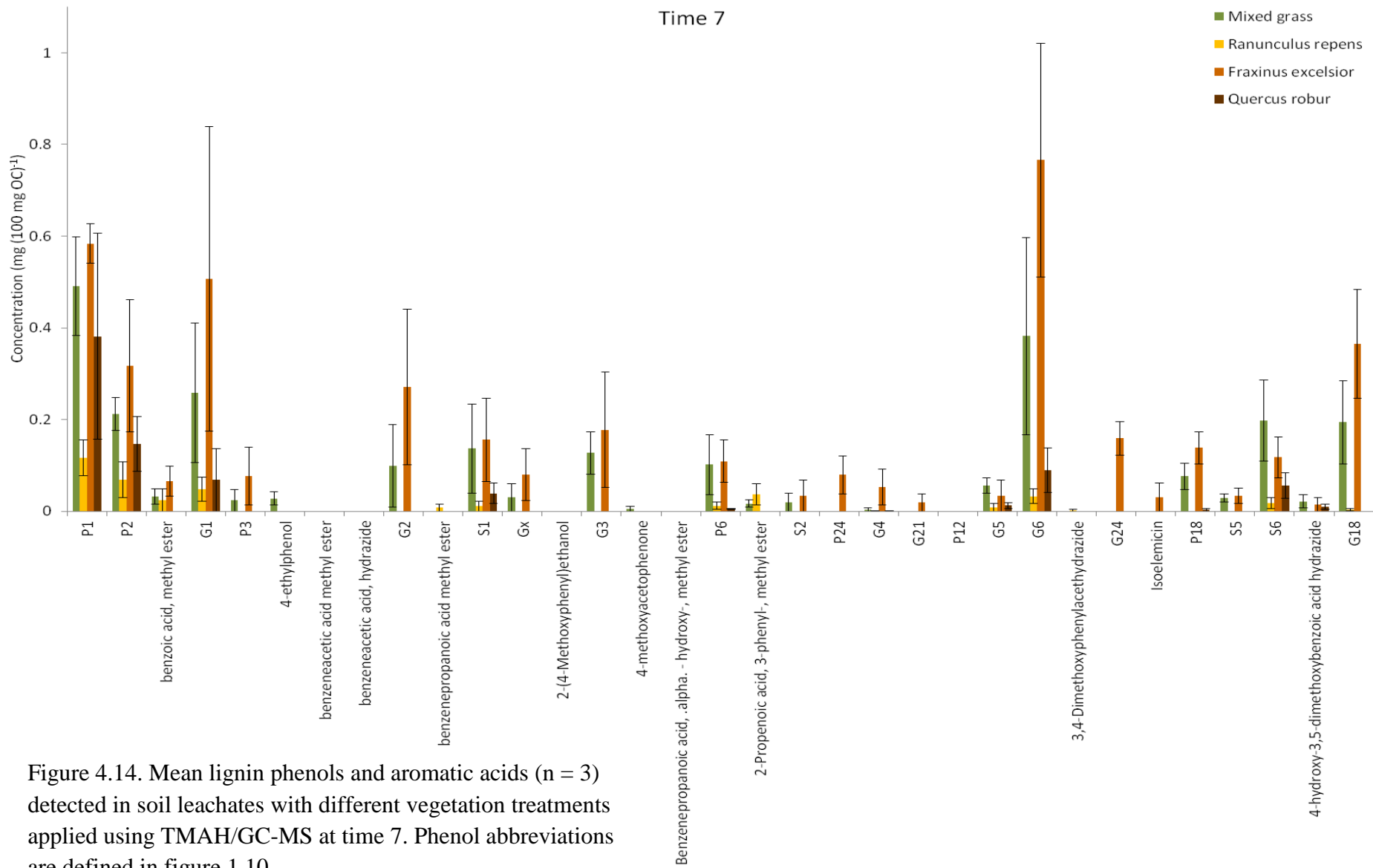


Figure 4.14. Mean lignin phenols and aromatic acids (n = 3) detected in soil leachates with different vegetation treatments applied using TMAH/GC-MS at time 7. Phenol abbreviations are defined in figure 1.10.

At times 1 and 2, mixed grass, *R. repens* and *F. excelsior* leached more total lignin than *Q. robur*. Dominant phenols at time 1 (figure 4.8) for all litter types were P1 and P2. Mixed grass leached significantly more G3 (F pr. = 0.043) and G18 (F pr. = 0.012) than other litter types. At time 2 (figure 4.9), *R. repens* leached more total lignin, comprising principally: P1, S1, and P6. Mixed grass was significantly different from other litter types for G3 (F pr. = 0.011), and mixed grass and *F. excelsior* were significantly different (F pr. = 0.015) from *R. repens* and *Q. robur* in G18 concentration.

At times 3 and 4 total lignin concentrations for mixed grass, *R. repens*, *F. excelsior* reduced to converge with *Q. robur* (figure 4.6). Dominant phenols in leachates for each litter at time 3 and 4 are shown in figures 4.10 and 4.11 respectively. At time 4, mixed grass was significantly different from other litter types for G2 (F pr. = <0.001), S1 (F pr. = 0.002), and G3 (F pr. = <0.001). G3 was also dominant in mixed grass at time 3 (figure 4.10), but not significantly different as there was none detected for other litter types.

At time 5 there was a dramatic increase in total lignin phenols leached for *R. repens*, *F. excelsior* and mixed grass, whereas only a slight increase for *Q. robur* (figure 4.6). *R. repens* had the greatest total lignin concentration which comprised mainly carboxylic acid compounds (figure 4.12) including: P24, G6, P6, S6, P1, and other non-lignin derived aromatic acids such as benzoic acid, methyl ester and benzeneacetic acid, methyl ester. Many of these compounds were detected in *R. repens* leachate at a greater concentration than in fresh or degraded *R. repens* litter. At time 5, *F. excelsior* was significantly different from other litter types in G1 (F pr. = 0.037) and G2 (F pr. = 0.027). Mixed grass and *F. excelsior* were significantly different from *R. repens*, and *Q. robur* in G3 (F pr. = 0.044).

At time 6, there was a sharp reduction in total lignin leached for all vegetation types except *Q. robur* which remained at a similar level as time 5 (figure 4.6). Total lignin concentration in leachate for *R. repens* was significantly different from other litter types (F pr. = 0.030). Dominant lignin phenols leached at time 6 (figure 4.13) were: G6, P1, P2, G18, S6, and G3. Mixed grass was significantly different from other litter types for G3 (F pr. = 0.008). There were multiple significant differences between litter types for P18 (F pr. = <0.001) and G18 (F pr. = <0.001): For both compounds, *R. repens* was similar to *Q. robur*, and these were different from mixed grass, which was also different from *F. excelsior*.

At time 7 (after 671 days), total lignin phenol concentrations leached from *F. excelsior* and mixed grass increased sharply whereas *R. repens* and *Q. robur* showed no change (figure 4.6). *F. excelsior* was significantly different from other litter types in total lignin concentration (F pr. = 0.038). Dominant lignin phenols leached (figure 4.14) were: G6, P1, G1, G18, and P2. *R. repens* was significantly different from mixed grass and *F. excelsior* for P1 (F pr. = 0.046). For G6, *R. repens* was similar to *Q. robur*, and these were different from *F. excelsior* (F pr. = 0.045). For P18, *R. repens* was similar to *Q. robur*, and mixed grass was similar to *F. excelsior*, although these two groups were significantly different from each other (F pr. = 0.005). *F. excelsior* was different from other litter types in G18 (F pr. = 0.015).

Additionally, from time 5 onwards, there was an increase in relative abundance of higher molecular weight phenols in leachates. This may arise if there are differences in retention of different phenols in soils, which is explored in Chapter 6.

4.4 Discussion

The hypotheses tested in this experiment were: dominant lignin phenols found in topsoil leachate DOM are the same as those in the source litter type (H3); and total lignin concentrations determined in leachate increase with increasing topsoil temperature (H4). The following discussion explores the main findings and concludes with acceptance of H3 for specific phenols for certain litter types and rejection of H3 for other phenols. H4 was accepted for mixed grass, *R. repens*, and *F. excelsior* because total lignin, and many specific phenol concentrations, increased as a proportion of TOC at higher seasonal temperature, although it was rejected for *Q. robur*.

4.4.1 Mass loss of litter, total C, total N, and total lignin phenols

After 671 days (1.8 years) *Q. robur* lost 23% of the initial litter mass applied, which is considerably less than the 57% and 58% lost for *Quercus crispula* after 2 years degradation *in-situ* in a litterbag degradation experiment (Ono et al., 2013), which may be due to the home field advantage, a phenomenon where litter decomposes more quickly in its home environment than in an away environment (Bocock et al., 1960, Hunt et al., 1988, Gholz et al., 2000, Wallenstein et al., 2013) in their study. Percentage mass loss of C, N, and total lignin in vegetation was greater for *R. repens* than other litter types (figure 4.2) possibly because considerably less mass of fresh *R. repens*

vegetation was applied to the soil lysimeters than the other litter treatments at the start of the experiment, so that by the end of the experiment only traces of *R. repens* remained. In this study, mean C mass loss for mixed grass was 48.3% after 671 days. This is considerably less than 87.5% mass loss for *L. perenne* in a litterbag experiment over 28 weeks (Sanaullah et al., 2012), which may be due to the fact that they degraded only 5g fresh litter (dry weight, DW), whereas in this study 189 g DW mixed grass litter was degraded. Litter mass loss % for *F. excelsior* from fresh (140 g DW) to degraded litter was 43% after 671 days, whereas 58% mass loss was observed for mountain ash (*Sorbus aucuparia*) after 27 months (810 days) in field degradation conditions based on 2 g (DW) litter samples (Kalbitz et al., 2006).

Total lignin phenols in mixed grass from fresh to degraded litter increased from 1.37 ± 0.19 to 1.91 ± 0.15 mg/100 mg OC (not significant) which was greater than the increase in total lignin from 1.9 ± 0.1 to 2.2 ± 0.7 mg/100 mg OC detected by Sanaullah et al., (2012). This increase was attributed to litter mass loss occurring in two phases: during the first phase (< 11 months) plant material is degraded as a whole, rather than selectively, whereas after 11 months, readily degradable components such as polysaccharides were selectively degraded (Chabbi and Rumpel, 2004, Sanaullah et al., 2012). An increase in total lignin concentration from fresh to degraded grasses (*Imperata cylindrica* and *Aristida stricta*) was also observed in an 8 month litter degradation study (Bray et al., 2012). Total lignin phenol concentrations decreased (not significantly) from fresh to degraded *Q. robur* litter, although in another study total lignin concentrations for *Q. robur* increased from green leaves to litter after three months of decomposition (Sariyildiz and Anderson, 2005).

4.4.2 Lignin phenol composition of litters and leachate

Some dominant phenols detected in litter were detected in topsoil leachates for each litter type, therefore H3 was accepted or rejected on a phenol specific basis.

All litter types in this study yielded methylated *p*-hydroxyphenyl, guaiacyl, syringyl, and cinnamyl lignin phenols upon analysis by TMAH/GC-MS. The relative dominance of cinnamyl phenols such as P18 and G18 in this study are characteristic of non-woody angiosperm vegetation (Hedges and Mann, 1979a, Clifford et al., 1995). P3 and G3 are also associated with non-woody lignin (Clifford et al., 1995, Chefetz et al., 2000), and these four phenols were present in all litter types in this study. Caution needs to be exercised with regard to allocating specific lignin phenols to specific litter types since

the majority of phenols were detected in all litter types, although in differing relative proportions.

For the four litter types studied, P6 was dominant in fresh mixed grass. S6 and G2 were dominant in fresh *Q. robur* litter. G18, dominant in mixed grass or *F. excelsior* in this study, was also dominant in grassland litter & fermentation, and organic horizons, together with P6 and S6 in other studies (Huang et al., 1998, Mason et al., 2012). In degraded litter, G2 was dominant in *Q. robur*. G3 and P18 were dominant in mixed grass. G18 was dominant in mixed grass or *F. excelsior*.

Organic carbon normalised concentrations of P6, G18, G3, and P18 were similar in fresh and degraded mixed grass, although less stable in *R. repens* and *Q. robur* (figure 4.5). Perhaps these phenols were degraded at the same rate as bulk litter C in mixed grass, resulting in their stable OC normalised concentration.

Translocation of dominant lignin phenols from litter to leachate

Due to the statistical relationship between their abundances in the litter and leachates, some lignin phenols dominant in the litter were assumed to be transferred into the dissolved phase and transported through soil. For instance, G3, dominant in degraded mixed grass litter, was also dominant in mixed grass leachates at times 1, 2, 3, 4, and 6 (figures 4.8 – 4.11, 4.13, respectively). However, from 381 days degradation onwards (times 5, 6, and 7), *F. excelsior* also leached G3 in relatively high abundance. G18 which was dominant in fresh and degraded mixed grass or *F. excelsior* litter was also dominant in soil leachates from these vegetation types (figures 4.8 – 4.14). G6 although not dominant, was transferred from *Q. robur* litter to its leachate at similar normalised concentrations.

Some compounds dominant in the litter were less abundant than expected in the soil leachates. G2, which was dominant in fresh and degraded *Q. robur* litter (figure 4.5), was never more abundant in *Q. robur* leachates than other litter types (figures 4.8 – 4.14). Additionally, P18 was dominant in degraded mixed grass litter compared to other degraded litter types, but was either not dominant in mixed grass leachate or was relatively dominant in leachates from both mixed grass and *F. excelsior*. Although G2 and P18 were present in low abundance in all litter leachates (figures 4.8 – 4.14), this does not necessarily mean that they did not enter the dissolved phase in greater abundance. They may have become stabilised in soil through sorption, or P18 may have undergone oxidative degradation of its side chain as has been observed in guaiacyl

lignin during the fungal degradation of Scots pine (Dijkstra et al., 1998). In the sorption of DOM to the mineral matrix and metals therein, aromatic and carboxyl C can be preferentially removed from solution (Kaiser et al., 1997) including acidic lignin phenols (Kaiser et al., 2004). However, other carboxyl containing phenols such as G6 and G18 were relatively dominant in leachates (figures 4.8 – 4.14). Previous work investigating biodegradation of DOM showed an enrichment of lignin-derived aromatic compounds after 90 day incubation suggesting selective decomposition of carbohydrates (Kalbitz et al., 2003) and amino acid substrates, (Marschner and Kalbitz, 2003), therefore it is unlikely that microbial oxidation of dissolved lignin to CO₂ would explain reductions in dissolved lignin concentrations, although little is known about this process at the compound specific level. It has already been shown that phase changes of lignin between dissolved and sorbed states can dramatically alter lignin parameters such as acid: aldehyde, S/V, and C/V ratios from their original source values by up to ten-fold due to the processes of solubilisation, leaching, and sorption without any degradation occurring (Hernes et al., 2007).

4.4.3 Leached lignin phenol concentrations with respect to temperature

Summed total lignin phenol concentrations increased with increasing topsoil temperature for mixed grass, *R. repens*, and *F. excelsior* (figure 4.6), therefore H4 was accepted for these litter types. Summed total lignin phenol concentrations for *Q. robur* did not correlate with temperature, therefore H4 was rejected for this litter type. This may be due to relatively high hydrolysable tannin concentrations in *Q. robur* (Filley et al., 2006), which are known to inhibit microbial activity and provide a protection mechanism against plant herbivory (Schultz et al., 1992).

There were some inconsistencies in the relationship between total lignin phenol concentration and topsoil temperature such as for the samples collected after 82 and 459 days (10/08/2010 and 22/08/2011, respectively). After 459 days (22/08/2011), total lignin concentration for mixed grass and *F. excelsior* reduced to similar levels as late summer the previous year (10/08/2010) and *R. repens* reduced to a level similar to that for winter sampling (06/12/2010 and 08/02/2011). Previous research has shown that the active SOC pool reaches a maximum size in late spring/early summer, as does the microbial respiration rate for grass stands and deciduous forests (Kirschbaum, 2013). Research has shown that lignin degradation is cometabolic occurring in the presence of readily utilizable substrates such as carbohydrates (Crawford, 1981, Klotzbucher et al., 2011b), and lignin can have a shorter residence time in soil compared to

polysaccharides (Kiem and Kogel-Knabner, 2003), n-alkanes, proteins, and total saccharides (Schmidt et al., 2011), suggesting that lignin can be preferentially degraded. Furthermore, since the process of adsorption is a reversible equilibrium reaction and often exothermic (Pignatello, 2000), Le Chatelier's principle states an increase in temperature will shift the equilibrium towards the reactants (i.e. desorption). Hence an increase in temperature should increase the rate of SOC desorption compared to adsorption (Conant et al., 2011). Therefore with increased desorbed SOM, and increased microbial degradation of SOM, including lignin, in late spring/early summer, it is feasible that the water-transportable component of SOC including lignin phenols should be increased at this time. Subsequent SOC degradation rates would therefore be reduced due to the remaining pool being depleted in available substrate, despite favourable decomposition temperatures (Kirschbaum, 2013), which would also result in reduced lignin leaching. The lower lignin concentrations observed for *R. repens* could also be due to less litter initially applied to lysimeters and only traces of *R. repens* litter remained at this stage in the experiment. With the onset of spring (21/03/2012) after 671 days, total lignin concentrations for *F. excelsior* and mixed grass increased towards a maximum again with rising soil temperatures, whereas *R. repens* maintained winter levels of total lignin concentration. *Q. robur* maintained the same concentration as the two previous sampling events. If leachates had been collected during the autumn or winter of 2012, it is likely that total concentrations for *F. excelsior* and mixed grass would have reduced below those attained in late August as the soil temperature reduced.

It is concluded in this study based on the evidence available that the leachate results are a product of lignin degradation and transport processes. Additionally, the lignin phenols characterised were those detected by thermochemolysis GC/MS, and were not necessarily identical in molecular structure to those leaching through soil. This is because this technique is designed to break the lignin macromolecule down into its constituent monomers by principally degrading the β -O-4 linkage (Clifford et al., 1995).

4.5 Conclusions

Lignin phenols in topsoil leachate were the same as those detected in the litter for mixed grass and *F. excelsior* (G3 and G18). However, P18 which was dominant in degraded mixed grass was not dominant in mixed grass leachate. S6, dominant in fresh *Q. robur*; and G2 dominant in fresh and degraded *Q. robur* litter were not dominant in its

leachates. P1 was relatively dominant in degraded *R. repens* litter and was also dominant in its leachates, although it also leached relatively large amounts of phenols and aromatics containing carboxylic acid groups. Hypothesis 3 was therefore accepted or rejected on a litter type- and phenol-specific basis (table 4.5).

Table 4.5. Litter types and lignin phenols where hypothesis 3 could be accepted, labelled ✓.

Phenol	Mixed grass	<i>R. repens</i>	<i>F. excelsior</i>	<i>Q. robur</i>
G3	✓		✓	
G18	✓		✓	
P1		✓		

Total lignin phenol concentrations in leachate increased with increasing topsoil temperature for mixed grass, *R. repens*, and *F. excelsior*, with maximum concentrations detected in late spring/early summer. This indicates that the overall rate of the combined processes of decomposition, solubilisation, and transport for many lignin phenols increase with increasing temperature. Hypothesis 4 was therefore accepted for these litter types. Total lignin phenol concentrations in *Q. robur* leachates gradually increased through time, independently of temperature, therefore hypothesis 4 was rejected for *Q. robur*. However, some individual lignin phenol concentrations did correlate with temperature.

As an important component of SOC, this study indicates that most lignin phenols leach from soil with increasing seasonal temperature, coinciding with times of maximum active SOC pool size and soil microbial respiration rate (Kirschbaum, 2013). There may therefore be important consequences for lignin phenols as part of soil carbon stocks for locations experiencing global warming.

Chapter 5: Lignin phenols in soils and natural waters as indicators of land use type

5.1 Introduction

Understanding soil organic matter (SOM) processes is essential to enhance agricultural productivity to address food security and mitigate climate change (Powlson et al., 2011), and the loss of organic matter from land to water by erosion or leaching requires further investigation (Lal, 2004). Identification of sources of organic matter input to watercourses, and the impact of land use on its organic composition (Williams et al., 2010), is also important with regards to issues of water quality (Guo et al., 2011) as well as for the distillery industry (Reid et al., 1993). The benefits of enhanced understanding of the impact of land use and management on water chemistry and quality are therefore manifold.

Lignin is the most abundant aromatic biopolymer comprising 4-hydroxyphenylpropanoid units (Ralph et al., 2004) accounting for an estimated 30% organic carbon in the biosphere (Boerjan et al., 2003). Therefore, lignin represents a major carbon input into soils, where it can have a shorter residence time than bulk SOM (Kiem and Kogel-Knabner, 2003, Schmidt et al., 2011). To account for the considerable quantities of lignin in terrestrial ecosystems it must either be removed through complete mineralisation to CO₂ by white-rot fungi (Kirk and Farrell, 1987), partially degraded into compounds not recognisable as lignin-derived, transported as particulate organic matter in surface flow, or lost as a component of dissolved organic matter (DOM). Partial lignin decomposition by white-rot degradation releases phenols (Robertson et al., 2008a) that are soluble in water. Given the magnitude of the input, transport of lignin phenols as a component of DOM in soils must be an important flux of C that remains poorly understood. Lignin monomers identified in natural samples are characteristic of vascular vegetation types (Hedges and Mann, 1979a, Clifford et al., 1995), and dissolved lignin phenols have been detected in fresh and marine waters (Louchouart et al., 2000), thus lignin phenols detected in natural waters are used as evidence of terrestrial input (Opsahl and Benner, 1997, Opsahl et al., 1999). However, fractionation of lignin phenols can occur between source litter-to-leachate, and subsequent sorption to soil can result in changes in parameters such as acid:aldehyde ratios, syringyl:vanillyl and cinnamyl:vanillyl ratios (Hernes et al., 2007). It is therefore surprising that there is

little information about the comparison between dissolved lignin phenols in local waters and those in the adjacent soil for different land uses.

5.1.1 Aims and hypotheses

In this study the influence of local land use (grassland, moorland and woodland) on the lignin phenols exported from the soil organic (O) horizon, through the soil A horizon, and into adjacent watercourses was examined by collecting soil cores and water samples for each land use. Lignin degradation products were detected using pyrolysis-gas chromatography/mass spectrometry in the presence of tetramethylammonium hydroxide (TMAH).

Hypotheses

H5. Lignin phenols detected in soils and in the DOM of adjacent water outlets are a function of land use type.

H6. Normalised total lignin phenol concentration in water outlets is not significantly different from their concentration in soil, for their respective land use type.

5.2 Methodology

5.2.1 Experimental design

Soil, dung, and water samples were collected in triplicate. Each soil replicate comprised of 5 cores.

5.2.2 Approach

Sample sites were selected to represent contrasting local land use type (grassland, ancient woodland, moorland) and water outflows from the vicinity of Rothamsted Research, North Wyke (Chapter 2, section 2.1). Soil, water, and livestock dung samples were collected from the locations described in Chapter 2, table 2.1, using the techniques described in Chapter 2, sections 2.3 and 2.4, respectively. 10 mL for each of the pH adjusted water samples was analysed for total organic carbon as described in Chapter 2, section 2.6.2 before extracting the remainder of each sample using SPE described in Chapter 2, section 2.6.3. Soil pH and TOC was determined as described in Chapter 2, sections 2.6.1 and 2.6.4, respectively.

Lignin phenols were characterised using on-line pyrolysis-GC-MS in the presence of TMAH as described in Chapter 2, section 2.7.2, except that sample weights analysed differed. Samples (10 mg for grassland and forest soil organic horizons, 5 mg for peat organic horizons, 20 mg for grassland and forest soil A horizons, 7 mg for peat A-horizons, 0.5 to 1.5 mg for DOM extract, and 2 mg for dung) were weighed into a quartz pyrolysis tube. Also, for soil samples > 12 mg, 10 μ L of an aqueous solution of TMAH (25%; w/w) was added to the sample instead of 5 μ L. The remainder of the procedure was the same.

Statistical analysis was carried out as described in Chapter 2, section 2.9. In addition, a principal component analysis (PCA) biplot was constructed from collapsed mean lignin phenol concentration data, i.e. where sample analysis with TMAH yielded both a methylated and unmethylated analogue of the same lignin phenol, these concentrations were summed together and reported as the methylated product.

5.3 Results and discussion

5.3.1 *Total lignin phenols*

Total lignin phenol concentrations in soil O and A horizons, and DOM from grassland, woodland and moorland are reported in figure 5.1. DOM samples from Taw Barton Farm, Sticklepath, and Josephs Carr sites represent grassland land use. DOM samples from Tributary of River Taw, and Orchard Dean Copse stream represent woodland land use. The River Taw DOM sample represents mixed land use: grassland, woodland and moorland (Chapter 2, table 2.1). Soil with respect to horizons and their formation are described in Chapter 1, section 1.8.

Greater total lignin concentrations normalised to TOC were detected in soil O horizons than A horizons for grassland, woodland and moorland land uses (figure 5.1), although this difference was only significant for grassland according to the FPLSD test. This may arise if lignin was preferentially lost from the A horizon, through mineralisation or leaching or due to higher lignin inputs into, or retention in, the O horizon.

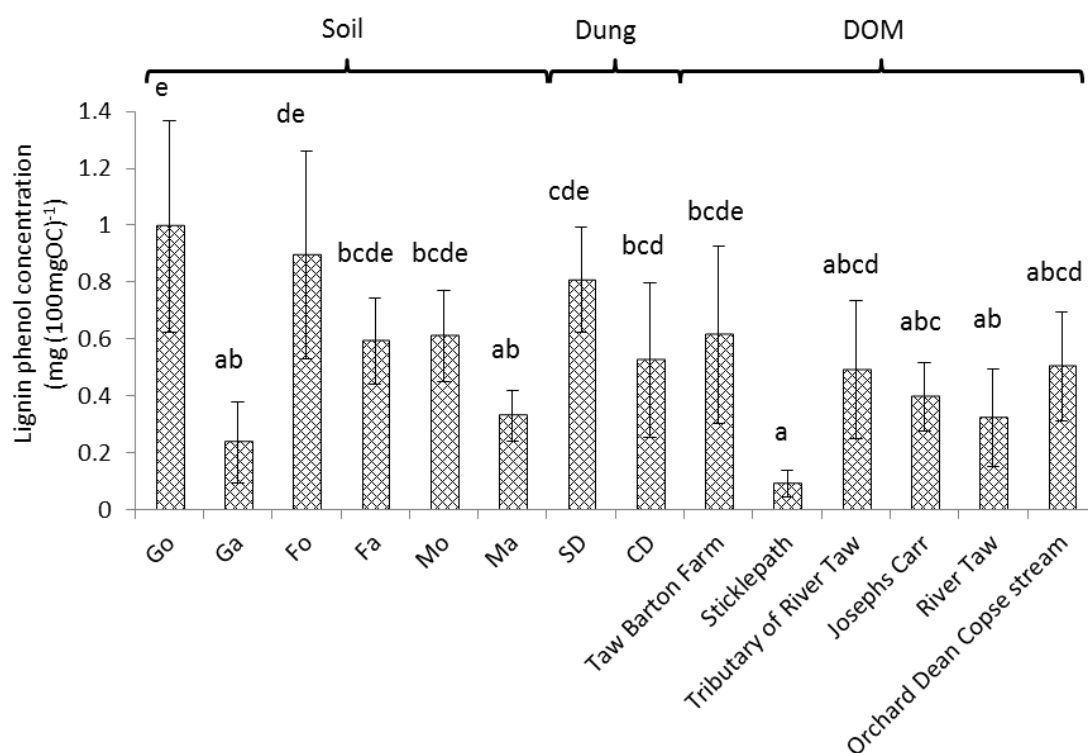


Figure 5.1. Mean (\pm standard error of the mean, $n = 3$) total lignin phenol concentrations of soils, dung, and dissolved organic matter (DOM) extracts, defined as the sum of lignin phenols in table 5.1. G = grassland, F = woodland, M = moorland. Subscripts o and a denote the soil organic and A horizons respectively. SD = sheep dung, and CD = cattle dung. Letters above each column group label the statistical difference grouping according to the Fisher's protected least significant difference test.

Soil A-horizon pH (5.7, 5.0, and 4.2) was lower than that of O horizons (6.7, 5.5, and 4.9) for grassland, woodland, and moorland respectively. Thus, conditions in the A horizons were more amenable for microbial lignin degradation, such as by white-rot fungi, the principal lignin degraders (Thevenot et al., 2010), where optimal lignin degradation by the white-rot fungus *Phanerochaete chrysosporium*, for example, has been shown to occur at pH 4 – 4.5 (Kirk et al., 1978). This difference in total lignin phenol concentration from the O to the A horizon was greatest for grassland, with a 75% decrease. This could be due to additional dung input from ruminants which could increase total lignin concentration in the organic horizon since it has been shown that dung is relatively enriched in lignin compared to fresh grass (Kondo et al., 1994), and that dung-lignin has been shown to remain in the top 5 cm of the soil profile rather than being transferred down the soil profile (Bol et al., 2000, Dungait et al., 2005). Additionally, roots have a high lignin content and may contribute lignin to soils (Abiven et al., 2005). Higher total lignin concentrations in grasslands were also observed in the

A_h horizon than the B_m horizon below it, for a range of chernozem soils (Feng and Simpson, 2007) and from the F horizon to the B horizon (Mason et al., 2012). Recent work comparing a moorland and Sitka spruce soil identified a decrease in total lignin concentration from the H1 horizon to the B horizon in the moorland soil. However, in the Sitka spruce soil, total lignin concentrations decreased initially with depth from the F horizon to the H1 horizon, before increasing in the H2 horizon then decreasing again in the B horizon. This trend was attributed to horizon inversion due to land preparation (Mason et al., 2009). The greater total lignin concentrations observed in woodland soil O horizons than A horizons in this study were likely to be attributed to degrading litter which was included in the analysis of the O horizon. Decreasing lignin phenol concentrations with increasing depth have also been observed in oak (*Quercus robur*) dominated woodland soils from the F2 + H horizon down to the mineral C horizons (Nierop and Filley, 2007) and in the soils and soil-DOM of coniferous forests (Guggenberger and Zech, 1994).

Carbon normalised total dissolved lignin concentrations were similar to total lignin concentrations in soil O and A horizons, for their respective land use (figure 5.1). The Fisher's protected least significant difference (FPLSD) test grouped the concentration data statistically, reported as letters above each column in figure 5.1, highlighting significant differences. Therefore, hypothesis 6, that normalised total lignin phenol concentration in water outlets is not significantly different from its concentration in soil, was accepted. Consequently, we propose that a considerable proportion of lignin is lost from soils through leaching. However, total lignin concentration in the Sticklepath drain was considerably lower which may be because a non-measurable proportion of the water collected from this site originates from an underground spring which may have contributed non-lignin-derived organic matter.

Furthermore, there were no significant differences in total lignin concentrations between different soil organic horizons, different soil A horizons, nor in DOM, from grassland, woodland, and moorland land use types, with the exception of the Sticklepath DOM, likely due to a proportion of it deriving from an underground spring (figure 5.1). This indicates that none of the land uses investigated released more lignin phenols from its soil than another.

5.3.2 Lignin phenols in soils and DOM from different land use type

Lignin phenols extracted from grassland soil O-, A-horizon, and extracted DOM are reported in figure 5.2, and the numbered letters representing lignin phenols are defined in figure 1.10.

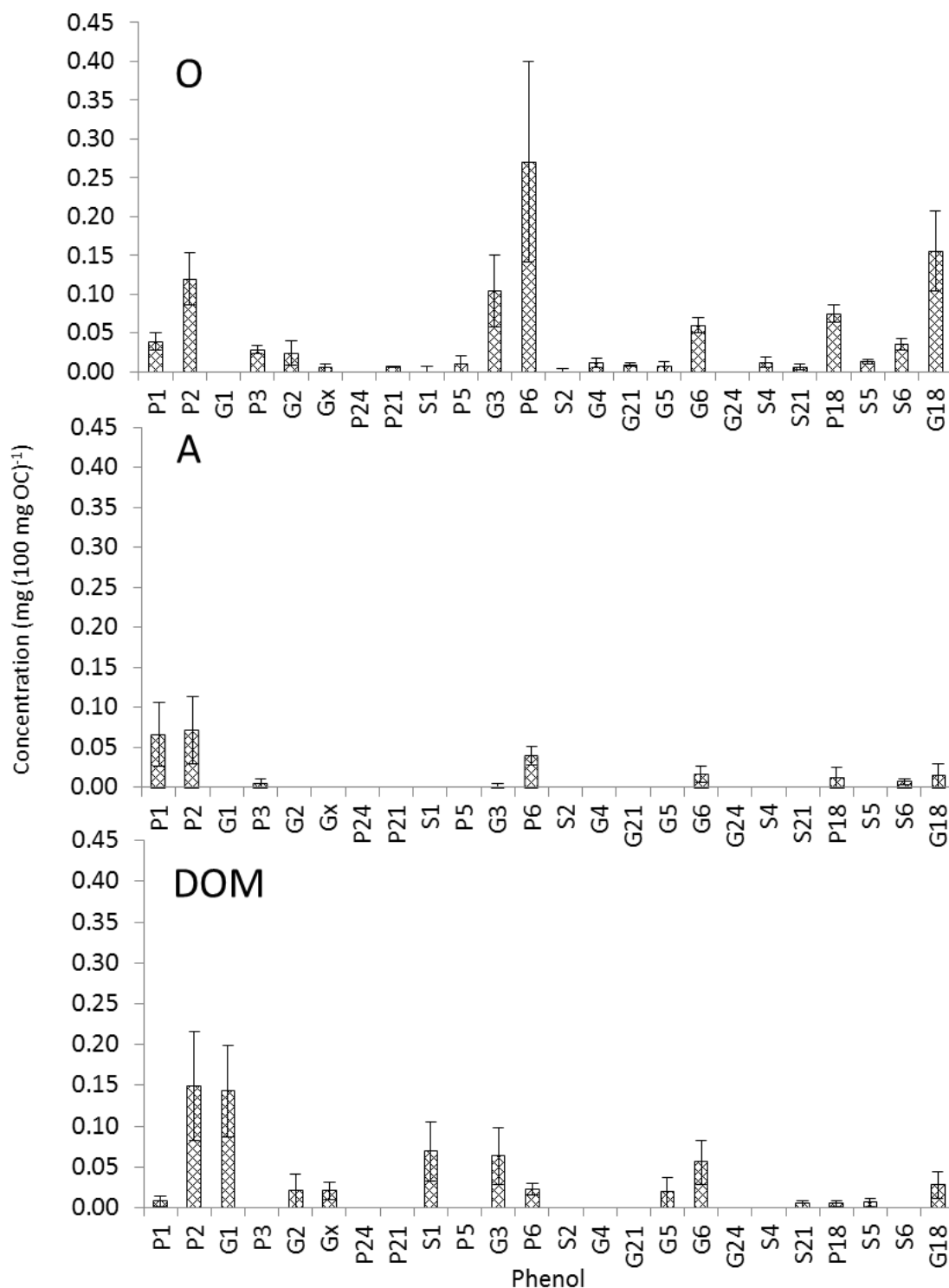


Figure 5.2. Mean (\pm standard error of the mean, $n = 3$) grazed grassland lignin phenol concentrations in soil organic- (O), A-horizon (A), and DOM (Taw Barton Farm). Lignin phenol abbreviations are defined in figure 1.10.

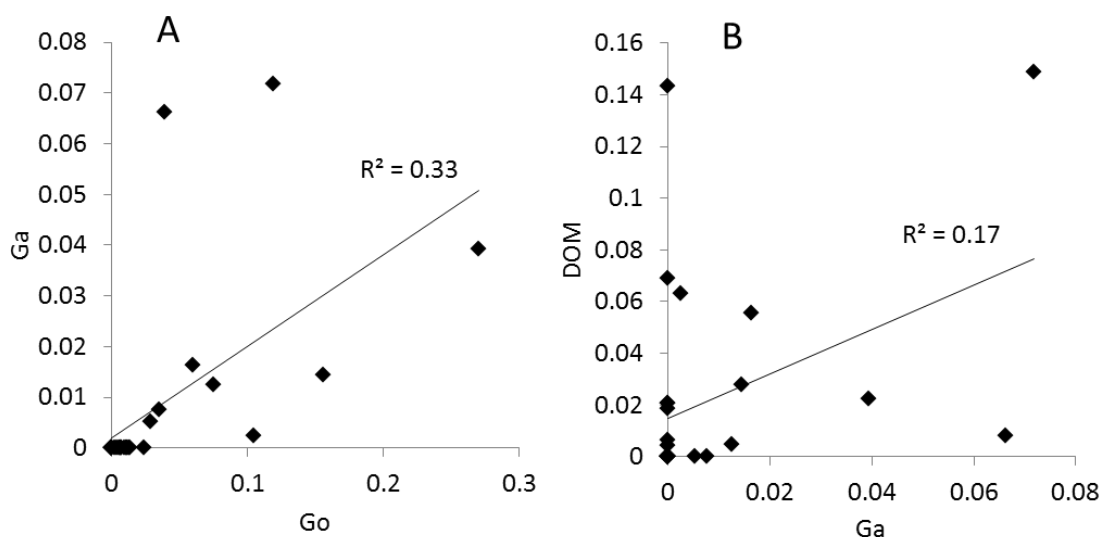


Figure 5.3. Lignin phenol correlations between grassland soil organic (Go) and A horizons (Ga, plot A) and between the A horizon and DOM (Taw Barton Farm, plot B).

P6 and G18 lignin phenols were dominant in the soil organic horizon (figure 5.2), whereas in the A horizon their concentrations were substantially reduced. P1 and P2 were dominant in the A horizon, and overall there were fewer lignin phenols. There were also reductions in P3, G6, P18, and S6 concentrations. There was little correlation between the concentration of individual lignin phenols between the grassland soil O and A horizons (figure 5.3A, $R^2 = 0.33$, $P = 0.086$), and between the A horizon and grassland DOM (figure 5.3B, $R^2 = 0.17$, $P = 0.387$). The dominant P6 and G18 peaks in the grassland O horizon in this study were important lignin-derived compounds observed in other grassland studies (Huang et al., 1998, Mason et al., 2012), and G18 and P18 are indicative of non-woody lignin (Hedges and Mann, 1979a) as well as P3 and G3 (Clifford et al., 1995, Chefetz et al., 2000). Dominant compounds in grassland DOM (figure 5.2 DOM, Taw Barton Farm drain) included P2 and G1. The concentration of dissolved G6 increased to a value higher than that of the A- but lower than that of the O horizon. G1 and G6 in this study are shown to be important in woodlands, and its detection here can be explained by the presence of oak and willow trees overhanging the pond. However, Huang et al. (1998) also observed G1 and G6 in autumn and spring DOM from upland grassland where G6 was the most abundant lignin-derived compound.

In the woodland ecosystem, P2 and G6 were dominant lignin-degradation products in the O- and A-horizons, and woodland DOM (figure 5.4 and table 5.1: Orchard Dean Copse stream).

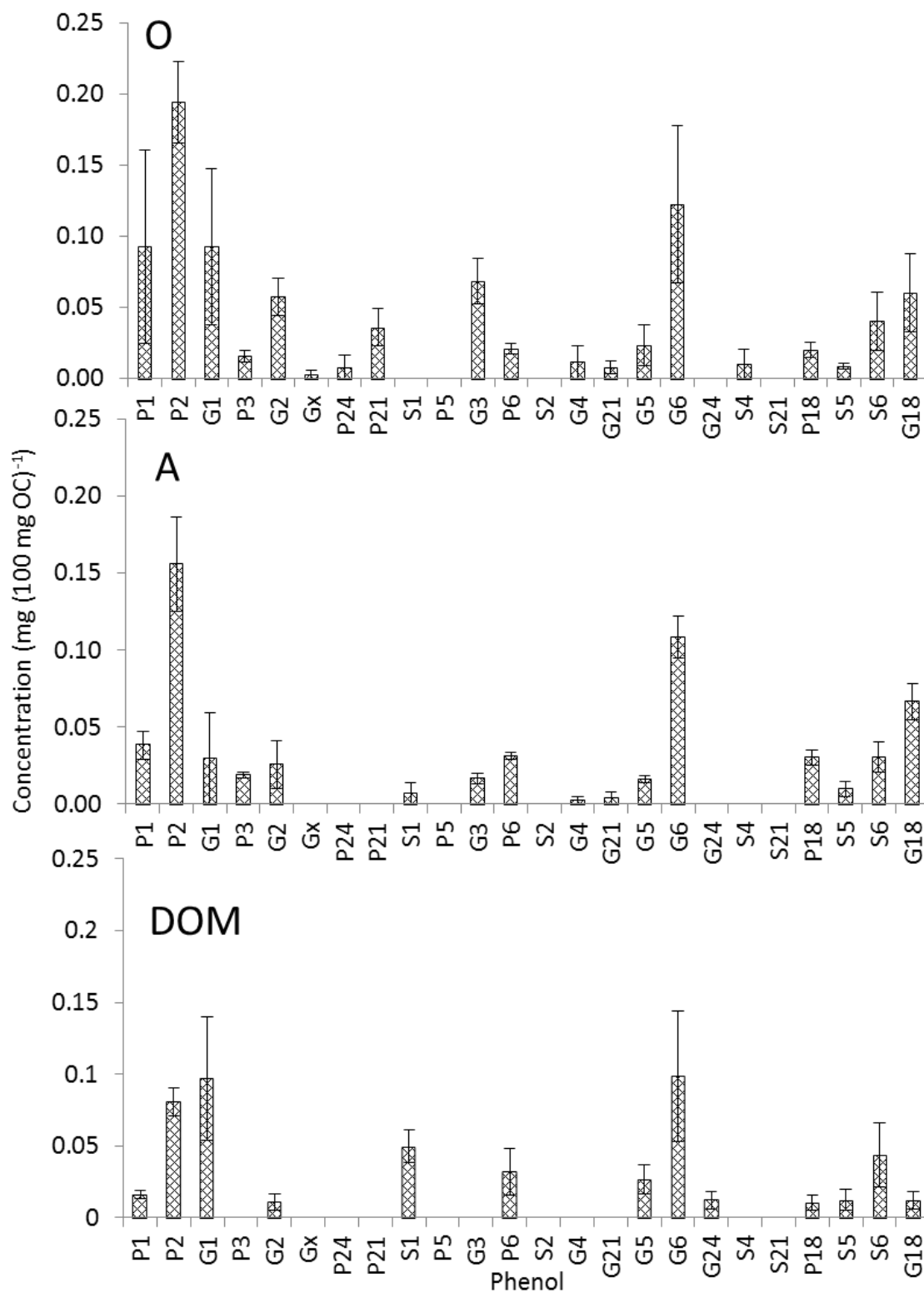


Figure 5.4. Mean (\pm standard error of the mean, $n = 3$) woodland lignin phenol concentrations in soil organic- (O), A-horizon (A), and DOM from Oak woodland (Orchard Dean Copse stream). Lignin phenol abbreviations are defined in figure 1.10.

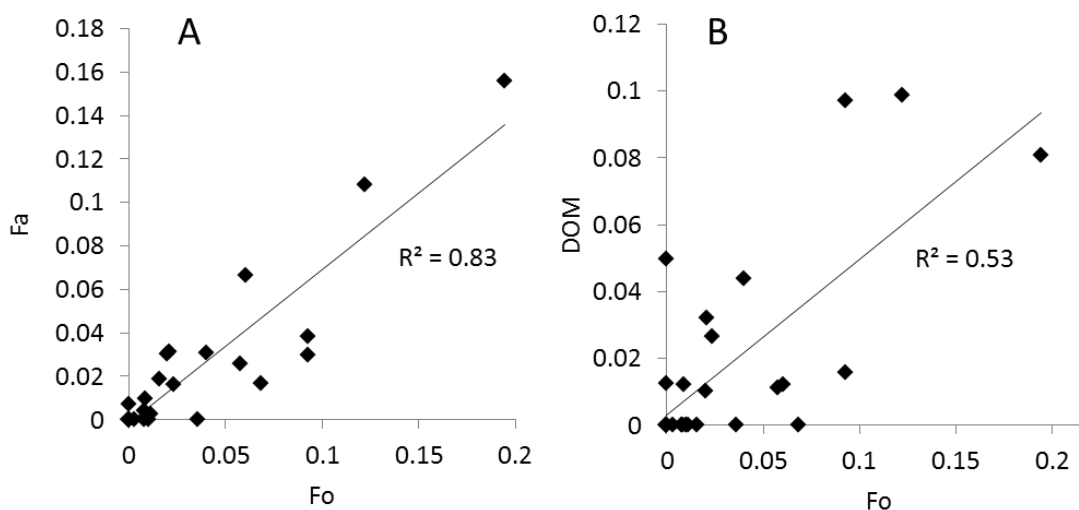


Figure 5.5. Lignin phenol correlations between woodland soil organic (Fo) and A horizons (Fa, plot A) and between the organic horizon and DOM (Orchard Dean Copse stream, plot B).

P1 and G1 were also dominant in the organic horizon although P1 and P2 gradually reduce in concentration down the profile and into the dissolved phase, whereas G1 reduced in concentration in the A horizon although it was dominant in DOM (figure 5.4). There was a good correlation between lignin phenol concentrations in woodland soil O and A horizons (figure 5.5A, $R^2 = 0.83$, $P = <0.000$), and a weaker correlation between those for the O horizon and woodland DOM (figure 5.5B, $R^2 = 0.53$, $P = 0.004$). In a Sitka spruce soil G6 was the most dominant peak in the F and A1 horizons, although P2 was not reported as it would have been outside the chromatographic region of the partial GC traces published. In the same study, G1 was identified as a minor peak down the soil profile (Mason et al., 2009). In a beech woodland soil, P1 and G1 were amongst the most dominant lignin phenols in the L-, F-, and H-horizons. G6 was also detected but was not a dominant peak (Nierop and Buurman, 1999). The data in this experiment suggests that a dominance of P2, G6, and G1 phenols may be indicative of oak dominated woodland ecosystems.

In the moorland O and A horizons, P2 and G3 were dominant compounds (figure 5.6), though reduced in concentration in the A horizon to approximately two thirds of that in the O horizon. In the moorland DOM (figure 5.6, table 5.1: River Taw), P2 and G6 were dominant, with G3 a minor component. The relatively dominant G6, together with G1, could be due to tree ecosystem lignin input since trees were growing along much of the length of the River Taw.

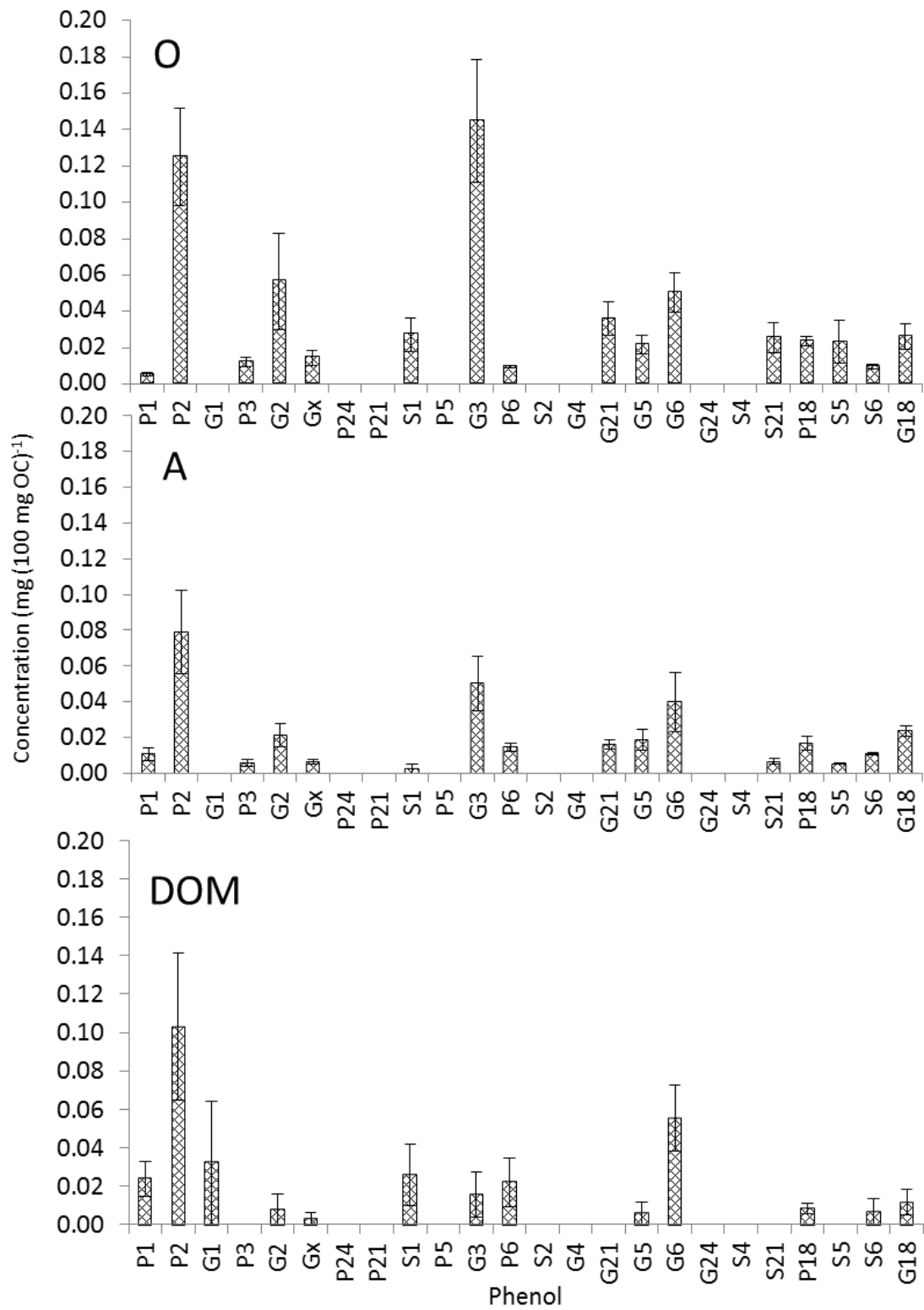


Figure 5.6. Mean (\pm standard error of the mean, $n = 3$) moorland lignin phenol concentrations in soil organic- (O), A-horizon (A), and River Taw DOM (DOM). Lignin phenol abbreviations are defined in figure 1.10.

There was a good correlation between lignin phenol concentrations in moorland soil O and A horizons (figure 5.7A, $R^2 = 0.83$, $P = <0.000$), and a weaker correlation between soil A horizon and DOM (figure 5.7B, $R^2 = 0.64$, $P = 0.000$).

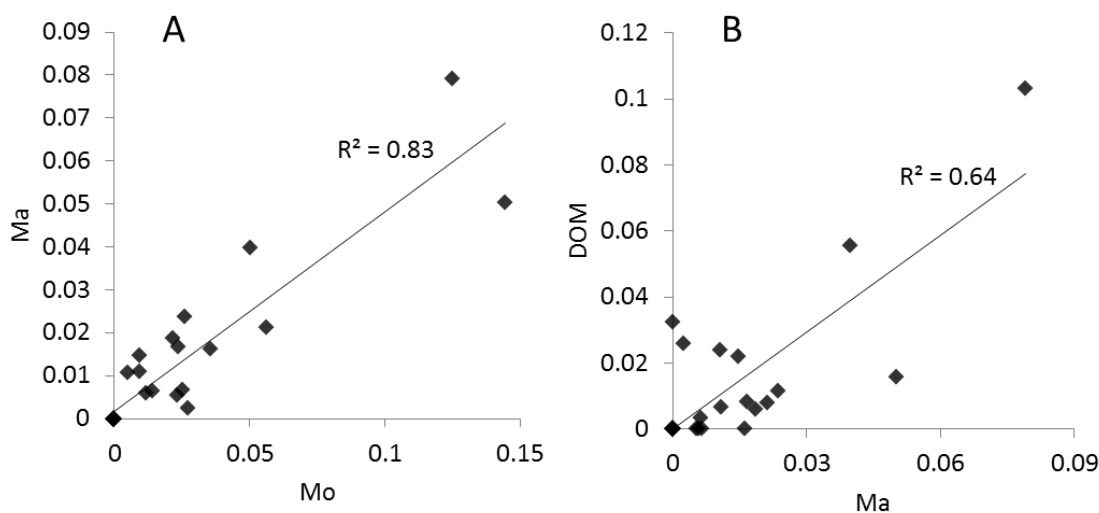


Figure 5.7. Lignin phenol correlations between moorland soil organic (Mo) and A horizons (Ma, plot A) and between the A horizon and DOM (River Taw, plot B).

The concentrations of lignin phenols identified in DOM extracts from each of the six sites are reported in table 5.1. G6 was relatively more abundant at woodland sites (Tributary of River Taw, Josephs Carr pond, River Taw, and Orchard Dean Copse stream). G1 was one of the more dominant lignin peaks at Taw Barton Farm drain, Tributary of River Taw, Josephs Carr pond, and Orchard Dean Copse stream. S6 was detected in the River Yeo, Josephs Carr pond and Orchard Dean Copse stream, which were all within, or in close proximity to oak-dominated woodland. S6 was also detected in peaty gley soils in a Sitka spruce afforested moorland (Mason et al., 2009) and in unimproved grassland (Mason et al., 2012), suggesting that a dominance of S6 does not indicate land use type.

Table 5.1. Mean (\pm standard error of the mean (s.e.), $n = 3$) dissolved lignin phenol concentrations from the six water samples. TBF = Taw Barton Farm drain, S = Sticklepath drain, TRT = Tributary of River Taw, JC = Josephs Carr pond, RT = River Taw, ODC = Orchard Dean Copse stream. The last six compound names with abbreviations (Abb.) in the table identify lignin degradation products detected in soils but not in water samples.

lignin compound	Abb.	mean concentration ($\mu\text{g (100 mg OC)}^{-1}$)											
		TBF	s.e.	S	s.e.	TRT	s.e.	JC	s.e.	RT	s.e.	ODC	s.e.
methoxybenzene	P1	8.3	6.6	7.4	4.4	21.5	11.8	17.0	3.1	23.8	9.1	15.9	2.9
4-methoxytoluene	P2	148.6	66.9	7.5	3.1	97.8	33.5	98.8	13.5	103.1	38.6	80.9	9.9
1,2-dimethoxybenzene	G1	143.2	56.3	10.9	6.4	104.2	54.9	71.6	23.8	32.2	32.2	97.0	43.2
4-methoxybenzeneethylene	P3	0	0	7.3	4.3	0	0	0	0	0	0	0	0
3,4-dimethoxytoluene	G2	20.7	20.7	0.8	0.8	11.9	11.9	3.4	1.9	8.0	8.0	11.1	5.6
4-methoxybenzaldehyde	P4	0	0	1.6	1.6	0	0	0	0	0	0	0	0
3-methoxy-4-hydroxyethylbenzene	Gx	20.7	10.8	0	0	18.2	9.2	0	0	3.2	3.2	0	0
1,2,3-trimethoxybenzene	S1	68.9	36.1	1.0	1.0	76.6	41.4	30.4	7.3	25.8	16.2	49.6	11.3
3,4-dimethoxybenzeneethylene	G3	63.3	34.8	19.0	7.1	0	0	4.8	4.8	15.6	11.8	0	0
4-methoxybenzoic acid methyl ester	P6	22.4	6.9	6.0	6.0	20.2	4.5	29.1	8.5	22.0	12.8	32.1	16.6
3,4,5-trimethoxytoluene	S2	0	0	0	0	4.7	4.7	0	0	0	0	0	0
1-(3,4-dimethoxyphenyl)-3-propene	G21	0	0	0	0	2.7	2.7	0	0	0	0	0	0
3,4-dimethoxyacetophenone	G5	18.8	18.8	0.9	0.9	24.7	11.0	7.4	3.7	5.8	5.8	26.7	10.1
3,4-dimethoxybenzoic acid methyl ester	G6	55.4	26.4	15.9	8.0	48.8	21.9	75.3	21.5	55.4	17.4	98.8	45.4
3,4-dimethoxybenzeneacetic acid methyl ester	G24	0	0	0	0	0	0	3.9	3.9	0	0	12.4	6.2
2-Propenoic acid, 3-(4-methoxyphenyl) methyl ester (E)-	P18	5.0	3.0	1.5	1.5	6.7	2.7	8.8	2.4	8.3	2.6	10.3	5.3
1-(3,4,5-trimethoxyphenyl)-3-propene	S21	4.4	4.4	0	0	3.1	3.1	0	0	0	0	0	0
3,4,5-trimethoxyacetophenone	S5	6.3	4.6	0	0	11.6	6.2	16.4	12.7	0	0	12.4	7.4
3,4,5-trimethoxybenzoic acid methyl ester	S6	0	0	0	0	24.9	14.9	20.0	11.0	6.7	6.7	43.8	22.0
2-propenoic acid, 3-(3,4-dimethoxyphenyl) methyl ester	G18	27.7	16.4	10.4	2.2	12.4	7.0	9.1	2.9	11.5	6.7	12.1	6.1
2-propenoic acid, 3-(3,4,5-trimethoxyphenyl) methyl ester	S18	0	0	0	0	0.9	0.9	0	0	0	0	0	0
3,4-dimethoxybenzaldehyde	G4												
4-methoxyacetophenone	P5												
3-(3,4-dimethoxyphenyl)-propanoic acid methyl ester	G12												
1-(4-methoxyphenyl)-3-propene	P21												
1-(3,4-dimethoxyphenyl)-3-propene	G21												
4-methoxybenzeneacetic acid	P24*												

5.3.3 Dung

G3, P18 and G18 were dominant lignin phenols in sheep and cattle dung, and were present at higher concentrations in sheep dung (figure 5.8). These were also relatively abundant in the grassland O horizon, which is likely due to ruminant grass diets.

Alternatively, dung grass lignin could contaminate the natural grass lignin signature since grassland soil cores were collected from grazed grassland, which would suggest that the grassland organic horizon lignin degradation product pattern was a mixture of natural grass and dung-grass. P3, G3, S1, S3, S5, S22, 4-(2-Z-propenyl)syringol, and 4-(2-E-propenyl)syringol lignin degradation products have been observed in dung using off-line pyrolysis (Dungait et al., 2008), although concentrations were not reported for comparison with this study.

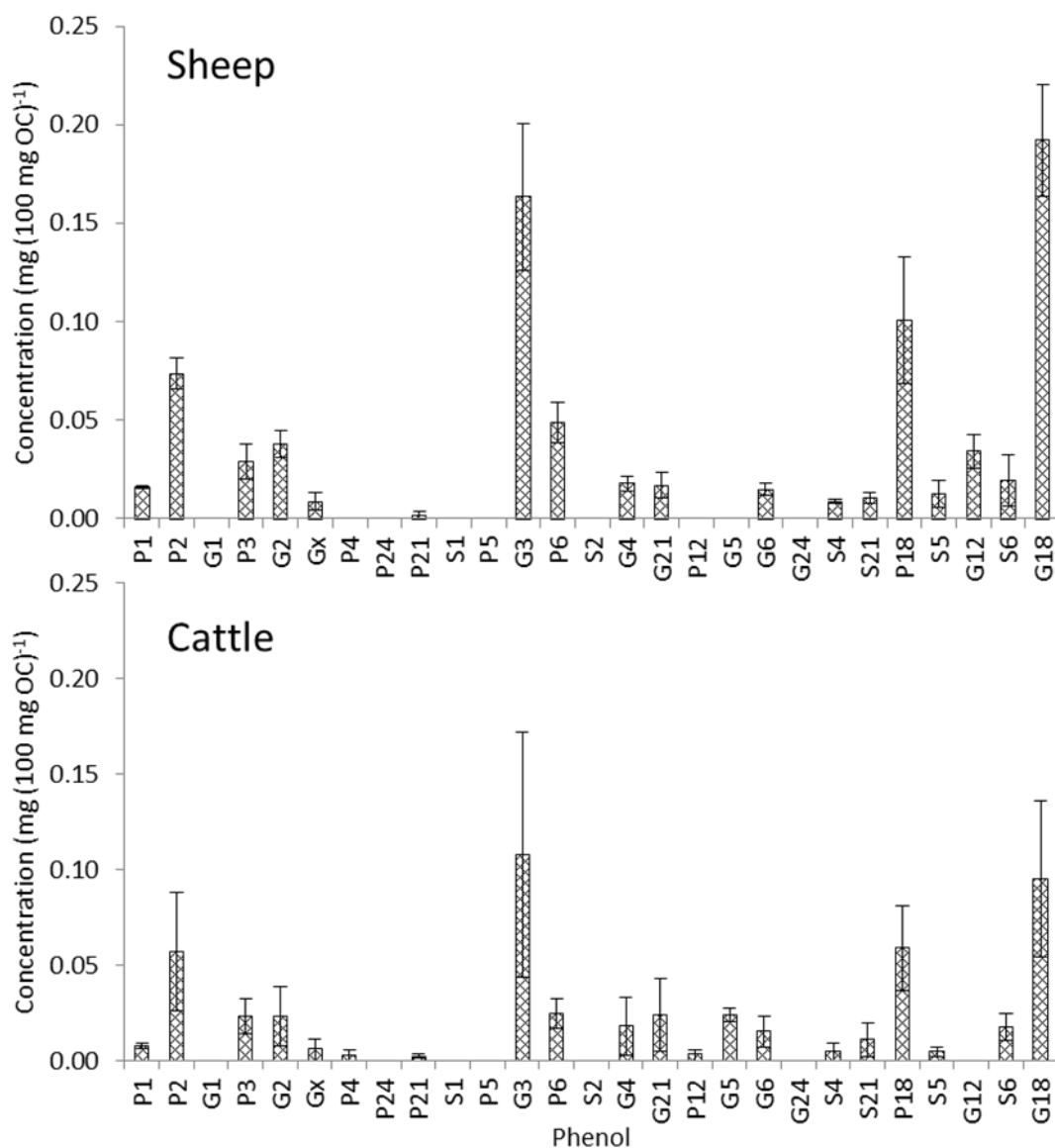


Figure 5.8. Mean (\pm standard error of the mean, $n = 3$) lignin phenol concentrations in sheep and cattle dung. Lignin phenol abbreviations are defined in figure 1.10.

5.3.4 Lignin phenols as indicators of land use type

Concentrations of individual lignin phenol data (individuals) and soil O and A horizon and DOM samples (variates) are displayed in a principal component biplot with first and second components on the x and y axis, respectively (figure 5.9). Phenols positioned in the same line as a soil or DOM sample have a strong association with that sample.

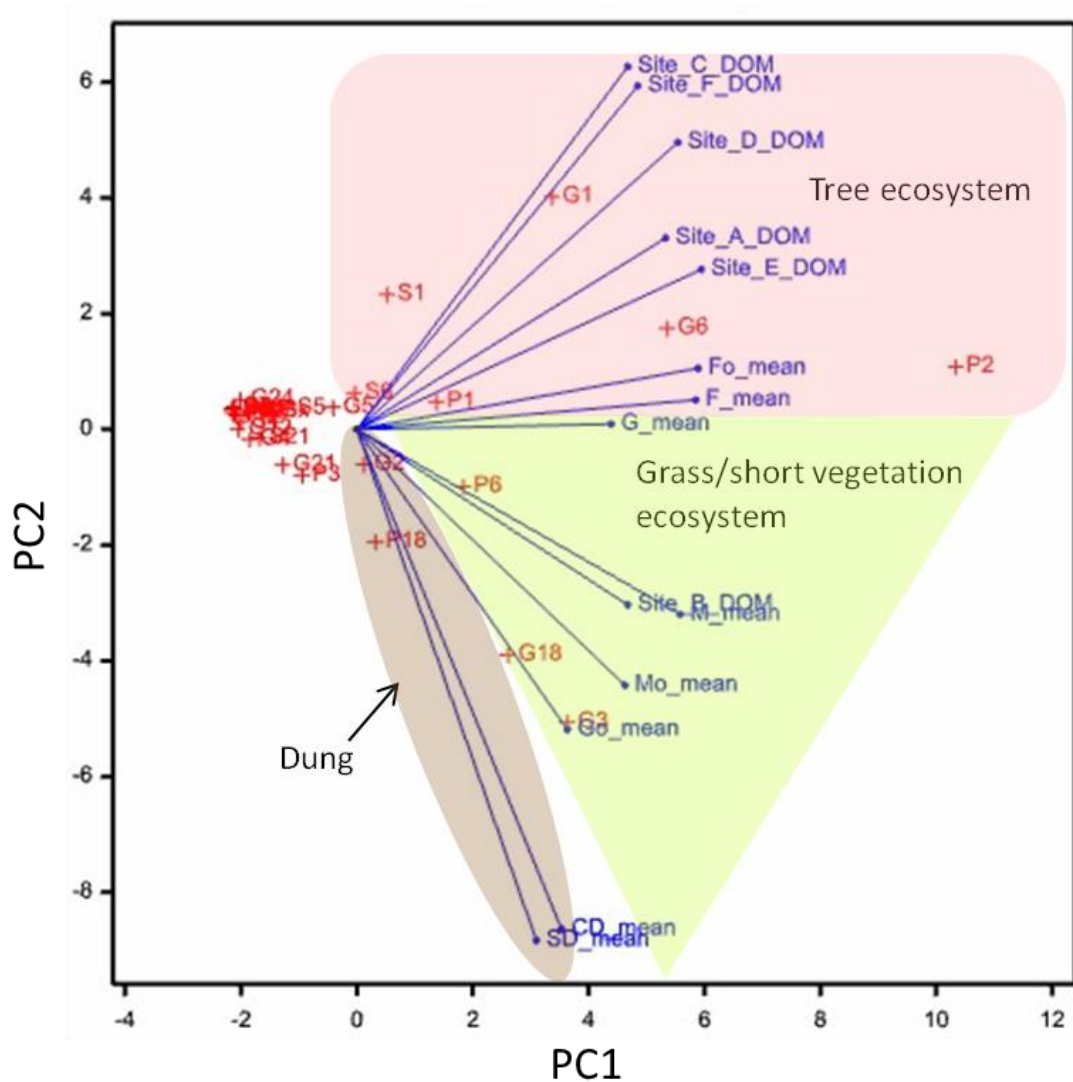


Figure 5.9. A principal component biplot of first and second components of individuals (individual lignin phenol concentrations, shown in red, table 5.1), and variates (different soil and dissolved organic matter samples, shown in blue). Site A_DOM, Site B_DOM, Site C_DOM, Site D_DOM, Site E_DOM, Site F_DOM, represent dissolved lignin samples from Taw Barton Farm, Sticklepath drain, Tributary of River Taw, Josephs Carr pond, River Taw, and Orchard Dean Copse stream, respectively. Go_mean, G_mean, Fo_mean, F_mean, Mo_mean, and M_mean represent soil organic and A horizon samples for grassland, woodland, and moorland land uses, respectively. Tree, and grass/short vegetation ecosystems, and dung-association regions are labelled.

The plot could be divided into regions of land use type, allowing lignin phenols associated with each region act as indicators of that land use. In the uppermost part of the plot are phenols associated with tree ecosystems: G1, G6, S6, P1, and P2, although P1 and P2 are positioned close to the tree-grass/short vegetation ecosystem border as they were abundant in both land use types. In the middle of the plot is a region associated with grass/short vegetation ecosystems where key lignin phenols included: P6, G3, and G18. Finally, in the lower-left of the plot is a region associated with sheep and cattle dung, where P18 was a key lignin phenol. The majority of DOM samples were located in the tree-association region, which can be explained by the presence of trees close to the sampling location, indicating that nearby trees can strongly contribute to the composition of a dissolved lignin sample. Therefore, hypothesis 5, that lignin phenols detected in soils and in the DOM of adjacent water outlets are a function of land use type, was accepted.

5.4 Conclusions

For grassland, woodland, and moorland land uses, a greater number of lignin phenols were detected in the soil O and A horizons than in the dissolved phase, with the exception of grassland A horizons. Virtually all lignin phenols detected in the dissolved phase were also detected in their respective soil O and A horizons. Normalised total dissolved lignin phenol concentrations from all three land uses were not significantly different to those in their respective soil O and A horizons, thus H6 was accepted. This suggests that a considerable amount of lignin, comparable to its proportion in SOM, is being lost from soils through leaching. There were no significant differences in normalised total lignin concentrations between different soil organic horizons, different soil A horizons, nor in DOM, from grassland, woodland, and moorland land use types. This indicates that lignin phenols were not lost in greater quantities from the soils of any of the land use types investigated.

Additionally, a dominance of specific lignin phenols were indicative of land use type, leading to the acceptance of H5. This study provides valuable molecular level information to understanding lignin's behaviour in soil carbon sequestration.

Chapter 6. Transport of phenols through soil

6.1 Introduction

Contrary to the traditional view that lignin is a relatively recalcitrant component of SOC (Crawford, 1981), it decomposes into monomer phenols (Chen et al., 1982). There is increasing evidence to suggest that lignin is not necessarily stabilised in soils (Kiem and Kogel-Knabner, 2003, Amelung et al., 2008, Bol et al., 2009, Thevenot et al., 2010), relative to ‘labile’ compounds, e.g. carbohydrates (Huang et al., 1998, Gleixner et al., 2002, Schmidt et al., 2011). Up to 74% of lignin was lost from senescent *Rhizophora mangle* leaf material in the dissolved phase through leaching (Benner et al., 1990), demonstrating that lignin decomposition products are soluble and can be transported by leaching through soils. Published data about the amount of lignin transported in the dissolved phase in soils is scarce. Previous research reported that when *Phanerochaete chrysosporium* (a white-rot fungi) degrades ¹⁴C-labelled aspen wood in static liquid culture, it releases almost as much ¹⁴C-derived lignin in water-soluble form as in ¹⁴CO₂ (Reid et al., 1982). Indeed, in this thesis it has been determined that total lignin phenols normalised to total soil organic carbon amounts in natural freshwaters can be as great as those in soils (see Chapter 5). It is therefore important to determine the relative rate of transport of lignin phenols through soil in order to understand if certain lignin breakdown products have a longer residence time in soils than others (Dungait et al., 2008) due to retention mechanisms. Roots are an important pathway for lignin input into the soil, and Rasse et al. (2005) suggest mechanisms whereby root SOC may be protected and retained in soils. Such mechanisms include: greater chemical recalcitrance of root tissues compared to shoots, which may be intrinsic or via selective incorporation of Al and Fe ions into root litter material; physical protection through aggregation; and physico-chemical protection through interaction with minerals (figure 6.1). However, there has been little study of the effect of soil site saturation on transport of apparently reactive lignin molecules. Because lignin monomer types are a function of vegetation type ((Hedges and Mann, 1979a, Clifford et al., 1995), and Chapters 4 and 5), the potential exists to establish whether specific lignin phenols are more likely to be transported than others, and to identify vegetation types in which these less readily transportable phenols are more abundant. This thesis therefore hypothesizes that this knowledge could provide a new tool to increase soil organic carbon stocks.

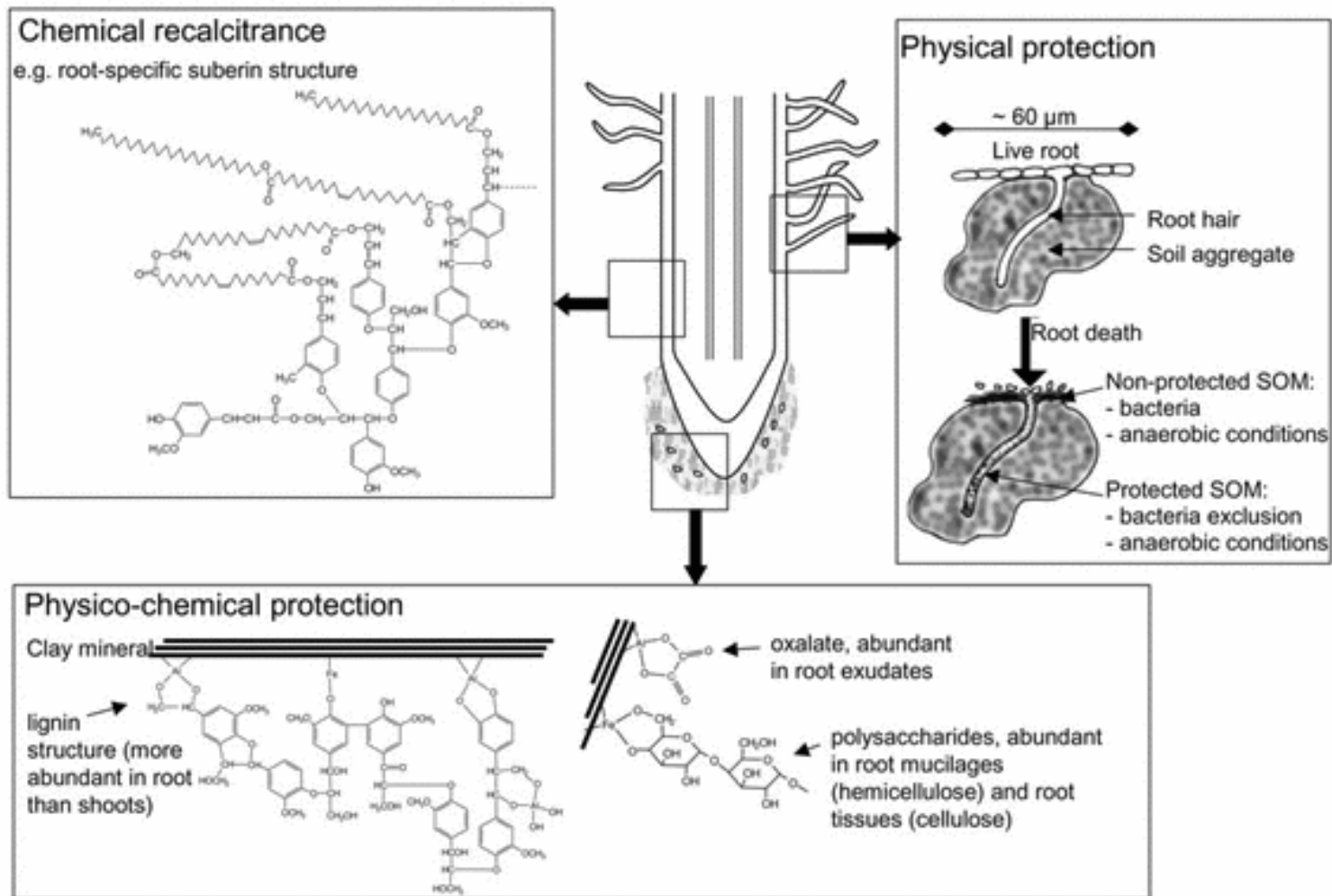


Figure 6.1. Processes resulting in protection of root carbon in soils (Rasse et al., 2005).

When lignin enters the soil it is exposed to the processes of degradation and transport, which may be concomitant or non-concurrent. Previous research has determined the abundance of total lignin in soil samples, but this constitutes a ‘snap shot’ and does not reveal which lignin components are immobile and stabilised and which are being transported through the soil matrix at that instant. It is also unknown whether the mass of lignin input dictates the rate of leaching of lignin monomers from the soil. Therefore, this experiment was designed to:

- (i) isolate the transported component of lignin as its phenol monomers,
- (ii) determine relative rates of transport of those monomers, and
- (iii) explore the effect of different mass inputs of lignin on rates of transport.

Differentiation between ‘new’ and ‘old’ lignin can be achieved either by application of specific lignin phenols not already present in the soil, such as synthetic lignin phenols, or through the use of isotopically labelled (^{14}C or ^{13}C) lignin phenols, at natural abundance, e.g. (Dignac et al., 2005, Bahri et al., 2006, Dungait et al., 2008, Dungait et al., 2010) or synthetically labelled monomers (Kirk et al., 1975). Previous research showed that dung-derived lignin phenols with propenyl side chains, particularly in the *Z* isomer conformation, were more stable in soils than the *E* isomer, as they were detected in soil 0-1 cm horizons after one year, and acetyl- and 2-propanone- side chains attached to syringyl units became relatively more abundant (Dungait et al., 2008), suggesting that all these side chain types may be less prone to leaching.

Other research has shown that < 12% of organic matter from cattle dung in soil remains in the top 5 cm of silty-clay soil (Dungait et al., 2005), although a subsequent investigation of particulate size fractions of cattle slurry using ^{15}N -labelled material showed that the majority was in the top 5 cm (Dungait, Williams et al., in preparation). Therefore, a substantial proportion of livestock-derived OM applied to soil is at risk of loss as leachate or surface runoff as particulate OM and sediment-bound components (Lloyd et al., 2012). Furthermore, there is evidence to suggest that dung application can induce priming effects that trigger increased leaching of SOC (Bol et al., 1999) or CO_2 emissions (Vanlauwe et al., 1994, Hogberg and Ekblad, 1996). Therefore in this study, the soluble portion of natural abundance ^{13}C isotope cattle dung was used as a source of lignin monomers to investigate lignin phenol leaching through packed soil cores.

6.1.1 Aims and hypotheses

The aims of this experiment were (i) to determine the relative rates of transport of different lignin monomers through topsoil after the application of the soluble fraction of dung, and (ii) to investigate whether these rates vary with different application rates.

Hypotheses

H7. Different lignin phenols leach at different relative rates through soil as a function of molecular structure.

H8. The mass of lignin phenols leached from soil cores is directly proportional to the application rate of the soluble fraction of dung.

6.2 Methodology

6.2.1 Experimental design

A completely randomised experiment (table 6.1) was designed to explore the rate of transport of lignin from the soluble fraction of dung (dung DOC) through packed soil cores placed in lysimeters into leached water. The soil cores were randomised using a random number generator at the beginning of the experiment and after each sampling event. The treatments were three rates of slurry application (see below).

Table 6.1. Experimental design for the allocation of slurry treatments to packed soil cores and the re-randomisation of cores after each sampling event.

Core ID	treatment	Lysimeter location				
		Starting position	after 1st sampling	after 2nd sampling	after 3rd sampling	after 4th sampling
1	65 m ³ ha ⁻¹	2	1	5	11	13
2	65 m ³ ha ⁻¹	7	4	3	1	4
3	65 m ³ ha ⁻¹	4	10	2	13	8
4	65 m ³ ha ⁻¹	10	6	7	5	6
5	65 m ³ ha ⁻¹	9	13	9	2	2
6	163 m ³ ha ⁻¹	6	11	6	3	1
7	163 m ³ ha ⁻¹	13	2	10	8	9
8	163 m ³ ha ⁻¹	1	8	13	6	5
9	163 m ³ ha ⁻¹	8	5	11	7	11
10	163 m ³ ha ⁻¹	5	3	1	12	3
11	Control 1	11	9	4	4	7
12	Control 2	12	12	12	9	10
13	Control 3	3	7	8	10	12

6.2.2 Preparation of soil cores, dung DOC, irrigation, and sampling

Rivington soil was collected as described in Chapter 2, table 2.1 and section 2.3. The soil was packed into cores, C4 dung DOC was prepared and applied to cores, the soil cores subsequently received simulated rainfall, and leachates were collected as described in Chapter 2, section 2.5.2, and shown in figure 6.2 in this chapter.

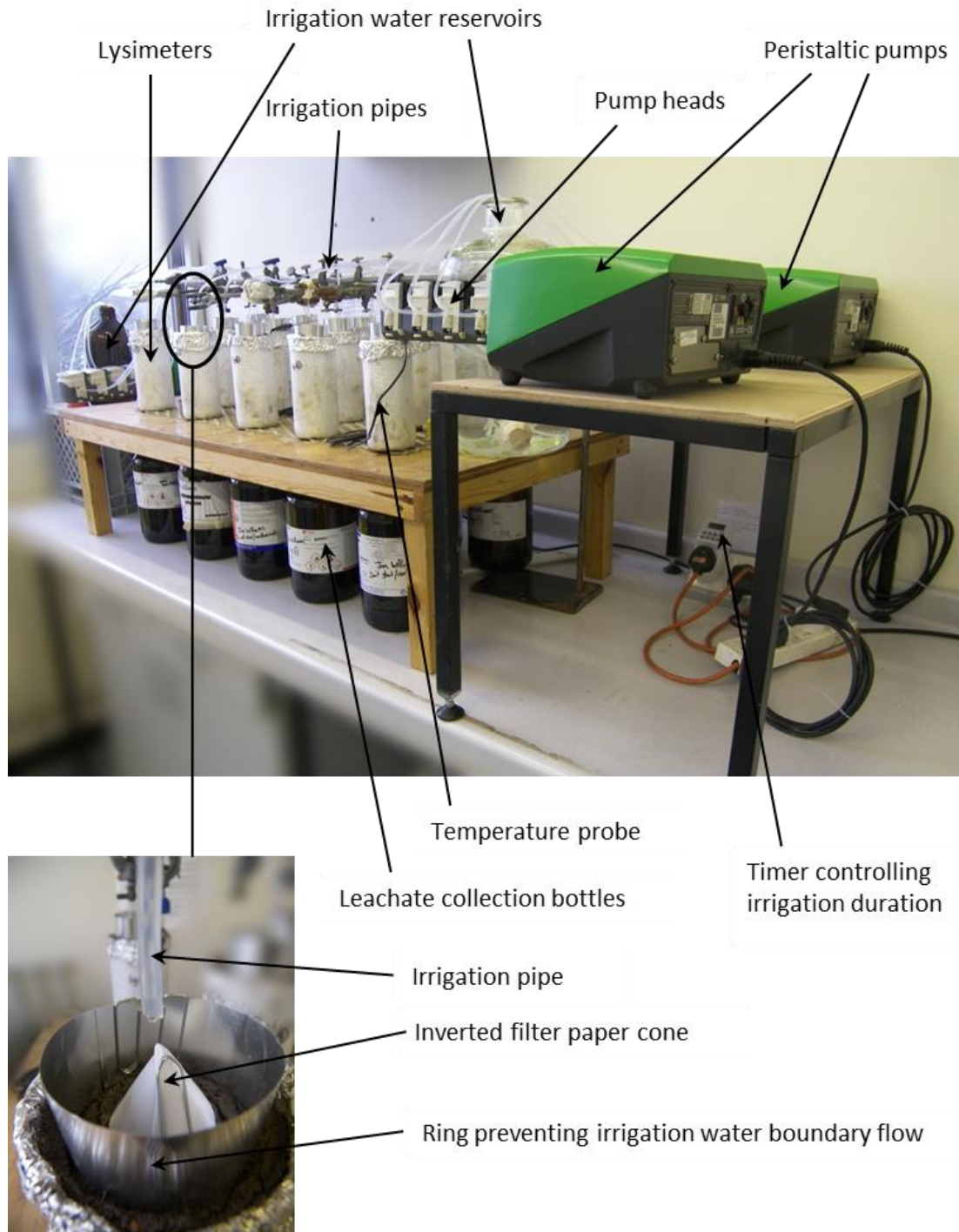


Figure 6.2. Experimental setup showing how irrigation water was pumped to each lysimeter, and subsequent leachate collection. The Insert shows the top of a lysimeter, utilising an inverted cone of filter paper to distribute irrigation water evenly.

6.2.3 Data handling, sample derivatisation and analysis

All of the release curve results in this study are expressed on the x axis in terms of number of soil pore volumes of leachate passed rather than as units of time, since the intensity and duration of rainfall events in nature vary spatially and temporally. One pore volume has been defined as the amount of space in the soil core occupied by pores or fractures, and can be calculated as the soil porosity multiplied by the total volume of the soil core (Forslund et al., 2011). Thus, for the dimensions of the soil cores used in this study, packed to a soil ρ_b of 1.92 g cm^{-3} , one pore volume equated to 178 mL, and for the purposes of this experiment, 0.53 pore volumes of water was applied daily to soil cores to simulate rainfall. Therefore, leachate volumes collected are expressed on figure x axes as a multiple of 178 mL.

Dung DOC and leachates were analysed for dissolved organic carbon (DOC) as described in Chapter 2, section 2.6.2. Leachates and an aliquot (40 mL) of dung DOC were extracted using solid phase extraction (SPE), before an aliquot of the SPE residue was analysed for bulk total carbon and ^{13}C isotope analysis, as described in Chapter 2, sections 2.6.3 and 2.6.4, respectively. Another aliquot of the solid extract was derivatised with BSTFA as described in Chapter 2, sections 2.7.1, except that 5 μL of 5 α -androstane (0.1 mg/mL) was added to each sample as an internal standard instead of 3 μL . GC-MS analysis of the derivatised total solvent extract was performed as described in Chapter 2, section 2.8.2.

The identities and concentrations of the dissolved lignin monomers detected in the applied dung DOC are reported in section 6.3.1 and table 6.2. Lignin phenols in the slurry could exist in monomeric, dimeric, or oligomeric forms. Derivatisation with BSTFA was performed to enable the original monomeric forms to be detected without risk of generating new monomers through the breakage of inter-unit linkages in dimer or oligomer forms, which could occur with thermochemolysis techniques (Clifford et al., 1995), and CuO oxidation (Hedges and Ertel, 1982), for example.

Statistical analysis of the data was carried out as described in Chapter 2, section 2.9. Replication was 5 for application slurry treatments $65 \text{ m}^3 \text{ ha}^{-1}$ and $163 \text{ m}^3 \text{ ha}^{-1}$ and 3 for the Control treatment.

6.2.4 Predictions of mass of DOC and total lignin phenols leached

Equation 6.1 was used to predict the mass of DOC leached at 163 m³ ha⁻¹ (DOC_p) treatment application rate.

$$DOC_p = (DOC_{65} - DOC_c) \times 2.5 + DOC_c \quad \text{Equation 6.1}$$

Where:

$$DOC_{65} = 8.981x^{0.5308}$$

$$DOC_c = -0.1447x^2 + 3.7145x + 1.1704$$

x = number of pore volumes

Where, DOC_{65} is the mean measured mass of leachate DOC at 65 m³ ha⁻¹, DOC_c is the mean measured mass of control leachate DOC, and the constant 2.5 is the multiplication factor between the two treatment application rates.

Equation 6.2 was used to predict the mass of total lignin phenols leached following 163 m³ ha⁻¹ (TP_p) treatment application rate.

$$TP_p = (TP_{65} - TP_c) \times 2.5 + TP_c \quad \text{Equation 6.2}$$

Where TP_{65} is the measured mass of total lignin phenols leached at 65 m³ ha⁻¹ application rate, TP_c is the measured mass of total lignin phenols leached from the control cores, and the constant 2.5 is the multiplication factor between the two treatment application rates.

6.3 Results

6.3.1 Soluble dung C characterisation

DOC concentration in the dung C was 1465.6 ± 8.4 mg L⁻¹. The soluble fraction of the dung was 4.2‰ depleted in ¹³C compared to the bulk dung solids (δ¹³C = -12.6‰). The soil was -27.8‰ and the slurry was -16.8‰ giving a Δ¹³C value of 11‰.

Twelve major compounds were identified in the soluble dung (table 6.2) comprising P and G units only. G* monomer units refer to catechol compounds (compounds with two adjacent hydroxyl groups attached to a phenyl ring) that may be microbially

decomposed lignin G units (Kirk and Adler, 1969, Kirk et al., 1970). The phenols have a saturated or unsaturated side chain consisting of one, two, or three carbons, and all with a carboxyl group with the exception of 3,4-dihydroxycinnamyl alcohol, tris(trimethylsilyl)-. The code given in column two of table 6.2 identifies the phenols that were also extracted from the leachates and are used to refer to the compounds in the remainder of this chapter. G12 was present in the highest concentration in the soluble dung C ($1.41 \mu\text{g L}^{-1}$). The molecular structures of the 12 phenols reported in table 6.2 detected in leachates, including the syringyl phenol S6 which was detected in leachate but not in the applied dung DOC, are given in figure 6.3. These phenol molecular structures are the same as those reported in Chapter 1, figure 1.10 except that these are the trimethylsilyl ether or ester derivatives resulting from derivatisation with BSTFA, whereas in figure 1.10 the methylated derivatives are shown, that results from derivatisation with TMAH.

Table 6.2. Mean (\pm standard deviation; $n = 3$) concentrations ($\mu\text{g L}^{-1}$) of major lignin phenols extracted from the soluble fraction of cattle dung. Compound labels instead of the full compound name are used in the text.

Compound	Compound label	Monomer unit type	Concentration ($\mu\text{g/L}$)	σ ($\mu\text{g/L}$)
4-[(trimethylsilyloxy)-benzoic acid TMS ester	P6	P	1.05	2.35
4-(trimethylsiloxy)-hydrocinnamic acid methyl ester	P12	P	116.84	86.17
4-(trimethylsiloxy)-hydrocinnamic acid TMS ester		P	566.85	194.80
3-methoxy-4-[(trimethylsilyloxy)-benzoic acid TMS ester	G6	G	28.05	26.68
3-methoxy-4-[(trimethylsilyloxy)-benzeneacetic acid ethyl ester		G	357.11	433.90
3,4-bis[(trimethylsilyloxy)-benzoic acid TMS ester		G*	19.42	20.26
3,4-bis(trimethylsiloxy)-hydrocinnamic acid methyl ester		G*	179.36	119.67
3-methoxy-4[(trimethylsilyloxy)-benzenepropanoic acid TMS ester	G12	G	1409.99	483.34
4-(trimethylsiloxy)-cinnamic acid TMS ester	P18	P	37.26	83.32
3,4-bis(trimethylsiloxy)-hydrocinnamic acid TMS ester	G12*	G*	482.23	169.50
3,4-dihydroxycinnamyl alcohol, tris(trimethylsilyl)-ferulic acid, trimethylsiloxy, TMS ester	G18	G	72.30	38.13
Total lignin monomer phenols			3292.55	722.68

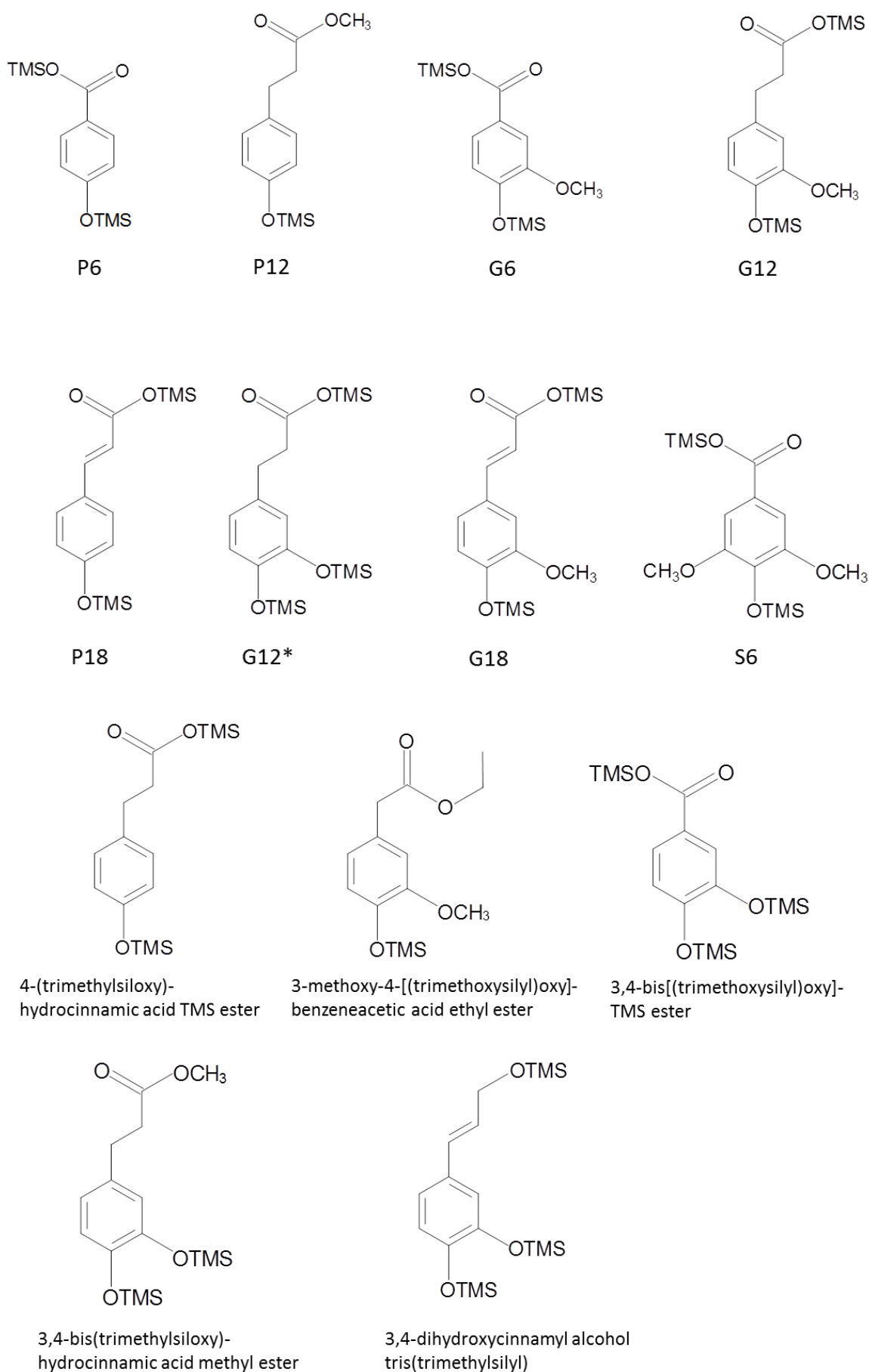


Figure 6.3. Molecular structure of phenols identified in soluble dung DOC and leachates reported in table 6.2.

6.3.2 Leachate DOC

Figure 6.4 is a cumulative release, or breakthrough curve where the area above the curve represents the mass fraction of DOC or specific phenolic compounds retained in the soil and the area below the curve represents the mass fraction leached from the soil core, following simulated rainfall application. The shape of a resulting breakthrough curve for chloride, for example, has been shown to be a function of soil texture (grain size), pore water velocity, diffusion coefficient, and soil column length (Shukla et al., 2000). Leachate DOC cumulative release results are shown in figure 6.4.

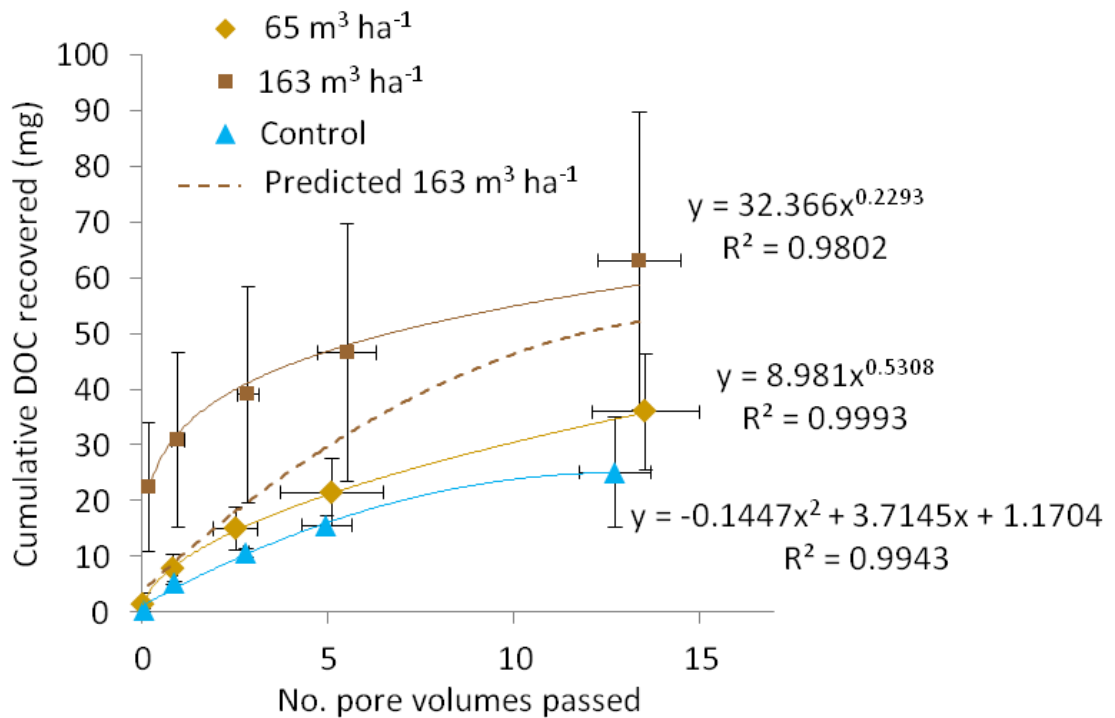


Figure 6.4. Mean values (and cumulative σ) for cumulative release of dung DOC in leachate from soil cores at 65 and 163 m³ ha⁻¹ application rates, where the control treatment (blue) received no dung DOC. The predicted amount of DOC leached following 163 m³/ha slurry application is shown (brown circles and dotted line) calculated using equation 6.1.

The total amount of DOC leached at the end of the experiment for the control, 65 m³ ha⁻¹, and 163 m³ ha⁻¹ treatments were 25, 36, and 63 mg, with an average per pore volume passed of 2.0, 2.7, and 4.7 mg, respectively. Only 27% (11 mg) and 37% (38 mg) of the soluble fraction of dung-DOC applied to cores was recovered after passage of 13.5 pore volumes for the 65 and 163 m³ ha⁻¹ treatments respectively. Therefore the remaining 73% (30 mg) and 63% (65 mg), respectively, was either retained in the soil, possibly sorbed, or was oxidised to CO₂ during the course of the experiment. The large cumulative

standard deviation (σ) for the $163 \text{ m}^3 \text{ ha}^{-1}$ treatment was due to the large variance in initial mass of leached DOC, attributable to variable soil leachate volumes (7 – 46 mL), which was translated into subsequent data points. After passage of approximately 0.1 pore volume, the mass of DOC leached from the $163 \text{ m}^3 \text{ ha}^{-1}$ treatment was significantly different from the $65 \text{ m}^3 \text{ ha}^{-1}$ and control treatments ($F_{pr} = 0.035$). This was because most of the DOC leached as direct leachate immediately following application. After passage of approximately 0.9 pore volumes, $163 \text{ m}^3 \text{ ha}^{-1}$ was significantly different from the control ($F_{pr} = 0.008$) but not significantly different from the $65 \text{ m}^3 \text{ ha}^{-1}$ treatment. After passage of approximately 2.7 pore volumes, 163 and $65 \text{ m}^3 \text{ ha}^{-1}$ treatments were significantly different from the control treatment ($F_{pr} = 0.007$), but not different from each other. After passage of approximately 5.2 and 13.2 pore volumes there were no significant differences between treatments ($F_{pr} = 0.106$ and 0.170 , respectively).

The predicted cumulative mass of DOC release (figure 6.4) at $163 \text{ m}^3 \text{ ha}^{-1}$ application rate calculated using equation 6.1 was always less than that observed, especially after approximately 0.2 pore volumes had passed where the predicted $163 \text{ m}^3 \text{ ha}^{-1}$ released 19.6 mg less DOC than that measured. After passage of 13.4 pore volumes, the difference between predicted and observed DOC released converged to 10.7 mg, indicating that the main difference between predicted and measured DOC leached following DOC input occurred within the passage of the first pore volume.

6.3.3 Leached total lignin phenols

The amount of summed total identified lignin phenols (table 6.2) in leachates is shown in figure 6.5. The control soils leached no lignin phenols initially, with the greatest mass released ($0.18 \mu\text{g}$) after 12.7 pore volumes had passed. The greatest mass of total lignin phenols released for the 65 and $163 \text{ m}^3 \text{ ha}^{-1}$ treatments were $2.3 \mu\text{g}$ and $60 \mu\text{g}$, after 5.1 and 0.2 pore volumes had passed, respectively. Therefore the lower input of dissolved lignin phenols led to their gradual release, whereas most total lignin phenols applied at $163 \text{ m}^3 \text{ ha}^{-1}$ leached after 0.2 pore volumes had passed. The large σ for the $163 \text{ m}^3 \text{ ha}^{-1}$ treatment was large initially ($\pm 71 \mu\text{g}$; 0.2 pore volumes), partly attributable to variable soil leachate volumes (7 – 46 mL), before reducing thereafter to between a range of ± 0.4 to ± 10.3 . Variance was more consistent for the $65 \text{ m}^3 \text{ ha}^{-1}$ and control treatments, ranging between ± 0.9 and ± 4.1 , and between ± 0 and ± 0.3 , respectively. There were

no significant differences between application treatments due to the large variance in the data.

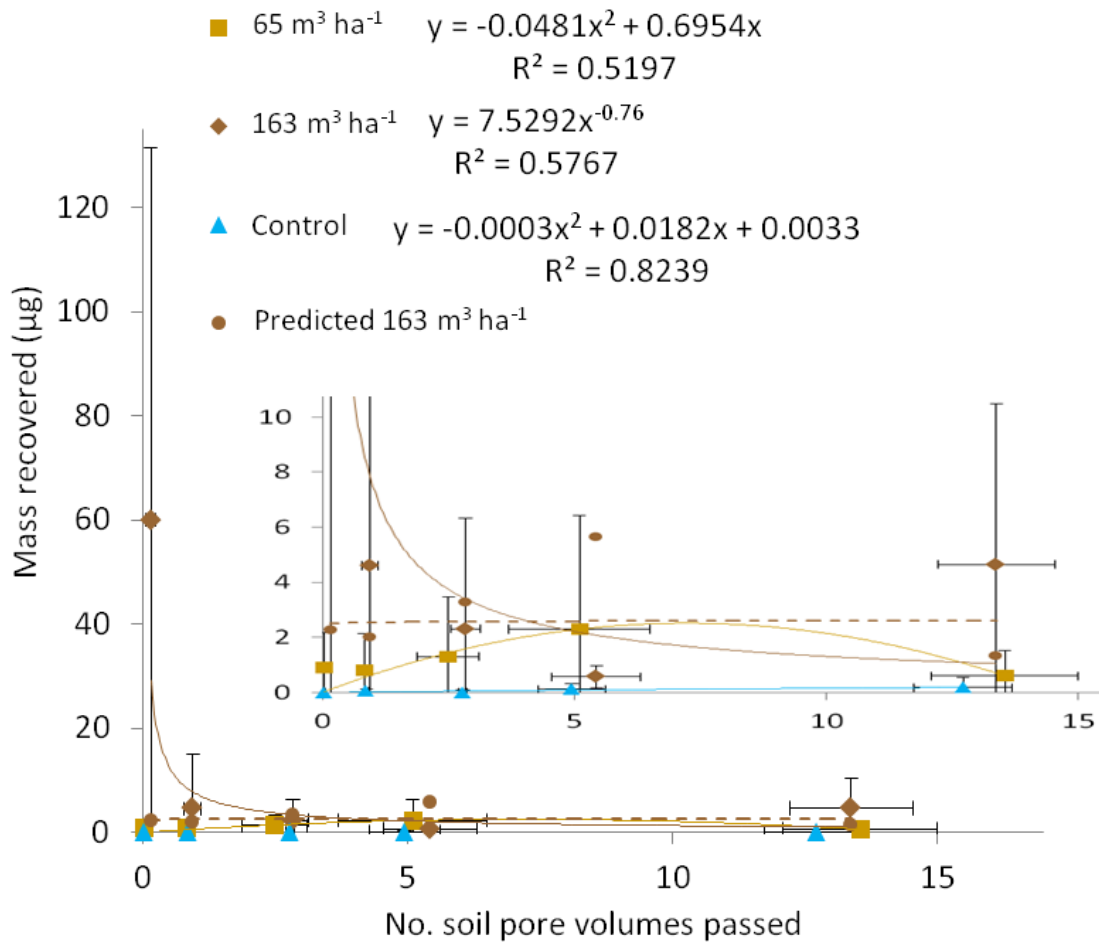


Figure 6.5. Release curves for mean ($\pm \sigma$) recovery of total lignin phenols applied to soil cores at 0 ($n = 3$), 65 ($n = 5$), and 163 m³ ha⁻¹ ($n = 5$) application rates. Total lignin defined as the sum of the compound concentrations listed in table 6.2. Predicted mass of total lignin phenols recovered in leachate at 163 m³ ha⁻¹ slurry application rate is also shown (brown circles and dashed line), calculated using equation 6.2. The insert is an expanded view of 0 – 10 μ g mass recovered.

Figure 6.5 also shows the predicted mass of total lignin phenols leached at 163 m³ ha⁻¹ application rate, calculated using equation 6.2. Individual observation data points at 65 m³ ha⁻¹ application rate were used to calculate the predicted total mass of lignin phenols leached instead of using the fitted curves in figure 6.5 due to their low R^2 values. The predicted mass of total lignin phenols leached was 27 times less than that detected at 163 m³ ha⁻¹ after 0.2 pore volumes had passed, although after 1 pore volume had passed the measured mass released was 2.3 fold greater than that predicted.

6.3.4 Leached lignin phenols

Release curves of eight phenols (P6, G6, G12, P18, G12*, P12, G18, S6) of the phenols detected in the slurry DOM (table 6.2) and subsequent leachates are shown in figure 6.6. These eight phenols were chosen as they represent P, G, and S phenols with varying side chain lengths from one to three carbons that are either saturated or unsaturated. Furthermore, some of these phenols were useful land use indicators based on the findings from Chapters 4 and 5.

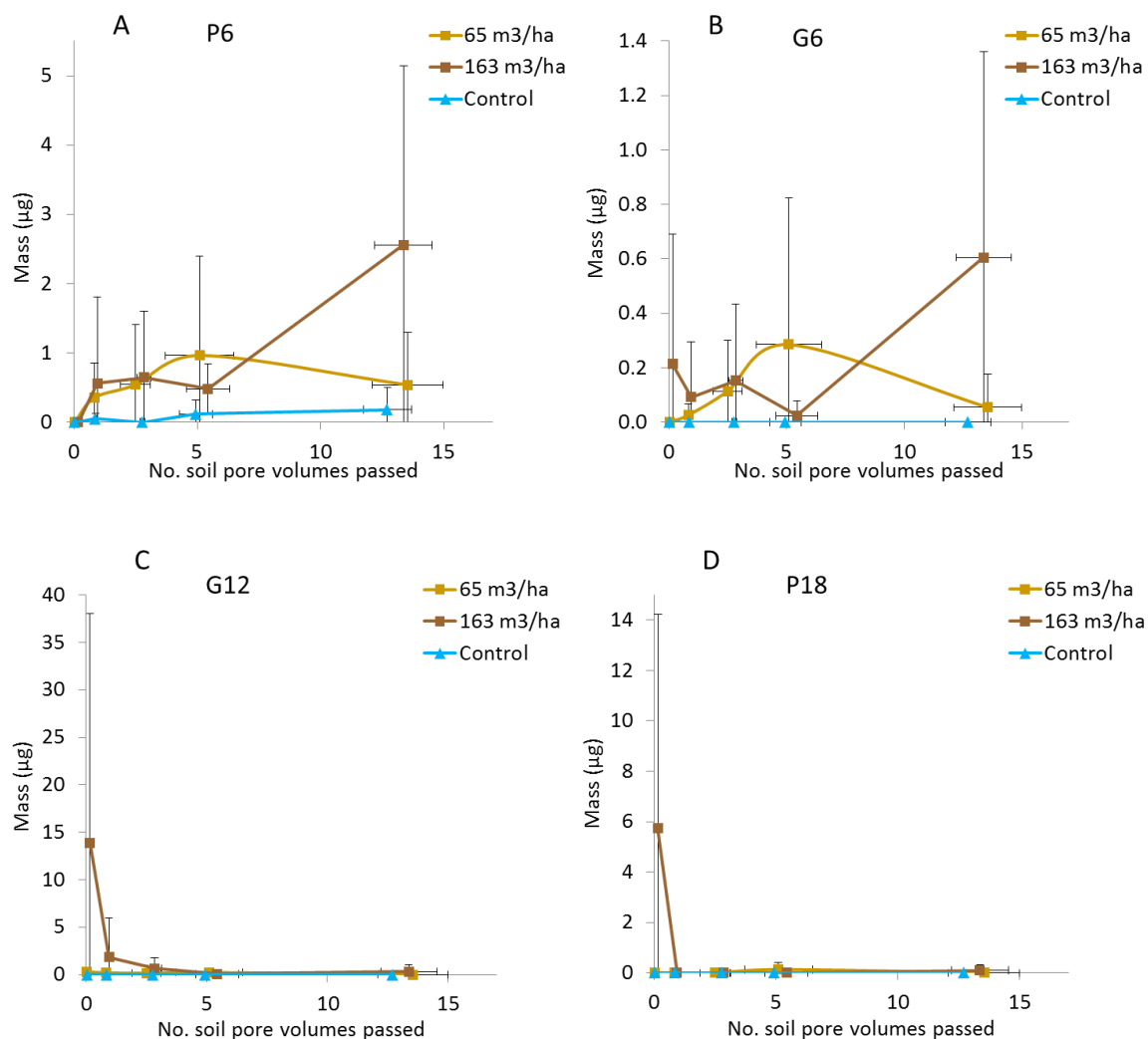


Figure continued on the next page.

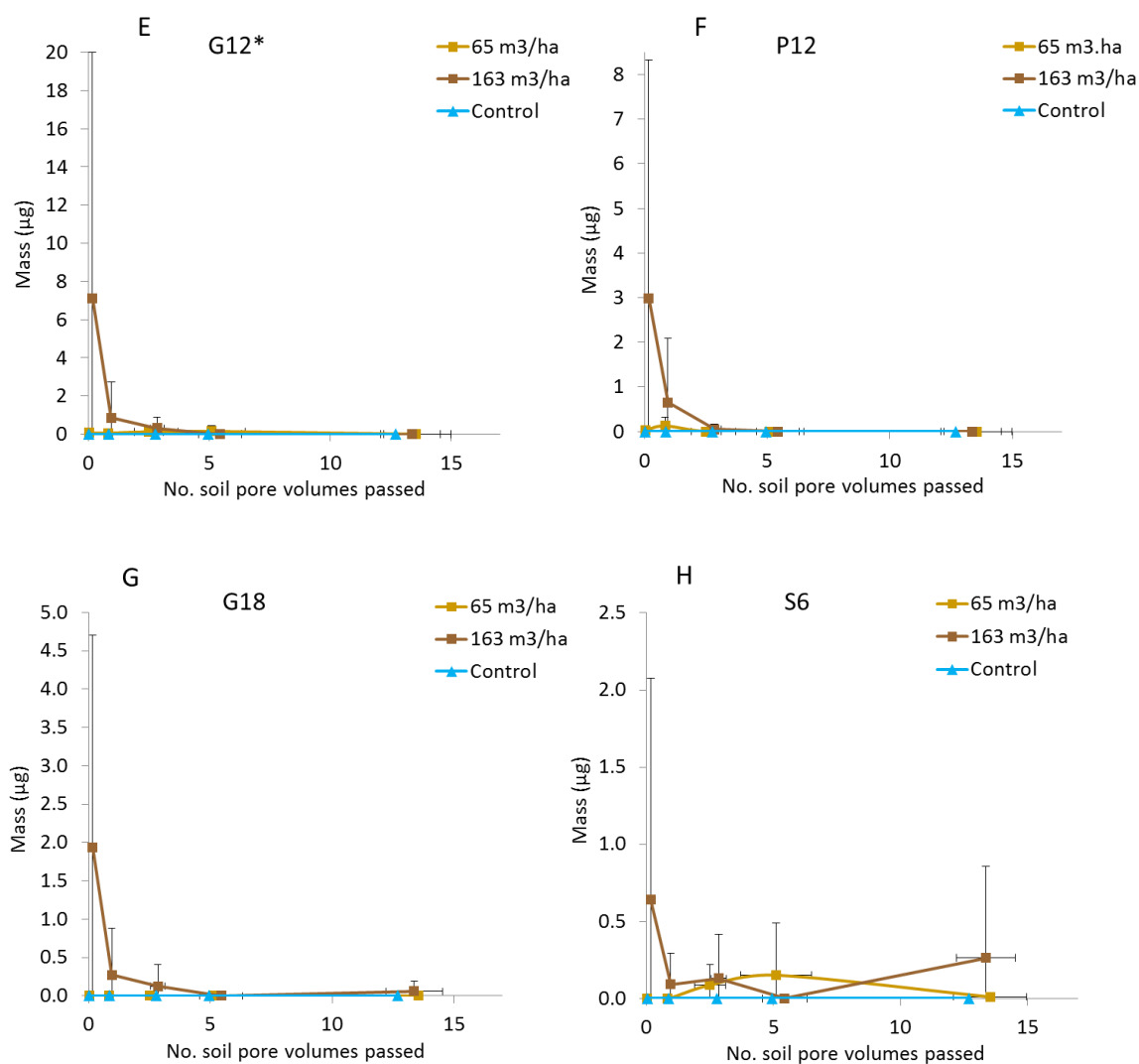


Figure 6.6. Release curves for mean masses (and standard deviation, $n = 5$) of P6, G6, G12, P18, G12*, P12, G18, and S6 lignin phenols determined in leachates from soil cores after application of dung DOC at 0, 65, and 163 $\text{m}^3 \text{ha}^{-1}$. Compound labels are defined in table 6.2.

Figure 6.6 shows that the majority of each lignin phenol leached from the 163 $\text{m}^3 \text{ha}^{-1}$ treatment during passage of the first pore volume, where the mass of individual phenols ranged between 14 μg (G12) and 0.6 μg (S6). However, due to the large variance, these were not significantly different from the control cores. Lignin phenols with C1 side chain (P6, G6, and S6) were more variable with increasing pore volumes passed, indicating they had more interaction with the soil matrix affecting subsequent release, or that they were the oxidation products of longer side chain lignin phenols (Dijkstra et al., 1998).

Mean recovery ratios were calculated for seven of the eight phenols in figure 6.6 as mass recovered in leachate at the end of the experiment after control subtraction (Mass) divided by initial mass applied to soil cores (Mass₀, table 6.3). No Mass/Mass₀ ratio was determined for S6 since no S6 was detected in the slurry DOM applied.

Table 6.3. Mean (n = 5) recovery (Mass/Mass₀) ratios of individual lignin monomers, total lignin phenols, and dissolved organic carbon (DOC) recovered in leachates after passage of 13.5 pore volumes. Differences in masses recovered at 65 and 163 m³ ha⁻¹ application rates are expressed as a Multiplication factor. Compound labels are defined in table 6.2.

Compound	Mean Mass/Mass ₀		Multiplication factor
	65 m ³ ha ⁻¹	163 m ³ ha ⁻¹	
P6	66.61	51.68	1.9
P12	0.05	0.45	24.1
G6	0.61	0.55	2.3
G12	0.02	0.17	18.8
P18	0.13	2.24	44.6
G12*	0.03	0.25	21.3
G18	0	0.47	
Total phenols	0.06	0.31	12.8
DOC	0.27	0.37	3.5

Mass/Mass₀ values for applied DOC recovered in leachate after passage of 13.5 pore volumes were 0.27 and 0.37 for 65 and 163 m³ ha⁻¹ application rates, respectively. Greater Mass/Mass₀ ratios were observed for individual phenols, total phenols, and DOC at 163 m³ ha⁻¹ than 65 m³ ha⁻¹ application rates, with the exception of P6 and G6. Mass/Mass₀ at 65 m³ ha⁻¹ application rate ranged from 0 (G18) to 0.61 (G6), and at 163 m³ ha⁻¹ ranged from 0.17 (G12) to 2.24 (P18). The mass recovery of P6 gave anomalous results at 65 and 163 m³ ha⁻¹ application rates in that 67 and 52 fold more mass was recovered in leachate than applied, respectively, after control subtraction. More P18 was also recovered in leachate at the 163 m³ ha⁻¹ application rate than that applied (Mass/Mass₀ = 2.24). No G18 was recovered in leachate at 65 m³ ha⁻¹, whereas at 163 m³ ha⁻¹ almost half the amount applied was recovered (Mass/Mass₀ = 0.47). By contrast, G6 mass recovery was more consistent by exhibiting similar Mass/Mass₀ ratios of 0.61 and 0.55 at 65 and 163 m³ ha⁻¹ application rates, respectively. Mass/Mass₀ ratios for total phenols were 0.06 and 0.31, which were less than those for bulk DOC (0.27 and 0.37) at 65 and 163 m³ ha⁻¹ application rates, respectively, indicating that in general lignin phenols were selectively retained in soils relative to DOC. However, P6 and G6

selectively leached at $65 \text{ m}^3 \text{ ha}^{-1}$ application rate, whereas at $163 \text{ m}^3 \text{ ha}^{-1}$ application rate P6, P12, G6, P18, and G18 all preferentially leached relative to DOC. There were no statistically significant differences in Mass/Mass₀ ratios between slurry application rates.

The multiplication factor (table 6.3) is the factor by which the mean mass of leached DOC, total lignin phenols, or individual lignin phenols increased as a consequence of the 2.5 fold increase in treatment application rate (from 65 to $163 \text{ m}^3 \text{ ha}^{-1}$), that was determined at the end of the experiment (after passage of 13.5 soil pore volumes). Multiplication factors varied from 1.9 (P6) to 44.6 (P18). Multiplication factors for phenols with a saturated or unsaturated C3 side chains (P12, G12, P18, G12*), and summed total phenols were all considerably greater than 2.5 showing that the increase in treatment application rate resulted in an exaggerated increase in mass of lignin phenols leached. This provides evidence for the rejection of hypothesis 8. However, since the Mass/Mass₀ ratios for G12, G12*, and total lignin phenols for $163 \text{ m}^3/\text{ha}$ application rate were still less than that of DOC, overall, lignin phenols were selectively retained in soil. The remaining phenols listed in table 6.3 selectively leached, and P12, P18, and G18, which were selectively retained in soils with respect to DOC at $65 \text{ m}^3 \text{ ha}^{-1}$ application rate, selectively leached at $163 \text{ m}^3 \text{ ha}^{-1}$ application rate. No factor could be calculated for G18 as none leached at the $65 \text{ m}^3 \text{ ha}^{-1}$ application rate. G6 was the only phenol with a similar multiplication factor (2.3) comparable to the 2.5 times increase in dung DOC application rate, therefore was the only phenol where hypothesis 8 could be accepted.

6.4 Discussion

The hypotheses that were tested in this experiment were that different lignin phenols leach at different relative rates through soil as a function of molecular structure (H7), and the mass of lignin phenols leached from soil cores is directly proportional to the application rate of the soluble fraction of dung (H8). The following discussion explores the major outcomes and concludes with the acceptance of H7 because different phenols had contrasting leaching dynamics, but rejection of H8 because the effect of dose was disproportionate to the mass of lignin recovery, and concludes that the rate of application is the over-riding driver of dissolved lignin movement through soils.

6.4.1 *Relative leaching rates of lignin phenols*

Different lignin phenols leached at different relative rates through the soil, and this was a function of molecular structure.

The summed mass of total lignin phenols leached increased gradually with the number (<13.5) of pore volumes passed following dung DOC application at $65 \text{ m}^3 \text{ ha}^{-1}$ (figure 6.5). Total lignin phenols comprised 0.22% of the bulk DOC. The leaching dynamics of lignin phenols with C1 side chains (i.e. P6, G6 and S6) was more variable (figure 6.6A, B and H, respectively). This indicates either more interaction with the soil matrix and subsequent release, or, their provenance as oxidation products of longer side chain phenols, as described for the fungal degradation of Scots pine (Dijkstra et al., 1998). It is likely that the duration of this experiment was sufficient for recovery of the fungal biomass in the prepacked soils, as suggested in previous work for soils incubated for up to 10 days (Dungait et al., 2011).

Mass/Mass₀ ratios for individual phenols (table 6.3) provided further evidence to suggest different rates of transport through soils. The recovery at the lower application rate suggest that the phenols were retained in soil in order from strongest to weakest retention with respect to DOC: G18 > G12 > G12* > P12 > P18. Phenols that preferentially leached from soil in order of strongest to weakest retention in soil were: G6 and P6. Therefore it appears that both lignin phenol type i.e. P, G, or possibly S, and side chain length influence the behaviour of lignin phenols in soil: G phenols were retained more than P phenols, and phenols with longer side chains were retained more than shorter side chains. Additionally, the degree of side chain saturation could also be important: phenols with unsaturated side chains appeared to be retained in soil more readily than those with saturated side chains. Therefore H7, lignin phenols leach at different rates as a function of molecular structure, was accepted.

There is an apparent contradiction here where phenols with C3 side chains appeared to leach faster than C1 side chains (figure 6.6), whereas Mass/Mass₀ ratios (table 6.3) indicate that C3 side chains were retained in soil more than C1 side chains. A possible explanation may be that phenols with C3 side chains were present in greater concentrations than those with C1 side chains in the dung DOC applied to the soil cores (table 6.2). Therefore there would be more opportunities for sorption of phenols with C3 side chains to the soil matrix following dung DOC application. Subsequent oxidation of C3 side chains to C1 side chains by fungi (Dijkstra et al., 1998), and their subsequent desorption and release from soil as C1 side chains would reduce Mass/Mass₀ ratios for phenols with a C3 side chain whilst simultaneously elevating Mass/Mass₀ ratios for C1 side chain phenols. This process also provides a mechanism by which phenols with C1 side chain could be continuously present in leachates, as observed in figure 6.6. A

requirement for this mechanism to function is that C3 side chain phenols are retained in soils more readily than phenols with C1 side chain.

All of the phenolic side chains detected in the soluble fraction of dung DOC used in this experiment contained a carboxyl group, therefore it was not possible to speculate about release of lignin with side chains containing other functional groups such as alcohol, ketone, or vinyl groups. Dungait, et al. (2008) applied whole dung to soil and estimated incorporation over one year using the C4 natural abundance, and found that lignin phenol side chain structure including: methyl, vinyl, ethyl, acetyl, propenyl, and propan-2-one groups, affected their rates of incorporation, degradation, or transformation in soil after heavy rainfall, providing further evidence that side chain structure influences rate of transport.

6.4.2 Effect of application rate of soluble fraction of dung on the mass of lignin phenols leached

The effect of dose (65 or $163 \text{ m}^3 \text{ ha}^{-1}$) was disproportionate to the mass of lignin recovery with far higher masses leached at the higher dose; therefore, the rate of application is the over-riding driver of dissolved lignin movement through soils.

The summed mass of total lignin phenols leached at $163 \text{ m}^3 \text{ ha}^{-1}$ (2.5 times the lower application rate) was 27 times more than predicted after 0.2 pore volumes had passed (figure 6.5). This equated to an initial flux of total lignin phenols of 140, 5.3, and 2.1 g ha^{-1} for 163, predicted 163, and $65 \text{ m}^3 \text{ ha}^{-1}$, respectively. A similar phenomenon was observed with bulk DOC whereby 8 times more DOC leached than predicted at the same 2.5 times increase in application rate after 0.2 pore volumes had passed (figure 6.4). Furthermore, multiplication factors (table 6.3) provided evidence that for most phenols, there was not a proportional increase in mass leached following a 2.5 times increase dung DOC application rate, rather considerably more mass leached. Therefore H8, that the mass of lignin phenols leached from soil cores is directly proportional to the application rate of the soluble fraction of dung was rejected.

Approximately one third of the DOC was transported very rapidly (< 0.2 pore volumes) and lost as direct leachate, equating to an initial flux of $52.3 \text{ kg DOC ha}^{-1}$, which was 16 times greater than the initial flux ($3.4 \text{ kg DOC ha}^{-1}$) following dung DOC application at $65 \text{ m}^3 \text{ ha}^{-1}$. In previous work exploring the movement of dung C, ten times more mass

of DOC leached from dung amended soil cores following the first simulated rainfall event (Bol et al., 1999). These observations are important because it suggests that heavy precipitation and more frequent winter flooding as predicted by climate models for the UK and Western Europe (Jenkins et al., 2009, Lavers et al., 2013) will increase the amount of DOC leached through soils and lost to waterways. Research has indicated long term increases in DOC in UK rivers and lakes (Worrall et al., 2003, Worrall et al., 2004) by an average of 91% in upland waters (Evans et al., 2005), attributable to large scale drivers such as the response effects of plant and decomposer C dynamics to atmospheric pollutant N deposition, or reduced soil solution acidity associated with decreasing S deposition (Evans et al., 2008) and land management practices such as burning blanket peat moorland (Clutterbuck and Yallop, 2010). Whilst quantities of DOC lost from agricultural systems is considerably less than the amount of C stored in crops and soils, they are still very important to the water industry in the production of acceptable drinking water (Dungait et al., 2012a), where for example greater concentrations of what the authors termed ‘humic substances’ increased the chlorine demand of the treatment process and result in increased total trihalomethane concentrations (Alarconherrera et al., 1994).

Natural abundance stable ^{13}C isotope analysis was used to differentiate between SOC and dung DOC in the leachate because the additional DOC and total lignin phenols released at the higher rate of dung DOC application could either be derived from the soluble component of dung, soil DOC, or a combination of both. The first leachate (0.2 pore volumes) from the $163\text{ m}^3\text{ ha}^{-1}$ treatment had a bulk $\delta^{13}\text{C}$ value which was very similar to the bulk $\delta^{13}\text{C}$ value of the dung DOC (section 6.3.1). This suggested that the direct leachate was derived solely from the dung DOC, although this does not mean that the lignin phenols were not at least partially, derived from SOC. Such displacement of SOC and pool substitution mechanisms in soil-dung-water interactions have been proposed previously (Bol et al., 1999). The mechanisms controlling the contribution of SOC to leachates are considered in section 6.4.3 below.

There were differences between the leaching dynamics of individual phenols. For example, no G18 leached at $65\text{ m}^3\text{ ha}^{-1}$ by the end of the experiment, whereas at $163\text{ m}^3\text{ ha}^{-1}$, approximately half the G18 applied was recovered ($\text{Mass}/\text{Mass}_0 = 0.47$). Therefore, the discrepancy between source of bulk DOC and individual lignin phenols in leachate suggest that components of DOC, and even different compounds within the same class of compounds, interacted with the soil matrix in different ways during leaching. Slurry

application at $163 \text{ m}^3 \text{ ha}^{-1}$ appeared to trigger excess leaching and recovery of P18, not observed in the control or $65 \text{ m}^3 \text{ ha}^{-1}$ application rates. Furthermore, approximately twice the mass of P18 as that applied was recovered after $163 \text{ m}^3 \text{ ha}^{-1}$ application compared to the lower rate.

As expected, more DOC was leached from the soils at both application rates compared with total lignin phenols, because phenols are a minor component of DOC. Other components of DOC include carbohydrates constituting $< 35\%$ of riverine DOC (Wang et al., 2013a), proteinaceous material such as amino acids (Lytle and Perdue, 1981), fatty acids, and n-alkanes (Frazier et al., 2003). Of the lignin phenols that leached from the soil at the higher rate, the masses of G12 and G12* were lowest suggesting these compound are most likely to be stored in soils. Gymnosperm lignin largely comprises guaiacyl type lignin (Hedges and Mann, 1979a), so in terms of the potential to change land used to increase C sequestration, it might be speculated based on the findings of this experiment, that softwood afforestation might be an appropriate land use. Phenols that preferentially leached from soil in order of strongest to weakest retention in soil were: P12 > G18 > G6 > P18 > P6.

6.4.3 Mechanisms of SOC contribution to leachates

The measured DOC results and statistical analysis suggests that adding greater volumes of water affects the amount of DOC leached, and that the DOC leached contained a component of SOC in addition to added soluble dung C. Differences in the order of retention strength between phenols applied at different rates may have arisen because of a range of physical, chemical, or biological mechanisms.

(i) Physical mechanisms could be the effect of the extra water rapidly added, associated with greater treatment application which could alter or disrupt soil aggregate structure. This is because soil aggregate-size stability testing, such as the wet-sieving method described previously (Beare and Bruce, 1993), for example, relies on rapid exposure of soil aggregates to water to assess their water stability. Aggregates are important since much of the organic remnants of plant product inputs into soils after microbial decomposition is enclosed within soil aggregates and closely associated with mineral surfaces (Hedges and Oades, 1997), the latter being the most important factor in SOC stabilisation irrespective of soil type, vegetation, and land use (Schrumpp et al., 2013). Upon aggregate disruption, it is likely that the newly exposed SOC would be prone to leaching in the aqueous environment. The soil in this experiment was sieved prior to

packing the cores, which to some extent replicates soil tillage processes by destroying soil aggregate structure, and previous research has shown that cultivation reduces soil aggregate stability (Beare and Bruce, 1993, Cambardella and Elliott, 1993). Therefore, it is likely that the SOC contribution to leachate DOC is attributable to physical disruption of soil aggregates.

(ii) Chemical mechanisms could include some form of dynamic exchange whereby the addition of the soluble component of dung triggered the release of SOC and native soil lignin phenols and subsequent, more favourable sorption of other components of the soluble fraction of dung to soil sorption sites.

There were differences in the comparative leaching rates between phenols applied at 65 or 163 m³ ha⁻¹ application rate, i.e. the soil cores either held the volume of the dung DOC applied, or leached up to a maximum of 15 mL (mean = 1 mg DOC of the 41 mg applied), whereas at 163 m³ ha⁻¹ application rate, leachate volumes ranged from 21.4 to 45.6 mL (mean = 22 mg of the 103 mg applied) before any simulated rainfall was applied. This may have led to rapid saturation of soil sorption sites thus preventing variation in phenol transport rate through natural sorption and desorption. However, at 65 and 163 m³ ha⁻¹ application, G12 and G12* had similar Mass/Mass₀ ratios of 0.02 and 0.03 respectively, and 0.17 and 0.25 respectively. This similarity could be because G12 and G12* have nearly identical molecular structures (figure 6.3.), the difference being that G12* originally had a hydroxyl group on the 3 position of the phenyl ring in place of a methoxy group in G12.

(iii) Biological mechanisms could include priming, as described above, although the extra substrate addition associated with the higher application rate created an enhanced priming effect. Since no data such as respiration rates or phospholipid fatty acid data was recorded during this experiment, it is difficult to speculate about biological mechanisms. Another contribution to the increased DOC might be the release of SOC by priming of the soil microbial biomass by addition of available C and N as suggested by (Bol et al., 1999) who reported that up to 50% of leachate C was native soil C derived after application of dung C.

6.5 Conclusions

Different lignin phenols leached at different rates depending on their molecular structure. Mass/Mass₀ ratios indicated that phenols with C3 side chains (G12, P18, G12*, P12, and G18) were selectively retained in soils compared to C1 side chains. Concentrations of lignin phenols with C1 side chains comprising carboxyl groups (P6, G6, and S6) were detected in leachates were variable with increasing pore volumes passed, likely attributable to fungal side chain oxidation (Dijkstra et al., 1998), and subsequent leaching. Furthermore, Mass/Mass₀ recovery ratios for the 65 m³ ha⁻¹ application rate revealed that guaiacyl phenols tended to be retained in soil more strongly than *p*-hydroxyphenyl phenols. Only G12 and G12* were selectively retained relative to bulk DOC at 65 and 163 m³ ha⁻¹ application rates.

The mass of summed total lignin phenols and DOC leached was not proportional to their application rate. More mass of both leached at 163 m³ ha⁻¹ than at 65 and 0 m³ ha⁻¹ application rates, and more than predicted, where some of this extra phenol mass could have been SOC derived from the effect of the extra water associated with greater application rate disrupting soil aggregates.

Initial DOC fluxes were 52.3, 3.4, and 1.1 kg DOC ha⁻¹ for 163, 65, and 0 m³ ha⁻¹ dung DOC application rates, and initial total lignin phenol fluxes of 140, 5.3, and 0 g ha⁻¹ for the same dung DOC application rates, respectively. This indicates that application rate is a dominant driver of dissolved lignin and DOC movement through soils. This work provides valuable insight into lignin phenol leaching behaviour, which when combined with the findings from other work in this thesis could allow fluxes of leached lignin from different land uses to be predicted, in order to increase soil C stocks. These findings indicate that gymnosperm vegetation, with its high guaiacyl lignin content, would increase lignin phenol residence times in soil through reduced leaching.

Chapter 7. Synthesis and future research

7.1 Overall thesis aims and objectives

Adoption of restorative land uses and recommended management practices can increase soil organic carbon (SOC) stocks to mitigate climate change as well as provide other ecosystem services such as promoting healthy soils for food security, agro-industries, and water quality (Lal, 2004). Vascular plant tissues comprise 20-30% lignin (Kirk and Farrell, 1987), which thus represents a considerable soil carbon input. Lignin has traditionally been perceived as a component of the stable fraction of SOC, although recent advances indicate that it is not necessarily preserved in soils (Thevenot et al., 2010, Schmidt et al., 2011). Therefore, questions remain regarding its fate after entering the soil. Presumably, lignin may be decomposed to CO₂, transformed to non-lignin compounds, or broken down into water transportable components that have been detected in a range of natural waters (Opsahl et al., 1999, Louchouart et al., 2000).

(H₀) The central hypothesis being tested by this thesis was that a significant proportion of lignin in soils is solubilised and lost from the soil by transport in water.

The overarching aim of this project was to understand the contribution of lignin to the soluble fraction of SOC and its delivery to associated watercourses in a range of terrestrial ecosystems by addressing four major questions:

- (1) What is the dominant form of lignin moving through soils and into water courses?
- (2) Does the form of lignin differ between soil and vegetation types and land use type?
- (3) Do lignin decomposition products and concentrations vary seasonally?
- (4) What is the rate of lignin movement through the soil?

Four experiments were designed to answer eight specific sub-hypotheses (H1 to H8) described in sections 7.2.1, 7.2.2, 7.2.3, and 7.2.4 below. A summary of the evidence for the acceptance or rejection of each hypothesis provided by the experimentation undertaken in this study is provided below each. The conclusions are then synthesized into larger trends and which are described into terms of 'the bigger picture' before addressing future research needs.

7.2 Thesis hypotheses and conclusions

7.2.1 Methodology comparison study (Chapter 3)

The aim of this experiment was to determine the optimum extraction and analysis techniques for water-borne lignin: Solid phase extraction (SPE) was compared with freeze-drying (FD) to extract water-borne lignin; and thermally assisted hydrolysis and methylation using tetramethylammonium hydroxide (TMAH/GC-MS) was compared with GC-FID of trimethylsilyl derivatives to detect lignin phenols.

H1. Freeze-drying (FD) extracts a greater concentration of water-transportable lignin-derived compounds from natural fresh water samples than solid phase extraction (SPE).

H1 was rejected because SPE was more consistent than FD for recovering total water transportable phenols from all the natural freshwaters tested, and with smaller standard errors of the mean. Additionally, more phenol compounds were detected following SPE than FD for a given analysis technique. This was attributed to SPE being better at extracting organic matter than FD.

H2. TMAH/GC-MS analysis detects greater concentration of water-borne lignin than GC-FID of trimethylsilyl derivatives.

H2 was accepted. TMAH/GC-MS provided greater concentrations of detectable summed lignin phenols for both extraction techniques. SPE combined with TMAH/GC-MS enabled detection of a wide array of P, G, and S type lignin phenols exhibiting a variety of side chain structures from zero to three carbons in length with alkyl, alkenyl, ketone, aldehyde, and carboxyl functional groups. Therefore SPE followed by TMAH/GC-MS was used to detect water transportable phenols in subsequent experiments except Chapter 6 which used GC-MS of BSTFA derivatives. This is because in Chapter 6 it was essential that phenols were detected with the same molecular structure as that when applied, whereas lignin phenols can be modified during TMAH/GC-MS analysis (Hatcher and Minard, 1995, Filley et al., 1999).

7.2.2 Investigation of leaf litter lignin decomposition and subsequent loss as dissolved organic matter over time in a model system (Chapter 4)

This polytunnel-based experiment explored the lignin phenols detected in fresh and degraded vegetation types representing different land uses, and their leachates, as well as investigating the relationship with temperature, to test the following hypotheses:

H3. Dominant lignin phenols found in topsoil leachate DOM are similar to those in the source litter input.

Lignin phenols in topsoil leachates were similar to those detected in the source litter from a mixed grass sward and *Fraxinus excelsior* for G3 and G18 (see Chapter 1, figure 1.10 for definition of phenol abbreviations). However, P18 which was dominant in degraded mixed grass litter was not dominant in the mixed grass leachate. S6, dominant in fresh *Quercus robur* litter, and G2 dominant in fresh and degraded *Q. robur* litter, were not dominant in its leachates. P1 was relatively dominant in degraded *Rununculus repens* litter, and was also dominant in its leachates, although it also leached relatively large amounts of phenols and aromatics containing carboxylic acid groups. H3 was therefore accepted or rejected on a litter type- and phenol-specific basis. Those phenols where H3 was accepted are reported in Chapter 4, table 4.5.

H4. Total lignin concentrations determined in leachate increase with increasing topsoil temperature.

Total lignin phenol concentrations in leachate increased with increasing topsoil temperature for mixed grass, *R. repens*, and *F. excelsior* litter treatments, with maximum concentrations detected in late spring/early summer. This indicates that the overall rate of the combined processes of decomposition, solubilisation, and transport for many lignin phenols increase with increasing temperature. H4 was therefore accepted for these litter types. Total lignin phenol concentrations in *Q. robur* leachates gradually increased through time, independently of temperature, therefore H4 was rejected for *Q. robur*. However, some individual lignin phenol concentrations in *Q. robur* leachate did correlate with temperature including P1 and P2.

7.2.3 Lignin phenols in soils and natural waters as indicators of land use type (Chapter 5)

A land use study investigated the lignin phenols in soil organic, A horizons, and in the dissolved phase from adjacent water outlets from grassland, woodland, and moorland ecosystems. The following hypotheses were tested:

H5. Lignin phenols detected in soils and in the DOM of adjacent water outlets are a function of land use type.

H5 was accepted because a dominance of specific lignin phenols were indicative of land use type. Dominant phenols associated with woody ecosystems were: G1, G6, S6, P1, and P2. Dominant phenols associated with grass/moorland ecosystems included P6, G3, and G18, although P1 and P2 were also dominant in this ecosystem. The phenol associated with dung from ruminant livestock was P18.

H6. Normalised total lignin phenol concentrations in water outlets is not significantly different from their concentration in soil, for each land use type.

Virtually all lignin phenols detected in DOM from water outlets were also detected in the soil organic and A horizons for grassland, woodland and moorland land uses. Normalised total dissolved lignin phenol concentrations in water from all three land uses were not significantly different to those in their respective soil O and A horizons, thus H6 was accepted. This suggests that a considerable amount of lignin, is being lost from soils through leaching and that this is comparable to its proportion in SOM. Also there was no significant difference in losses of lignin phenols between each land use type.

7.2.4 Transport of phenols through soil (Chapter 6)

This experiment used the dissolved fraction of natural abundance C4 labelled dung as a source of phenols to compare the rates of transport of different phenols through soil after application of two rates of dung DOC, to test the following hypotheses:

H7. Different lignin phenols leach at different relative rates through soil as a function of molecular structure.

H7 was accepted because different lignin phenols leached at different rates depending on their molecular structure. Mass/Mass₀ recovery ratios indicated that phenols with C3 side chains (G12, P18, G12*, P12, and G18) were selectively retained in soils compared to C1 side chains. Lignin phenols with C1 side chains comprising carboxyl groups (P6, G6, and S6) were detected in leachates at variable concentrations with increasing pore volumes passed, likely attributable to side chain oxidation by fungi (Dijkstra et al., 1998), generating a continuous, albeit variable in concentration, supply of C1 side chain phenols and their subsequent leaching. Mass/Mass₀ ratios for the 65 m³ ha⁻¹ application rate indicated that guaiacyl phenols tended to be retained in soil more strongly than *p*-hydroxyphenyl phenols, and only G12 and G12* were selectively retained relative to bulk DOC at 65 and 163 m³ ha⁻¹ application rates.

H8. The mass of lignin phenols leached from soil cores is directly proportional to the application rate of the soluble fraction of dung.

The mass of summed total lignin phenols and DOC leached was not proportional to their application rate. Greater mass of both total lignin phenols and DOC leached at the upper application rate, and were greater than predicted, therefore H8 was rejected. However, G6 exclusively displayed a similar Multiplication factor (2.3) comparable to the 2.5 times increase in dung DOC application rate; therefore H8 could be accepted for this phenol.

Following application of dung DOC at 163, 65, and 0 m³ ha⁻¹, initial DOC fluxes exiting topsoil as direct leachate were 52.3, 3.4, and 1.1 kg DOC ha⁻¹, respectively. Total lignin phenol fluxes at the same application rates were 140, 5.3, and 0 g ha⁻¹. This indicates that water application rate was the dominant driver of dissolved lignin and DOC movement through soils.

7.3 Synthesis of outcomes

In chapter 5 (H6) it was established that **a considerable proportion of lignin phenols were lost from soils through leaching from grassland, woodland and moorland land uses**. Furthermore, the **total amount of lignin leached from soil, as a proportion of TOC, increased with increasing seasonal temperature reaching a maximum in late spring/early summer** (Chapter 4, H4). Chapter 6 determined that the mass of

lignin phenols leached was disproportionate to their application rate (H8) i.e. that at higher application rates, greater mass of total lignin phenols leached than expected. Therefore **the water was an important driver for dissolved lignin phenol and DOC transport through soils**. Global climate predictions indicate warming (Solomon et al., 2007) with an increase in heavy rainfall and winter flooding events over northern and western Europe (Lavers et al., 2013), and an increase in the intensity of precipitation events in tropical regions (Meehl and Stocker, 2007). In the Russian Arctic, rising permafrost depths and decreasing thickness of the frozen layer in seasonally frozen ground could lead to increased river runoff (Frauenfeld et al., 2004). Therefore, based on the findings from H4 and H8, **it can be speculated that increased amounts of dissolved lignin phenols will be generated upon warming and subsequently leached more rapidly, than at present.**

Some dominant lignin phenols associated with each fresh and/or degraded litter type and their leachates at the species level (see section 7.2.2, H3) **were also dominant lignin phenols at the ecosystem scale, within their respective land use** (see section 7.2.3, H5). For example, P6 was dominant in fresh mixed grass litter (Chapter 4, section 4.3.2), G3 and G18 dominant in fresh and degraded mixed grass litter and DOM (H3, Chapter 4, section 4.4.2), were also dominant in soil organic horizons, and detected in soil A and DOM in the grassland ecosystem (H5, Chapter 5 figure 5.2). G3 was also dominant in soil organic and A horizons in the moorland ecosystem (H5, Chapter 5 figure 5.6). In fresh *Q. robur* litter, relatively dominant lignin phenols were: P2 and S6 (Chapter 4, section 4.3.2). These phenols were also dominant in woodland ecosystems in the soil organic-, A horizon, and DOM respectively (section 7.2.3, H5, Chapter 5 figure 5.4). However, for *F. excelsior* G18 was a dominant phenol in fresh and degraded litter and leachates (H3, Chapter 4 figures 4.5 and 4.7), although G18 was more strongly associated with grassland rather than woodland ecosystems, perhaps because the woodland ecosystems examined in this thesis were *Q. robur* rather than *F. excelsior* dominated.

Chapter 6 (H7) established that **different lignin phenols were transported through soils at different rates as a function of molecular structure**. Guaiacyl phenols tended to be retained in soil more strongly than *p*-hydroxyphenyl phenols, and that longer side chains tended to be retained better than short side chains. Unfortunately no syringyl phenols were detected in the dung DOC applied to soil cores, so it was not possible to determine recovery Mass/Mass₀ ratios for these phenols. Combining the findings from

H3, H5, and H7 and that gymnosperm vegetation contains principally guaiacyl lignin phenols (Hedges and Mann, 1979a, Clifford et al., 1995), it may be controversially speculated that growing gymnosperm vegetation, such as coniferous afforestation, may be a suitable land use to increase soil C sequestration. Further evidence to support this is that G units have been shown to turnover slower than S and C units (Bahri et al., 2006), and previous research indicates a significant increase in soil C stocks of $1.0 \text{ t C ha}^{-1} \text{ year}^{-1}$ under principally coniferous plantations to a depth of 1 m between 1978 and 2009 (Chapman et al., 2013). However, balancing competing land uses to sequester C as well as forestry, food production (livestock, cereals, vegetables, and fruit), urbanisation, and energy farms (biofuels, wind, solar) to support an increasing global population, on declining land area due to rising sea levels (Levermann et al., 2013) represents the present and future challenges.

7.4 Future research

In addressing the fate and transport of lignin in the soil-water continuum, this thesis has explored lignin phenols in vegetation litter and soils, as one end member of the soil-water continuum. It has also investigated dissolved lignin from agricultural drains, seasonal streams, and minor rivers. The other end member, not explored in this study, is the ocean. Much of the previous research in lignin phenols in soils and DOM has focussed on determination of phenol molecular structures and their concentrations. Soils, and particularly waterways are temporally dynamic environments, therefore this previous research, even with sufficient spatial replication, constitutes at best a ‘snapshot’ of the biogeochemical processes occurring at any given time. More research investigating fluxes of lignin phenols through soils and hydrological pathways is required to better understand the ‘lignin cycle’ as a component of the C cycle. Rivers transport approximately $2.5 \times 10^{10} \text{ kg DOC year}^{-1}$ to the ocean (Meybeck, 1982). Total lignin phenol concentrations detected in major rivers are $1.26 \pm 0.71 \text{ mg (100 mg OC)}^{-1}$ in the River Mississippi (Benner and Opsahl, 2001), $0.68\text{-}0.96 \text{ mg (100 mg OC)}^{-1}$ at the outlets of the Rivers Ob, and Yenisei (Opsahl et al., 1999). A lignin flux of $1.2 \times 10^8 \text{ kg year}^{-1}$ has been determined part way along the River Amazon at Óbidos (Ertel et al., 1986), which constitutes 0.5% of the total DOC riverine flux to the ocean. Therefore these major rivers and others such as the River Congo must be important conduits for the transport of lignin from terrestrial to marine environments, with considerable fluxes that need to be estimated.

Purely from a climate change rather than a food security perspective, the considerable proportion of lignin phenols leached and lost from soils (see chapter 5, H6) need not necessarily be a concern for global C sequestration from a climate change perspective, if they are subsequently stabilized in watercourses or ocean sediments. Whilst previous research has detected lignin phenols in ocean columns (Opsahl and Benner, 1997), little is known about the flux of lignin phenols or carbon derived from lignin phenols from various natural waters back to the atmosphere as CO₂ via photooxidation or microbial oxidation. Recent advances indicate that enhanced flooding events (as predicted in global climate change scenarios) can cause rapid loss of stored carbon from soil to the atmosphere via aquatic ecosystem processes (Bianchi et al., 2013). Furthermore, 30-50% of bulk Amazon River respiration has been estimated to constitute terrestrially-derived phenols, including lignin (Ward et al., 2013). With water covering two thirds of the Earth's surface, this must be an important flux to understand, for all classes of organic molecules, if we want to reduce atmospheric CO₂ concentrations.

In addition, there is little research into the flux of lignin in soils released as CO₂ to the atmosphere for different land uses. Up to 8% of lignin was evolved as CO₂ after 14 days degradation by actinomycetes in an incubation experiment (McCarthy and Broda, 1984). The white-rot fungi *Sporotrichum pulverulentum* degraded approximately 50% of the lignin from wheat seedlings as CO₂ after 15 days in an incubation experiment at 37 °C (McCarthy et al., 1984). Previous research indicates a strong correlation between emissions of respired CO₂ from soil amended with different vegetation litters and the disappearance of DOC (Marschner and Noble, 2000). Therefore, microbial respiration could represent a major pathway by which lignin is lost from soils in natural environments.

Figure 7.1 shows the 'lignin cycle', first presented in Chapter 1, figure 1.12, modified by identifying the lignin fluxes and pools described above in this section, that need to be investigated in future research in order to better understand the fate of lignin as a component of the global carbon cycle.

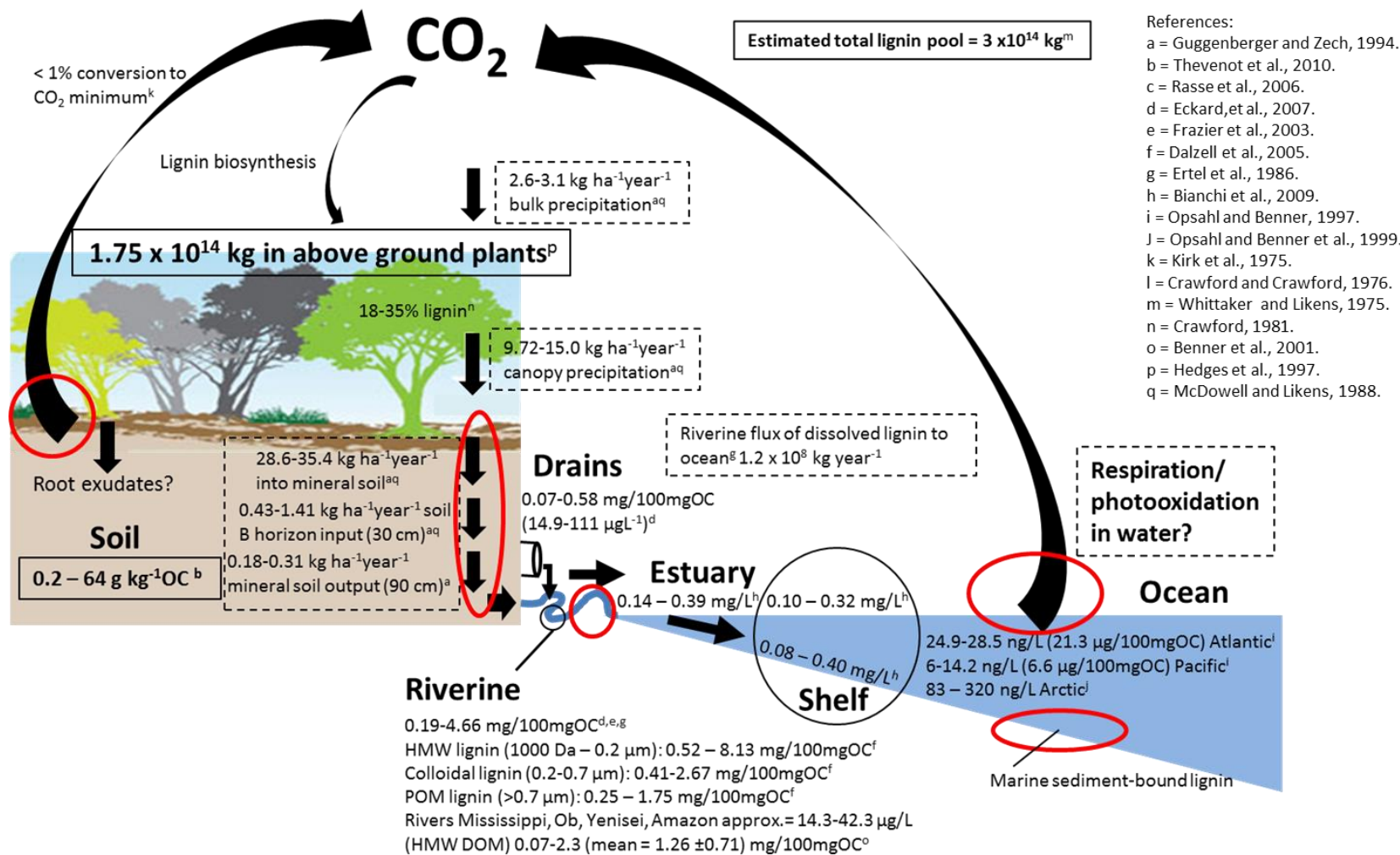


Figure 7.1. The lignin cycle, identifying future research lignin flux determination requirements highlighted in red.

To address these major research questions, methodological advances are needed in several areas:

(i) Reduction in the errors for the SPE and TMAH/GC-MS techniques used in this thesis. A lack of previous studies using both of these techniques or FD followed by GC-FID prevents comparison of the methodological errors. However, previous research investigating lignin phenols using SPE extraction (Louchouart et al., 2000), or detection of lignin phenols using TMAH/GC-MS from water samples (Frazier et al., 2003) and in soil samples (Mason et al., 2009, Mason et al., 2012) have incurred smaller errors. The standard errors of the mean reported for dissolved lignin concentrations in water samples in Chapters 3 and 5 this study are likely to be elevated due to seasonal variation since these water samples were collected at different times of the year (May, July, and January). Lignin phenols detected in soils and vegetation samples using TMAH/GC-MS were also of experimental replicates, rather than analytical replicates, in order to capture the natural range of variation within different vegetation species and ecosystems. Thus, in order to fully investigate methodological errors exclusively for the extraction and detection of dissolved lignin phenols, it would be necessary to design an experiment comparing extraction and detection approaches using lignin phenol standard solutions.

(ii) Better techniques to determine lignin oligomeric structure. Common degradative approaches e.g. pyrolysis techniques including TMAH/GC-MS can generate biproducts not in the original lignin macromolecular structure (Filley et al., 1999, Clifford et al., 1995), and CuO oxidation tends to generate products with less side chain structure than TMAH/GC-MS (Hatcher et al., 1995, Wysocki et al., 2008). Lignin dimer structures have been investigated previously using TMAH/GC-MS (Nakagawa-Izumia et al., 2004), although lignin dimer/monomer ratios investigated using CuO oxidation are characteristic of lignin source (Goni and Hedges, 1992, Opsahl and Benner, 1995, Dignac and Rumpel, 2006) such as grasses (monocotyledons), angiosperms and conifers (Otto and Simpson, 2006). Investigation of lignin dimers using TMAH/GC-MS in SOC and DOC may strengthen the associations identified between lignin thermochemolysis products and land use type, furthering the work in Chapter 5 (H5). Also, development of HPLC and LC-IRMS techniques may provide more information about the transport of higher molecular weight lignin oligomeric structures, and

(iii) Compound specific ^{14}C radiocarbon analysis of lignin phenols will help to determine which lignin forms have a longer residence time in soil and natural waters.

This would allow determination of which phenols or oligomers are more stable in soils, and which land uses or management practices facilitate their stabilisation.

The research in Chapter 4 could be extended by separating degradation and transport processes to carry out separate long-term degradation and transport experiments to understand the effects of seasonality on each. In addition, the effect of subsoils with regard to fractionation of lignin degradation products through sorption and desorption processes was not investigated in Chapter 4. Research has indicated that highly condensed and substituted aromatic compounds are preferentially retained with increasing soil depth in peatland soils with an underlying mineral horizon (Kalbitz, 2001).

Specific questions that need to be addressed

In order to improve our understanding of lignin biogeochemistry, with respect to the lignin cycle (see Chapter 1, figure 1.12) the following questions need to be addressed:

- What is the dissolved lignin flux through soils under grassland, moorland, gymnosperm (coniferous), and angiosperm woodland land uses? Therefore which land uses are more amenable to store lignin in soils?
- What is the flux of lignin in soils released to the atmosphere as CO₂ from different land uses?
- What is the flux of dissolved and particulate lignin in the major global rivers to the oceans?
- Are oceans a lignin phenol sink? What is the residence time for dissolved-, particulate-, and sorbed lignin in the oceans?
- What is the flux of lignin phenols from natural waters to the atmosphere as CO₂?

References

- ABBOTT, G. D., SWAIN, E. Y., MUHAMMAD, A. B., ALLTON, K., BELYEA, L. R., LAING, C. G. & COWIE, G. L. 2013. Effect of water-table fluctuations on the degradation of Sphagnum phenols in surficial peats. *Geochimica Et Cosmochimica Acta*, 106, 177-191.
- ABIVEN, S., RECOUS, S., REYES, V. & OLIVER, R. 2005. Mineralisation of C and N from root, stem and leaf residues in soil and role of their biochemical quality. *Biology and Fertility of Soils*, 42, 119-128.
- AESCHBACHER, M., GRAF, C., SCHWARZENBACH, R. P. & SANDER, M. 2012. Antioxidant Properties of Humic Substances. *Environmental Science & Technology*, 46, 4916-4925.
- AIKEN, G. R., THURMAN, E. M., MALCOLM, R. L. & WALTON, H. F. 1979. Comparison Of XAD Macroporous Resins For The Concentration Of Fulvic-Acid From Aqueous-Solution. *Analytical Chemistry*, 51, 1799-1803.
- ALARCONHERRERA, M. T., BEWTRA, J. K. & BISWAS, N. 1994. Seasonal-Variations In Humic Substances And Their Reduction Through Water-Treatment Processes. *Canadian Journal of Civil Engineering*, 21, 173-179.
- ALLISON, I., BINDOFF, N. L., BINDSCHADLER, R. A., COX, P. M., DE NOBLET, N., ENGLAND, M. H., FRANCIS, J. E., GRUBER, N., HAYWOOD, A. M., KAROLY, D. J., KASER, G., LE QUERE, C., LENTON, T. M., MANN, M. E., MCNEIL, B. I., PITMAN, A. J., RAHMSTORF, S., RIGNOT, E., SCHELLNHUBER, H. J., SCHNEIDER, S. H., SHERWOOD, S. C., SOMERVILLE, R. C. J., STEFFEN, K., STEIG, E. J., VISBECK, M. & WEAVER, A. J. 2009. The Copenhagen Diagnosis. The University of New South Wales Climate Change Research Centre (CCRC), Sydney, Australia.
- AMADOR, J. A., MILNE, P. J., MOORE, C. A. & ZIKA, R. G. 1990. Extraction Of Chromophoric Humic Substances From Seawater. *Marine Chemistry*, 29, 1-17.
- AMELUNG, W., BRODOWSKI, S., SANDHAGE-HOFMANN, A. & BOL, R. 2008. Combining Biomarker With Stable Isotope Analyses For Assessing The Transformation And Turnover Of Soil Organic Matter. In: SPARKS, D. L. (ed.) *Advances in Agronomy, Vol 100*.
- AMELUNG, W., FLACH, K. W. & ZECH, W. 1999. Lignin in particle-size fractions of native grassland soils as influenced by climate. *Soil Science Society of America Journal*, 63, 1222-1228.
- AMON, R. M. W. & BENNER, R. 1996. Bacterial utilization of different size classes of dissolved organic matter. *Limnology and Oceanography*, 41, 41-51.
- ANDREN, O. & KATTERER, T. 1997. ICBM: The introductory carbon balance model for exploration of soil carbon balances. *Ecological Applications*, 7, 1226-1236.
- AUSTIN, A. T. & BALLARE, C. L. 2010. Dual role of lignin in plant litter decomposition in terrestrial ecosystems. *Proceedings of the National Academy of Sciences of the United States of America*, 107, 4618-4622.
- BAHRI, H., DIGNAC, M.-F., RUMPEL, C., RASSE, D. P., CHENU, C. & MARIOTTI, A. 2006. Lignin turnover kinetics in an agricultural soil is monomer specific. *Soil Biology and Biochemistry*, 38, 1977-1988.
- BEARE, M. H. & BRUCE, R. R. 1993. A Comparison Of Methods For Measuring Water-Stable Aggregates - Implications For Determining Environmental-Effects On Soil Structure. *Geoderma*, 56, 87-104.
- BENNER, R., BIDDANDA, B., BLACK, B. & MCCARTHY, M. 1997. Abundance, size distribution, and stable carbon and nitrogen isotopic compositions of marine organic matter isolated by tangential-flow ultrafiltration. *Marine Chemistry*, 57, 243-263.
- BENNER, R. & OPSAHL, S. 2001. Molecular indicators of the sources and transformations of dissolved organic matter in the Mississippi river plume. *Organic Geochemistry*, 32, 597-611.
- BENNER, R., WELIKY, K. & HEDGES, J. I. 1990. Early Diagenesis Of Mangrove Leaves In A Tropical Estuary - Molecular-Level Analyses Of Neutral Sugars And Lignin-Derived Phenols. *Geochimica Et Cosmochimica Acta*, 54, 1991-2001.

- BIANCHI, T. S., DIMARCO, S. F., SMITH, R. W. & SCHREINER, K. M. 2009. A gradient of dissolved organic carbon and lignin from Terrebonne-Timbalier Bay estuary to the Louisiana shelf (USA). *Marine Chemistry*, 117, 32-41.
- BIANCHI, T. S., GARCIA-TIGREROS, F., YVON-LEWIS, S. A., SHIELDS, M., MILLS, H. J., BUTMAN, D., OSBURN, C., RAYMOND, P., SHANK, G. C., DIMARCO, S. F., WALKER, N., REESE, B. K., MULLINS-PERRY, R., QUIGG, A., AIKEN, G. R. & GROSSMAN, E. L. 2013. Enhanced transfer of terrestrially derived carbon to the atmosphere in a flooding event. *Geophysical Research Letters*, 40, 116-122.
- BLYTH, A. J. & WATSON, J. S. 2009. Thermochemolysis of organic matter preserved in stalagmites: a preliminary study. *Organic Geochemistry*, 40, 1029-1031.
- BOCOCK, K. L., GILBERT, O., CAPSTICK, C. K., TWINN, D. C., WAID, J. S. & WOODMAN, M. J. 1960. Changes In Leaf Litter When Placed On The Surface Of Soils With Contrasting Humus Types .1. Losses In Dry Weight Of Oak And Ash Leaf Litter. *Journal of Soil Science*, 11, 1-9.
- BOERJAN, W., RALPH, J. & BAUCHER, M. 2003. Lignin biosynthesis. *Annual Review of Plant Biology*, 54, 519-546.
- BOL, R., AMELUNG, W., FRIEDRICH, C. & OSTLE, N. 2000. Tracing dung-derived carbon in temperate grassland using C-13 natural abundance measurements. *Soil Biology & Biochemistry*, 32, 1337-1343.
- BOL, R., BOLGER, T., CULLY, R. & LITTLE, D. 2003. Recalcitrant soil organic materials mineralize more efficiently at higher temperatures. *Journal of Plant Nutrition and Soil Science-Zeitschrift Fur Pflanzenernahrung Und Bodenkunde*, 166, 300-307.
- BOL, R., OSTLE, N. J., FRIEDRICH, C., AMELUNG, W. & SANDERS, I. 1999. The influence of dung amendments on dissolved organic matter in grassland soil leachates - Preliminary results from a lysimeter study. *Isotopes in Environmental and Health Studies*, 35, 97-109.
- BOL, R., POIRIER, N., BALESIDENT, J. & GLEIXNER, G. 2009. Molecular turnover time of soil organic matter in particle-size fractions of an arable soil. *Rapid Communications in Mass Spectrometry*, 23, 2551-2558.
- BOLAN, N. S., BASKARAN, S. & THIAGARAJAN, S. 1996. An evaluation of the methods of measurement of dissolved organic carbon in soils, manures, sludges, and stream water. *Communications in Soil Science and Plant Analysis*, 27, 2723-2737.
- BOSATTA, E. & AGREN, G. I. 1999. Soil organic matter quality interpreted thermodynamically. *Soil Biology & Biochemistry*, 31, 1889-1891.
- BOUTTON, T. W. & YAMASAKI, S. (eds.) 1996. *Stable Carbon Isotope Ratios of Soil Organic Matter and Their Use as Indicators of Vegetation and Climate Change*. : Marcel Dekker, Inc.
- BOWEN, S. R., GREGORICH, E. G. & HOPKINS, D. W. 2009. Biochemical properties and biodegradation of dissolved organic matter from soils. *Biology and Fertility of Soils*, 45, 733-742.
- BRADFORD, M. A., DAVIES, C. A., FREY, S. D., MADDOX, T. R., MELILLO, J. M., MOHAN, J. E., REYNOLDS, J. F., TRESEDER, K. K. & WALLENSTEIN, M. D. 2008. Thermal adaptation of soil microbial respiration to elevated temperature. *Ecology Letters*, 11, 1316-1327.
- BRADY, N. C. & WEIL, R. R. 2002. *The Nature and Properties of Soils*, Prentice Hall.
- BRADY, N. C. & WEIL, R. R. 2008. *The Nature and Properties of Soils*, Pearson Prentice Hall.
- BRAY, S. R., KITAJIMA, K. & MACK, M. C. 2012. Temporal dynamics of microbial communities on decomposing leaf litter of 10 plant species in relation to decomposition rate. *Soil Biology & Biochemistry*, 49, 30-37.
- BRUTTINI, R., ROVERO, G. & BALDI, G. 1991. Experimentation And Modelling Of Pharmaceutical Lyophilization Using A Pilot-Plant. *Chemical Engineering Journal and the Biochemical Engineering Journal*, 45, B67-B77.
- BRUUN, S., CHRISTENSEN, B. T., HANSEN, E. M., MAGID, J. & JENSEN, L. S. 2003. Calibration and validation of the soil organic matter dynamics of the Daisy model with data from the Askov long-term experiments. *Soil Biology & Biochemistry*, 35, 67-76.

- BSI 1995. BS7755 Soil Quality Part 3: Chemical Methods Section 3.2: Determination of pH.
- BUTMAN, D. & RAYMOND, P. A. 2011. Significant efflux of carbon dioxide from streams and rivers in the United States. *Nature Geoscience*, 4, 839-842.
- CAMBARDELLA, C. A. & ELLIOTT, E. T. 1993. Carbon And Nitrogen Distribution In Aggregates From Cultivated And Native Grassland Soils. *Soil Science Society of America Journal*, 57, 1071-1076.
- CAMPBELL, M. M. & SEDEROFF, R. R. 1996. Variation in lignin content and composition - Mechanism of control and implications for the genetic improvement of plants. *Plant Physiology*, 110, 3-13.
- CHABANNES, M., RUEL, K., YOSHINAGA, A., CHABBERT, B., JAUNEAU, A., JOSELEAU, J. P. & BOUDET, A. M. 2001. In situ analysis of lignins in transgenic tobacco reveals a differential impact of individual transformations on the spatial patterns of lignin deposition at the cellular and subcellular levels. *Plant Journal*, 28, 271-282.
- CHABBI, A. & RUMPEL, C. 2004. Decomposition of plant tissue submerged in an extremely acidic mining lake sediment: phenolic CuO-oxidation products and solid-state(13)C NMR spectroscopy. *Soil Biology & Biochemistry*, 36, 1161-1169.
- CHALLINOR, J. M. 1995. Characterisation of wood by pyrolysis derivatisation - gas chromatography/mass spectrometry. *Journal of Analytical and Applied Pyrolysis*, 35, 93-107.
- CHAMBERS, B., NICHOLSON, N., SMITH, K., PAIN, B., CUMBY, T. & SCOTFORD, I. 2001. Managing Livestock Manures. In: ADAS, RESEARCH, I. O. G. A. E. & INSTITUTE, S. R. (eds.) 2 ed.
- CHAPMAN, S. J., BELL, J. S., CAMPBELL, C. D., HUDSON, G., LILLY, A., NOLAN, A. J., ROBERTSON, A. H. J., POTTS, J. M. & TOWERS, W. 2013. Comparison of soil carbon stocks in Scottish soils between 1978 and 2009. *European Journal of Soil Science*, 64, 455-465.
- CHEFETZ, B., CHEN, Y., CLAPP, C. E. & HATCHER, P. G. 2000. Characterization of organic matter in soils by thermochemolysis using tetramethylammonium hydroxide (TMAH). *Soil Science Society of America Journal*, 64, 583-589.
- CHEN, C., CHANG, H. & KIRK, T. K. 1982. Aromatic-Acids Produced During Degradation Of Lignin In Spruce Wood By Phanerochaete-chrysosporium. *Holzforschung*, 36, 3-9.
- CHEN, C. L., CHANG, H. & KIRK, T. K. 1983. Carboxylic-Acids Produced Through Oxidative Cleavage Of Aromatic Rings During Degradation Of Lignin In Spruce Wood By Phanerochaete-Chrysosporium. *Journal of Wood Chemistry and Technology*, 3, 35-57.
- CHEN, Y.-R. & SARKANEN, S. 2010. Macromolecular replication during lignin biosynthesis. *Phytochemistry*, 71, 453-462.
- CHRIST, M. J. & DAVID, M. B. 1996. Temperature and moisture effects on the production of dissolved organic carbon in a Spodosol. *Soil Biology & Biochemistry*, 28, 1191-1199.
- CHRISTENSEN, J. H., BAUCHER, M., O'CONNELL, A. P., VAN MONTAGU, M. & BOERJAN, W. (eds.) 2000. *Control of lignin biosynthesis*, Dordrecht: Kluwer.
- CHRISTMAN, R. F. & GHASSEMI, M. 1966. Chemical Nature of Organic Color in Water. *Journal American Water Works Association*, 58, 723-741.
- CLIFFORD, D. J., CARSON, D. M., MCKINNEY, D. E., BORTIATYNSKI, J. M. & HATCHER, P. G. 1995. A new rapid technique for the characterisation of lignin in vascular plants: thermochemolysis with tetramethylammonium hydroxide (TMAH). *Organic Geochemistry*, 23, 169-175.
- CLUTTERBUCK, B. & YALLOP, A. R. 2010. Land management as a factor controlling dissolved organic carbon release from upland peat soils 2 Changes in DOC productivity over four decades. *Science of the Total Environment*, 408, 6179-6191.
- COLEMAN, K., JENKINSON, D. S., CROCKER, G. J., GRACE, P. R., KLIR, J., KORSCHENS, M., POULTON, P. R. & RICHTER, D. D. 1997. Simulating trends in soil organic carbon in long-term experiments using RothC-26.3. *Geoderma*, 81, 29-44.
- CONANT, R. T., PAUSTIAN, K. & ELLIOTT, E. T. 2001. Grassland management and conversion into grassland: Effects on soil carbon. *Ecological Applications*, 11, 343-355.

- CONANT, R. T., RYAN, M. G., AGREN, G. I., BIRGE, H. E., DAVIDSON, E. A., ELIASSON, P. E., EVANS, S. E., FREY, S. D., GIARDINA, C. P., HOPKINS, F. M., HYVONEN, R., KIRSCHBAUM, M. U. F., LAVALLEE, J. M., LEIFELD, J., PARTON, W. J., STEINWEG, J. M., WALLENSTEIN, M. D., WETTERSTEDT, J. A. M. & BRADFORD, M. A. 2011. Temperature and soil organic matter decomposition rates - synthesis of current knowledge and a way forward. *Global Change Biology*, 17, 3392-3404.
- CONANT, R. T., STEINWEG, J. M., HADDIX, M. L., PAUL, E. A., PLANTE, A. F. & SIX, J. 2008. Experimental warming shows that decomposition temperature sensitivity increases with soil organic matter recalcitrance. *Ecology*, 89, 2384-2391.
- CRAWFORD, R. L. 1981. *Lignin Biodegradation and Transformation*, New York, John Wiley & Sons.
- DALZELL, B. J., FILLEY, T. R. & HARBOR, J. M. 2005. Flood pulse influences on terrestrial organic matter export from an agricultural watershed. *Journal of Geophysical Research-Biogeosciences*, 110.
- DAVIDSON, E. A. & JANSSENS, I. A. 2006. Temperature sensitivity of soil carbon decomposition and feedbacks to climate change. *Nature*, 440, 165-173.
- DEL RIO, J. C., MCKINNEY, D. E., KNICKER, H., NANNY, M. A., MINARD, R. D. & HATCHER, P. G. 1998. Structural characterization of bio- and geo-macromolecules by off-line thermochemolysis with tetramethylammonium hydroxide. *Journal of Chromatography A*, 823, 433-448.
- DENMAN, K., HOFMANN, E. & MARCHANT, H. 1996. *Marine Biotic Responses to Environmental Change and Feedbacks to Climate* [Online]. Available: http://lmacweb.env.uea.ac.uk/green_ocean/publications/Eco/Denman96.pdf.
- DIGNAC, M.-F. & RUMPEL, C. 2006. Relative distributions of phenol dimers and hydroxy acids in a cultivated soil and above ground maize tissue. *Organic Geochemistry*, 37, 1634-1638.
- DIGNAC, M. F., BAHRI, H., RUMPEL, C., RASSE, D. P., BARDOUX, G., BALESSENT, J., GIRARDIN, C., CHENU, C. & MARIOTTI, A. 2005. Carbon-13 natural abundance as a tool to study the dynamics of lignin monomers in soil: an appraisal at the Closeaux experimental field (France). *Geoderma*, 128, 3-17.
- DIJKSTRA, E. F., BOON, J. J. & VAN MOURIK, J. M. 1998. Analytical pyrolysis of a soil profile under Scots pine. *European Journal of Soil Science*, 49, 295-304.
- DITTMAR, T., KOCH, B., HERTKORN, N. & KATTNER, G. 2008. A simple and efficient method for the solid-phase extraction of dissolved organic matter (SPE-DOM) from seawater. *Limnology and Oceanography-Methods*, 6, 230-235.
- DITTMAR, T., WHITEHEAD, K., MINOR, E. C. & KOCH, B. P. 2007. Tracing terrigenous dissolved organic matter and its photochemical decay in the ocean by using liquid chromatography/mass spectrometry. *Marine Chemistry*, 107, 378-387.
- DREWES, J. E., MITTERWALLNER, J., GRUENHEID, S. & BELLONA, C. A Novel Approach Using Reverse Osmosis/Electrodialysis (RO/ED) to Concentrate and Isolate Organic Carbon From Water Samples. Water Quality Technology Conference, November 2002 Seattle, WA. 252-269.
- DUNGAIT, A. J. J., STEAR, N. S., VAN DONGEN, B. E., BOL, R. & EVERSLED, R. P. 2008. Off-line pyrolysis and compound-specific stable carbon isotope analysis of lignin moieties: a new method for determining the fate of lignin residues in soil. *Rapid Communications in Mass Spectrometry*, 22, 1631-1639.
- DUNGAIT, J. A. J., BOL, R. & EVERSLED, R. P. 2005. Quantification of dung carbon incorporation in a temperate grassland soil following spring application using bulk stable carbon isotope determinations. *Isotopes in Environmental and Health Studies*, 41, 3-11.
- DUNGAIT, J. A. J., BOL, R., LOPEZ-CAPEL, E., BULL, I. D., CHADWICK, D., AMELUNG, W., GRANGER, S. J., MANNING, D. A. C. & EVERSLED, R. P. 2010. Applications of stable isotope ratio mass spectrometry in cattle dung carbon cycling studies. *Rapid Communications in Mass Spectrometry*, 24, 495-500.

- DUNGAIT, J. A. J., CARDENAS, L. M., BLACKWELL, M. S. A., WU, L., WITHERS, P. J. A., CHADWICK, D. R., BOL, R., MURRAY, P. J., MACDONALD, A. J., WHITMORE, A. P. & GOULDING, K. W. T. 2012a. Advances in the understanding of nutrient dynamics and management in UK agriculture. *Science of the Total Environment*, 434, 39-50.
- DUNGAIT, J. A. J., HOPKINS, D. W., GREGORY, A. S. & WHITMORE, A. P. 2012b. Soil organic matter turnover is governed by accessibility not recalcitrance. *Global Change Biology*, 18, 1781-1796.
- DUNGAIT, J. A. J., KEMMITT, S. J., MICHALLON, L., GUO, S., WEN, Q., BROOKES, P. C. & EVERSHED, R. P. 2011. Variable responses of the soil microbial biomass to trace concentrations of ¹³C-labelled glucose, using ¹³C-PLFA analysis. *European Journal of Soil Science*, 62, 117-126.
- ECKARD, R. S., HERNES, P. J., BERGAMASCHI, B. A., STEPANAUSKAS, R. & KENDALL, C. 2007. Landscape scale controls on the vascular plant component of dissolved organic carbon across a freshwater delta. *Geochimica Et Cosmochimica Acta*, 71, 5968-5984.
- ERTEL, J. R., HEDGES, J. I., DEVOL, A. H., RICHEY, J. E. & RIBEIRO, M. D. G. 1986. Dissolved Humic Substances Of The Amazon River System. *Limnology and Oceanography*, 31, 739-754.
- EVANS, C., GOODALE, C., CAPORN, S., DISE, N., EMMETT, B., FERNANDEZ, I., FIELD, C., FINDLAY, S., LOVETT, G., MEESENBURG, H., MOLDAN, F. & SHEPPARD, L. 2008. Does elevated nitrogen deposition or ecosystem recovery from acidification drive increased dissolved organic carbon loss from upland soil? A review of evidence from field nitrogen addition experiments. *Biogeochemistry*, 91, 13-35.
- EVANS, C. D., MONTEITH, D. T. & COOPER, D. M. 2005. Long-term increases in surface water dissolved organic carbon: Observations, possible causes and environmental impacts. *Environmental Pollution*, 137, 55-71.
- FAIX, O., MEIER, D. & GROBE, I. 1987. Studies On Isolated Lignins And Lignins In Woody Materials By Pyrolysis-Gas Chromatography-Mass Spectrometry And Off-Line Pyrolysis-Gas Chromatography With Flame Ionization Detection. *Journal of Analytical and Applied Pyrolysis*, 11, 403-416.
- FENG, X. & SIMPSON, M. J. 2007. The distribution and degradation of biomarkers in Alberta grassland soil profiles. *Organic Geochemistry*, 38, 1558-1570.
- FENG, X. & SIMPSON, M. J. 2008. Temperature responses of individual soil organic matter components. *Journal of Geophysical Research-Biogeosciences*, 113.
- FERNANDEZ, I., MAHIEU, N. & CADISCH, G. 2003. Carbon isotopic fractionation during decomposition of plant materials of different quality. *Global Biogeochemical Cycles*, 17.
- FILLEY, T. R., HATCHER, P. G., SHORTLE, W. C. & PRASEUTH, R. T. 2000. The application of C-13-labeled tetramethylammonium hydroxide (C-13-TMAH) thermochemolysis to the study of fungal degradation of wood. *Organic Geochemistry*, 31, 181-198.
- FILLEY, T. R., MINARD, R. D. & HATCHER, P. G. 1999. Tetramethylammonium hydroxide (TMAH) thermochemolysis: proposed mechanisms based upon the application of ¹³C-labeled TMAH to a synthetic model lignin dimer. *Organic Geochemistry*, 30, 607-621.
- FILLEY, T. R., NIEROP, K. G. J. & WANG, Y. 2006. The contribution of polyhydroxyl aromatic compounds to tetramethylammonium hydroxide lignin-based proxies. *Organic Geochemistry*, 37, 711-727.
- FISHER, M. J., RAO, I. M., AYARZA, M. A., LASCANO, C. E., SANZ, J. I., THOMAS, R. J. & VERA, R. R. 1994. Carbon Storage By Introduced Deep-Rooted Grasses In The South-American Savannas. *Nature*, 371, 236-238.
- FORSLUND, A., MARKUSSEN, B., TOENNER-KLANK, L., BECH, T. B., JACOBSEN, O. S. & DALSGAARD, A. 2011. Leaching of *Cryptosporidium parvum* Oocysts, *Escherichia coli*, and a *Salmonella enterica* Serovar Typhimurium Bacteriophage through Intact Soil Cores following Surface Application and Injection of Slurry. *Applied and Environmental Microbiology*, 77, 8129-8138.

- FRAUENFELD, O. W., ZHANG, T. J., BARRY, R. G. & GILICHINSKY, D. 2004. Interdecadal changes in seasonal freeze and thaw depths in Russia. *Journal of Geophysical Research-Atmospheres*, 109.
- FRAZIER, S. W., KAPLAN, L. A. & HATCHER, P. G. 2005. Molecular Characterization of Biodegradable Dissolved Organic Matter Using Bioreactors and [¹²C/¹³C] Tetramethylammonium Hydroxide Thermochemolysis GC-MS. *Environmental Science & Technology*, 39, 1479-1491.
- FRAZIER, S. W., NOWACK, K. O., GOINS, K. M., CANNON, F. S., KAPLAN, L. A. & HATCHER, P. G. 2003. Characterization of organic matter from natural waters using tetramethylammonium hydroxide thermochemolysis GC-MS. *Journal of Analytical and Applied Pyrolysis*, 70, 99-128.
- FREUDENBERG, K. 1965. Lignin - Its Constitution And Formation From P-Hydroxycinnamyl Alcohols. *Science*, 148, 595-&.
- FROBERG, M., GRIP, H., TIPPING, E., SVENSSON, M., STROMGREN, M. & KLEJA, D. B. 2013. Long-term effects of experimental fertilization and soil warming on dissolved organic matter leaching from a spruce forest in Northern Sweden. *Geoderma*, 200/201, 172-179.
- FUJI, K., ICHIKAWA, K., NODE, M. & FUJITA, E. 1979. Hard Acid And Soft Nucleophile System - New Efficient Method For Removal Of Benzyl Protecting Group. *Journal of Organic Chemistry*, 44, 1661-1664.
- GARDNER, W. S. & MENZEL, D. W. 1974. Phenolic Aldehydes As Indicators Of Terrestrially Derived Organic-Matter In Sea. *Geochimica Et Cosmochimica Acta*, 38, 813-822.
- GEIB, S. M., FILLEY, T. R., HATCHER, P. G., HOOVER, K., CARLSON, J. E., JIMENEZ-GASCO, M. D. M., NAKAGAWA-IZUMI, A., SLEIGHTER, R. L. & TIEN, M. 2008. Lignin degradation in wood-feeding insects. *Proceedings of the National Academy of Sciences of the United States of America*, 105, 12932-12937.
- GELLERSTEDT, G. 2007. *Lignin Complexity: Fundamental And Applied Issues*. [Online]. Available: <http://rfparois.free.fr/LIG2G/Seminaire%20LIG2G-WEB-vs-tout-public.htm>.
- GHOLZ, H. L., WEDIN, D. A., SMITHERMAN, S. M., HARMON, M. E. & PARTON, W. J. 2000. Long-term dynamics of pine and hardwood litter in contrasting environments: toward a global model of decomposition. *Global Change Biology*, 6, 751-765.
- GIARDINA, C. P. & RYAN, M. G. 2000. Evidence that decomposition rates of organic carbon in mineral soil do not vary with temperature. *Nature*, 404, 858-861.
- GLEIXNER, G., POIRIER, N., BOL, R. & BALESSENT, J. 2002. Molecular dynamics of organic matter in a cultivated soil. *Organic Geochemistry*, 33, 357-366.
- GLENN, J. K., MORGAN, M. A., MAYFIELD, M. B., KUWAHARA, M. & GOLD, M. H. 1983. An Extracellular H₂O₂-Requiring Enzyme Preparation Involved In Lignin Biodegradation By The White Rot Basidiomycete Phanerochaete-Chrysosporium. *Biochemical and Biophysical Research Communications*, 114, 1077-1083.
- GONI, M. A. & HEDGES, J. I. 1992. Lignin Dimers - Structures, Distribution, And Potential Geochemical Applications. *Geochimica Et Cosmochimica Acta*, 56, 4025-4043.
- GONI, M. A., RUTTENBERG, K. C. & EGLINTON, T. I. 1997. Source and contribution of terrigenous organic carbon to surface sediments in the Gulf of Mexico. *Nature*, 389, 275-278.
- GRASSET, L., VLCKOVA, Z., KUCERIK, J. & AMBLES, A. 2010. Characterization of lignin monomers in low rank coal humic acids using the derivatization/reductive cleavage method. *Organic Geochemistry*, 41, 905-909.
- GREEN, F. & HIGHLEY, T. L. 1997. Mechanism of brown-rot decay: Paradigm or paradox. *International Biodeterioration & Biodegradation*, 39, 113-124.
- GRUNEWALD, G., KAISER, K., JAHN, R. & GUGGENBERGER, G. 2006. Organic matter stabilization in young calcareous soils as revealed by density fractionation and analysis of lignin-derived constituents. *Organic Geochemistry*, 37, 1573-1589.

- GUGGENBERGER, G. & ZECH, W. 1994. Composition And Dynamics Of Dissolved Carbohydrates And Lignin-Degradation Products In Two Coniferous Forests, Ne Bavaria, Germany. *Soil Biology & Biochemistry*, 26, 19-27.
- GUO, L. B. & GIFFORD, R. M. 2002. Soil carbon stocks and land use change: a meta analysis. *Global Change Biology*, 8, 345-360.
- GUO, X. J., XI, B. D., YU, H. B., MA, W. C. & HE, X. S. 2011. The structure and origin of dissolved organic matter studied by UV-vis spectroscopy and fluorescence spectroscopy in lake in arid and semi-arid region. *Water Science and Technology*, 63, 1010-1017.
- HARTLEY, I. P. & INESON, P. 2008. Substrate quality and the temperature sensitivity of soil organic matter decomposition. *Soil Biology & Biochemistry*, 40, 1567-1574.
- HATCHER, P. G. & MINARD, R. D. 1995. Comment on the origin of benzenecarboxylic acids in pyrolysis methylation studies. *Organic Geochemistry*, 23, 991-994.
- HATCHER, P. G., NANNY, M. A., MINARD, R. D., DIBLE, S. D. & CARSON, D. M. 1995. Comparison of two thermochemolytic methods for the analysis of lignin in decomposing gymnosperm wood: The CuO oxidation method and the method of thermochemolysis with tetramethylammonium hydroxide (TMAH). *Organic Geochemistry*, 23, 881-888.
- HAYNES, W. M. (ed.) 2010. *CRC Handbook of Chemistry and Physics*: CRC Press.
- HEDGES, J. I. & ERTEL, J. R. 1982. Characterization Of Lignin By Gas Capillary Chromatography Of Cupric Oxide Oxidation-Products. *Analytical Chemistry*, 54, 174-178.
- HEDGES, J. I., KEIL, R. G. & BENNER, R. 1997. What happens to terrestrial organic matter in the ocean? *Organic Geochemistry*, 27, 195-212.
- HEDGES, J. I. & MANN, D. C. 1979a. Characterisation Of Plant-Tissues By Their Lignin Oxidation-Products. *Geochimica Et Cosmochimica Acta*, 43, 1803-1807.
- HEDGES, J. I. & MANN, D. C. 1979b. Lignin Geochemistry Of Marine-Sediments From The Southern Washington Coast. *Geochimica Et Cosmochimica Acta*, 43, 1809-1818.
- HEDGES, J. I. & OADES, J. M. 1997. Comparative organic geochemistries of soils and marine sediments. *Organic Geochemistry*, 27, 319-361.
- HERBERT, B. E. & BERTSCH, P. M. 1995. *Characterization Of Dissolved And Colloidal Organic Matter In Soil Solution - A Review*.
- HERNES, P. J. & BENNER, R. 2002. Transport and diagenesis of dissolved and particulate terrigenous organic matter in the North Pacific Ocean. *Deep-Sea Research Part I-Oceanographic Research Papers*, 49, 2119-2132.
- HERNES, P. J. & BENNER, R. 2003. Photochemical and microbial degradation of dissolved lignin phenols: Implications for the fate of terrigenous dissolved organic matter in marine environments. *Journal of Geophysical Research-Oceans*, 108.
- HERNES, P. J. & BENNER, R. 2006. Terrigenous organic matter sources and reactivity in the North Atlantic Ocean and a comparison to the Arctic and Pacific oceans. *Marine Chemistry*, 100, 66-79.
- HERNES, P. J., ROBINSON, A. C. & AUFDENKAMPE, A. K. 2007. Fractionation of lignin during leaching and sorption and implications for organic matter "freshness". *Geophysical Research Letters*, 34.
- HIGUCHI, T. 2004. Microbial degradation of lignin: Role of lignin peroxidase, manganese peroxidase, and laccase. *Proceedings of the Japan Academy*, 80, 204-214.
- HIGUCHI, T., ITO, Y., SHIMADA, M. & KAWAMURA, I. 1967. Chemical Properties Of Milled Wood Lignin Of Grasses. *Phytochemistry*, 6, 1551-&.
- HOGBERG, P. & EKBLAD, A. 1996. Substrate-induced respiration measured in situ in a C-3-plant ecosystem using additions of C-4-sucrose. *Soil Biology & Biochemistry*, 28, 1131-1138.
- HOLTMAN, K. M., CHANG, H. M., JAMEEL, H. & KADLA, J. F. 2003. Elucidation of lignin structure through degradative methods: Comparison of modified DFRC and thioacidolysis. *Journal of Agricultural and Food Chemistry*, 51, 3535-3540.
- HUANG, Y., EGLINTON, G., VAN DER HAGE, E. R. E., BOON, J. J., BOL, R. & INESON, P. 1998. Dissolved organic matter and its parent organic matter in grass upland soil horizons studied by analytical pyrolysis techniques. *European Journal of Soil Science*, 49, 1-15.

- HUNT, H. W., INGHAM, E. R., COLEMAN, D. C., ELLIOTT, E. T. & REID, C. P. P. 1988. Nitrogen Limitation Of Production And Decomposition In Prairie, Mountain Meadow, And Pine Forest. *Ecology*, 69, 1009-1016.
- IKEDA, T., HOLTMAN, K., KADLA, J. F., CHANG, H. M. & JAMEEL, H. 2002. Studies on the effect of ball milling on lignin structure using a modified DFRC method. *Journal of Agricultural and Food Chemistry*, 50, 129-135.
- IPCC (ed.) 2001. *Climate Change 2001: The Scientific Basis. Contribution of Working Group I to the Third Assessment Report of the Intergovernmental Panel on Climate Change*: Chambridge University Press.
- JENKINS, G. J., MURPHY, J. M., SEXTON, D. M. H., LOWE, J. A., JONES, P. & KILSBY, C. G. 2009. UK Climate Projections: Briefing report. . Met Office Hadley Centre, Exeter, UK.
- JENKINSON, D. S. & RAYNER, J. H. 1977. Turnover Of Soil Organic-Matter In Some Of Rothamsted Classical Experiments. *Soil Science*, 123, 298-305.
- JIN, L., SCHULTZ, T. P. & NICHOLAS, D. D. 1990. Structural Characterization Of Brown-Rotted Lignin. *Holzforschung*, 44, 133-138.
- JONES, L., ENNOS, A. R. & TURNER, S. R. 2001. Cloning and characterization of irregular xylem4 (irx4): a severely lignin-deficient mutant of Arabidopsis. *Plant Journal*, 26, 205-216.
- KAISER, K., GUGGENBERGER, G. & HAUMAIER, L. 2004. Changes in dissolved lignin-derived phenols, neutral sugars, uronic acids, and amino sugars with depth in forested Haplic Arenosols and Rendzic Leptosols. *Biogeochemistry*, 70, 135-151.
- KAISER, K., GUGGENBERGER, G., HAUMAIER, L. & ZECH, W. 1997. Dissolved organic matter sorption on subsoils and minerals studied by C-13-NMR and DRIFT spectroscopy. *European Journal of Soil Science*, 48, 301-310.
- KALBITZ, K. 2001. Properties of organic matter in soil solution in a German fen area as dependent on land use and depth. *Geoderma*, 104, 203-214.
- KALBITZ, K., GLASER, B. & BOL, R. 2004. Clear-cutting of a Norway spruce stand: implications for controls on the dynamics of dissolved organic matter in the forest floor. *European Journal of Soil Science*, 55, 401-413.
- KALBITZ, K. & KAISER, K. 2008. Contribution of dissolved organic matter to carbon storage in forest mineral soils. *Journal of Plant Nutrition and Soil Science-Zeitschrift Fur Pflanzenernahrung Und Bodenkunde*, 171, 52-60.
- KALBITZ, K., KAISER, K., BARGHOLZ, J. & DARDENNE, P. 2006. Lignin degradation controls the production of dissolved organic matter in decomposing foliar litter. *European Journal of Soil Science*, 57, 504-516.
- KALBITZ, K., SCHWESIG, D., RETHEMEYER, J. & MATZNER, E. 2005. Stabilization of dissolved organic matter by sorption to the mineral soil. *Soil Biology & Biochemistry*, 37, 1319-1331.
- KALBITZ, K., SCHWESIG, D., SCHMERWITZ, J., KAISER, K., HAUMAIER, L., GLASER, B., ELLERBROCK, R. & LEINWEBER, P. 2003. Changes in properties of soil-derived dissolved organic matter induced by biodegradation. *Soil Biology & Biochemistry*, 35, 1129-1142.
- KALBITZ, K., SOLINGER, S., PARK, J. H., MICHALZIK, B. & MATZNER, E. 2000. Controls on the dynamics of dissolved organic matter in soils: A review. *Soil Science*, 165, 277-304.
- KICKLIGHTER, D. W., BRUNO, M., DONGES, S., ESSER, G., HEIMANN, M., HELFRICH, J., IFT, F., JOOS, F., KADUK, J., KOHLMAIER, G. H., MCGUIRE, A. D., MELILLO, J. M., MEYER, R., MOORE, B., NADLER, A., PRENTICE, I. C., SAUF, W., SCHLOSS, A. L., SITCH, S., WITTENBERG, U. & WURTH, G. 1999. A first-order analysis of the potential role of CO₂ fertilization to affect the global carbon budget: a comparison of four terrestrial biosphere models. *Tellus Series B-Chemical and Physical Meteorology*, 51, 343-366.
- KIEM, R. & KOGEL-KNABNER, I. 2003. Contribution of lignin and polysaccharides to the refractory carbon pool in C-depleted arable soils. *Soil Biology & Biochemistry*, 35, 101-118.
- KIM, S., SIMPSON, A. J., KUJAWINSKI, E. B., FREITAS, M. A. & HATCHER, P. G. 2003. High resolution electrospray ionization mass spectrometry and 2D solution NMR for the

- analysis of DOM extracted by C-18 solid phase disk. *Organic Geochemistry*, 34, 1325-1335.
- KIRK, T. K. & ADLER, E. 1969. Catechol Moieties in Enzymatically Liberated Lignin. *Acta Chemica Scandinavica*, 23, 705-707.
- KIRK, T. K., CONNORS, W. J., BLEAM, R. D., HACKETT, W. F. & ZEIKUS, J. G. 1975. Preparation And Microbial Decomposition Of Synthetic C-14 Lignins. *Proceedings of the National Academy of Sciences of the United States of America*, 72, 2515-2519.
- KIRK, T. K. & COWLING, E. B. 1984. Biological Decomposition Of Solid Wood. *Advances in Chemistry Series*, 455-487.
- KIRK, T. K. & FARRELL, R. L. 1987. Enzymatic Combustion - The Microbial-Degradation Of Lignin. *Annual Review of Microbiology*, 41, 465-505.
- KIRK, T. K., LARSSON, S. & MIKSCH, G. E. 1970. Aromatic Hydroxylation Resulting From Attack Of Lignin By A Brown-Rot Fungus. *Acta Chemica Scandinavica*, 24, 1470-1472.
- KIRK, T. K., SCHULTZ, E., CONNORS, W. J., LORENZ, L. F. & ZEIKUS, J. G. 1978. Influence Of Culture Parameters On Lignin Metabolism By Phanerochaete-Chrysosporium. *Archives of Microbiology*, 117, 277-285.
- KIRSCHBAUM, M. U. F. 2006. The temperature dependence of organic-matter decomposition - still a topic of debate. *Soil Biology & Biochemistry*, 38, 2510-2518.
- KIRSCHBAUM, M. U. F. 2013. Seasonal variations in the availability of labile substrate confound the temperature dependence of organic matter decomposition. *Soil Biology & Biochemistry*, 57, 568-576.
- KLEIN, M. T. & VIRK, P. S. 1983. Model Pathways In Lignin Thermolysis .1. Phenethyl Phenyl Ether. *Industrial & Engineering Chemistry Fundamentals*, 22, 35-45.
- KLINGBERG, A., ODERMATT, J. & MEIER, D. 2005. Influence of parameters on pyrolysis-GC/MS of lignin in the presence of tetramethylammonium hydroxide. *Journal of Analytical and Applied Pyrolysis*, 74, 104-109.
- KLOTZBUCHER, T., FILLEY, T. R., KAISER, K. & KALBITZ, K. 2011a. A study of lignin degradation in leaf and needle litter using C-13-labelled tetramethylammonium hydroxide (TMAH) thermochemolysis: Comparison with CuO oxidation and van Soest methods. *Organic Geochemistry*, 42, 1271-1278.
- KLOTZBUCHER, T., KAISER, K., GUGGENBERGER, G., GATZEK, C. & KALBITZ, K. 2011b. A new conceptual model for the fate of lignin in decomposing plant litter. *Ecology*, 92, 1052-1062.
- KOGEL-KNABNER, I. 2002. The macromolecular organic composition of plant and microbial residues as inputs to soil organic matter. *Soil Biology & Biochemistry*, 34, 139-162.
- KONDO, T., OHSHITA, T. & KYUMA, T. 1994. Comparison Of Phenolic-Acids In Lignin Fractions From Forage Grasses Before And After Digestion By Sheep. *Animal Feed Science and Technology*, 47, 277-285.
- KURODA, K. & NAKAGAWA-IZUMI, A. 2006. Analytical pyrolysis of lignin: Products stemming from beta-5 substructures. *Organic Geochemistry*, 37, 665-673.
- LAL, R. 2004. Soil carbon sequestration to mitigate climate change. *Geoderma*, 123, 1-22.
- LAL, R. 2013. Enhancing ecosystem services with no-till. *Renewable Agriculture and Food Systems*, 28, 102-114.
- LAPIERRE, C., MONTIES, B. & ROLANDO, C. 1988. Thioacidolysis Of Diazomethane-Methylated Pine Compression Wood And Wheat Straw Insitu Lignins. *Holzforschung*, 42, 409-411.
- LARA, R. J. & THOMAS, D. N. 1994. XAD-Fractionation Of New Dissolved Organic-Matter - Is The Hydrophobic Fraction Seriously Underestimated. *Marine Chemistry*, 47, 93-96.
- LAVERS, D. A., ALLAN, R. P., VILLARINI, G., LLOYD-HUGHES, B., BRAYSHAW, D. J. & WADE, A. J. 2013. Future Changes In Atmospheric Rivers And Their Implications For Winter Flooding In Britian. *Environmental Research Letters*, 8, 034010.
- LAWOKO, M., HENRIKSSON, G. & GELLERSTEDT, G. 2005. Structural differences between the lignin-carbohydrate complexes present in wood and in chemical pulps. *Biomacromolecules*, 6, 3467-3473.

- LEO, R. F. & BARGHOORN, E. S. 1970. Phenolic Aldehydes - Generation From Fossil Woods And Carbonaceous Sediments By Oxidative Degradation. *Science*, 168, 582-&.
- LEVERMANN, A., CLARK, P. U., MARZEION, B., MILNE, G. A., POLLARD, D., RADIC, V. & ROBINSON, A. 2013. The multimillennial sea-level commitment of global warming. *Proceedings of the National Academy of Sciences of the United States of America*, 110, 13745-50.
- LISKA, I. 2000. Fifty years of solid-phase extraction in water analysis - historical development and overview. *Journal of Chromatography A*, 885, 3-16.
- LISKI, J., ILVESNIEMI, H., MAKELA, A. & WESTMAN, C. J. 1999. CO₂ emissions from soil in response to climatic warming are overestimated - The decomposition of old soil organic matter is tolerant of temperature. *Ambio*, 28, 171-174.
- LLOYD, C. E. M., MICHAELIDES, K., CHADWICK, D. R., DUNGAIT, J. A. J. & EVERSHED, R. P. 2012. Tracing the flow-driven vertical transport of livestock-derived organic matter through soil using biomarkers. *Organic Geochemistry*, 43, 56-66.
- LOMBARDI, A. T., HIDALGO, T. M. R. & VIEIRA, A. A. H. 2005. Copper complexing properties of dissolved organic materials exuded by the freshwater microalgae *Scenedesmus acuminatus* (Chlorophyceae). *Chemosphere*, 60, 453-459.
- LOUCHOUARN, P., OPSAHL, S. & BENNER, R. 2000. Isolation and Quantification of Dissolved Lignin from Natural Waters Using Solid-Phase Extraction and GC/MS. *Analytical Chemistry*, 72, 2780-2787.
- LU, F. & RALPH, J. 1997. Derivatization Followed by Reductive Cleavage (DFRC method), a New Method for Lignin Analysis: Protocol for Analysis of DFRC Monomers. *Journal of Agricultural and Food Chemistry*, 45, 2590-2592.
- LU, F. C. & RALPH, J. 1998. The DFRC method for lignin analysis. 2. Monomers from isolated lignins. *Journal of Agricultural and Food Chemistry*, 46, 547-552.
- LYTLE, C. R. & PERDUE, E. M. 1981. Free, Proteinaceous, And Humic-Bound Amino-Acids In River Water Containing High-Concentrations Of Aquatic Humus. *Environmental Science & Technology*, 15, 224-228.
- MARSCHNER, B. & KALBITZ, K. 2003. Controls of bioavailability and biodegradability of dissolved organic matter in soils. *Geoderma*, 113, 211-235.
- MARSCHNER, B. & NOBLE, A. D. 2000. Chemical and biological processes leading to the neutralisation of acidity in soil incubated with litter materials. *Soil Biology & Biochemistry*, 32, 805-813.
- MARTIN, F., DEL RIO, C., GONZALEZVILA, F. J. & VERDEJO, T. 1995. Thermally Assisted Hydrolysis And Alkylation Of Lignins In The Presence Of Tetra-Alkylammonium Hydroxides. *Journal of Analytical and Applied Pyrolysis*, 35, 1-13.
- MARTIN, J. P., HAIDER, K. & KASSIM, G. 1980. Biodegradation And Stabilization After 2 Years Of Specific Crop, Lignin, And Polysaccharide Carbons In Soils. *Soil Science Society of America Journal*, 44, 1250-1255.
- MASON, S. L., FILLEY, T. R. & ABBOTT, G. D. 2009. The effect of afforestation on the soil organic carbon (SOC) of a peaty gley soil using on-line thermally assisted hydrolysis and methylation (THM) in the presence of C-13-labelled tetramethylammonium hydroxide (TMAH). *Journal of Analytical and Applied Pyrolysis*, 85, 417-425.
- MASON, S. L., FILLEY, T. R. & ABBOTT, G. D. 2012. A comparative study of the molecular composition of a grassland soil with adjacent unforested and afforested moorland ecosystems. *Organic Geochemistry*, 42, 1519-1528.
- MCCARTHY, A. J. & BRODA, P. 1984. Screening For Lignin-Degrading Actinomycetes And Characterization Of Their Activity Against C-14 Lignin-Labeled Wheat Lignocellulose. *Journal of General Microbiology*, 130, 2905-2913.
- MCCARTHY, A. J., MACDONALD, M. J., PATERSON, A. & BRODA, P. 1984. Degradation Of C-14-Labeled Lignin Wheat Lignocellulose By White-Rot Fungi. *Journal of General Microbiology*, 130, 1023-1030.
- MCCARTHY, M., HEDGES, J. & BENNER, R. 1996. Major biochemical composition of dissolved high molecular weight organic matter in seawater. *Marine Chemistry*, 55, 281-297.

- MCDOWELL, W. H. & LIKENS, G. E. 1988. Origin, Composition, And Flux Of Dissolved Organic-Carbon In The Hubbard Brook Valley. *Ecological Monographs*, 58, 177-195.
- MEEHL, G. A. & STOCKER, T. F. 2007. *Global Climate Projections*, Cambridge University Press.
- MELLOR, J. D. 1978. *Fundamentals of freeze-drying*, London, Academic Press.
- MEYBECK, M. 1982. Carbon, Nitrogen, And Phosphorus Transport By World Rivers. *American Journal of Science*, 282, 401-450.
- MEYERSSCHULTE, K. J. & HEDGES, J. I. 1986. Molecular Evidence For A Terrestrial Component Of Organic-Matter Dissolved In Ocean Water. *Nature*, 321, 61-63.
- MICHALZIK, B. & MATZNER, E. 1999. Dynamics of dissolved organic nitrogen and carbon in a Central European Norway spruce ecosystem. *European Journal of Soil Science*, 50, 579-590.
- MOLDOVEANU, S. C. (ed.) 1998. *Analytical Pyrolysis of Natural Organic Polymers*, Amsterdam: Elsevier.
- MOLDOVEANU, S. C. 2001. Pyrolysis GC/MS, Present and Future (Recent Past and Present Needs). *Journal of Microcolumn Separations*, 13, 102-125.
- MORAN, M. A., WICKS, R. J. & HODSON, R. E. 1991. Export Of Dissolved Organic-Matter From A Mangrove Swamp Ecosystem - Evidence From Natural Fluorescence, Dissolved Lignin Phenols, And Bacterial Secondary Production. *Marine Ecology Progress Series*, 76, 175-184.
- MURTY, D., KIRSCHBAUM, M. U. F., MCMURTRIE, R. E. & MCGILVRAY, A. 2002. Does conversion of forest to agricultural land change soil carbon and nitrogen? a review of the literature. *Global Change Biology*, 8, 105-123.
- NAKAGAWA-IZUMIA, A., KURODA, K. & OZAWA, T. 2004. Thermochemolytic behavior of beta-beta lignin structures in the presence of tetramethylammonium hydroxide (TMAH). *Organic Geochemistry*, 35, 763-774.
- NIEROP, K. G. J. & BUURMAN, P. 1999. Water-soluble organic matter in incipient podzols: accumulation in B horizons or in fibres? *European Journal of Soil Science*, 50, 701-711.
- NIEROP, K. G. J. & FILLEY, T. R. 2007. Assessment of lignin and (poly-)phenol transformations in oak (*Quercus robur*) dominated soils by C-13-TMAH thermochemolysis. *Organic Geochemistry*, 38, 551-565.
- NIEROP, K. G. J. & FILLEY, T. R. 2008. Simultaneous analysis of tannin and lignin signatures in soils by thermally assisted hydrolysis and methylation using (13)C-labeled TMAH. *Journal of Analytical and Applied Pyrolysis*, 83, 227-231.
- O'DRISCOLL, N. J., SICILIANO, S. D., PEAK, D., CARIGNAN, R. & LEAN, D. R. S. 2006. The influence of forestry activity on the structure of dissolved organic matter in lakes: Implications for mercury photoreactions. *Science of the Total Environment*, 366, 880-893.
- ONO, K., HIRADATE, S., MORITA, S. & HIRAI, K. 2013. Fate of organic carbon during decomposition of different litter types in Japan. *Biogeochemistry*, 112, 7-21.
- OPSAHL, S. & BENNER, R. 1995. Early Diagenesis Of Vascular Plant-Tissues - Lignin And Cutin Decomposition And Biodegradation Implications. *Geochimica Et Cosmochimica Acta*, 59, 4889-4904.
- OPSAHL, S. & BENNER, R. 1997. Distribution and cycling of terrigenous dissolved organic matter in the ocean. *Nature*, 386, 480-482.
- OPSAHL, S. & BENNER, R. 1998. Photochemical reactivity of dissolved lignin in river and ocean waters. *Limnology and Oceanography*, 43, 1297-1304.
- OPSAHL, S., BENNER, R. & AMON, R. M. W. 1999. Major flux of terrigenous dissolved organic matter through the Arctic Ocean. *Limnology and Oceanography*, 44, 2017-2023.
- OTTO, A. & SIMPSON, M. J. 2006. Evaluation of CuO oxidation parameters for determining the source and stage of lignin degradation in soil. *Biogeochemistry*, 80, 121-142.
- PARTON, W. J., STEWART, J. W. B. & COLE, C. V. 1988. Dynamics Of C, N, P And S In Grassland Soils - A Model. *Biogeochemistry*, 5, 109-131.
- PENG, J. P., LU, F. C. & RALPH, J. 1998. The DFRC method for lignin analysis. 4. Lignin dimers isolated from DFRC-degraded loblolly pine wood. *Journal of Agricultural and Food Chemistry*, 46, 553-560.

- PIGNATELLO, J. J. 2000. The measurement and interpretation of sorption and desorption rates for organic compounds in soil media. *Advances in Agronomy*, Vol 69, 69, 1-73.
- POMETTO III, A. L. & CRAWFORD, D. L. 1986. Effects of pH on Lignin and Cellulose Degradation by *Streptomyces viridosporus*. *Applied and Environmental Microbiology*, 52, 246-250.
- POWLSON, D. S., BROOKES, P. C., WHITMORE, A. P., GOULDING, K. W. T. & HOPKINS, D. W. 2011. Soil Organic Matters. *European Journal of Soil Science*, 62, 1-4.
- RALPH, J. & GRABBER, J. H. 1996. Dimeric beta-ether thioacidolysis products resulting from incomplete ether cleavage. *Holzforschung*, 50, 425-428.
- RALPH, J., LAPIERRE, C., MARITA, J. M., KIM, H., LU, F. C., HATFIELD, R. D., RALPH, S., CHAPPLE, C., FRANKE, R., HEMM, M. R., VAN DOORSSELAERE, J., SEDEROFF, R. R., O'MALLEY, D. M., SCOTT, J. T., MACKAY, J. J., YAHIAOUI, N., BOUDET, A. M., PEAN, M., PILATE, G., JOUANIN, L. & BOERJAN, W. 2001. Elucidation of new structures in lignins of CAD- and COMT-deficient plants by NMR. *Phytochemistry*, 57, 993-1003.
- RALPH, J., LUNDQUIST, K., BRUNOW, G., LU, F., KIM, H., SCHATZ, P. F., MARITA, J. M., HATFIELD, R. D., RALPH, S. A., CHRISTENSEN, J. H. & BOERJAN, W. 2004. Lignins: Natural polymers from oxidative coupling of 4-hydroxyphenylpropanoids. *Phytochemistry Reviews*, 3, 29-60.
- RASSE, D. P., DIGNAC, M. F., BAHRI, H., RUMPEL, C., MARIOTTI, A. & CHENU, C. 2006. Lignin turnover in an agricultural field: from plant residues to soil-protected fractions. *European Journal of Soil Science*, 57, 530-538.
- RASSE, D. P., RUMPEL, C. & DIGNAC, M. F. 2005. Is soil carbon mostly root carbon? Mechanisms for a specific stabilisation. *Plant and Soil*, 269, 341-356.
- REID, I. D., ABRAMS, G. D. & PEPPER, J. M. 1982. Water-Soluble Products From The Degradation Of Aspen Lignin By *Phanerochaete-chrysosporium*. *Canadian Journal of Botany-Revue Canadienne De Botanique*, 60, 2357-2364.
- REID, K. J. G., SWAN, J. S. & GUTTERIDGE, C. S. 1993. Assessment Of Scotch Whiskey Quality By Pyrolysis Mass-Spectrometry And The Subsequent Correlation Of Quality With The Oak Wood Cask. *Journal of Analytical and Applied Pyrolysis*, 25, 49-62.
- RIMMER, D. L. 2006. Free radicals, antioxidants, and soil organic matter recalcitrance. *European Journal of Soil Science*, 57, 91-94.
- RIMMER, D. L. & ABBOTT, G. D. 2011. Phenolic compounds in NaOH extracts of UK soils and their contribution to antioxidant capacity. *European Journal of Soil Science*, 62, 285-294.
- ROBERTSON, S. A., MASON, S. L., HACK, E. & ABBOTT, G. D. 2008a. A comparison of lignin oxidation, enzymatic activity and fungal growth during white-rot decay of wheat straw. *Organic Geochemistry*, 39, 945-951.
- ROBERTSON, S. A., MASON, S. L., HACK, E. & ABBOTT, G. D. 2008b. A comparison of lignin oxidation, enzymatic activity and fungal growth during white-rot decay of wheat straw (vol 39, pg 945, 2008). *Organic Geochemistry*, 39, 1816-1816.
- ROLANDO, C., MONTIES, B. & LAPIERRE, C. (eds.) 1992. *Methods in Lignin Chemistry*, Heidelberg: Springer-Verlag.
- RUMPEL, C., KOGEL-KNABNER, I. & BRUHN, F. 2002. Vertical distribution, age, and chemical composition of organic, carbon in two forest soils of different pedogenesis. *Organic Geochemistry*, 33, 1131-1142.
- SAIZJIMENEZ, C., HERMOSIN, B. & ORTEGA-CALVO, J. J. 1993. Pyrolysis/Methylation - A Method For Structural Elucidation Of The Chemical Nature Of Aquatic Humic Substances. *Water Research*, 27, 1693-1696.
- SANAULLAH, M., RUMPEL, C., CHARRIER, X. & CHABBI, A. 2012. How does drought stress influence the decomposition of plant litter with contrasting quality in a grassland ecosystem? *Plant and Soil*, 352, 277-288.
- SARIYILDIZ, T. & ANDERSON, J. M. 2005. Variation in the chemical composition of green leaves and leaf litters from three deciduous tree species growing on different soil types. *Forest Ecology and Management*, 210, 303-319.

- SCHLESINGER, W. H. 1977. Carbon Balance In Terrestrial Detritus. *Annual Review of Ecology and Systematics*, 8, 51-81.
- SCHLICHTING, A., RIMMER, D. L., ECKHARDT, K.-U., HEUMANN, S., ABBOTT, G. D. & LEINWEBER, P. 2013. Identifying potential antioxidant compounds in NaOH extracts vegetation by untargeted mass spectrometric screening. *Soil Biology & Biochemistry*, 58, 16-26.
- SCHMIDT, M. W. I., TORN, M. S., ABIVEN, S., DITTMAR, T., GUGGENBERGER, G., JANSSENS, I. A., KLEBER, M., KOEGEL-KNABNER, I., LEHMANN, J., MANNING, D. A. C., NANNIPIERI, P., RASSE, D. P., WEINER, S. & TRUMBORE, S. E. 2011. Persistence of soil organic matter as an ecosystem property. *Nature*, 478, 49-56.
- SCHRUMPF, M., KAISER, K., GUGGENBERGER, G., PERSSON, T., KOEGEL-KNABNER, I. & SCHULZE, E. D. 2013. Storage and stability of organic carbon in soils as related to depth, occlusion within aggregates, and attachment to minerals. *Biogeosciences*, 10, 1675-1691.
- SCHULTZ, J., HUNTER, M. & APPEL, H. 1992. Antimicrobial Activity of Polyphenols Mediates Plant-Herbivore Interactions. In: HEMINGWAY, R. & LAKS, P. (eds.) *Plant Polyphenols*. Springer US.
- SHARP, J. H., BENNER, R., BENNETT, L., CARLSON, C. A., FITZWATER, S. E., PELTZER, E. T. & TUPAS, L. M. 1995. Analysis Of Dissolved Organic-Carbon In Seawater - The JGOFS EQPAC Methods Comparison. *Marine Chemistry*, 48, 91-108.
- SHRESTHA, R. K., LAL, R. & RIMAL, B. 2013. Soil carbon fluxes and balances and soil properties of organically amended no-till corn production systems. *Geoderma*, 197, 177-185.
- SHUKLA, M. K., KASTANEK, F. J. & NIELSEN, D. R. 2000. Transport of chloride through water-saturated soil columns. *Bodenkultur*, 51, 235-246.
- SIMPSON, N. J. K. 2000. *Solid-Phase Extraction: Principles, Techniques, and Applications*, New York, Marcel Dekker, Inc.
- SOLOMON, S., QIN, D. & MANNING, M. 2007. *Technical Summary*, Cambridge University Press.
- SORENSEN, H. 1962. Decomposition of Lignin by Soil Bacteria and Complex Formation between Autoxidized lignin and Organic Nitrogen Compounds. *Journal of General Microbiology*, 27, 21-34.
- SPENCER, R. G. M., AIKEN, G. R., DYDA, R. Y., BUTLER, K. D., BERGAMASCHI, B. A. & HERNES, P. J. 2010. Comparison of XAD with other dissolved lignin isolation techniques and a compilation of analytical improvements for the analysis of lignin in aquatic settings. *Organic Geochemistry*, 41, 445-453.
- TANS, P. & KEELING, R. 2013. *Trends in Atmospheric Carbon Dioxide* [Online]. Scripps Institution of Oceanography. Available: <http://www.esrl.noaa.gov/gmd/ccgg/trends/>.
- THEVENOT, M., DIGNAC, M.-F. & RUMPEL, C. 2010. Fate of lignins in soils: A review. *Soil Biology & Biochemistry*, 42, 1200-1211.
- TIEN, M. & KIRK, T. K. 1983. Lignin-Degrading Enzyme From The Hymenomycete Phanerochaete-Chrysosporum Burds. *Science*, 221, 661-662.
- TJOELKER, M. G., OLEKSYN, J. & REICH, P. B. 2001. Modelling respiration of vegetation: evidence for a general temperature-dependent Q(10). *Global Change Biology*, 7, 223-230.
- US-DOE 2008. Carbon Cycling and Biosequestration: Integrating Biology and Climate Through Systems Science; Report from the March 2008 Workshop. DOE/SC-108, U.S. Department of Energy Office of Science.
- VAN BERGEN, P. F., NOTT, C. J., BULL, I. D., POULTON, P. R. & EVERSHED, R. P. 1998. Organic geochemical studies of soils from the Rothamsted Classical Experiments - IV. Preliminary results from a study of the effect of soil pH on organic matter decay. *Organic Geochemistry*, 29, 1779-1795.
- VAN DER HAGE, E. R. E. 1995. *Pyrolysis mass spectrometry of lignin polymers*. Doctor of Philosophy Publication, University of Amsterdam.
- VAN DER HAGE, E. R. E., MULDER, M. M. & BOON, J. J. 1993. Structural Characterization Of Lignin Polymers By Temperature-Resolved In-Source Pyrolysis Mass-Spectrometry And

- Curie-Point Pyrolysis-Gas Chromatography Mass-Spectrometry. *Journal of Analytical and Applied Pyrolysis*, 25, 149-183.
- VANE, C. H. 2003. The molecular composition of lignin in spruce decayed by white-rot fungi (*Phanerochaete chrysosporium* and *Trametes versicolor*) using pyrolysis-GC-MS and thermochemolysis with tetramethylammonium hydroxide. *International Biodeterioration & Biodegradation*, 51, 67-75.
- VANE, C. H. & ABBOTT, G. D. 1999. Proxies for land plant biomass: closed system pyrolysis of some methoxyphenols. *Organic Geochemistry*, 30, 1535-1541.
- VANE, C. H., ABBOTT, G. D. & HEAD, I. M. 2001a. The effect of fungal decay (*Agaricus bisporus*) on wheat straw lignin using pyrolysis-GC-MS in the presence of tetramethylammonium hydroxide (TMAH). *Journal of Analytical and Applied Pyrolysis*, 60, 69-78.
- VANE, C. H., MARTIN, S. C., SNAPE, C. E. & ABBOTT, G. D. 2001b. Degradation of lignin in wheat straw during growth of the oyster mushroom (*Pleurotus ostreatus*) using off-line thermochemolysis with tetramethylammonium hydroxide and solid-state C-13 NMR. *Journal of Agricultural and Food Chemistry*, 49, 2709-2716.
- VANLAUWE, B., DENDOOVEN, L. & MERCKX, R. 1994. Residue Fractionation And Decomposition - The Significance Of The Active Fraction. *Plant and Soil*, 158, 263-274.
- VETTER, T. A., PERDUE, E. M., INGALL, E., KOPRIVNJAK, J. F. & PFROMM, P. H. 2007. Combining reverse osmosis and electrodialysis for more complete recovery of dissolved organic matter from seawater. *Separation and Purification Technology*, 56, 383-387.
- WALDROP, M. P. & FIRESTONE, M. K. 2004. Altered utilization patterns of young and old soil C by microorganisms caused by temperature shifts and N additions. *Biogeochemistry*, 67, 235-248.
- WALLENSTEIN, M. D., HADDIX, M. L., AYRES, E., STELTZER, H., MAGRINI-BAIR, K. A. & PAUL, E. A. 2013. Litter chemistry changes more rapidly when decomposed at home but converges during decomposition-transformation. *Soil Biology & Biochemistry*, 57, 311-319.
- WALLENSTEIN, M. D., HADDIX, M. L., LEE, D. D., CONANT, R. T. & PAUL, E. A. 2012. A litter-slurry technique elucidates the key role of enzyme production and microbial dynamics in temperature sensitivity of organic matter decomposition. *Soil Biology & Biochemistry*, 47, 18-26.
- WANG, C., HAN, G., JIA, Y., FENG, X. & TIAN, X. 2012a. Insight into the temperature sensitivity of forest litter decomposition and soil enzymes in subtropical forest in China. *Journal of Plant Ecology*, 5, 279-286.
- WANG, H., HE, Z., LU, Z., ZHOU, J., VAN NOSTRAND, J. D., XU, X. & ZHANG, Z. 2012b. Genetic Linkage of Soil Carbon Pools and Microbial Functions in Subtropical Freshwater Wetlands in Response to Experimental Warming. *Applied and Environmental Microbiology*, 78, 7652-7661.
- WANG, X., CAI, Y. & GUO, L. 2013a. Variations in abundance and size distribution of carbohydrates in the lower Mississippi River, Pearl River and Bay of St Louis. *Estuarine Coastal and Shelf Science*, 126, 61-69.
- WANG, X., GOUAL, L. & COLBERG, P. J. S. 2012c. Characterization and treatment of dissolved organic matter from oilfield produced waters. *Journal of Hazardous Materials*, 217, 164-170.
- WANG, Z.-P., HAN, X.-G., CHANG, S. X., WANG, B., YU, Q., HOU, L.-Y. & LI, L.-H. 2013b. Soil organic and inorganic carbon contents under various land uses across a transect of continental steppes in Inner Mongolia. *Catena*, 109, 110-117.
- WARD, N. D., KEIL, R. G., MEDEIROS, P. M., BRITO, D. C., CUNHA, A. C., DITTMAR, T., YAGER, P. L., KRUSCHE, A. V. & RICHEY, J. E. 2013. Degradation of terrestrially derived macromolecules in the Amazon River. *Nature Geoscience*, 6, 530-533.
- WEISHAAR, J. L., AIKEN, G. R., BERGAMASCHI, B. A., FRAM, M. S., FUJII, R. & MOPPER, K. 2003. Evaluation of specific ultraviolet absorbance as an indicator of the chemical composition and reactivity of dissolved organic carbon. *Environmental Science & Technology*, 37, 4702-4708.

- WHITE, A., CANNELL, M. G. R. & FRIEND, A. D. 2000. CO₂ stabilization, climate change and the terrestrial carbon sink. *Global Change Biology*, 6, 817-833.
- WHITTAKER, R. & LIKENS, G. 1975. The Biosphere and Man. *In: LIETH, H. & WHITTAKER, R. (eds.) Primary Productivity of the Biosphere*. Springer Berlin Heidelberg.
- WILLIAMS, C. J., YAMASHITA, Y., WILSON, H. F., JAFFE, R. & XENOPOULOS, M. A. 2010. Unraveling the role of land use and microbial activity in shaping dissolved organic matter characteristics in stream ecosystems. *Limnology and Oceanography*, 55, 1159-1171.
- WOLF, S., EUGSTER, W., POTVIN, C., TURNER, B. L. & BUCHMANN, N. 2011. Carbon sequestration potential of tropical pasture compared with afforestation in Panama. *Global Change Biology*, 17, 2763-2780.
- WORRALL, F., BURT, T. & SHEDDEN, R. 2003. Long term records of riverine dissolved organic matter. *Biogeochemistry*, 64, 165-178.
- WORRALL, F., HARRIMAN, R., EVANS, C. D., WATTS, C. D., ADAMSON, J., NEAL, C., TIPPING, E., BURT, T., GRIEVE, I., MONTEITH, D., NADEN, P. S., NISBET, T., REYNOLDS, B. & STEVENS, P. 2004. Trends in dissolved organic carbon in UK rivers and lakes. *Biogeochemistry*, 70, 369-402.
- WYSOCKI, L. A., FILLEY, T. R. & BIANCHI, T. S. 2008. Comparison of two methods for the analysis of lignin in marine sediments: CuO oxidation versus tetramethylammonium hydroxide (TMAH) thermochemolysis. *Organic Geochemistry*, 39, 1454-1461.
- YAN, Y., TIAN, J., FAN, M., ZHANG, F., LI, X., CHRISTIE, P., CHEN, H., LEE, J., KUZYAKOV, Y. & SIX, J. 2012. Soil organic carbon and total nitrogen in intensively managed arable soils. *Agriculture Ecosystems & Environment*, 150, 102-110.
- ZHANG, J., LOYNACHAN, T. E. & RAICH, J. W. 2011. Artificial soils to assess temperature sensitivity of the decomposition of model organic compounds: effects of chemical recalcitrance and clay-mineral composition. *European Journal of Soil Science*, 62, 863-873.
- ZOGG, G. P., ZAK, D. R., RINGELBERG, D. B., MACDONALD, N. W., PREGITZER, K. S. & WHITE, D. C. 1997. Compositional and functional shifts in microbial communities due to soil warming. *Soil Science Society of America Journal*, 61, 475-481.
- ZSOLNAY, A. 1996. Chapter 4 - Dissolved Humus in Soil Waters. *In: ALESSANDRO, P. (ed.) Humic Substances in Terrestrial Ecosystems*. Amsterdam: Elsevier Science B.V.